

Novel Applications of Magnesium Base Systems in Preparative Organic Chemistry and Asymmetric Synthesis

Thesis submitted to the University of Strathclyde in partial fulfilment of the requirements for the degree of Doctor of Philosophy

By

Peter Katai

University of Strathclyde

2018

Department of Pure and Applied Chemistry

University of Strathclyde

Thomas Graham Building

295 Cathedral Street

Glasgow

G1 1XL

Declaration of copyright

This thesis is the result of the author's original research. It has been composed by the author and has not been previously submitted for examination which has led to the award of a degree.

The copyright of this thesis belongs to the author under the terms of the United Kingdom Copyright Acts as qualified by University of Strathclyde Regulation 3.50. Due acknowledgement must always be made of the use of any material contained in, or derived from, this thesis.

Signature:

A handwritten signature in black ink, appearing to read "Peter Vlatari". The signature is written in a cursive style with some loops and flourishes.

Date: 27-Sep-2018

Abstract

During this research project the synthesis of sp^3 -rich azepanes was envisioned using our asymmetric deprotonation strategy as a key step build in chirality. First a series of chiral enol phosphates were prepared in good to high yields with high enantioselectivities (up to 99:1) using a C_2 -symmetric magnesium base developed in the Kerr group. Thereafter a series of trisubstituted alkenes were synthesized by a cross coupling strategy using phenylmagnesium bromide and to our delight, after a detailed optimisation, the desired products were obtained with high to excellent yields. The scope of the nucleophilic coupling partner was also successfully expanded for primary and secondary alkyl Grignard reagents, which are known to be more challenging coupling partners and the desired products were obtained in high to excellent yields. When the primary alkyl cross coupled products were used as substrates the desired 7-membered azepanes were obtained after a one pot ozonolysis-reductive amination sequence, with good yields and high *ers* in a diastereoselective manner. Neither in the cross coupling step nor in the tandem ozonolysis-reductive amination erosion of the enantioselectivity was not observed. In the case of the secondary and aryl coupled products, with identical conditions the ring closure does not occur, and the corresponding aliphatic ϵ -amino ketones could be obtained with moderate to good yields in an enantiomerically enriched fashion. Further optimisation of the reaction conditions allowed us to prepare the desired chiral azepanes even with these challenging substrates.

In parallel with this a series of conformationally locked cyclobutanones were synthesised and desymmetrised with a C_2 -symmetric magnesium base, developed in our group. The enol phosphates were isolated with significantly lower enantiomeric ratios (57:43 to 59:41) than the previously reported values (95:5 to 99:1). In order to explain the observed differences a Kumada coupling reaction was developed for the cross coupling of enol phosphates with phenylmagnesium bromide. The products were obtained in moderate to high yields and separation of these products revealed that the enantioselectivity of the products was identified incorrectly previously. In addition the structure of the C_2 -symmetric magnesium base was also investigated by DOSY NMR and revealed that under standard conditions a mixed alkylmagnesium amide forms instead of the previously assumed bisamide. With these results in hand, a novel mixed magnesium amide system was identified computationally as an efficient base, for the asymmetric deprotonation of cyclobutanones. Finally, the desired amine was prepared through a three step synthetic sequence.

Acknowledgement

First, I would like to thank Billy for the opportunity to be part of his research group and his continuous professional support during the last 4 years. I also would like to thank Laura and Dave for their encouragement during group meetings and reviewing my yearly reports and the final thesis. I would like to thank for all of those, that I shared the lab with (Renan, Leo, Liam, Garry, Adele, Giorgia, Paul, Raymond, Jemma and Scott) and special thanks for avoiding Pizza Hut on Fat Fridays for 3.5 years. Most of all, I'd like to thank Reka for sharing all the ups and downs that a PhD brings, with me in the last 4 years and supporting me. Last but not least, I would like to thank my parents for their encouragement, love and guidance during this time.

Abbreviations

Ac	Acetyl group
b.p.	Boiling point
CIP	Contact ion pair
D	Deuterium atom
DABCO	1,4-diazabicyclo[2.2.2]octane
DCM	Dichloromethane
DBU	1,8-diazabicyclo[5.4.0]undec-7-ene
DOSY	Diffusion-ordered spectroscopy
dr	Diastereomeric ratio
ee	Enantiomeric excess
Et ₂ O	Diethyl ether
EQ	External quench
er	Enantiomeric ratio
h	hour
HMPA	Hexamethylphosphoramide
IQ	Internal quench
IR	Infrared spectroscopy
LDA	Lithium di- <i>iso</i> -propylamide
M	mmol/mL
min	minute
MW	Microwave irradiation
NMR	Nuclear magnetic resonance
	s singlet
	d doublet
	t triplet
	q quartet

	m	multiplet
	br	broad
nOe		Nuclear Overhauser effect
NOESY		Nuclear Overhauser effect Spectroscopy
PE		Petroleum ether
rt		Room temperature
sat.		Saturated
SET		Single electron transfer
SSIP		Solvent separated ion pair
TBDMS		<i>Tert</i> -butyldimethylsilyl
Tf		Triflate
THF		Tetrahydrofuran
TLC		Thin layer chromatography
TMEDA		Tetramethylethylenediamine
TMP		2,2,6,6-tetramethylpiperidine
TMS		Trimethylsilyl
UV		Ultraviolet
2-MeTHF		2-methyltetrahydrofuran

Contents

1	Introduction	- 9 -
2	Chiral Lithium Amide Bases	- 11 -
2.1	Enantioselective Rearrangement of Epoxides	- 12 -
2.2	Synthesis of Chiral Tricarbonyl (η^6 -arene)chromium Complexes	- 14 -
2.2.1	Aromatic Functionalisation	- 14 -
2.2.2	Benzylic Functionalisation.....	- 16 -
2.2.3	Deprotonation of Prochiral Ketones.....	- 18 -
2.3	Catalytic Enantioselective Deprotonation with Sub-Stoichiometric Quantities of Chiral Base.....	- 32 -
2.4	Summary	- 39 -
3	Magnesium Amide Bases.....	- 40 -
4	Structure of Magnesium Amides	- 42 -
5	Homoleptic Magnesium Bisamide Complexes	- 44 -
5.1	Discovery and Substrate Scope	- 44 -
5.2	Structural Development.....	- 52 -
5.2.1	Alteration of the Achiral and Chiral Sidearm.....	- 52 -
5.2.2	Chelating Amine Ligands.....	- 57 -
5.2.3	Polymer-supported Magnesium Bisamides.....	- 63 -
6	Heteroleptic Magnesium Amides	- 66 -
6.1	Advantages.....	- 66 -
6.2	Aryloxymagnesium Amides.....	- 66 -
6.3	Alkylmagnesium Amides	- 69 -
7	Carbon Centred Bases.....	- 71 -
7.1	Catalytic Asymmetric Deprotonation.....	- 71 -
7.2.1	Synthesis of Functionalised Enolates.....	- 76 -
7.2.2	Other Applications	- 80 -
8	Proposed Work	- 83 -
8.1	Synthesis of Chiral Azepanes.....	- 83 -
8.2	Asymmetric Deprotonation of Cylobutanones	- 85 -
8.3	Structural Analysis of the Base by NMR spectroscopy	- 86 -
9	Results and Discussion	- 88 -

9.1	Synthesis of Chiral sp ³ -rich Azepanes	- 88 -
9.1.1	Introduction	- 88 -
9.1.2	Computational Analysis of the 3D Properties of the Azepane Core.....	- 89 -
9.1.3	Synthesis of Racemic Enol Phosphates.....	- 90 -
9.1.4	Synthesis of Chiral Enol Phosphates	- 91 -
9.1.5	Cross Coupling.....	- 93 -
9.1.6	Development of a New Protocol	- 95 -
9.1.7	Substrate Scope for the Cross Coupling with Phenylmagnesium Bromide..	- 99 -
9.1.8	Mechanistic Insight in the Formation of the Homocoupled Enol Phosphate-	102 -
9.1.9	Extension of the Substrate Scope: Secondary Alkyl Grignard Reagents	- 111 -
9.1.10	Summary for the Cross Coupling	- 116 -
9.1.11	Ozonolysis-Reductive Amination	- 118 -
9.1.12	Further Azepane Targets.....	- 127 -
9.1.13	Summary and Future Work.....	- 142 -
9.2	Towards the Synthesis of chiral Pyrrolidines	- 143 -
9.2.1	Synthesis of Cyclobutanones	- 143 -
9.2.2	Synthesis of Racemic Enol Phosphates.....	- 146 -
9.2.3	Asymmetric Deprotonation of Cyclobutanones	- 147 -
9.2.4	Towards a Novel Amine Structure	- 158 -
9.2.5	Synthesis of the Novel Amine	- 164 -
9.2.6	Summary and Future Work.....	- 169 -
9.3	Structural Studies of Magnesium Amides	- 171 -
9.3.1	Summary for the Structural Studies of Magnesium Amides	- 181 -
10	Experimental	- 183 -
10.1	Reagents	- 183 -
10.2	General Instrumentation	- 184 -
10.3	General Procedures	- 184 -
10.4	Experimental Procedures	- 198 -
13	References	- 314 -

1 Introduction

By definition, a molecule is chiral if it is not superimposable on its mirror image.¹ In Nature, chirality plays a central role, with critical building blocks such as amino acids and carbohydrates exhibiting homochirality in living organisms. In order to prepare chemical substances that can sufficiently interact with these biopolymers, the stereochemistry of the reactive chemical substance has to be controlled. Indeed, the preparation of such molecules is a particularly challenging area of science due to the similar physical properties that chiral molecules exhibit. As a consequence, there is a high demand for the preparation of molecules in an asymmetric fashion. Most importantly, these molecules are ubiquitously used as agrochemicals and pharmaceuticals.² For example, 56% of the drugs currently in use are chiral products.³ Therefore, the generation and preservation of chiral information is one of the most important and popular fields in synthetic chemistry. However, the selective installation of stereocentres still presents a considerable challenge in organic synthesis.⁴ The development of such protocols is still demanding, despite the fact that several generations of scientists have worked to understand the key factors in these processes and develop rational guidelines for the synthesis of new molecules.

Historically, the synthesis of chiral targets was firstly achieved by the use of enantiomerically pure, naturally-occurring, starting materials, which is known as the chiral pool method (first generation asymmetric synthesis). The configuration of a new chiral centre is affected by the existing one and the relative energy difference between the diastereomeric transition states determines the selectivity of the transformation. This process is often termed as a substrate-controlled reaction in asymmetric synthesis. The main disadvantages of this strategy are the restricted availability of the source and the limited number of tolerated transformations without the loss of stereogenicity.⁵ A further method, referred to as second-generation asymmetric synthesis, employs a stoichiometric chiral auxiliary, which can be attached to a prochiral substrate to induce chirality *via* a diastereoselective reaction.⁶ These transformations are not restricted to the availability of the chiral starting material, although, it has to be highlighted that the attachment and removal of the chiral auxiliary increases the number of necessary reaction steps by two. Stoichiometric chiral reagents are also successfully used in asymmetric synthesis (often referred to as third generation asymmetric synthesis).⁷⁻⁹ In this case, the generation of chirality is achieved using an enantiomerically pure reactant, where the starting substrate is an achiral molecule. In addition, varying chiral organometallic reagents are easily prepared in high yield allowing a wide variety of synthetic transformations to be carried out.⁷⁻⁹ Finally, the generation of stereocentres can also be achieved by catalytic methods, which is known as fourth

generation asymmetric synthesis.¹⁰ Although the application of catalytic transformations are widely used to prepare chiral structures under milder conditions or through otherwise unavailable disconnections, this approach typically requires the use of often expensive metals, in order to efficiently catalyse asymmetric transformations. In addition, a chiral environment, generated by the ligands around the metal centre is required, and synthesis of these ligands can often be costly and time consuming. Due to these drawbacks, the application of these protocols on industrial scale synthesis is often challenging.

As mentioned above, stoichiometric chiral reagents have been extensively used for the preparation of highly functionalised molecules in a stereoselective manner. One of the most important chiral transformations with a stoichiometric chiral reagent is the enantioselective deprotonation of a prochiral substrate, which forms a highly reactive nucleophilic intermediate, which can be reacted with several different electrophiles to prepare enantiomerically enriched molecules.¹¹ Most frequently, chiral lithium amides have been used to successfully accomplish the asymmetric deprotonation process.^{7,9,12} In relation to this, our own research team is especially interested in the application of magnesium amides as chiral reagents in the synthesis of complex molecular frameworks. The outstanding ability of these reagents lies in their highly basic character, in parallel with their low nucleophilicity. These properties make these reagents exceptional chiral bases in the asymmetric deprotonation of organic substrates.

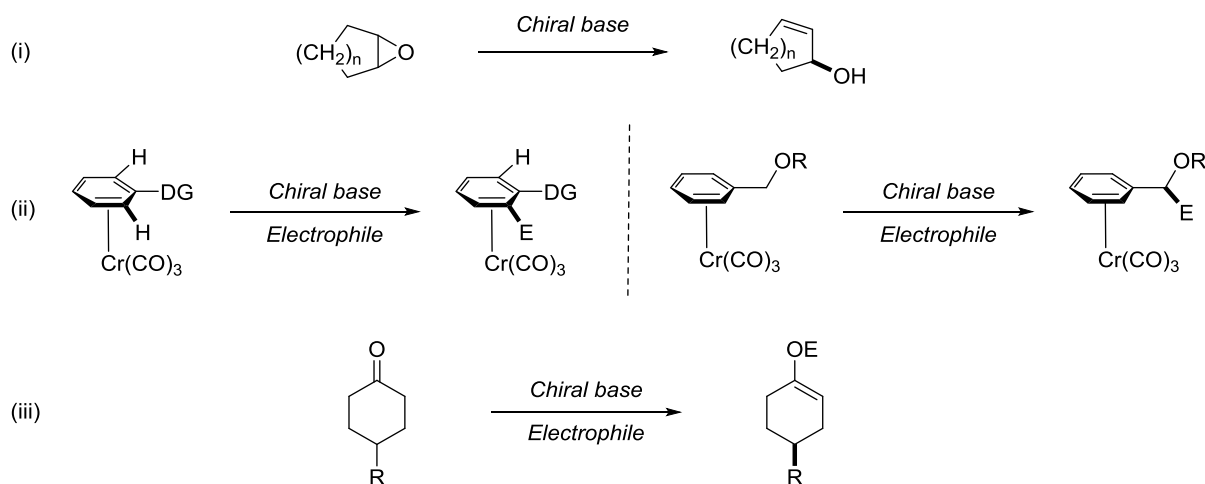
The following sections discuss, in turn, the development of both lithium and magnesium base species for application in asymmetric synthesis.

2 Chiral Lithium Amide Bases

Over the last twenty years, there has been a continuing effort towards the application of chiral bases in molecular desymmetrisation processes. In particular, chiral lithium amide bases have emerged to become one of the most popular classes of chiral bases. They have been extensively investigated by several research groups in order to understand the key parameters in the desymmetrisation of prochiral substrates.^{2,13-15} Such studies have involved investigations into the structure-selectivity relationship, including a series of crystallographic and NMR experiments. Furthermore, the role of different additives has been investigated to increase the efficiency of the process. Unsurprisingly, the information gained through these studies has resulted in an increased use of chiral base mediated reactions as the key steps in total syntheses.¹⁶

Chiral lithium amide bases have been successfully employed in the desymmetrisation of three main classes of organic substrates as shown in **Scheme 2.1**:

- (i) rearrangement of epoxides to allylic alcohols;¹³
- (ii) aromatic and benzylic functionalisation of tricarbonyl(η^6 -arene)chromium complexes;¹⁵
- (iii) asymmetric deprotonation of conformationally locked prochiral cyclohexanones and other cyclic ketones.¹⁷



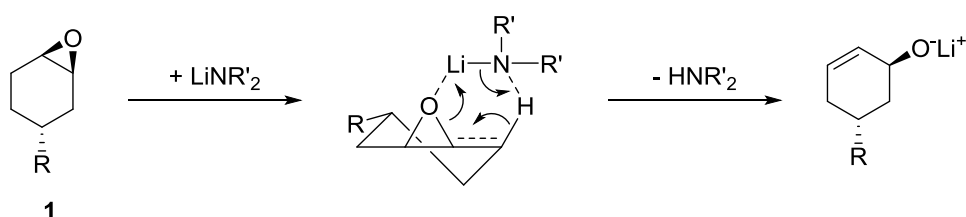
Scheme 2.1

All three classes of substrate possess a plane of symmetry or are achiral. With regard to obtaining enantiomerically enriched products in these desymmetrisation processes, the chiral base has to distinguish between a pair of equivalent but enantiotopic protons.

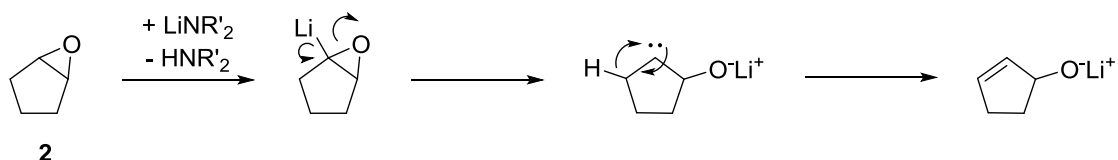
2.1 Enantioselective Rearrangement of Epoxides

The rearrangement of cyclic epoxides to allylic alcohols using achiral lithium amide species is a well-known process.¹⁸ The widely accepted mechanism for the transformation of, for example, cyclohexene oxide **1**, proceeds through a *syn* β -elimination¹⁹ of a *pseudo*-axial proton, although with cyclopentene oxide **2**, an alternative α -lithiation mechanism was also suggested (**Scheme 2.2**).²⁰

β -elimination:

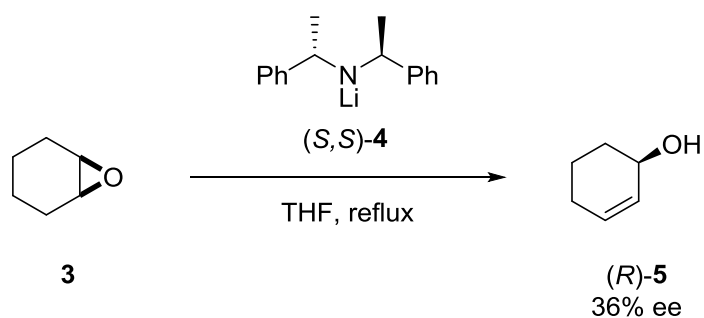


α -insertion:



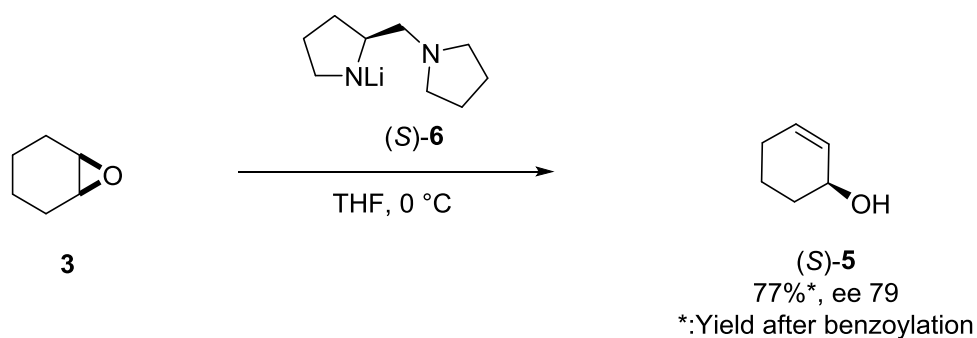
Scheme 2.2

Whitesell was the first to use a chiral lithium amide, (*S,S*)-**4**, in the asymmetric deprotonation of cyclohexene oxide **3** in 1980 (**Scheme 2.3**).²¹ The reaction was carried out in refluxing THF and the allylic alcohol (*R*)-**5** was obtained in a moderate 36% enantiomeric excess.



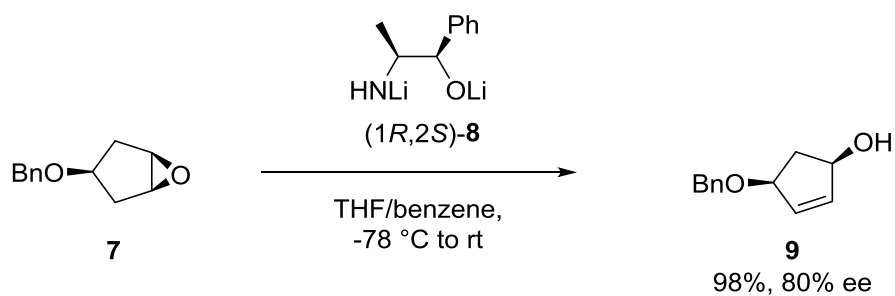
Scheme 2.3

Since this pioneering report, several research groups have improved on Whitesell's original protocol. To further increase the synthetic utility of the reaction, a series of novel lithium amide bases containing a second, electron donating, heteroatom were prepared. Firstly, Asami reported a proline-derived base, (*S*)-**6** (**Scheme 3.4**).^{6,7} The product (*S*)-**5** was obtained in a significantly higher 79% ee compared to Whitesell's amine, which gave 36% ee.



Scheme 2.4

More importantly, with base (*S,S*)-4 giving (*R*)-5 as the major enantiomer, and base (*S*)-6 giving (*S*)-5, these two protocols are complementary. Following these studies, Schlosser found that a mixed alkoxy amido base effectively increased the enantioselectivity in the desymmetrisation of oxiranes.²⁴ Based on these initial results, Murphy demonstrated that a more readily available chiral amine (*1R,2S*)-8 could also be used in the asymmetric deprotonation of cyclic epoxides to produce chiral allylic alcohols in higher ee (Scheme 2.5).^{25,26}

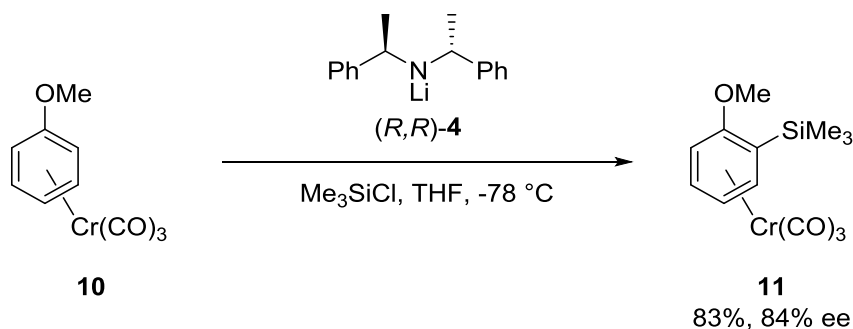


Scheme 2.5

2.2 Synthesis of Chiral Tricarbonyl (η^6 -arene)chromium Complexes

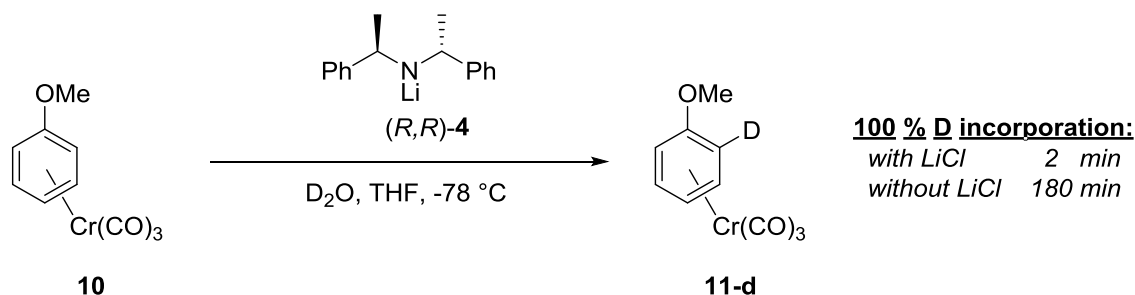
2.2.1 Aromatic Functionalisation

In 1994, Simpkins first demonstrated that a chiral lithium amide base (*R,R*)-**142** could differentiate between the *ortho*-protons in a prochiral (η^6 -arene)chromium tricarbonyl complex **148** (Scheme 2.6).^{27,28}



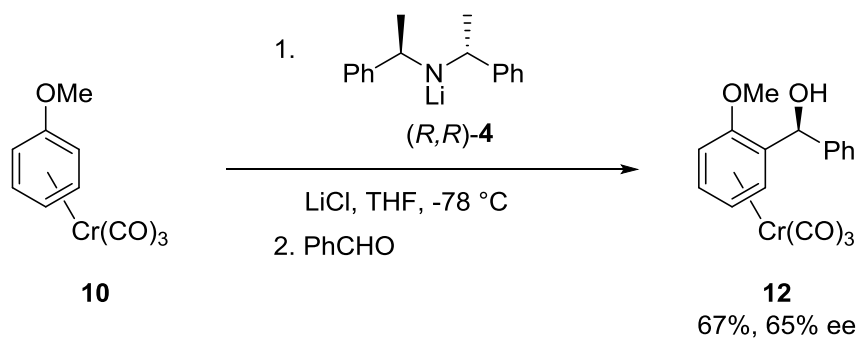
Scheme 2.6

The metallation was aided by a methoxy directing group, and the product **11** was obtained in high yield and good enantioselectivity after quenching with trimethylsilyl chloride. Subsequently, the metallation was followed by quenching with benzaldehyde as an electrophile, however only small amounts of the desired product was observed. In order to investigate this poor result, the organometallic intermediate was quenched with deuterated water. In the presence of lithium chloride, the reaction was dramatically accelerated (Scheme 2.9).²⁹



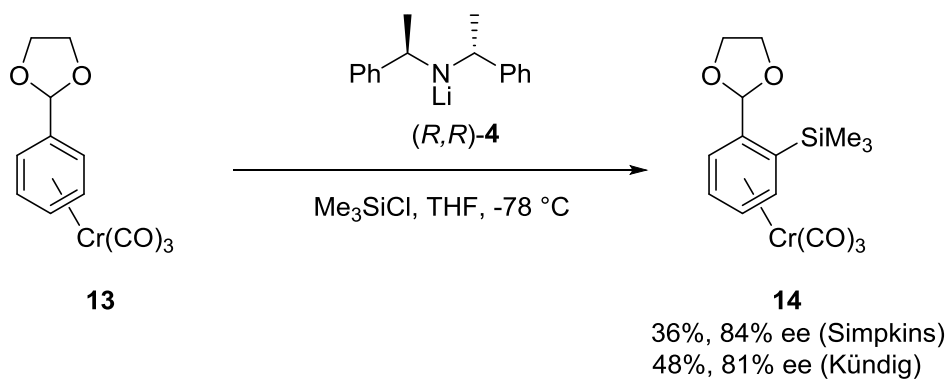
Scheme 2.7

With the optimised conditions in hand, benzaldehyde was eventually used successfully as an alternative electrophilic reactant in the desymmetrisation of (η^6 -arene)chromium tricarbonyl complex **10** (Scheme 2.8).^{28,29}



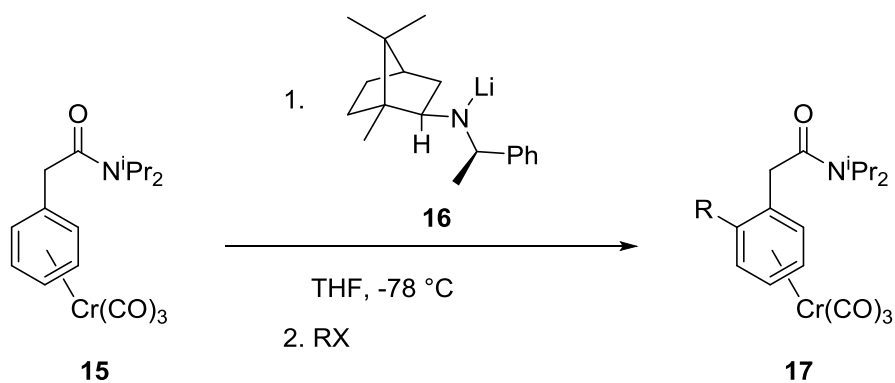
Scheme 2.8

However, the yield and ee values were still lower in comparison with **Scheme 2.6**. Other coordinating groups were also successfully used in the desymmetrisation of tricarboxyl (η^6 -arene)chromium complexes. In this manner, acetal **13**^{27,28,30} and amide **15**³⁰ were also used (**Scheme 2.9** and **Scheme 2.10**) in the *ortho*-functionalisation of these substrates.



Scheme 2.9

Finally, Kündig demonstrated that a wide range of different electrophiles can react with the lithiated organometallic species generated *in situ* by reaction of amide **15** with chiral base **16** (**Scheme 2.10**).³⁰ Generally, the *ortho*-substituted complexes were obtained in high yields and with ee values between 64-73%.



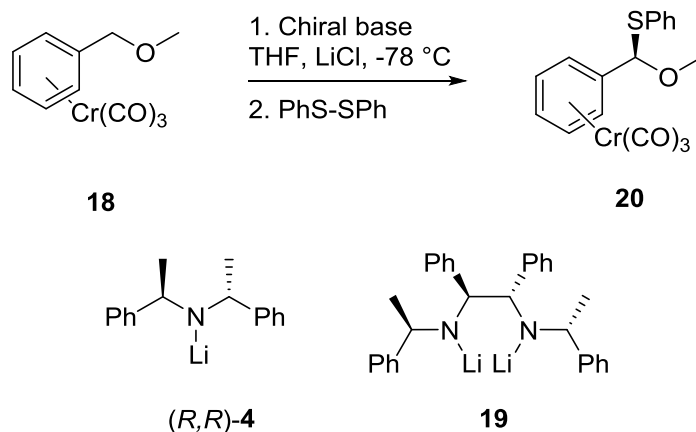
Scheme 2.10

Entry	R-X	Yield (%)	ee (%)
1	Me_3SiCl	86	67
2	MeOC(O)Cl	71	73
3	$\text{Me}_2\text{NC(O)Cl}$	85	68
4	MeI	93	64
5	DMF	93	69

Table 2.1

2.2.2 Benzylic Functionalisation

In the *ortho*-functionalisation of chromium complex **13**, both Simpkins and Kündig observed relatively low yields due to competing metalation at the benzylic position (*c.f.* **Scheme 2.9**).^{27,28,30} Inspired by their results, Simpkins^{28,31} and Gibson³² independently recognised the synthetic importance of this transformation to prepare enantiomerically enriched, benzyl-functionalised (η^6 -arene)chromium complexes. Initially, the same chiral base (*R,R*)-**4** was used in these reactions, as for the *ortho*-functionalisation, however, Gibson demonstrated the practical utility of a new diamine ligand, **157**, which significantly increased the ee and yield under similar conditions (**Scheme 2.11**).³²

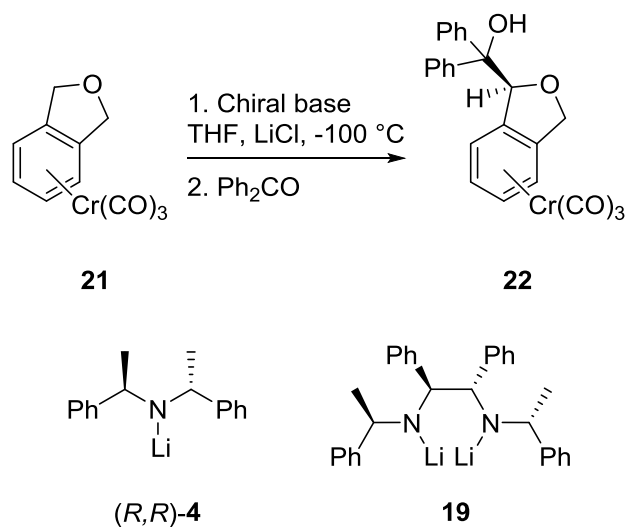


Scheme 2.11

Entry	Chiral base	Yield (%)	ee (%)
1	(<i>R,R</i>)-4	52	22
2	19	86	97

Table 2.2

The same effect was also observed by Simpkins with dihydroisobenzofuran chromium complex **21**. The lithiated organometallic, in this case, was trapped by benzophenone to give the chiral tertiary alcohol **22** as shown in **Scheme 2.12**.^{28,31}



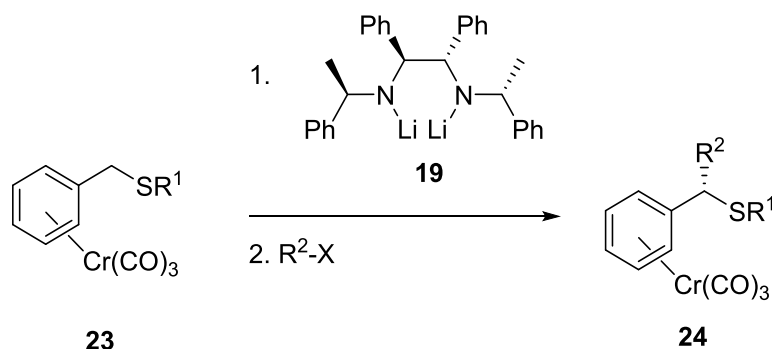
Scheme 2.12

Entry	Chiral base	Yield (%)	ee (%)
1	(<i>R,R</i>)-4	72	75
2	19	70	99

Table 2.3

Using chiral base (*R,R*)-4 or **19** the product was isolated in similar yields, while the ee with amide **19** was significantly higher. Moreover, the effect of different directing groups was also

investigated. For example, thioethers **23** were studied and several electrophiles were used with success (**Scheme 2.13**).³²



Scheme 2.13

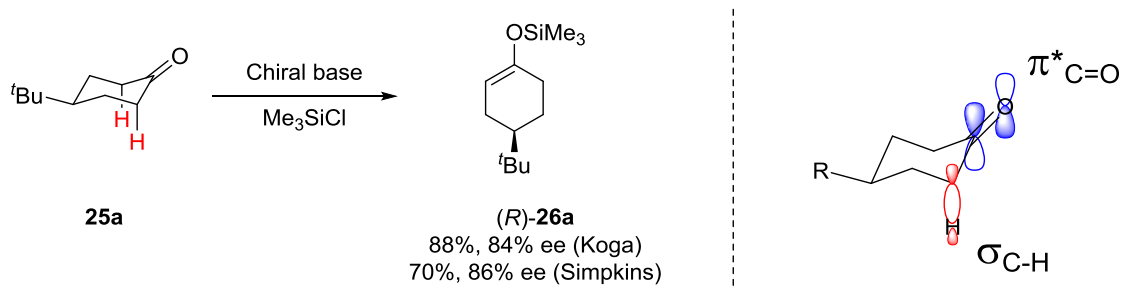
Entry	R ¹	R ²	Yield (%)	ee (%)
1	Me	Bn	91	88
2	Me	C ₁₁ H ₉	93	88
3	Me	Me ₃ Si	62	89
4	Bn	Me	84	91
5	Bn	C ₁₁ H ₉	83	91

Table 2.4

The corresponding complexes **24** were furnished in high ee and in generally good yields. However, in contrast with the *ortho*-functionalisation, when trimethylsilyl chloride was used as electrophile the yield dropped to 62% (entry 3 in **Table 2.4**).

2.2.3 Deprotonation of Prochiral Ketones

Independently, Simpkins³³ and Koga³⁴ both demonstrated that asymmetric deprotonation of prochiral ketones using chiral lithium amide bases is a viable process, producing silyl enol ethers in an enantiomerically enriched fashion (**Scheme 2.14**).

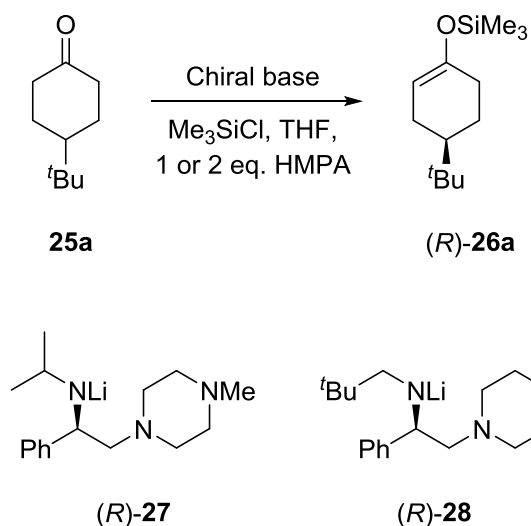


Scheme 2.14

In conformationally locked ketones, a stereoelectronic preference exists to remove the axial protons (red hydrogens in **Scheme 2.14**) due to the more effective overlapping interaction between the

developing negative charge and the antibonding orbital of the carbon oxygen double bond (right-hand side in **Scheme 2.14**).³⁵ The work of Koga and Simpkins thus demonstrated that a reactive chiral base can effectively distinguish between these two enantiotopic protons.

Based upon these results, Koga extensively studied the asymmetric deprotonation 4-*tert*-butylcyclohexanone analogues with novel bidentate bases (*R*)-**164** and (*R*)-**165** (**Scheme 2.15**).³⁶



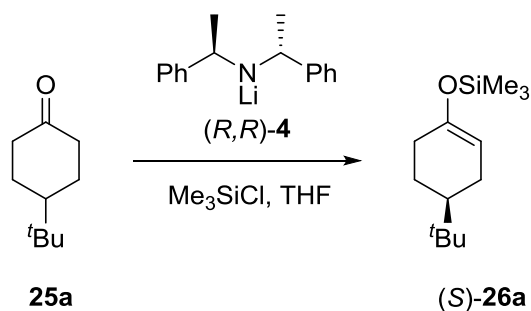
Scheme 2.15

Entry	Chiral base	Temp. (°C)	Yield (%)	ee (%)
1	(<i>R</i>)- 27	-78	87	77
2	(<i>R</i>)- 28	-78	82	82
3	(<i>R</i>)- 27	-105	52	89

Table 2.5

The corresponding silyl enol ether **26a** was obtained in high ee with both lithium amides (*R*)-**27** and (*R*)-**28**. In order to achieve a high yield, Corey's internal quench method was used in every case, which means that the reactive organometallic was added to a solution of the substrate and electrophilic reagent.³⁷ In addition, 1 - 2 equivalents of the Lewis base HMPA was shown to be essential to enable high enantioselectivity.

Following this study, Simpkins then showed that a more simple *C*₂-symmetric chiral base (*R,R*)-**4** could be used in the deprotonation of cyclohexanone **25a** (**Scheme 2.16**).³⁸



Scheme 2.16

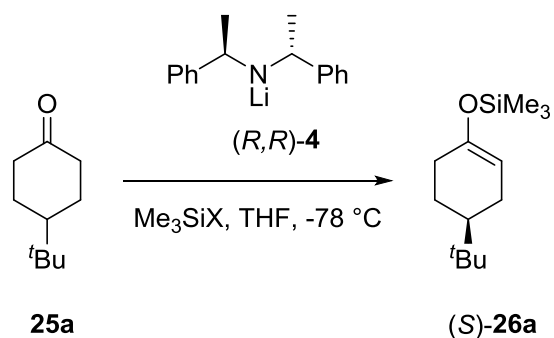
Entry	Temp (°C)	Yield (%)	ee (%)
1	-78	73	69
2	-90	66	88

Table 2.6

In both cases, the observed enantiomeric excesses were directly proportional to the reaction temperature. In conclusion, low temperatures were needed to reach high ee (entry 2 in **Table 2.6**), although the yield was compromised in these cases.

2.2.3.1 Effect of Salt Additives

In these early studies, both Koga³⁶ and Simpkins³³ reported the *in situ* trapping of the generated lithium enolates by an electrophilic reagent (internal quench). Interestingly, the enantiomeric ratios decreased drastically if the electrophilic trimethylsilyl chloride was added last to the reaction mixture (so-called external quench). To rationalise the observed effect, research efforts were focused on determining the role of lithium chloride, which can be generated under the reaction conditions. Firstly, Simpkins investigated the effect of different quenching techniques in the asymmetric deprotonation of 4-*tert*-butylcyclohexanone **25a** with chiral base (*R,R*)-**4** (**Scheme 2.17**).³⁹



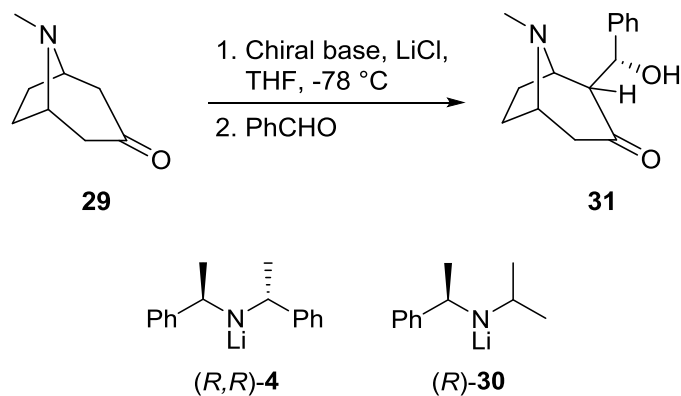
Scheme 2.17

Entry	X	Quench	LiCl (eq.)	ee (%)
1	Cl	Internal	-	69
2	Cl	External	-	23
3	Cl	External	0.5	83
4	Br	Internal	-	20

Table 2.7

Under internal quench conditions the enantioselectivity of the process increased from 23% (entry 2 in **Table 2.7**) to 69% ee (entry 1 in **Table 2.7**). On the other hand, the highest ee, 83%, was achieved by the addition of 0.5 equivalents of lithium chloride under external quench conditions (entry 3 in **Table 2.7**).

Reactions with different electrophiles and substrates were also carried out to determine the general role of lithium chloride in the asymmetric deprotonations. The same effect was observed by Simpkins^{38,39} and Majewski^{40,41} in the asymmetric aldol reaction of tropinone **29** (**Scheme 2.18**).



Scheme 2.18

Entry	Chiral base	Simpkins ^{28,29}		Majewski ^{30,31}	
		LiCl (eq.)	ee (%)	LiCl (eq.)	ee (%)
1		-	24	-	35
2		-	-	0.25	78
3	(R,R)-4	0.5	78	0.5	58
4		-	-	1	88
5		-	-	1.0*	95*
6		-	24	-	22
7	(R)-30	-	-	0.25	65
8		0.5	66	0.5	71
9		-	-	1	68

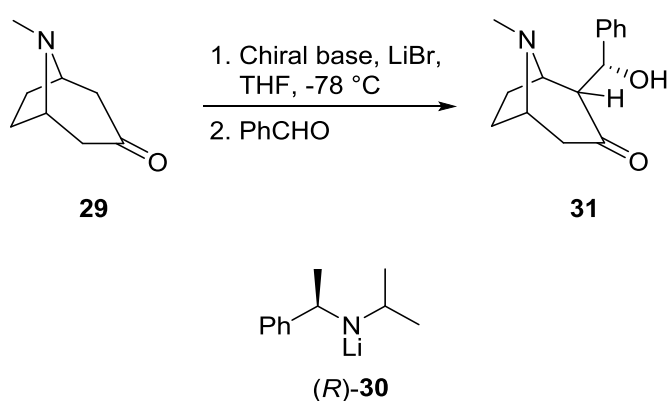
* Lithium chloride generated by premixing *n*-butyllithium and the hydrochloride salt of the amine precursor to chiral base (R,R)-4

Table 2.8

In both reports, the observed ee values were higher in the presence of lithium chloride. Moreover, an alternative method has been published to increase the selectivity. Instead of the hygroscopic amine, the less sensitive hydrochloride salt was used, which was deprotonated by 2 equivalents of *n*-butyllithium, generating the lithium amide base and lithium chloride additive *in situ* (entry 5 in **Table**

3.8). Indeed, in this case, Majewski was able to improve the enantioselectivity to an impressive 95% ee.

Other inorganic salts were also tested in the asymmetric deprotonation of tropinone **29**. In a detailed study, Simpkins investigated the effect of different lithium, sodium, magnesium and potassium salts, however, in each case, similar ee values were obtained as compared to the absence of any additive at all.³⁹ Furthermore, Majewski also obtained similar results with lithium perchlorate and lithium iodide, however, it was noted that lithium bromide has a similarly positive effect as lithium chloride in the asymmetric deprotonation of tropinone **29** when using base (*R*)-**30** (Scheme 2.19).⁴⁰

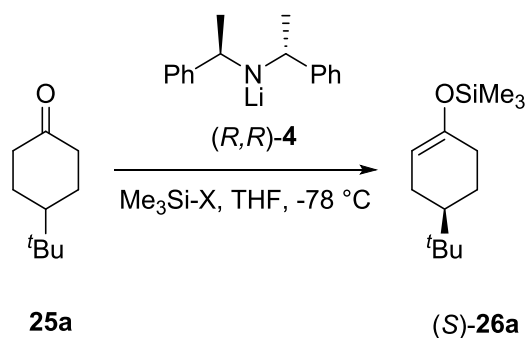


Scheme 2.19

Entry	Chiral base	LiBr (eq.)	ee (%)
1	(<i>R</i>)- 30	0	24
2	(<i>R</i>)- 30	1	69

Table 2.9

Due to the fact that inorganic lithium salts can be generated under standard reaction conditions, Koga has examined the effect of different electrophilic trimethylsilyl halides in the asymmetric functionalisation of 4-*tert*-butylcyclohexanone **25a** with chiral base (*R,R*)-**4** (Scheme 2.20).⁴²



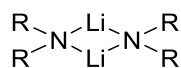
Scheme 2.20

Entry	X	Quench	Additive (eq.)	ee (%)
1	Cl	Internal	-	90
2	Br	Internal	-	65
3	I	Internal	-	31
4	Cl	External	-	44
5	Cl	External	LiCl (0.5)	87
6	Cl	External	LiCl (1.0)	88
7	Cl	External	LiCl (3.0)	88
8	Cl	External	LiBr (3.0)	86
9	Cl	External	LiI (3.0)	43

Table 2.10

Under internal quench conditions, the highest enantioselectivity was reached with trimethylsilyl chloride (entries 1-3 in **Table 2.10**). In summary, a similar trend to Simpkins' results was observed (*cf.* **Scheme 2.20** and **Scheme 2.17**).^{38,42} In both studies, the product (*S*)-**26a** formed in considerably lower ee under external quench conditions in the absence of additives. On the other hand, at least comparable ee was obtained when 0.5 equivalents of lithium chloride was added to the reaction mixture under external quench conditions. Higher amounts of lithium chloride did not improve the enantioselectivity (entries 5-7 in **Table 2.10**). In order to achieve a comparable effect with lithium bromide, 3.0 equivalents of the salt additive were required (entry 8 in **Table 2.10**). However, when lithium iodide was used the product (*S*)-**26a** was obtained with a significantly lower e.r. (entry 9 in **Table 2.10**).

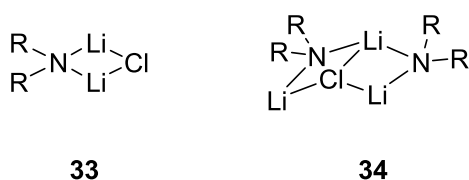
Keeping the previously reported results in mind, further research efforts were focused on the structural elucidation of different lithium amide bases in both liquid and solid phase. Koga performed a series of asymmetric deprotonation reactions with chiral base (*R,R*)-**4** to generate enantiomerically enriched silyl enol ethers.⁴² The structure of the chiral base (*S,S*)-**4** was characterized by ⁶Li and ¹⁵N NMR spectroscopy. Without lithium chloride, the main component was identified as a homo dimer **32** in THF solution (**Figure 2.1**).



32

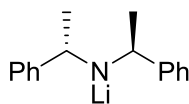
Figure 2.1

This observation was strengthened by the X-ray crystallographic analysis of chiral base (*R,R*)-**4**. In the solid state, a dimeric structure **32** was again revealed.⁴³ In this case, the crystals were obtained from a hexane-THF solution. With these results in hand, Koga suggested that the homo dimer, **32**, is responsible for the poor enantioselectivity. Moreover, ⁶Li and ¹⁵N NMR studies showed that in the presence of lithium chloride, two new species were formed in solution. They were identified as a mixed dimer **33** and a trimer **34**. The analogous trimeric structure has already been observed in the solid state structure of LDA in the presence of lithium chloride.⁴⁴ The mixed dimer **33** was identified as the major component in the THF solution of chiral base (*S,S*)-**4** and this species is believed to be responsible for the higher ee in the asymmetric deprotonation reactions (**Figure 2.2**).



33

34



(*S,S*)-**4**

Figure 2.2

The same phenomenon was observed with chelating chiral ligands (*R*)-**27** and (*R*)-**28** (**Figure 2.3**). Koga identified a similar dimeric structure with chiral amine (*R*)-**28** in solution (**Figure 2.3**), which likewise produced high enantioselectivities in the asymmetric deprotonation of 4-*tert*-butylhexanone **25a**.^{45,46}

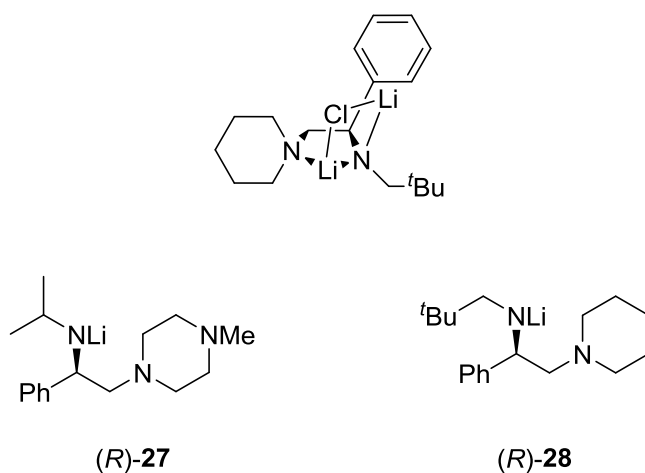
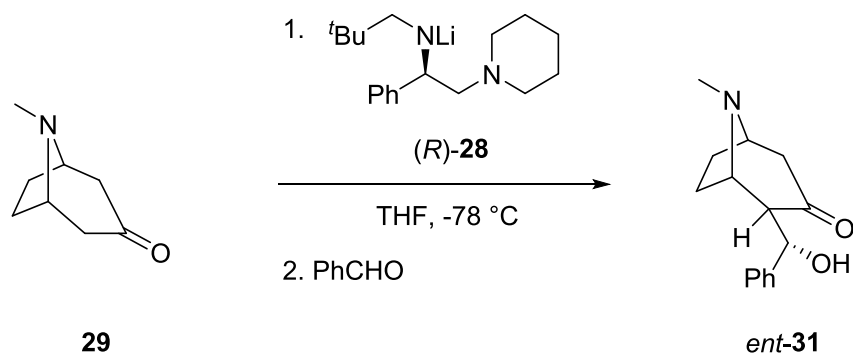


Figure 2.3

Unusually, when Majewski used chiral amine (*R*)-**28** in the asymmetric aldol reaction of tropinone **29**, the enantiomeric excess was independent of the amount of lithium salt (**Scheme 2.21**).⁴⁰ This shows that, whilst a good understanding of such base systems has been achieved, the individual systems can still be unpredictable and, indeed, substrate or base dependant.



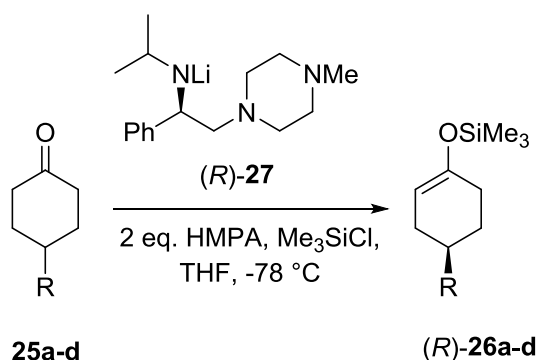
Scheme 2.21

Entry	LiCl (eq.)	ee (%)
1	-	90
2	0.5	90
3	1	90

Table 2.11

2.2.3.2 Substrate Scope and Application in Total Synthesis

At this point, research efforts began to focus on the application of chiral base mediated desymmetrisation to prepare a range of enantiomerically enriched cyclic ketones. Firstly, Koga extensively studied the asymmetric deprotonation of different 4-substituted cyclohexanones **25a** and **23** with chelating amines.^{36,47,48} Chiral amine (*R*)-**27** was effective in the generation of enantiomerically enriched silyl enol ethers (*R*)-**26a** (entries 1-3 in **Table 2.12**), although with the small methyl group in the 4-position the enantioselectivity decreased dramatically (entry 4 in **Table 2.12**).

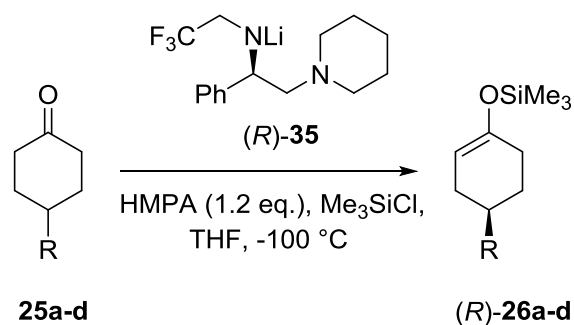


Scheme 2.22

Entry	R	Yield (%)	ee (%)
1	^t Bu (25a)	87	77
2	Ph (25b)	93	75
3	ⁱ Pr (25c)	85	78
4	Me (25d)	68	46

Table 2.12

Consequently, the deprotonation of the same substrates with chiral amine (*R*)-**35** were also investigated and the reactions afforded the appropriate products (*R*)-**26a-d** in higher ee and yield (**Scheme 2.23**). Indeed, a good yield of 76% and excellent enantioselectivity of 94% was observed when employing previously troublesome methyl-substituted substrate **26d** (entry 4 in **Table 3.13**).



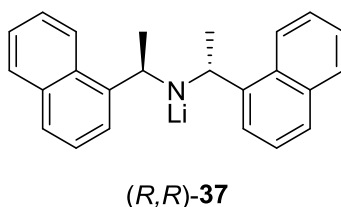
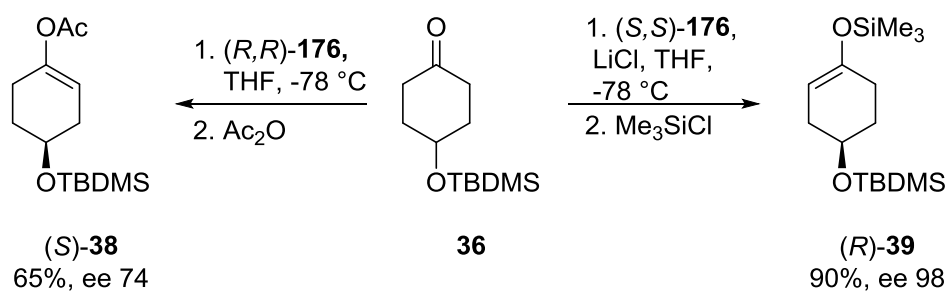
Scheme 2.23

Entry	R	Yield (%)	ee (%)
1	^t Bu (25a)	88	93
2	Ph (25b)	95	93
3	ⁱ Pr (25c)	92	95
4	Me (25d)	76	94

Table 2.13

However, in all of the reactions reported by Koga, low temperatures were employed and HMPA was required as an additive in order to achieve high enantioselectivities.

Next, Majewski investigated the desymmetrisation of silyl protected cyclohexanone **36** with chiral lithium amide **(R,R)-37** (Scheme 2.24).⁴⁹



Scheme 2.24

Under external quench conditions, the enolate was trapped by trimethylsilyl chloride and acetic anhydride. Either enantiomer could be obtained depending on the electrophile. The silyl enol ether

(*R*)-**39** was successfully used as an enantiomerically enriched starting material in the total synthesis of dihydroquilegiolide **40** (Figure 2.4).⁵⁰

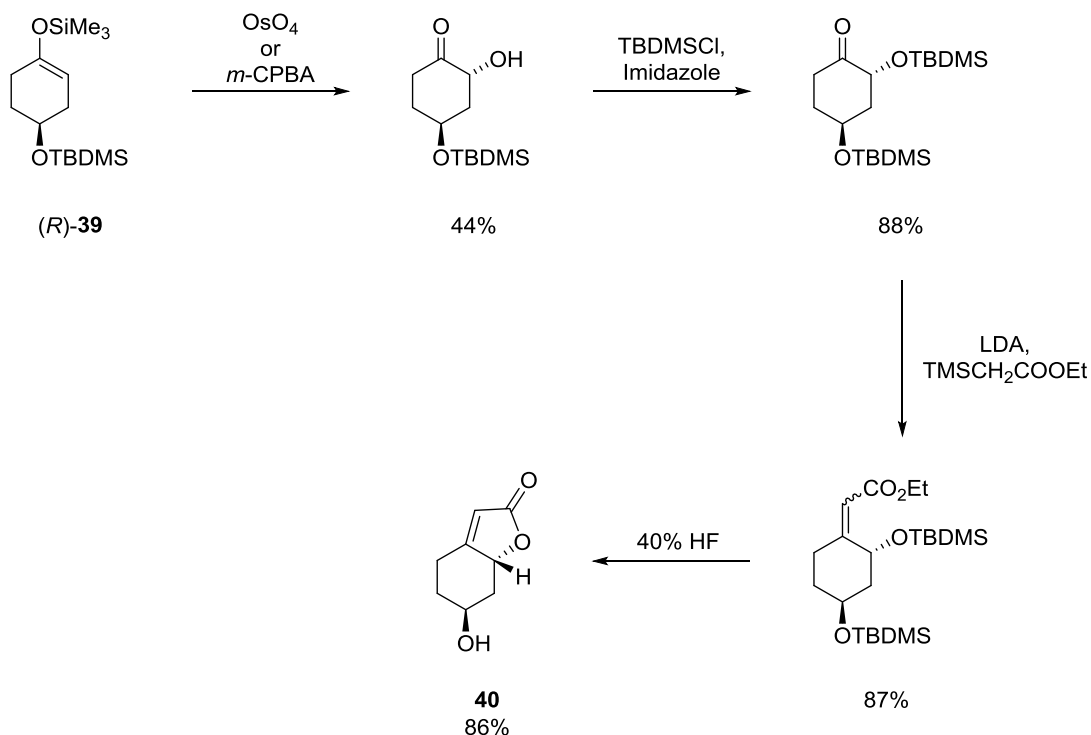
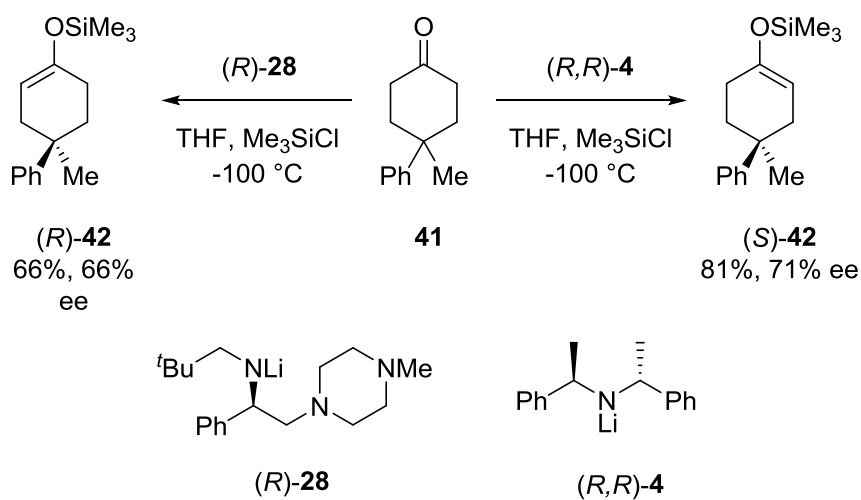


Figure 2.4

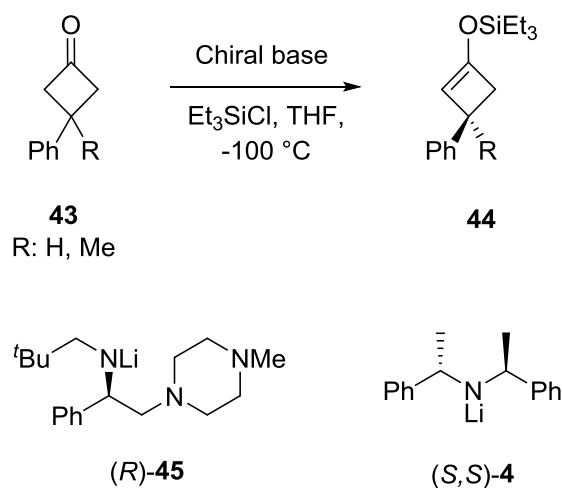
Adapting this methodology to the formation of chiral quaternary stereocentres, the asymmetric deprotonation of 4,4-disubstituted cyclohexanone **41** was investigated under internal quench conditions with several different chiral lithium amide bases.⁵¹ The best results were obtained with chiral base (*R*)-**28** and (*R,R*)-**4** (Scheme 2.25).⁵¹



Scheme 2.25

In general, the observed enantioselectivity was lower than the 4-*tert*-butyl- cyclohexanone **25a**, however both enantiomers were accessible with the appropriate amine (*R*)-**28** or (*R,R*)-**4**.

In addition, the smaller, 4-membered cyclobutanones **43** were also tested in the enantioselective deprotonation by Honda (Scheme 2.26).⁵² The highest enantioselectivity was reached when the monosubstituted (R=H **43a**) cyclobutanone was reacted with chiral base (*S,S*)-**4** under internal quench conditions.



Scheme 2.26

Entry	Substrate	Amine	Yield(%)	ee
1	R = H (43a)	(<i>R</i>)- 45	68	47
2	R = H (43a)	(<i>S,S</i>)- 4	67	92
3	R = Me (43b)	(<i>R</i>)- 45	65	60
4	R = Me (43b)	(<i>S,S</i>)- 4	85	12

Table 2.14

In addition, a series of lactones and acids **46-50** such as the natural product (-)-methyleneolactocin **50** were generated from the enantiomerically enriched cyclobutene products **44** (Figure 2.5).^{52,53}

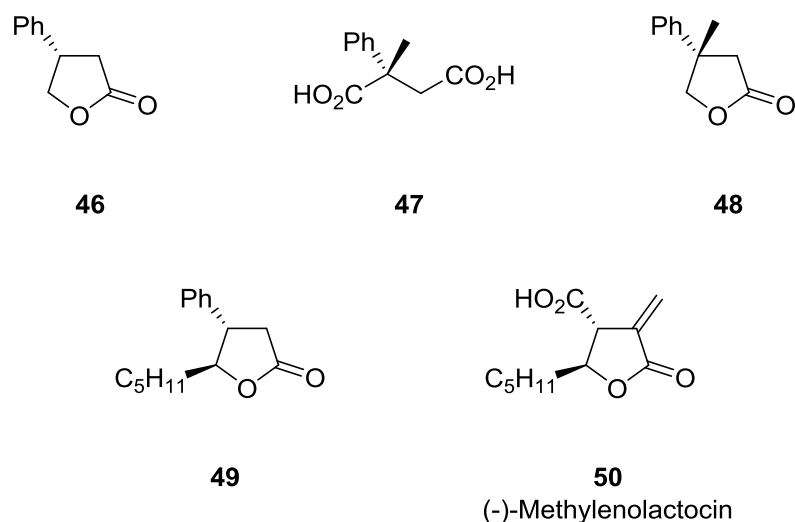
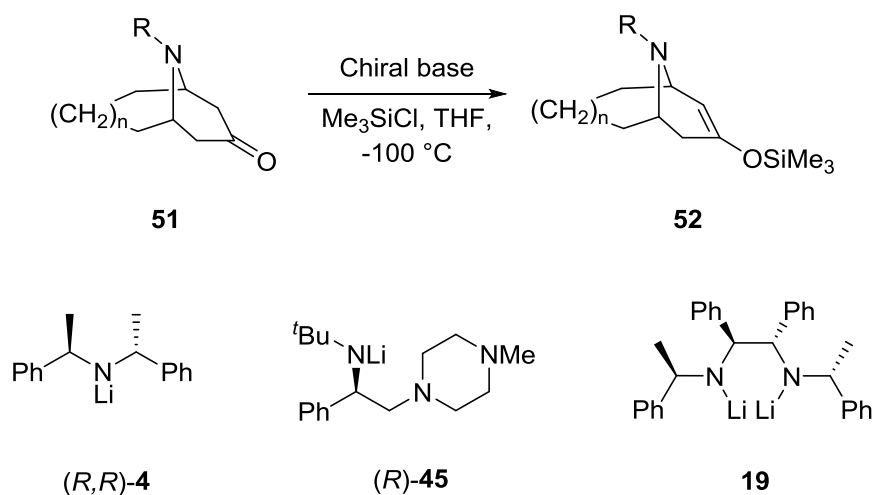


Figure 2.5

Finally, extended tropinone analogues were prepared by asymmetric deprotonation, in order to produce valuable building blocks for the synthesis of alkaloids. Momose conducted a series of experiments with carbamate protected azabicyclic ketones **51** with several different chiral lithium amides (**Scheme 2.27**).^{54,55}



Scheme 2.27

Entry	Chiral base	R	<i>n</i>	Yield (%)	ee (%)
1	(<i>R,R</i>)-4	COOMe	0	-	15-20
2	(<i>R</i>)-45	COOMe	1	94	93*
3	(<i>R</i>)-45	COOBn	2	75	90*
4	(<i>R</i>)-45	COOBn	0	89	90*
5	19	COOMe	0	84	78

*:Product is *ent*-52

Table 2.15

Generally, bidentate bases (*R*)-45 and 19 performed better than Simpkins' C_2 -symmetric base (*R,R*)-4. The generated silyl enol ether products 52 were used as starting materials in the total synthesis of a series of different alkaloids 53-55, such as (+)-pinidine hydrochloride, (+)-monomorine, and (-)-indolizidine 223AB (Figure 2.6)^{56,57}

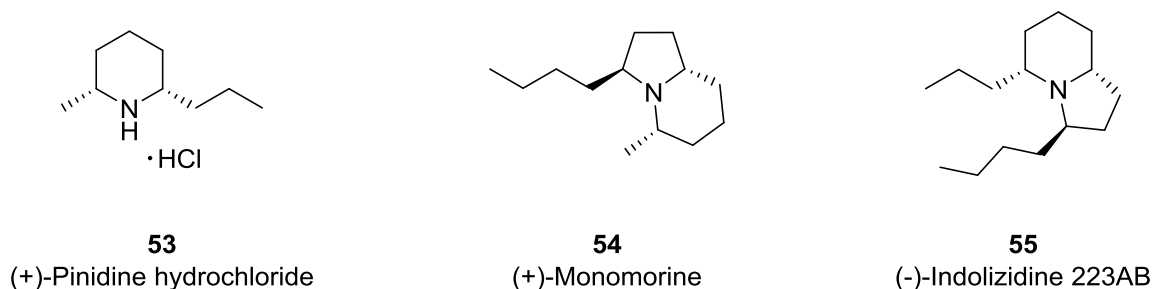
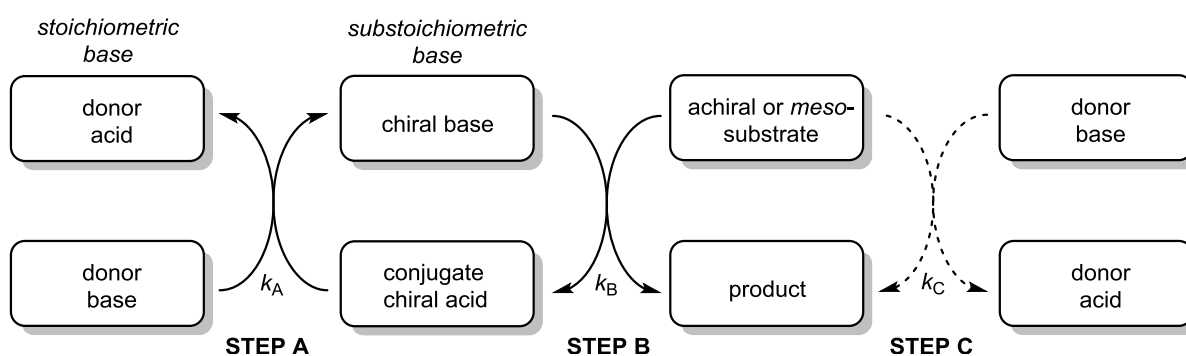


Figure 2.6

2.3 Catalytic Enantioselective Deprotonation with Sub-Stoichiometric Quantities of Chiral Base

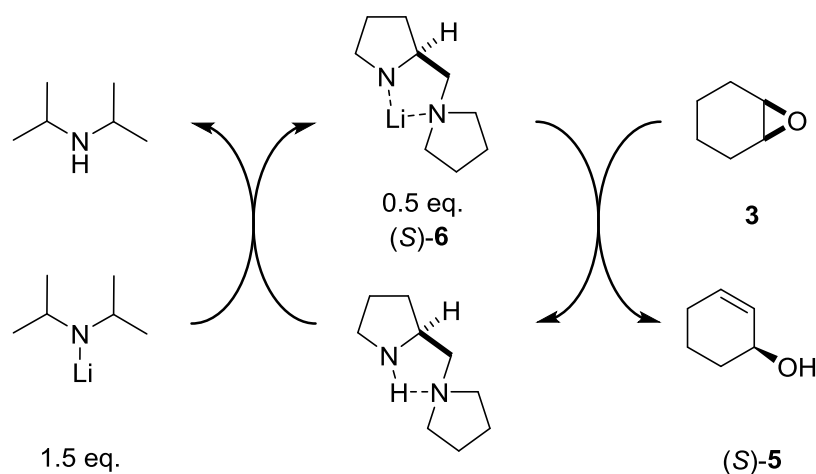
Despite the beneficial properties of catalytic transformations, enantioselective deprotonation protocols with a sub-stoichiometric amount of chiral bases are rarely reported in organic synthesis,⁵⁸ due to the complex catalytic cycle as shown in Scheme 2.28. The challenges with such protocols are the following. Firstly, the achiral base must be kinetically basic enough to mediate an efficient deprotonation, without playing the role of the base in the competitive stereorandom process. The former can be achieved, if the rate of the stereoselective deprotonation with the chiral amine is

higher than the rate of analogous nonstereoselective deprotonation with the achiral base ($k_B \gg k_C$). Furthermore, the regeneration of the sub-stoichiometric chiral base also has to be quicker than the subsequent deprotonation of the achiral or meso substrate ($k_A \gg k_C$). In addition, during the reaction the concentration of the achiral acid gradually increases, and can produce a series of different new supramolecular complexes. These aggregates can have a significant influence on the reaction outcome.



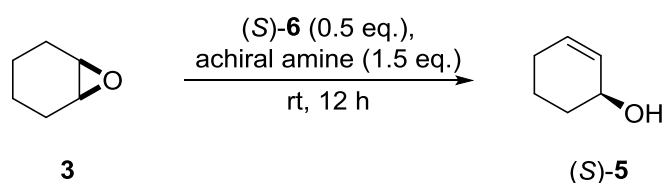
Scheme 2.28

Despite these issues, in 1994, Asami reported the first catalytic system for the enantioselective deprotonation of cyclohexene oxide **3** (Scheme 2.29).⁵⁹



Scheme 2.29

His research group investigated the effect of different parameters meticulously and demonstrated that the structure of the achiral lithium amide donor has a major impact on the reaction outcome (Scheme 2.30).



Scheme 2.30

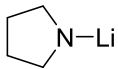
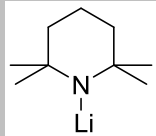
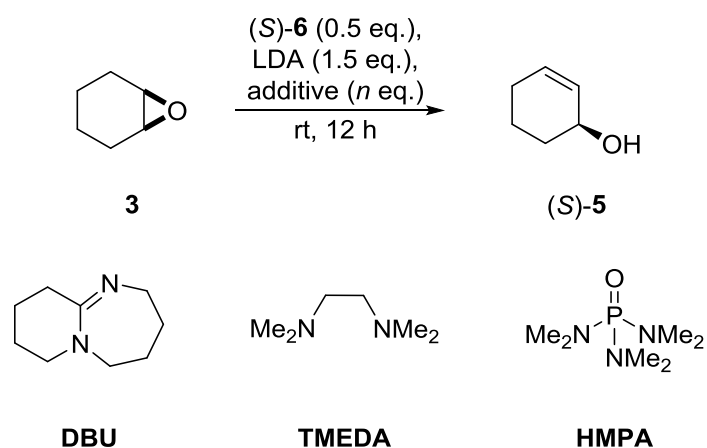
Entry	Achiral amine	% ee (% conv.)
1	LDA	48 (63)
2		37 (59)
3	Et ₂ NLi	37 (81)
4	(cyclohexyl) ₂ NLi	4 (38)
5		2 (72)

Table 2.16

The best enantioselectivity was obtained when lithium di-*iso*-propylamine was used as a stoichiometric donor (entry 1 in **Table 2.16**), because its sterically hindered nature possibly decreased the relative rate of the racemic deprotonation of the epoxide **3**. In contrast, low stereocontrol was observed with structurally similar and sterically less hindered secondary amides (*cf.* entry 1 with entries 2 and 3 in **Table 2.16**). Interestingly, highly encumbered achiral bases are provided the desired product **5** with a low enantiomeric ratio (entry 4 and 5 in **Table 2.16**). In addition, Asami also investigated the impact of different Lewis basic additives. In the absence of additive the product **5** was obtained with a good 63% conversion, but moderate 48% ee (entry 1 in **Table 2.17**). When the reaction was performed in the presence of 2 eq. DBU the yield and ee both increased to 61% and 71% respectively (entry 2 in **Table 2.17**). With higher amounts of DBU the yield and the ee was steadily increased (entries 3-5 in **Table 2.17**), while the highest selectivity and conversion (82% and 74% ee) was achieved with 10 eq. DBU (entry 5 in **Table 2.17**). In the presence of DBU and HMPA a similar ees and yields were observed in comparison with the additive free reaction (*cf.* entries 6 and 7 with entry 1 in **Table 2.17**).

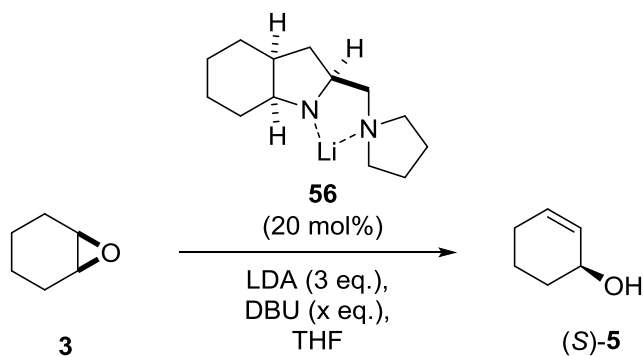


Scheme 2.31

Entry	Additive	Eq. of additive (<i>n</i>)	% ee (% conv.)
1	-	0	48 (63)
2	DBU	2	61 (71)
3	DBU	4	68 (79)
4	DBU	6	72 (81)
5	DBU	10	74 (82)
6	TMEDA	2	43 (67)
7	HMPA	2	54 (63)

Table 2.17

Additionally, an alternative amide **56** was tested in an attempt to further increase the yield in the deprotonation reaction of *meso*-cyclohexene oxide **3**.⁶⁰ In this case, the amount of DBU could be decreased from 0.20 eq. to 0.05 eq. without significant loss in the conversion (93-95%) although the ee slightly decreased from 88% to 85% (entries 1-3 **Scheme 2.32**). With lower amounts of DBU the ee and the yield decreased (entries 4 and 5 in **Scheme 2.32**).

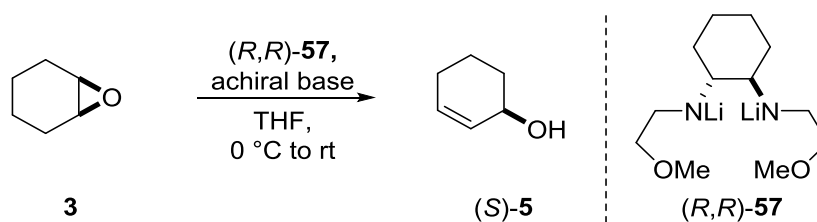


Scheme 2.32

Entry	DBU (eq.)	ee % (% conv.)
1	0.20	88 (95)
2	0.10	88 (93)
3	0.05	85 (93)
4	0.03	79 (92)
5	0.01	60 (74)

Table 2.18

Alexakis has investigated the application of a structurally more simple C_2 -symmetric diamide, (*R,R*)-**57**, as the source of asymmetric induction (Scheme 2.33).⁶¹ Despite the stoichiometric variant of this reaction providing a good conversion (68%) and ee 76 (entry 1 in Table 2.19), employing catalytic quantities of the chiral base resulted in lower reactivity 35-66% conversion and lower ees as compared to stoichiometric reaction (*cf.* entry 1 with entries 2-4 in Table 2.19). This was suggested to be caused by insufficient regeneration of the chiral base (*R,R*)-**189**.



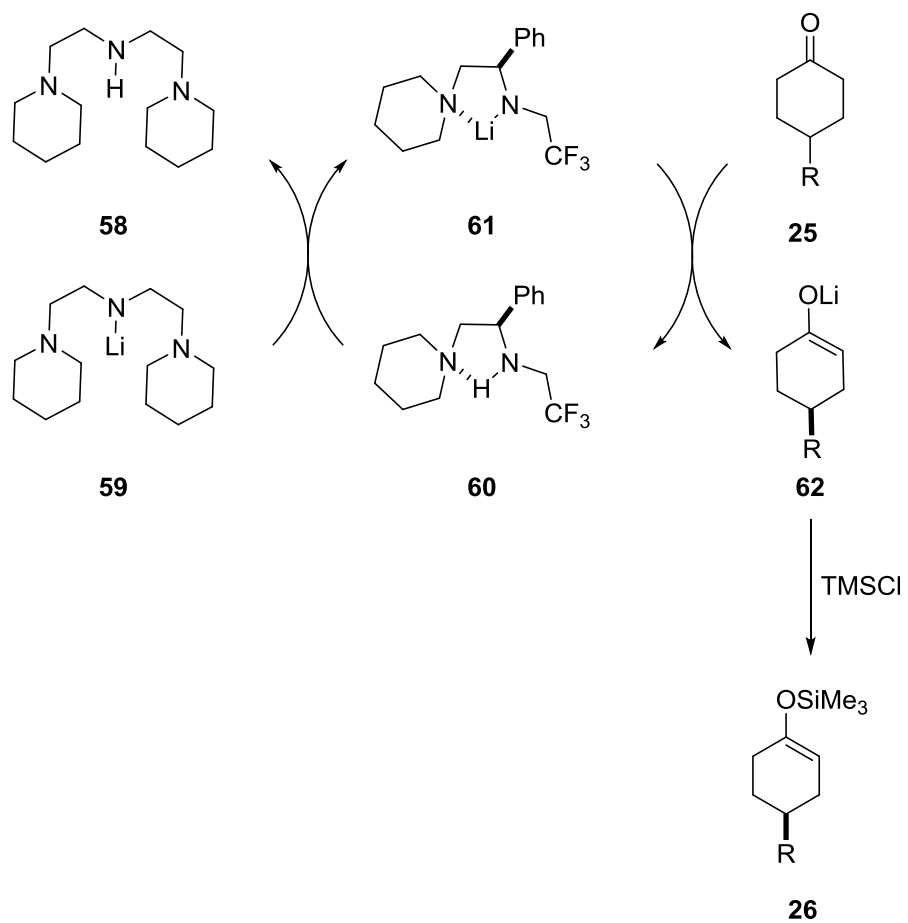
Scheme 2.33

Entry	(R,R) -189 (eq.)	Achiral base	Additive	ee % (conv. %)
1	1.0	-	-	76 (68)
2	0.2	n BuLi (1 eq.)*	-	67 (47)
3	0.2	LDA (1 eq.)	-	32 (66)
4	0.2	LDA (1 eq.)	DBU (6 eq.)	13 (35)

* Reaction was performed in benzene at 5 °C instead of 0°C then warmed to rt

Table 2.19

The catalytic asymmetric deprotonation of conformationally-locked ketones has been investigated by Koga using chiral base **61**.⁶² It was proposed that with a more hindered and more Lewis basic achiral amide, **59**, the competing unselective deprotonation could be suppressed, and, in addition, efficient recycling of the chiral amine could occur (**Scheme 2.34**). Indeed, a series of 4-substituted silyl enol ethers (R)-**26a-d** was generated in moderate to high enantiomeric excesses (ee 57-77%) and with good conversions 57-85% (**Table 3.19**). However, HMPA and DABCO were needed to achieve high levels of enantioselectivity and reactivity (*cf.* entry 5 with entries 1 and 7 in **Table 2.20**).



Scheme 2.34

Entry	Substrate (R group)	Chiral amine 192 (eq.)	Achiral amine 190 (eq.)	HMPA	DABCO	ee % (conv. %)
1	^t Bu (25a)	1.24	0.0	2.4	0.0	81% (85%)
2	Ph (25b)	1.24	0.0	2.4	0.0	80% (77%)
3	ⁱ Pr (25c)	1.24	0.0	2.4	0.0	79% (75%)
4	Me (25d)	1.24	0.0	2.4	0.0	78% (82%)
5	^t Bu (25a)	0.30	3.6	-	-	31% (57%)
6	^t Bu (25a)	0.30	2.4	2.4	0.0	70% (75%)
7	^t Bu (25a)	0.30	2.4	2.4	1.5	79% (83%)
8	Ph (25b)	0.30	2.4	2.4	1.5	76% (77%)
9	ⁱ Pr (25c)	0.30	2.4	2.4	1.5	76% (80%)
10	Me (25d)	0.30	2.4	2.4	1.5	75% (70%)

Table 2.20

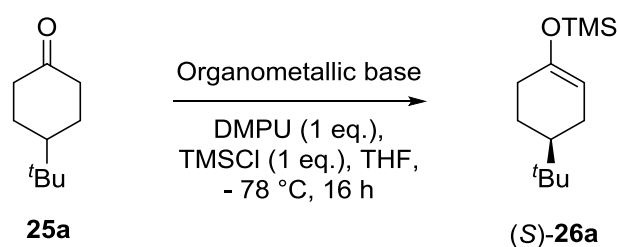
2.4 Summary

In the last 35 years a series of a series of lithium amide bases has been developed for the asymmetric functionalization of prochiral substrates. In this manner *meso*-epoxides, (η^6 -arene) chromium complexes and conformationally locked cyclic ketones have been successfully functionalised in a chiral manner. Although a series of chiral amines are reported the reactions are typically performed under cryogenic conditions to achieve high enantioselectivities. As a consequence often long reaction time required to achieve high conversion. In addition the complex aggregation state of lithium amide often hinders the application of protocol for novel substrates. Therefore chiral magnesium amides has been extensively studied to offer an alternative thermally more stable and less complex transformation of the synthesis of chiral enolates.

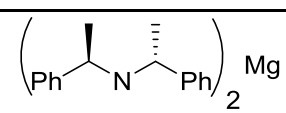
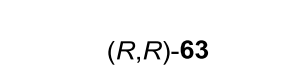
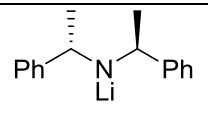

3 Magnesium Amide Bases

Although, chiral lithium amides are popular bases in organic synthesis,^{63–65} and have been used frequently to prepare enantiomerically-enriched products, the application of these reagents suffers from several drawbacks.⁶⁶ First and foremost, the nitrogen-lithium bond has a high ionic character,⁶⁷ which results in a low functional group tolerance. Moreover, to suppress by-product formation and increase enantioselectivity, the reactions often have to be performed at very low temperatures.^{63–65} Kerr proposed that the analogous magnesium bisamide complexes should overcome these difficulties, since these complexes have shown to be thermally stable and less ionic.⁶⁷ The main developments in relation to the desymmetrisation of conformationally locked cyclic ketones with magnesium amide bases, and the investigations into the structures of the bases themselves, will be summarised in the following sections.

Asymmetric deprotonation of a prochiral 4-substituted cyclohexanone with a chiral magnesium reagent, was reported for the first time with 4-*tert*-butylcyclohexanone **25a** by Kerr *et al.* (Scheme 3.1).³⁹



Scheme 3.1

Entry	Organometallic base	Temp. (°C)	Enantiomeric ratio (S):(R)	Conv. (%)
1		-78	94:6	97
2		0	86:14	93
3*		-78	85:15	62-89**
4*		0	76:24	62-89**

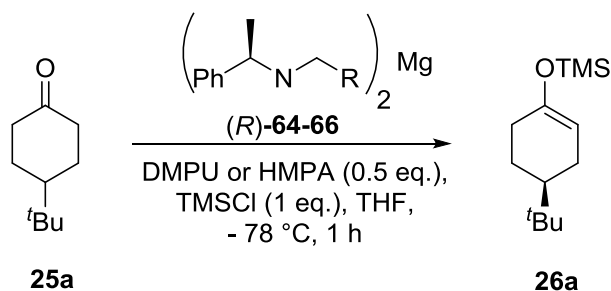
*: Reaction was carried out in the presence of 0.5 eq. LiCl instead of DMPU. **: Isolated yields were reported instead of conversion.

Table 3.1

Interestingly, when the reaction was performed with magnesium base (*R,R*)-**63** a higher enantioselectivity was observed at -78 °C, in comparison with the lithium analogue (*cf.* entries 1 and 3 in Table 4.1). In addition, with magnesium base (*R,R*)-**63** the enantiomeric ratio of the product (*S*-

26a at 0 °C was still high ((S):(R) = 86:14, entry 2 in **Table 4.1**), while with the analogous lithium base (*R,R*)-**4**, the enantiomeric ratio decreased to 76:24 (entry 4 in **Table 4.1**).

Additionally, in order to deaggregate higher lithium amide complexes, Lewis basic additive such as HMPA are commonly required,⁷⁻⁹ which, is a reagent with high toxicity. Kerr's research showed that in the asymmetric deprotonation of 4-*tert*-butylcyclohexanone **25a**, with a series of chiral magnesium amides, that toxic HMPA additive can be replaced by DMPU without any significant loss of enantioselectivity (**Table 3.2**).⁶⁸



Scheme 3.2

Entry	R group	Additive	Yield (%)	ee (%)
1	<i>i</i> Pr	HMPA	87	72:28
2	<i>i</i> Pr	DMPU	87	80:20
3	Vinyl	HMPA	80	82:18
4	Vinyl	DMPU	87	81:19
5	1-Naphthyl	HMPA	76	87:13
6	1-Naphthyl	DMPU	87	87:13

Table 3.2

In addition to the above described advantages of employing magnesium amide bases in this area of science, the less polar magnesium-nitrogen bond should tolerate more sensitive functional groups than the corresponding lithium amide species. Moreover, the divalent nature of magnesium permits the usage of a spectator ligand alongside a reactive one, i.e. using half the quantity of the precious chiral material relative to that required by the homochiral bisamide system.⁶⁶

In relation to the above, the structure of magnesium amides have been a recent focus of the Kerr research team and, indeed, form part of the work described in this thesis (*vide infra*). As such, the following sections introduce the varying structures of such species as well as detail recent efforts (from our laboratories and others) towards their application in deprotonation reactions.

4 Structure of Magnesium Amides

Magnesium amides are the most well studied organometallics within group 2. Indeed, a series of magnesium amide complexes have been reported and investigated by X-ray crystallography and NMR spectroscopy.⁶⁹ The structure of homo- and heteroleptic magnesium amide complexes shows a simple solution phase composition, where the magnesium atom is typically tetra coordinated and, depending on the nature of the ligands, exists as a monomer or a bridged dimer in solution (**Figure 5.1**).⁷¹

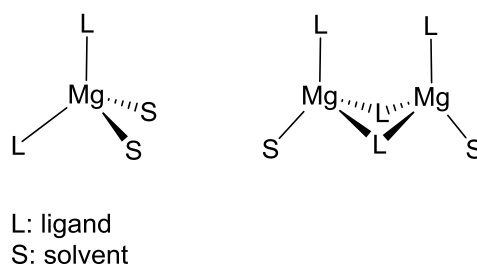
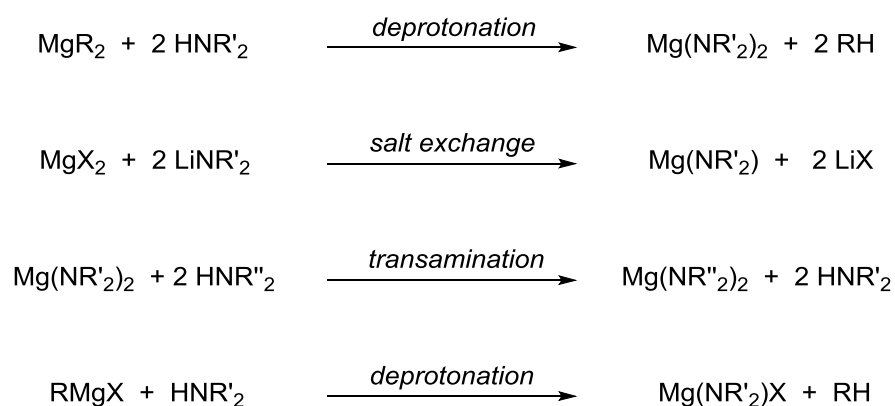


Figure 4.1

In comparison, the most frequently used lithium amides can form even higher aggregates, and generate a number of different supramolecular structures in solution.⁷¹ The individual contribution of the structurally different complexes to the observed selectivity and yield is unknown in most cases, therefore the application of structurally more simple organometallics reagents is highly desirable.

Magnesium amides can be synthesised by a number of different routes.^{66,69} The most frequently used is the deprotonation of an amine using a highly basic dialkylmagnesium species (**Scheme 4.1**). Additionally, salt exchange between a magnesium(II) halide and the lithium amide is also commonly used.⁷⁰ Finally, transamination reactions are also reported, and mixed magnesium amide complexes can be prepared in this way.⁷² If monoaminated complexes are required, the amine can be reacted with the Grignard analogue to generate what is commonly referred to as a Hauser base.



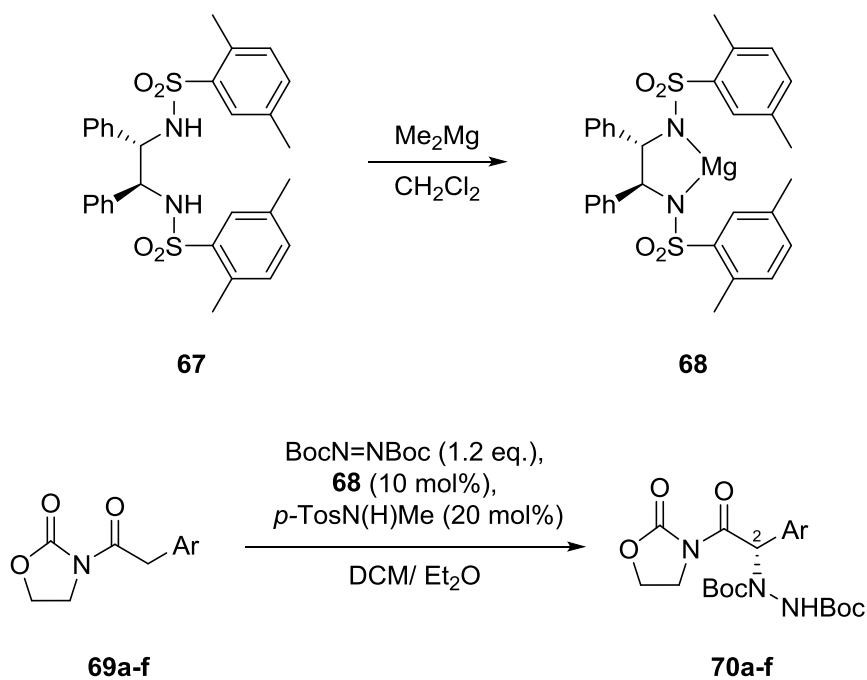
Scheme 4.1

The most simple bisamide species, magnesium dimethylamide, was obtained as an insoluble solid in the reaction of diethyl magnesium and dimethylamine, and a polymeric structure was suggested.⁷³ However, with bulkier ligands on the nitrogen atom ((R₂N)₂Mg, where R = phenyl⁷³, benzyl⁷⁴ and trimethylsilyl⁷⁵) dimeric structures were observed. The trimethylsilyl and benzyl analogues can be further deaggregated to obtain the monomeric species in the presence of several different Lewis bases, such as HMPA and pyridine.^{74,76} Overall, these results suggest that the aggregation state of magnesium in solution is predictable and reproducible. In addition, the position of the equilibrium between the monomeric and dimeric state can be readily tuned. In this sense, the amount and polarity of the solvent, as well as the stoichiometry and denticity of any Lewis base additive, are key parameters.

5 Homoleptic Magnesium Bisamide Complexes

5.1 Discovery and Substrate Scope

The first application of a chiral magnesium bisamide dates back to 1997 when Evans and Nelson demonstrated that such complexes can be used in sub-stoichiometric amounts in the enolisation and asymmetric amination of fused *N*-acyloxazolidinones **69a-f** as shown in **Scheme 5.1**.⁷⁷ Bismagnesium amide **68** was prepared in a simple fashion by reacting the parent amine **67** with bismethyl magnesium in dichloromethane. When the phenyl substituted substrate **69a** was used the desired **70a** product was obtained with a high yield (92%) and high e.r. (93:7) (entry 1 in **Table 5.1**). Importantly, the ee of the product **70a** could further be elevated by recrystallization. Electron withdrawing and electron donating substituents are both tolerated and the corresponding products **70b-c** were obtained with similarly high enantiomeric ratios ranging from 95:5 to 93:7, in excellent yields of 93%-97% (entries 2 and 3 in **Table 5.1**). Disubstituted aryl rings were also incorporated in the substrate structure and the products **70d-e** were obtained with a slightly lower enantiomeric ratios of 91:9 to 90:10, and still good yields (85% and 84%) (entries 4 and 5 in **Table 5.1**). Finally, the naphthyl substituted analogue **69f** was also delivered the desired product **70f** in a high 87% yield and excellent 91:9 e.r.



Scheme 5.1

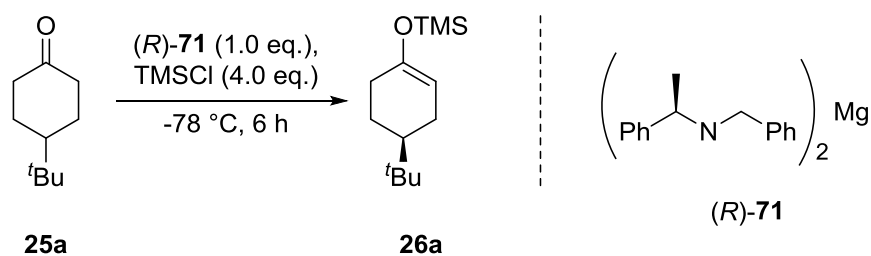
Entry	Product	Aryl group	Reaction time, h (temp. (°C))	e.r.(S):(R) (yield (%)) ^[*]	ee (%) ^[**]
1	70a	$\text{C}_6\text{H}_5\text{-}$	48 (-75)	93:7 (92)	>99
2	70b	$p\text{-F-C}_6\text{H}_4\text{-}$	48 (-65)	95:5 (97)	>99
3	70c	$p\text{-CH}_3\text{O-C}_6\text{H}_4\text{-}$	48 (-65)	93:7 (93)	99
4	70d		72 (-75)	91:9 (85)	>99
5	70e		60 (-75)	90:10 (84)	97
6	70f		48 (-65)	91:9 (87)	96

[*] Values reported are those for chromatographically purified hydrazides. [^{**}] Values reported are those for recrystallised hydrazides.

Table 5.1

Following this, little attention was focused on the enantioselective functionalisation of organic substrates by chiral magnesium amides until 2000, when Henderson and Kerr published the first enantioselective deprotonation of the conformationally locked ketone **25a**, using a novel homochiral magnesium bisamide (*R*)-**71** (Scheme 5.2).⁷⁸ The magnesium amide was first prepared by mixing 1 eq. of di-*n*-butyl magnesium and the corresponding amine, and thereafter the hexane solution was

refluxed for 90 min. Following the removal of the hexane solvent used to prepare the base (*R-71*), the deprotonation reaction was investigated taking consideration of the effect of different reaction solvents, and of the number of equivalents of additive required (**Scheme 5.2**). In the absence of HMPA in Et₂O was used as a solvent the desired silyl enol ether **26a** was not observed (entry 1 in **Table 5.2**). Although when 1 eq. HMPA was added the product was obtained with a good conversion (83%) and high e.r. (80:20) (entry 2 in **Table 5.2**). When the reaction was performed in DCM a lower conversion of 40% and e.r. 72:28 was detected. Interestingly, when THF was used a solvent the desired product **26a** could be obtained with a low conversion but excellent e.r. 90:10 (entry 4 in **Table 5.2**). When 1 eq. of HMPA was used as an additive in THF, the product **26a** was obtained with an excellent conversion 94% and similar e.r. of 86:14 (entry 5 in **Table 5.2**) in comparison to the additive free reaction (*cf.* entry 1 and entry 5 in **Table 5.2**). In the presence of the 2 eq. of the strongly coordinating HMPA additive, the reactivity dramatically decreased to 26% conversion but the product could be obtained with a similar e.r. 84:16 (entry 6 in **Table 5.2**) Interestingly, if the amount of the Lewis basic additive was decreased to 0.5 eq., the enantiomeric ratio increased to 91:9 (entry 7 in **Table 5.2**). Lower loading of HMPA decreased the conversion to 53% (entry 8 in **Table 5.2**). Most importantly, Kerr and his research group demonstrated again that high conversion of 89% and high enantiomeric ratio (90:10) could be achieved even in the absence of the toxic HMPA additive (entry 9 in **Table 5.2**).

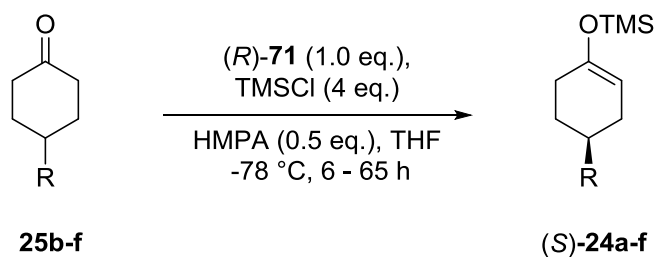


Scheme 5.2

Entry	Solvent	Additive (eq.)	Conversion (%)	e.r. (S):(R)
1	Et ₂ O	HMPA, 0.0	0	-
2	Et ₂ O	HMPA, 1.0	83	80:20
3	CH ₂ Cl ₂	HMPA, 1.0	40	72:28
4	THF	HMPA, 0.0	33	90:10
5	THF	HMPA, 1.0	94	86:14
6	THF	HMPA, 2.0	26	84:16
7	THF	HMPA, 0.5	82	91:9
8	THF	HMPA, 0.1	53	91:9
9	THF	DMPU, 0.5	89	90:10

Table 5.2

Kerr followed this optimisation with the disclosure that a range of 4-substituted analogues of type **25b-d** could be converted to the corresponding silyl enol ether products (**Table 6.3**).⁷⁸ The observed conversions 79-88% and enantiomeric ratios 87:13-95:5 were similarly high in all cases (entries 1-4 in **Table 5.3**).



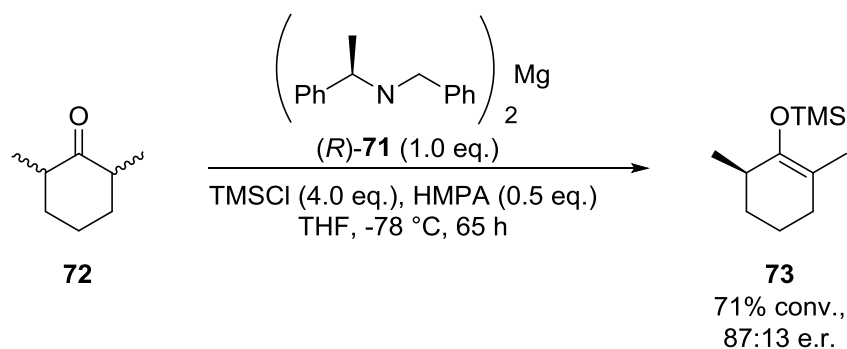
Scheme 5.3

Entry	R	Product	Conversion (%)	e.r. (S):(R)
1	Ph	(S)- 26b	79	87:13
2	<i>i</i> Pr	(S)- 26c	77	95:5
3	Me	(S)- 26d	81	91:9
4	<i>n</i> Pr	(S)- 26e	88	88:12

Table 5.3

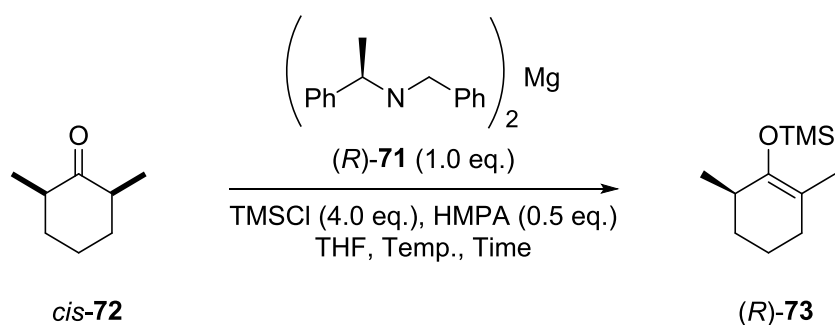
Although, the structure of the parent amine (*R*)-**71** was relatively simple, the synthetic utility of chiral magnesium bisamides was clearly highlighted in the generation of molecular asymmetry.

In 2001, Kerr et al. observed a kinetic resolution process with 2,6-disubstituted cyclohexanone **72** (Scheme 5.4).⁷⁹



Scheme 5.4

The diastereomeric mixture of 2,6-dimethylcyclohexanone **72**, present as an 82:18 ratio of *cis/trans* isomers was deprotonated by chiral amide base (*R*)-**71**. The silyl enol ether **73** was obtained with a 71 % conversion and in an 87:13 er. However, the unreacted *trans*-ketone **72** was also recovered, in an increased 74:26 ratio of enantiomers, which demonstrated the capability of the chiral base to mediate a kinetic resolution process. To further explore the potential of the reaction in a novel kinetic resolution processes, the *trans*- and *cis*-isomer of the 2,6-disubstituted ketone **72** was reacted with chiral base (*R*)-**71** individually.⁷⁹ With the *cis*-ketone **72**, the product, (*R*)-**73**, was formed with a 97:3 enantiomeric ratio, although the yield was moderate (25%) after 6 h (entry 1 in Table 5.4). The conversion towards the desired product (*R*)-**73** could be increased to 67% by extending the reaction time to 65 h (entry 2 in Table 5.4). The yield could also be increased to 67% conversion by performing the reaction at higher temperature -60 °C (entry 3 in Table 5.4) and the stereoselectivity reached comparable levels 94:6. A final boost in the conversion was also observed when the reaction was performed at -40 °C (entry 4 in Table 5.4) conversion (99%) with excellent 93:7 e.r.

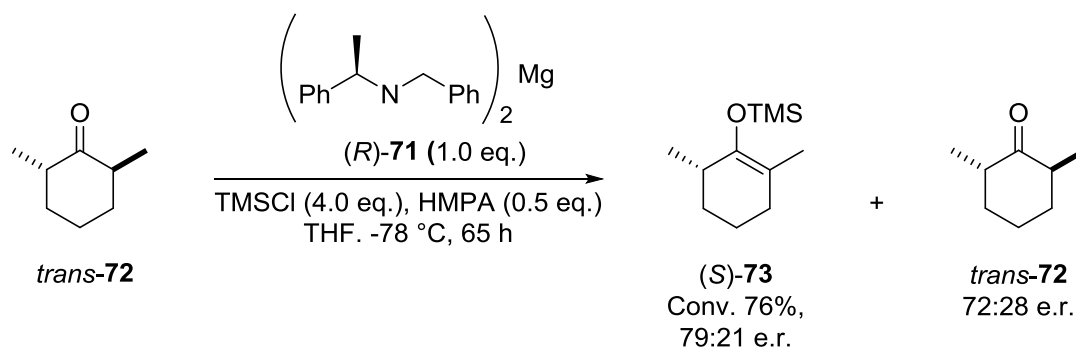


Scheme 5.5

Entry	Temp. (°C)	Reaction time (h)	Conversion (%)	e.r. (R):(S)
1	-78	6	25	97:3
2	-78	65	67	97:3
3	-60	6	67	94:6
4	-40	6	99	93:7

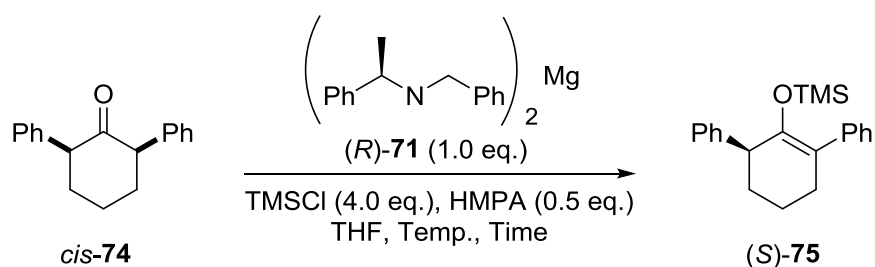
Table 5.4

When the reaction was performed with the racemic mixture of the *trans*-isomer, *trans*-**72**, the silyl enol ether (*S*)-**73** was obtained with good conversion 76%, and in high e.r. 79:21 (Scheme 5.6).⁷⁹ In parallel, the unreacted *trans*-ketone *trans*-**72** was returned in 72:28 e.r. The main component was identified as the (*R,R*)-enantiomer.



Scheme 5.6

In order to further explore the scope of this novel process, *cis*-**74** was also desymmetrised by chiral base (*R*)-**71**. The reaction with the 2,6-diphenyl substituted cyclohexanone *cis*-**74** produced the silyl enol ether (*S*)-**75** in a moderate yield and 87:13 enantiomeric ratio (entry 1 in Table 5.5).⁷⁹ Importantly, a similar level of enantiomeric induction was observed at the relatively elevated temperature of -40 °C 82:18 e.r., but the yield was significantly increased from 39% to 86% (entry 2 in Table 5.5).

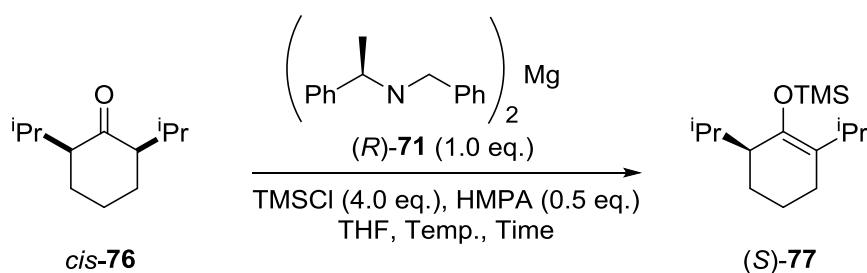


Scheme 5.7

Entry	Temp. (°C)	Reaction time (h)	Yield (%)	e.r. (R):(S)
1	-60	24	39	87:13
2	-40	8	86	82:18

Table 5.5

The same phenomenon was observed in the reaction of *cis*-2,6-di-*iso*-propylcyclohexanone, *cis*-**76** (Scheme 5.8). When the reaction was performed at -60 °C, the desired product *cis*-**77** was obtained with a good e.r. (99.4:0.6), but moderate conversion (66%) (entry 1 in Table 5.6). Increasing the temperature to obtain the desired product **77** with a similarly high e.r. (98.8:1.2) and excellent conversion of 99% (entry 2 in Table 5.6). Surprisingly, a remarkably high e.r. (91:9) was obtained even at room temperature (entry 3 in Table 5.6) only after 2 h, which highlights the advantageous thermal stability of the formed magnesium amide over the generally used lithium amides in asymmetric deprotonations.

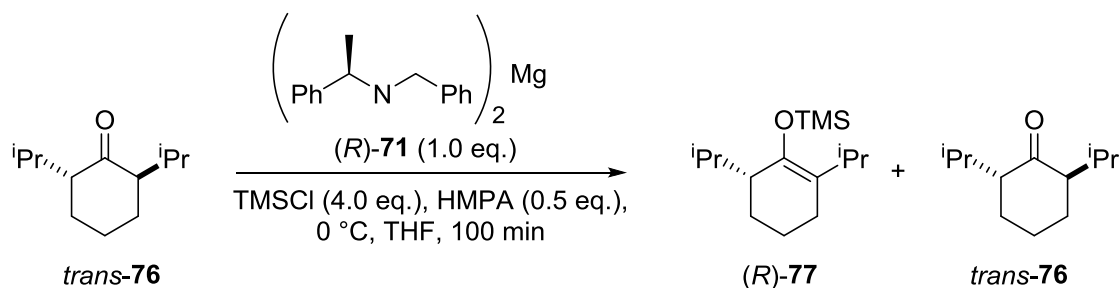


Scheme 5.8

Entry	Temp. (°C)	Reaction time (h)	Conversion (%)	e.r. (R):(S)
1	-60	6	66	99.4:0.6
2	-40	6	99	98.8:1.2
3	rt	2	99	91:9

Table 5.6

The *trans*-isomer of 2,6-di-*iso*-propylcyclohexanone, *trans*-76, was also exhibited similar behaviour. Whereby at -40 °C a relatively low but still good conversion 66% was observed with a good 81:19 e.r. (entry 1 in **Table 5.7**). Thereafter the reaction was performed at 0°C the product (*R*)-77 was obtained a similarly good conversion 59%, and with a slightly lower e.r. value of 76:24 (entry 2 in **Table 5.7**). Unfortunately, increasing the reaction time further decreased the e.r. of the product (*R*)-77 dramatically to 53:47 (entry 3 in **Table 5.7**).



Scheme 5.9

Entry	Temp. (°C)	Reaction time (h)	Conversion (%)	Product 77 e.r. (R):(S)	Recovered <i>trans</i> -76 e.r. (R):(S)
1	-40	67	66	81:19	94:6
2	0	1.66	59	76:24	80:20
3	0	19	>99	53:47	99:1

Table 5.7

5.2 Structural Development

Magnesium bisamides have shown a unique and exceptional stability and reactivity in asymmetric deprotonations. However, whilst developing the substrate scope, the demand for a comprehensive structure-reactivity study emerged. Systematic variation of the parent amine was proposed by alteration of the chiral and achiral side arms. Additionally, by analogy with lithium amides, the application of potentially chelating and C_2 -symmetric structures in asymmetric reactions were also investigated in our group.

5.2.1 Alteration of the Achiral and Chiral Sidearm

In order to further investigate the structure-reactivity relationship, the achiral sidearm of the parent amine was systematically varied. The prepared chiral amines (*R*)-**78**-(*R*)-**89** are outlined in **Figure 5.1**.⁸⁰

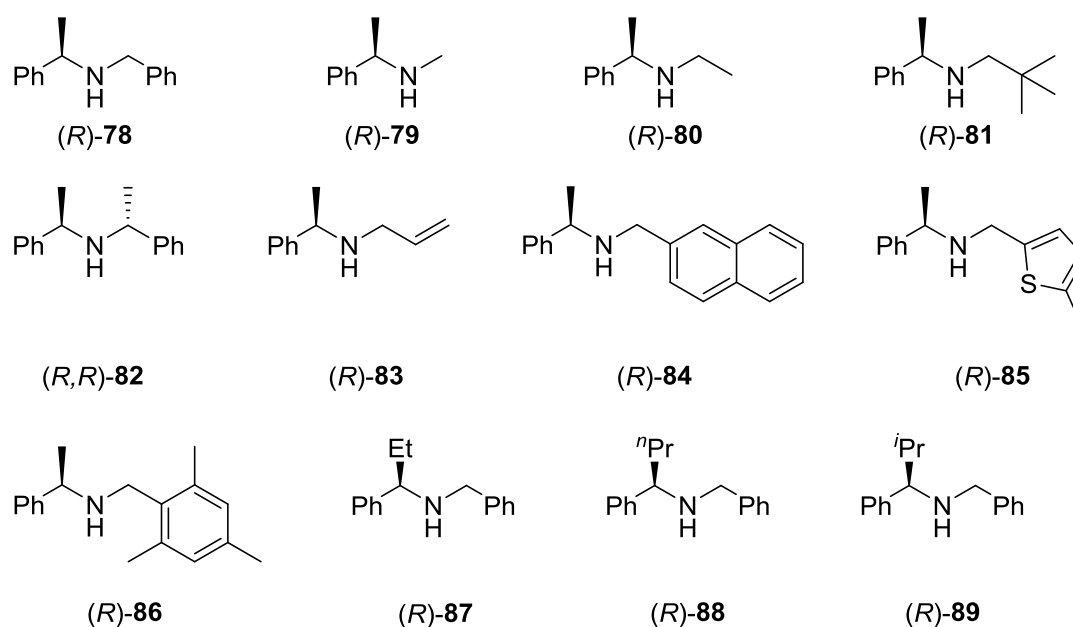
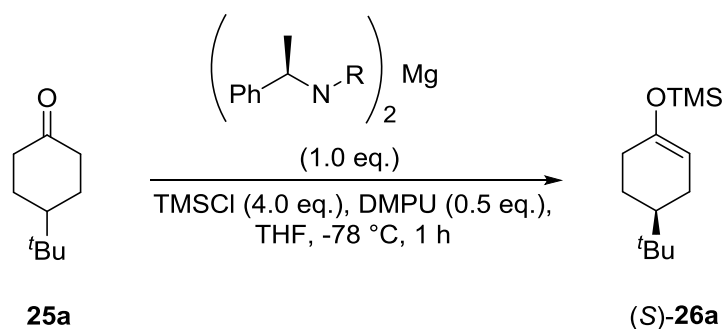


Figure 5.1

The results of the corresponding enantioselective deprotonation of 4-*tert*-butylcyclohexanone **25a** are summarised in **Scheme 5.10**.⁸⁰ Careful inspection of these results allowed the identification of general trends between the structure of the magnesium amide and the selectivity and reactivity. Firstly, with increasing size of the R substituent, the observed stereoselectivity gradually increased from 55:45-88:12 ((*R*)-**79**, (*R*)-**80** and (*R*)-**81** (entries 2-4 in **Table 5.8**). With the bulky neopentyl group (*R*)-**81**, the enantioselectivity obtained e.r. (88:12) was comparable with original amine (*R*)-**78** e.r. (90:10) (*cf.* entry 1 and 4 in **Table 5.8**). On the other hand, when amine (*R*)-**81** was used, the conversion toward the desired product (*S*)-**164a** significantly decreased to 17% (entry 4 in **Table 5.8**).

Other unsaturated systems were also investigated and in general, good conversions ranging between 83% and 97% were observed and similar selectivities of 80:20- 87:13 were obtained with amines (*R,R*)-**82**-(*R*)-**86** (entries 5-9 in **Table 5.8**). However, these compounds do not offer an increased selectivity in the asymmetric deprotonation of the benchmark conformationally locked ketone **25a** over the previously used magnesium bisamide (*R*)-**71** (entry 1 in **Table 5.8**) e.r. of 90:10 and 89% conversion.

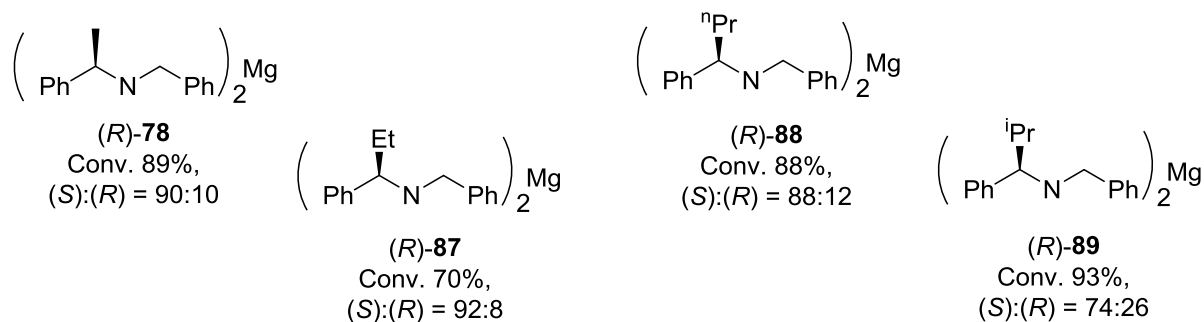
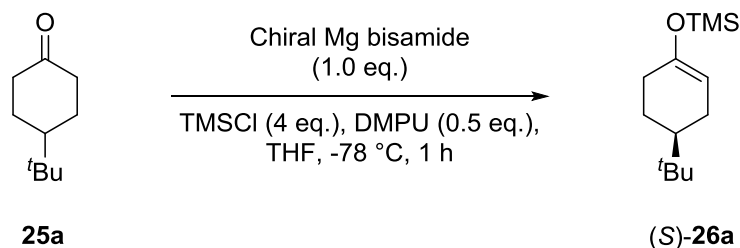


Scheme 5.10

Entry	Amine	R substituent	Conversion (%)	e.r. (S):(R)
1	(<i>R</i>)- 78	Bz	89	90:10
2	(<i>R</i>)- 79	Me	42	55:45
3	(<i>R</i>)- 80	Et	73	75:25
4	(<i>R</i>)- 81	Neopentyl	17	88:12
5	(<i>R,R</i>)- 82	CH*(Me)Ph	87	80:20
6	(<i>R</i>)- 83	Allyl	87	81:19
7	(<i>R</i>)- 84	CH ₂ (2-naphthyl)	87	87:13
8	(<i>R</i>)- 85	CH ₂ ((5-methyl)-2-thiophene)	83	87:13
9	(<i>R</i>)- 86	CH ₂ Mes	97	84:16

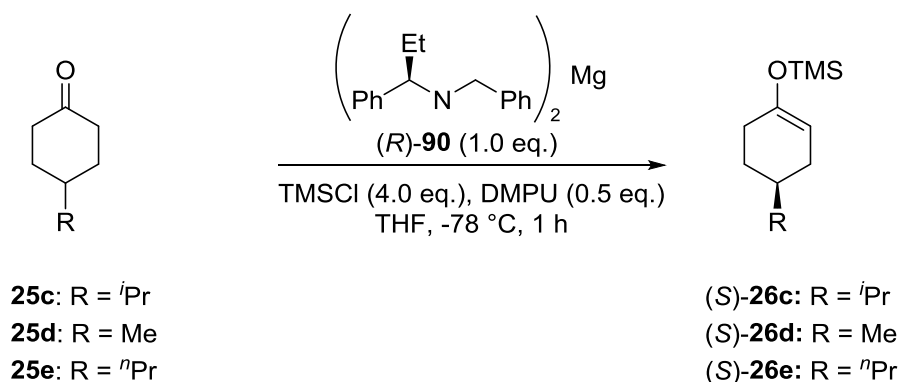
Table 5.8

Keeping these results in mind, a comprehensive investigation of the chiral sidearm was undertaken (**Scheme 5.11**).⁸¹ When the methyl group was replaced with a larger ethyl unit (*R*)-**87**, the selectivity was slightly increased from 90:10 to 92:8 and the conversion was slightly decreased to 70%. Interestingly, the sterically more encumbered amines were less effective in the desymmetrisation of ketone **25a**, the enantiomeric ratio of the product **26a** was decreased to 88:12 and 74:26 using (*R*)-**88** and (*R*)-**89**. Overall, the increasing size of the branching group at the α -position seems to have a negative effect on the selectivity of the process. In these cases, instead of HMPA the less toxic DMPU additive was used.



Scheme 5.11

To further extend the scope of this asymmetric deprotonation protocol, a series of 4-substituted ketones **25c-e** were deprotonated by **(R)-90**, which previously delivered the highest enantiomeric ratio in the asymmetric deprotonation of 4-*tert*-butylcyclohexanone **25a** (Scheme 5.12). Generally, moderate levels of conversion were achieved (53-68%), with excellent enantiomeric ratios (>90:10) (entries 1-3 in Table 5.9).



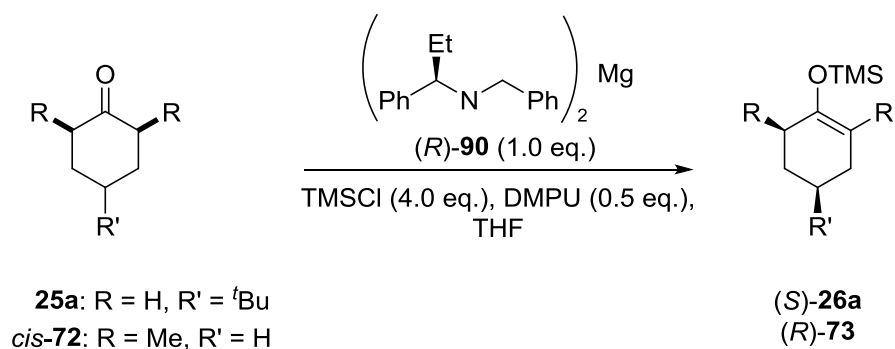
Scheme 5.12

Entry	R	Conversion (%)	e.r. (S):(R)
1	<i>i</i> Pr	53	95:5
2	Me	59	90:10
3	<i>n</i> Pr	65	91:9

Table 5.9

Thereafter, experiments were conducted at a higher temperature with homochiral magnesium amide base **(R)-90**, in order to investigate the effect of the reaction temperature on the process

(Scheme 5.13). Surprisingly, high levels of enantioselectivity were observed even at -40 °C with the 4-*tert*-butyl-substituted and *cis*-2,6-dimethylcyclohexanone *cis*-**210** e.r 80:20 and 87:13, respectively (entries 2 and 4 in Table 5.10) in comparison with the -78 °C reactions (entries 1 and 3 in Table 5.10).



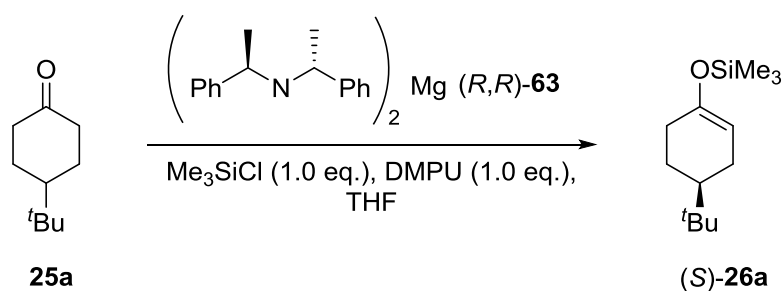
Scheme 5.13

Entry	Ketone	Temp (°C)	Conversion (%)	e.r.*
1	25a	-78	70	92:8
2	25a	-40	70	80:20
3	<i>cis</i> - 72	-78	57	96:4
4	<i>cis</i> - 72	-40	44	87:13

*: (S):(R) for entries 1-2 and (R):(S) for entries 3-4

Table 5.10

During the modification of the magnesium amide structure, it was observed that successful deprotonation of 4-substituted cyclohexanone derivatives **25** could be achieved at -40 °C. To further elevate the reaction temperature, and build a more economic and environmentally friendly protocol, new amines were tested in the asymmetric enolisation process of conformationally locked ketones, and a novel, more reactive and selective, C_2 -symmetric amine was reported by the Kerr group (Scheme 5.14).⁸² Amide (*R,R*)-**63** showed an unprecedented selectivities of 94:6-86:14 and high reactivity with conversions between 93% and 97% under a wide temperature range of -78 °C to 0°C in comparison (entries 1-5 in Table 5.11) with the previously reported systems. Even at 0 °C a high enantioselectivity of 86:14 was observed with an excellent conversion of 93% (entry 4 in Table 5.11.) In addition, at this temperature, the achieved enantioselectivity was comparable with the analogous lithium base at -78 °C (e.r. 85:15). In addition, only 1 eq. of DMPU additive and 1 eq. of trimethylsilyl chloride electrophile were used in the optimised system.

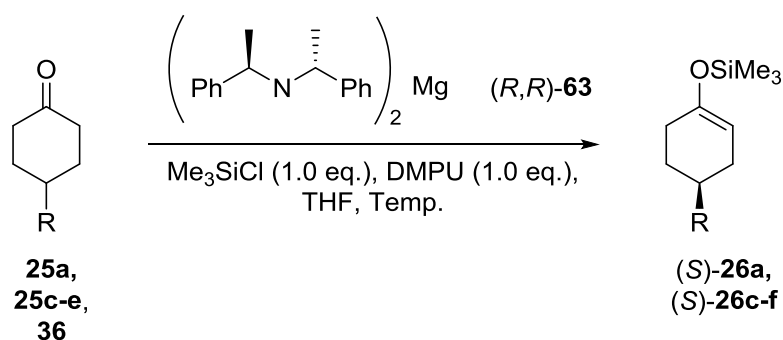


Scheme 5.14

Entry	Temp. (°C)	Conversion (%)	e.r. (S):(R)
1	-78	97	94:6
2	-60	93	92:2
3	-40	95	90:10
4	-20	97	88:12
5	0	93	86:14
6	23	89	75:25

Table 5.11

Encouraged by this initial result, the C_2 -symmetric magnesium bisamide complex (*R,R*)-**63** was used in the asymmetric deprotonation of a range of 4-substituted cyclohexanones **25a**, **25c-e** and **36** (Scheme 5.15). Kerr showed that excellent conversions of 91-96% and selectivities could be achieved in all tested substrates **25a**, **25c-e** and **36** (entries 1-5 in Table 5.12). Importantly, a protected alcohol **36** was tolerated under the applied conditions (entry 5 in Table 5.12) and the desired silyl enol ether **26f** was obtained with a high 91% conversion and excellent 92:8 e.r. The observed enantiomeric ratios (87:13-90:10) and yields were generally very high (92-96%) when the reactions were conducted at -20 °C (entries 6-10 in Table 5.12).



Scheme 5.15

Entry	R	Temp. (°C)	Yield ^[*] (%)	e.r. (S):(R)
1	^t Bu	-78	93 (66)	93:7
2	ⁱ Pr	-78	96 (67)	93:7
2	Me	-78	96 (69)	95:5
4	ⁿ Pr	-78	92 (65)	94:6
5	OTBDMS	-78	91 (68)	92:8
6	^t Bu	-20	93 (83)	88:12
7	ⁱ Pr	-20	95 (70)	87:13
8	Me	-20	96 (69)	90:10
9	ⁿ Pr	-20	96 (68)	89:11
10	OTBDMS	-20	92 (70)	87:13

[*] Isolated yield

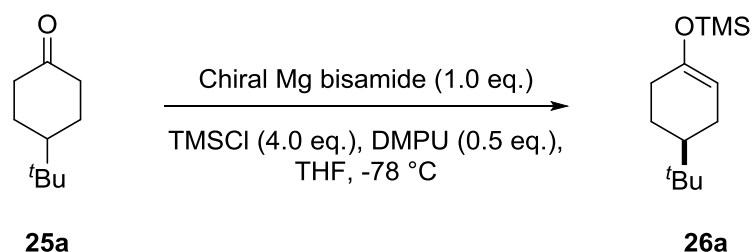
Table 5.12

In addition to the above, Kerr envisioned the synthesis of more sterically encumbered amines with the introduction of a second, potentially chelating heteroatom. It was anticipated that the interaction between the magnesium and the chiral ligand would be strengthened, allowing the reaction to be performed at higher temperatures with at least the same level of enantioselectivity.

5.2.2 Chelating Amine Ligands

As such, a more comprehensive library of suitable amine candidates was constructed through the preparation of 2-pyridyl (*R*)-**91**, 2-furyl (*S*)-**92**, 2-pyrrolyl (*S*)-**93** and 2-thiophenyl (*S*)-**94** analogues.⁸³ Moreover, a second series of saturated, chelating amines with an elongated linkage between the basic nitrogen and the second chelating atom were synthesised; (*R*)-**95**–(*R*)-**97**. Evaluation of these amines was performed in the benchmark deprotonation of 4-*tert*-butylcyclohexanone **25a** (Table 5.13).⁸³ Unfortunately, unsaturated heterocycles with a nitrogen or oxygen heteroatom did not offer any improvement neither in the conversion nor in the enantioselectivity in this benchmark deprotonation (entries 1-3 in Table 5.13). However when

thiophene was incorporated in the structure the the desired product **26a** was obtained with a good conversion (83%) and high e.r. (14:86) favouring the (*R*)-product (*R*)-**26a** (entry 4 in **Table 5.13**). Bases with 6-membered saturated heterocycles (*R*)-**95**-(*R*)-**97** were also tested, unfortunately they showed low stereoselectivities (50:50-51:49) in the asymmetric formation of silyl enol ether **26a**, and moderate to good conversions of 43-79% (entries 5-7 in **Table 5.13**).



Scheme 5.16

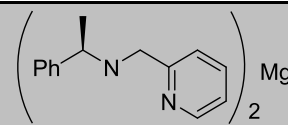
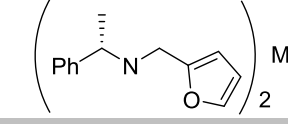
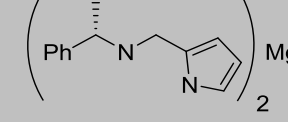
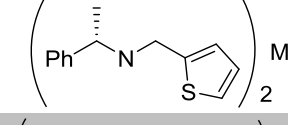
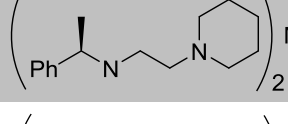
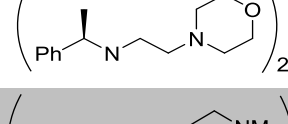
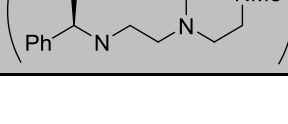
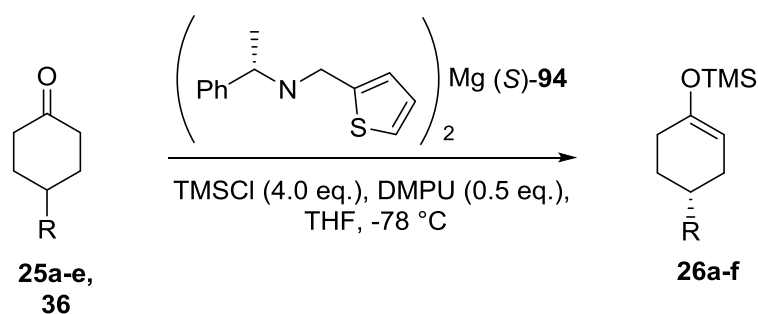
Entry	Mg bisamide	Conversion (%)	e.r. (<i>S</i>):(<i>R</i>)
1	 (<i>R</i>)-91	12	49:51
2	 (<i>S</i>)-92	19	42:58
3	 (<i>S</i>)-93	1	24:76
4	 (<i>S</i>)-94	83	14:86
5	 (<i>R</i>)-95	43	50:50
6	 (<i>R</i>)-96	64	50:50
7	 (<i>R</i>)-97	79	51:49

Table 5.13

As such, the activity of the magnesium bisamide (*S*)-**94** was tested against a range of different 4-substituted conformationally locked ketones **25b-e** and **36**. As such, a series of 4-alkyl substituted cyclohexanones **25a** and **25c-e** was used as a substrate and the desired (*S*)-enantiomers of the silyl enol ethers **26a-f** were generated in moderate to good yields (68-83%) and with similar enantiomeric

ratios (83:17-87:13) (entries 1-5 in **Table 5.14**). In addition, a silyl protected alcohol **36** was also desymmetrised with this novel magnesium amide (*S*)-**94** and the desired product (*S*)-**26f** was obtained with an a good conversion of 71% and good e.r. of 84:16 (entry 6 in **Table 5.14**).



Scheme 5.17

Entry	R	Conversion ^[*] (%)	e.r. (<i>S</i>):(<i>R</i>)
1	^t Bu	83 (75)	86:14
2	Ph	68 (49)	85:15
3	ⁱ Pr	73 (55)	87:13
4	Me	75 (62)	86:14
5	ⁿ Pr	72 (55)	83:17
6	OTBDMS	71 (55)	84:16

[*] Isolated yields in bracket

Table 5.14

In a further effort to probe the chiral amine structure, Kerr incorporated a second chiral centre within a series of new chelating amine bases. Six chiral bisamides, (*R,R*)-**98**, (*R,R*)-**99**, (*R,R*)-**100**, (*S,R*)-**98**, (*S,R*)-**99** and (*S,R*)-**100**, were prepared in this way (**Figure 5.2**).⁸⁴

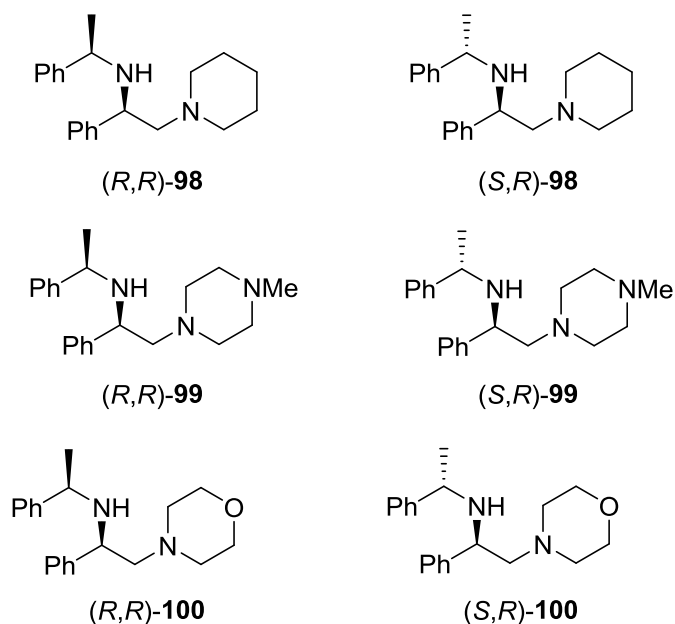
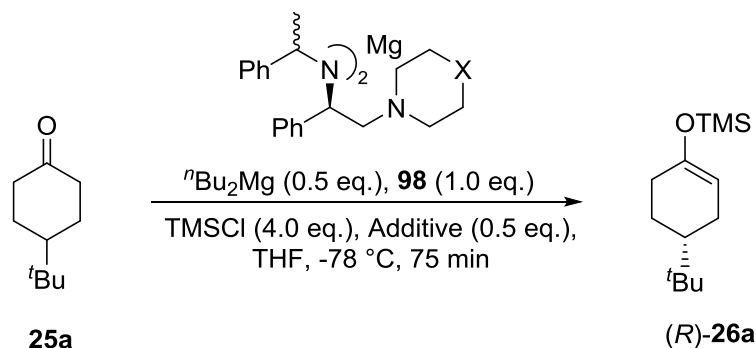


Figure 5.2

Firstly, amine **98** was used in the asymmetric deprotonation of 4-*tert*-butylcyclohexanone **25a**. The reaction was carried out with both diastereomers of amine **98** to determine the role of the second chiral centre in this asymmetric process (Scheme 5.18). Overall, high enantioselectivities of 93:7 and 88:12 were observed with excellent conversions of 90% and 88% for the asymmetric deprotonation of 4-*tert*-butylcyclohexanone **25a** (entries 1 and 2 in Table 5.15) after only 75 min. Although it was noted that the configuration of the second chiral centre has only a small influence on the selectivity of the reaction (*cf.* entry 1 and 2 in Table 5.15). Notably, indetically high enantiomeric ratios between 93:7 and 88:12 were observed even in the absence of Lewis basic additives with both bases (entries 3 and 4 in Table 5.15) in comparison with the reactions when DMPU was used as an additive, indicating that in the presence of a second chiral centre the Lewis basic additive is not a necessity to achieve good enantioselectivities.

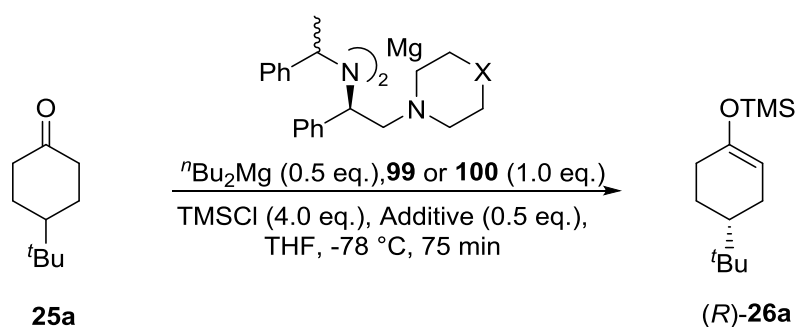


Scheme 5.18

Entry	Mg-amide	Additive	Conversion (%)	e.r. (R):(S)
1	(<i>R,R</i>)- 98	DMPU	90	93:7
2	(<i>S,R</i>)- 98	DMPU	88	88:12
3	(<i>R,R</i>)- 98	None	58	93:7
4	(<i>S,R</i>)- 98	None	87	88:12

Table 5.15

In addition to the above, two complexes **99** and **100** with a third chelating heteroatom were tested in the asymmetric deprotonation of substrate **25a**. The results are summarised in **Table 6.15**.⁸⁴ With the *N*-methylpiperazine analogue **99**, good enantioselectivities were achieved (92:8) with high conversions of 94% and 92% with both diastereomeric base (*R,R*)-**99** and (*S,R*)-**99** (entries 1 and 2 in **Table 5.16**). Interestingly when base (*R,R*)-**99** was used a high e.r. was observed even in the absence of DMPU (91:9) with a good conversion of 88% (entry 5 in **Table 5.16**). However in order to obtain high conversion, addition of DMPU was necessary for (*S,R*)-**99** (cf. entries 2 and 6 in **Table 5.16**). Similar trends were observed with the morpholine amide **100**. In the presence of DMPU the reaction afforded the desired chiral silyl enol ether **26a** with a good conversions of 88% and 83% and high e.r. values from 88:12 to 89:11 (entries 3 and 4 in **Table 5.16**). Again in the absence of DMPU base (*R,R*)-**242** afforded the desired product **26a** was obtained with similarly high conversion (86%) and e.r. (90:10) in comparison with the DMPU protocol (cf. entries 4 and 7 in **Table 5.16**). On the other hand, in the case of the diastereomeric (*S,R*)-base (*S,R*)-**100**, DMPU was required to achieve high conversion, as in the absence the product was detected with a decreased 55% conversion (entry 8 in **Table 5.16**). Overall these results also indicate that the second chiral centre has a minor impact on the enantioselectivity of the process (cf. even and odd entries in **Table 5.16**).

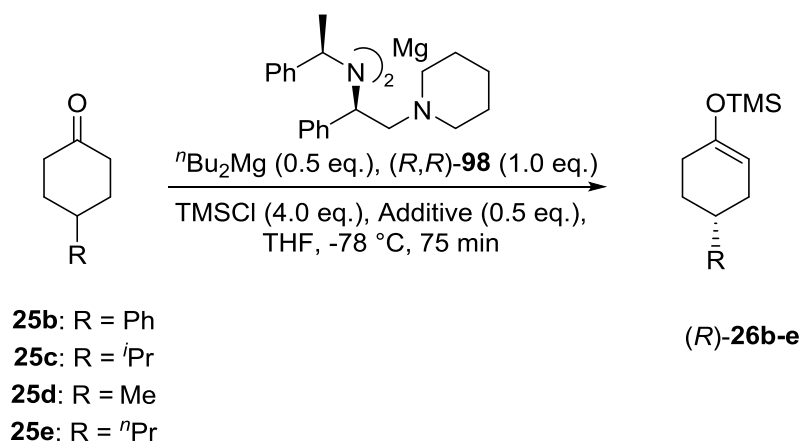


Scheme 5.19

Entry	Amine	X	Additive	Conversion (%)	e.r. (R):(S)
1	(R,R)-99	NMe	DMPU	94	92:8
2	(S,R)-99	NMe	DMPU	92	92:8
3	(R,R)-100	O	DMPU	96	88:12
4	(S,R)-100	O	DMPU	83	89:11
5	(R,R)-99	NMe	None	88	91:9
6	(S,R)-99	NMe	None	59	87:13
7	(R,R)-100	O	None	86	90:10
8	(S,R)-100	O	None	55	89:11

Table 5.16

Finally, using the best performing chelating amine (R,R)-98, the substrate scope of the asymmetric deprotonation was investigated with a series of 4-substituted cyclohexanones **25b-e** (Scheme 5.20). In general the desired silyl enol ethers **26b-e** were obtained with good to excellent 89-97% conversion and high e.r. values between 92:8 and 94:6 (entries 1-4 in Table 5.17). In the absence of DMPU similarly high e.r. were observed (93:7-94:6) but the conversion decreased to 60-78% in every case (entries 5-8 in Table 5.17)



Scheme 5.20

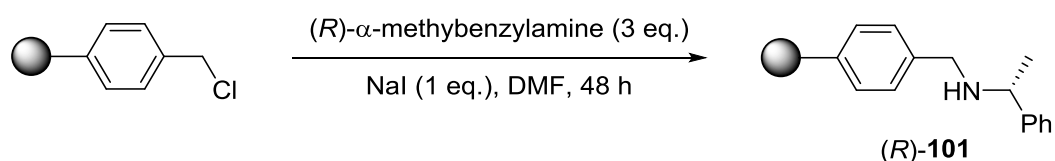
Entry	R	Additive	Conversion (%)	e.r. (R):(S)
1	Ph	DMPU	91	94:6
2	<i>i</i> Pr	DMPU	97	94:6
3	Me	DMPU	89	92:8
4	<i>n</i> Pr	DMPU	93	94:6
5	Ph	None	60	94:6
6	<i>i</i> Pr	None	78	94:6
7	Me	None	67	93:7
8	<i>n</i> Pr	None	76	94:6

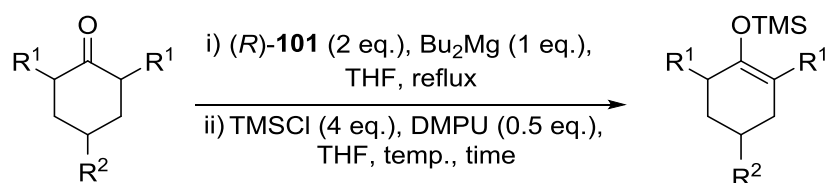
Table 5.17

During Kerr's development of the chiral amine structure, connection of the chiral amine to a polymer matrix was envisioned to develop a more user friendly asymmetric deprotonation protocol with a shorter work up.

5.2.3 Polymer-supported Magnesium Bisamides

A process with a polymer supported chiral base would be beneficial, since the expensive chiral reagent could be easily recovered with a simple filtration and therefore decrease the time required for the work up and purification, in addition in theory the base could be reused in further cycles. In 2001, Kerr demonstrated the asymmetric deprotonation of conformationally locked ketones is a viable and efficient transformation with polymer-supported magnesium bisamide.⁸⁵ In this regard, the chiral amine was attached to the Merrifield resin to give polymer-bound amine (*R*)-**101** and the desymmetrisation of several different cyclohexanone analogues was explored (**Scheme 5.21**). When 4-substituted cyclohexanones **25** were used the desired products **26** were observed with a lower e.r. 68:32-74:26 and good conversions of 74-89% (entries 1-5 in **Table 5.18**). In comparison with the homogenous reaction (**Table 5.3**). The conversion could be increased to 91% with the increase of the reaction temperature to rt, but the e.r. significantly decreased to 65:35 (*cf* entry 1 with entry 2 in **Table 5.18**). In addition 2,6-disubstituted cyclohexanones **72** and **76** were also used as substrate and at -78 °C a low conversions of 7% and 2% towards the desired silyl enol ether products **73** and **77** were detected (entries 6 and 9 in **Table 5.18**). Although by increasing the temperature to -40 °C high conversions were observed (86% and 69%) with good e.r. (73:27 and 91:9) (entries 7 and 10 in **Table 5.18**). The conversion could further improved to excellent levels by increasing the temperature to rt and interestingly slightly higher e.r. values of 75:25 and 93:7 were observed in these cases (entries 8 and 11 in **Table 5.18**). Overall, the polymer-supported protocol allowed for high conversions with temperatures up to room temperature being viable. Having said this, attachment to the Merrifield resin significantly eroded the enantioselectivity of the overall transformation, with the exception of 2,6-diisopropylcyclohexan-1-one substrate *cis*-**76**.



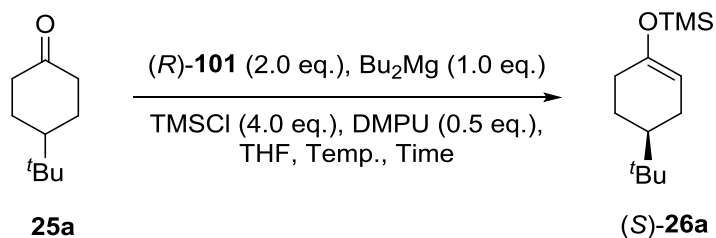


Scheme 5.21

Entry	Substrate	R ¹	R ²	Temp. (°C)	Time (h)	Conversion (%)	e.r. (S):(R)
1	25a	H	^t Bu	-78	4	78	74:26
2				rt	2	91	65:35
3				-78	4	89	68:32
4				-78	4	85	74:26
5				-78	4	74	68:32
6	cis-72	Me	H	-78	43	7	76:24
7				-40	24	86	73:27
8	cis-76	ⁱ Pr	H	rt	2	98	75:25
9				-78	19	2	-
10				-40	68	69	91:9
11	cis-76	ⁱ Pr	H	rt	2	97	93:7

Table 5.18

Nonetheless, Kerr and his research group also demonstrated that the chiral amine could be recycled up to 5 times without any detectable decrease in the e.r. of the product **26a** (entries 1-5 in Table 5.19) and they also demonstrated that the resin can be reused at even -78 °C.

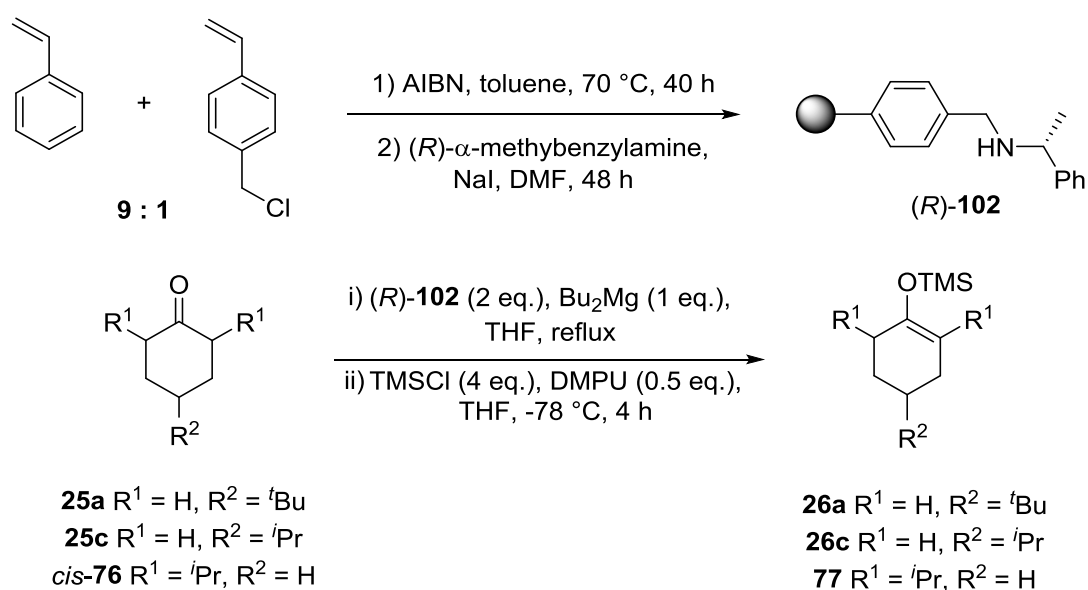


Scheme 5.22

Cycle	Temp. (°C)	Time (h)	Conversion (%)	e.r. (S):(R)
1	rt	2	91	65:35
2	rt	2	97	65:35
3	rt	2	86	65:35
4	rt	2	91	66:34
5	rt	2	92	66:34
6	-78	4	71	73:27

Table 5.19

Further developments by Kerr in this area showed that by using an alternative soluble polystyrene-based resin⁸⁶ for the preparation of the solid supported chiral amine (*R*)-**102**. When this reagent was used for asymmetric deprotonation of 4-substituted-cyclohexanones **25a** and **25c** the desired products **26a** and **26c** were obtained with good e.r. (83:17 and 80:20) and good to high conversion of 91% and 82% (entries 1 and 3 in **Table 5.20**). The conversion towards the desired products **26a** and **26e** could be further improved to excellent levels (99% and 96%) by performing the reaction at higher temperature, although the e.r. slightly decreased to 70:30 and 71:29 (entries 2 and 4 in **Table 5.20**). When the 2,6-disubstituted substrate *cis*-**76** was used identical e.r. ratios was detected even at rt in comparison with the -78 °C reaction (e.r. 93:7) and the product **77** was obtained with an almost quantitative conversion (entries 5-6 in **Table 5.20**).



Scheme 5.23

Entry	Ketone	Product	Temp. (°C)	Time (h)	Conversion (%)	e.r. (<i>S</i>):(<i>R</i>)
1	25a	(<i>S</i>)- 26a	-78	4	91	83:17
2	25a	(<i>S</i>)- 26a	rt	2	99	70:30
3	25c	(<i>S</i>)- 26c	-78	4	82	80:20
4	25c	(<i>S</i>)- 26c	rt	2	96	71:29
5	<i>cis</i> - 76	(<i>S</i>)- 77	-78	24	67	93:7
6	<i>cis</i> - 76	(<i>S</i>)- 77	rt	2	99	93:7

Table 5.20

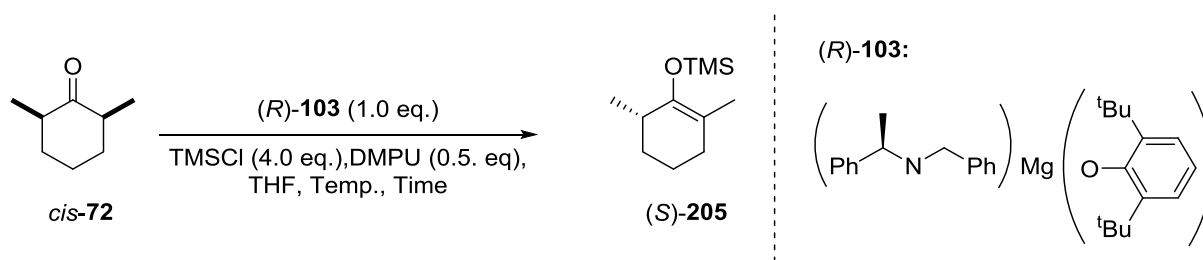
6 Heteroleptic Magnesium Amides

6.1 Advantages

The magnesium species described until this stage have been complexes bearing two identical amide ligands, i.e. homoleptic reagents. Indeed, the bivalent nature of magnesium theoretically allows the enantioselective functionalisation to be carried out using a reagent bearing only one chiral ligand and one spectator ligand, therefore there is the potential to use half of the quantity of precious chiral amine relative to that required by the homochiral bisamide system. Moreover, the modification of the spectator ligand would allow the overall reactivity of the corresponding heteroleptic magnesium amide to be fine-tuned. Accordingly, several heteroleptic magnesium complexes, such as, aryloxy^{-87,88} and alkylmagnesium amides⁸⁹ have been synthesised and compared in the benchmark deprotonation reaction of 4-*tert*-butyl-cyclohexanone **25a**.

6.2 Aryloxymagnesium Amides

In parallel with the application of novel homoleptic chiral magnesium amides in asymmetric synthesis, Kerr targeted a relatively simple heteroleptic complex bearing the electron rich 2,6-di-*tert*-butylphenolate structure as a spectator ligand in order to increase the overall stability of the heteroleptic magnesium base (*R*)-**103** (Scheme 6.1).⁹⁰ The use of this base revealed an unusual reactivity/selectivity profile. The results with (*R*)-**103** were disappointing at -78 °C, a low e.r. of 46:54 and good conversion of 78% was obtained (entry 1 in Table 6.1) in comparison with the benchmark deprotonation of 4-*tert*-butylcyclohexanone **25a** (entry 9 in Scheme 5.2). The novel heteroleptic base (*R*)-**103** afforded the desired silyl enol ether product **73** analogue in higher temperatures with a significantly higher e.r. (entries 2-4 in Table 6.1). The best result was achieved at room temperature, where a 62% conversion and 78:22 enantiomeric ratio was obtained (entry 3 in Table 7.1). At 40°C the product **73** was obtained with a good e.r. (83: 17) (entry 4 in Table 6.1), although the conversion was low (33%). Reactions at higher temperature afforded the desired product **73** with significantly lower e.r.values of 76:24 at 50°C and 67:33 at 66 °C (entries 5 and 6 in Scheme 6.1). It was also interesting to note that the absolute configuration of the major product, (*S*)-**73**, was the opposite to the corresponding bisamide reaction. This suggests that final stereochemical induction is not purely controlled by the amide ligand itself but, in fact, directed by the overall chiral environment within the magnesium base complex.

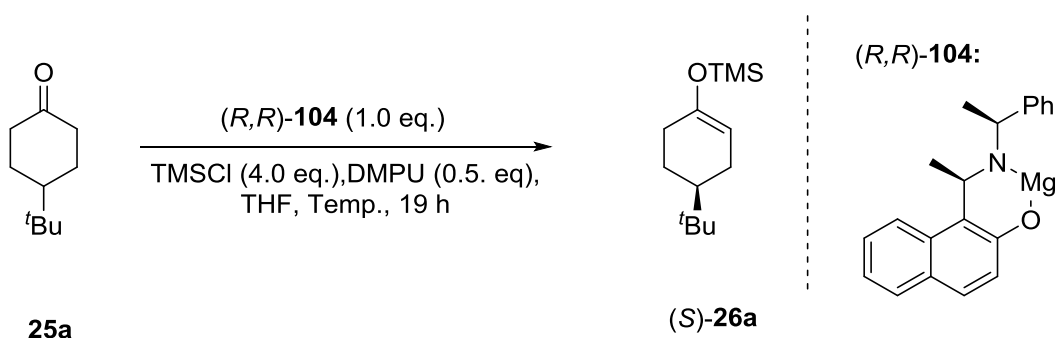


Scheme 6.1

Entry	Temp. (°C)	Time (h)	Conversion (%)	e.r. (<i>R</i>):(<i>S</i>)
1	-78	68	78	46:54
2	-40	68	54	76:24
3	rt	19	62	78:22
4	40	1	33	83:17
5	50	1	46	76:24
6	66	1	11	67:33

Table 6.1

In addition to these results, further stabilisation of the corresponding magnesium amide was envisioned with the implementation of a second donating atom. Kerr anticipated that the use of amino alcohols, which when derivatised to the magnesium complex, would generate a conformationally rigid metallocycle that may deliver modified selectivity profiles and potentially enable effective asymmetric induction at more accessible reaction temperatures. A temperature study in the asymmetric deprotonation of 4-*tert*-butylcyclohexanone **25a** revealed that comparable levels of enantioselectivities of 89:11-81:19 are achievable in a temperature range between -78 and -20 °C with steadily increasing conversion values from 13% to 89% (entries 1-4 in **Table 6.2**). At 0 °C the product **26a** could be also obtained with a relatively good conversion (69%) but lower e.r. of 71:29 (entry 5 in **Table 6.2**).

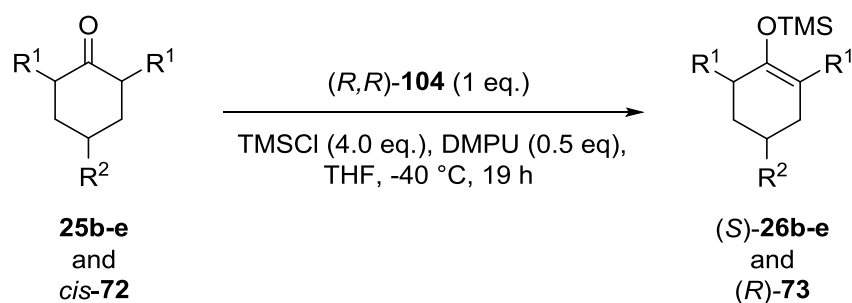


Scheme 6.2

Entry	Temp. (°C)	Conv. (%)	e.r. (S):(R)
1	-78	13	89:11
2	-60	77	85:15
3	-40	87	84:16
4	-20	89	81:19
5	0	69	71:29

Table 6.2

After optimisation, the generality of the process was also studied with several differently-substituted cyclohexanone analogues as shown in **Table 6.3**.⁸⁸ A series of 4-alkyl substituted cyclohexanones **25b-e** were desymmetrised with this protocol effectively at -40 °C to generate the corresponding chiral silyl enol ethers with good to excellent conversions of 89-90% and similarly good e. r. ranging from 78:22 to 84:16 (entries 1-3 in **Table 6.3**). The phenyl substituted cyclohexanone **25b** also afforded the desired product **26b** with a slightly lower e.r. (74:26) and good conversion of 81% (entry 4 in **Table 6.3**). Interestingly, the desymmetrization of a 2,6-di-methylcyclohexanone *cis*-**72** also delivered the desired product **73** with high e.r. (87:13), but moderate conversion of 56% (entry 5 in **Table 6.3**).



Scheme 6.3

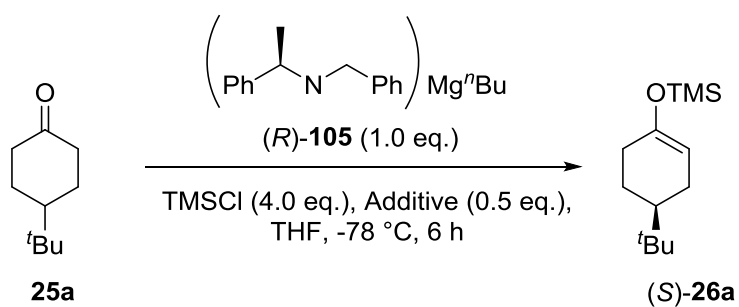
Entry	Product	R ¹	R ²	Conversion (%) ^[*]	e.r. (S):(R)
1	(S)- 26b	H	Ph	81 (71)	74:26
2	(S)- 26d	H	Me	87 (47)	78:22
3	(S)- 26e	H	ⁿ Pr	90 (79)	82:18
4	(R)- 73	Me	Me	56 (35)	13:87

[*] Isolated yields.

Table 6.3

6.3 Alkylmagnesium Amides

In a similar vein, the application of alkylmagnesium amide complexes in the asymmetric deprotonation of prochiral ketones was also studied. Complex (*R*)-**105** was tested with varying Lewis basic additives in the benchmark deprotonation of **25a** (Table 6.4).^{87,89} When HMPA was used with base (*R*)-**105** the desired product **26a** was obtained with a good conversion (88%) and high e.r. (84:16) (entry 1 in Table 6.4). The toxic HMPA additive could be switched to DMPU and the desired product **26a** could be obtained with a slightly lower but still high conversion (80%) and 86:14 e.r. (entry 2 in Table 6.4). Interestingly in the absence of additives the desired silyl enol ether **26a** was obtained with the highest e.r. (87:13), but the conversion slightly decreased to 61% (entry 3 in Table 6.4).

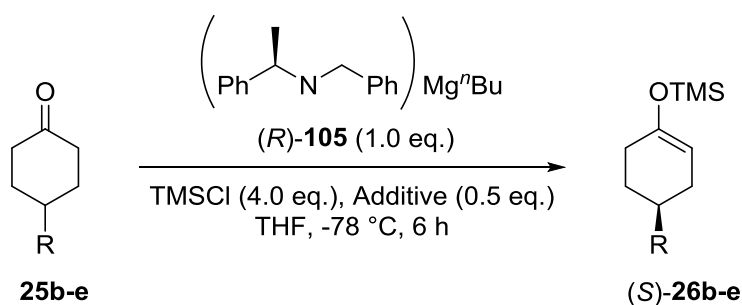


Scheme 6.4

Entry	Additive	Conversion (%)	e.r. (S):(R)
1	HMPA	88	84:16
2	DMPU	80	86:14
3	None	61	87:13

Table 6.4

Following this, four different 4-substituted cyclohexanones **25b-e** were tested, and, in every case, the products (*S*)-**26b-e** were obtained with high conversions of 83-85%, and high e.r. values of 83:17-86:14 when DMPU was added to the reaction (**Table 6.5**). Importantly similar levels of enantioselectivities (84:16-80:20) were observed with base (*R*)-**105** with a series of 4-substituted cyclohexanones **25b-e**, but the conversion was significantly lower, (between 47% and 70%) in every case (**Table 6.5**).



Scheme 6.5

Entry	Product	R	Additive	Conversion (%)	e.r. (S):(R)
1	(S)-26b	Ph	DMPU	83	86:14
			None	47	84:16
2	(S)-26c	<i>i</i> Pr	DMPU	85	86:14
			None	63	83:17
3	(S)-26d	Me	DMPU	84	83:17
			None	70	80:20
4	(S)-26e	<i>n</i> Pr	DMPU	84	86:14
			None	66	85:15

Table 6.5

7 Carbon Centred Bases

7.1 Catalytic Asymmetric Deprotonation

Previously, Kerr had demonstrated the applicability of magnesium amide complexes in the desymmetrisation of substituted cyclic ketones.^{78,81,82,89,91,92} During the pursuit of new, more efficient strategies, a catalytic version was envisioned, which offers several advantages over the previous protocols:

1. A sub-stoichiometric amount of the expensive chiral amine ligand is required, and
2. The chiral magnesium reagent would be generated *in situ* from a commercially available organometallic and the chiral amine

The general scheme is shown in **Figure 7.1**.⁸⁹

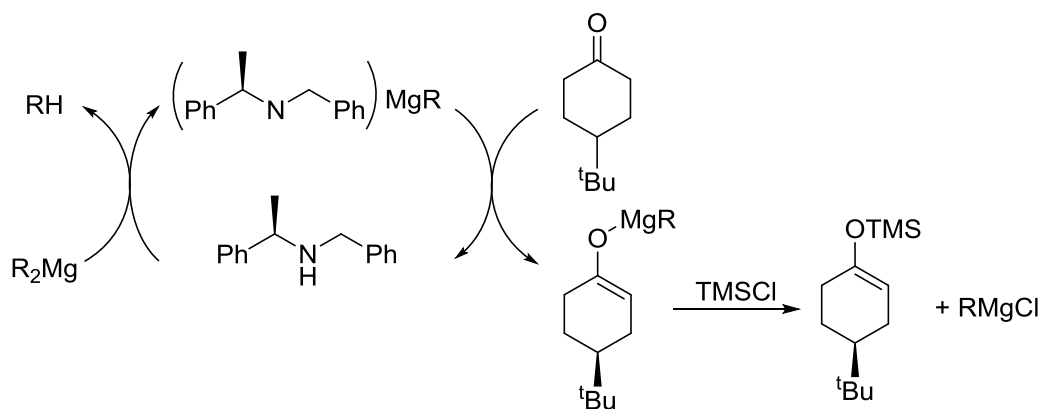
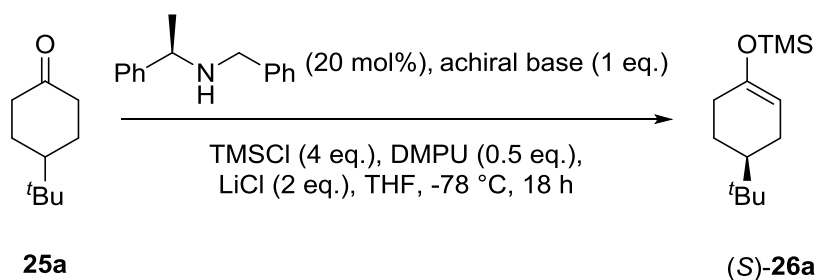


Figure 7.1

The chiral amine would be deprotonated by an achiral, strongly basic, dialkylmagnesium complex to prepare the mixed chiral magnesium species in solution. Thereafter, the mixed complex would induce chirality and distinguish between the two enantiomeric protons of the prochiral ketone. Finally, the resultant magnesium enolate species would be trapped by the electrophilic reagent, trimethylsilyl chloride, to obtain the enantiomerically enriched silyl enol ether product. Importantly, the bulk dialkylmagnesium species (or indeed the RMgCl species) should not react with the ketone substrate in an achiral fashion.

To initiate these studies, various achiral dialkylmagnesium sources were screened (**Scheme 7.1**). When di-*n*-butyl- and di-*iso*-propylmagnesium were employed as the achiral magnesium source, both the 1,2-addition product and the reduced product were observed and the desired product **26a** was obtained with a low yields of 29% and 17%, however the observed enantioselectivity was relatively high (83:17 and 70:30) (entries 1 and 2 in **Table 8.1**).⁸⁹ In an attempt to prevent the reduction pathway, homoleptic complexes with a sterically congested substituent (*tert*-butyl group) and without a β -hydrogen (mesityl) were synthesised. In this manner, di-*tert*-butylmagnesium and bismesitylmagnesium were used as achiral bases (entry 3 and entry 4 in **Table 8.1**). When di-*tert*-butylmagnesium was used in the absence of any additive, a low 3% yield and low e.r. of 58:42 was observed (entry 3 in **Table 7.1**). With 2 equivalents of lithium chloride, the product **26a** was obtained in higher yield (33%) and higher e.r. of 83:17 (entry 4 in **Table 7.1**). Bismesitylmagnesium offered no improvement, with a poor yield of 37% and moderate selectivity obtained of 61:39 e.r. (entry 5 in **Table 7.1**).



Scheme 7.1

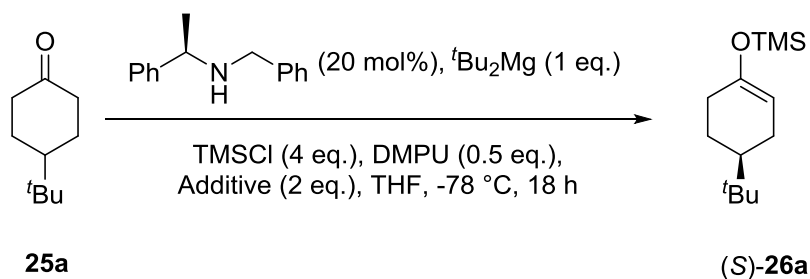
Entry	Achiral base	Yield (%)	e.r. (S):(R)
1*	$n\text{Bu}_2\text{Mg}$	29	83:17
2*	$i\text{Pr}_2\text{Mg}$	14	70:30
3**	$t\text{Bu}_2\text{Mg}$	3	58:42
4	$t\text{Bu}_2\text{Mg}$	33	83:17
5	Mes_2Mg	37	61:39

*: Alkylated and reduced by-products were also observed

** : Reaction was carried out in the absence of lithium chloride

Table 7.1

The activation of Grignard and related magnesium reagents by lithium chloride is well known *via* the formation of a more reactive mixed dimer complex.⁹³ Consequently, the effect of different salt additives was investigated with similar results being obtained relative to lithium chloride at -78°C (entry 1 in **Table 7.2**); lithium bromide (16% yield and e.r. 82:18, entry 2 in **Table 7.2**) and lithium *tert*-butoxide (37% yield and e.r. 75:35, entry 3 in **Table 7.2**).⁸⁹ Due to the poor yields across the board, the reaction was also performed using with the best additive, lithium chloride, at the higher temperatures with the aim to further increase the reactivity. At -60°C the product **26a** was obtained with a higher but still moderate 43% yield and decreased e.r. of 71:29 (entry 4 in **Table 7.2**) and at -40 °C a significantly higher yield of 83% was observed but the selectivity decreased to 59:41 (entry 5 in **Table 7.2**).



Scheme 7.2

Entry	Additive	Temp. (°C)	Yield (%)	e.r. (S):(R)
1	LiCl	-78	33	83:17
2	LiBr	-78	16	82:18
3	LiO ^t Bu	-78	37	75:35
4	LiCl	-60	43	71:29
5	LiCl	-40	83	59:41

Table 7.2

Based upon the modest selectivity and activity achieved in the initial efforts towards the development of a catalytic system, a new approach was proposed at this stage as shown in **Figure 7.2**.⁸⁹ A more acidic chiral amine (*R*)-**106** was utilised, with the incorporation of a strongly electron withdrawing CF₃ group in the amine structure.

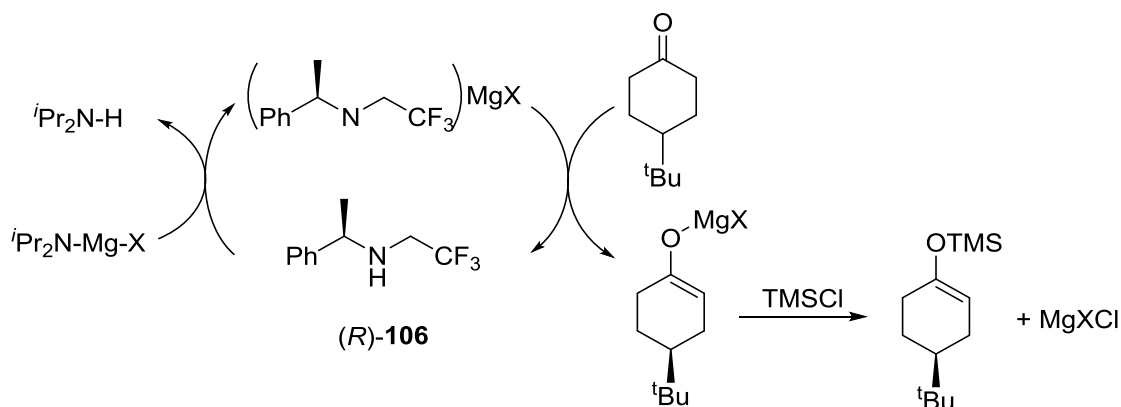
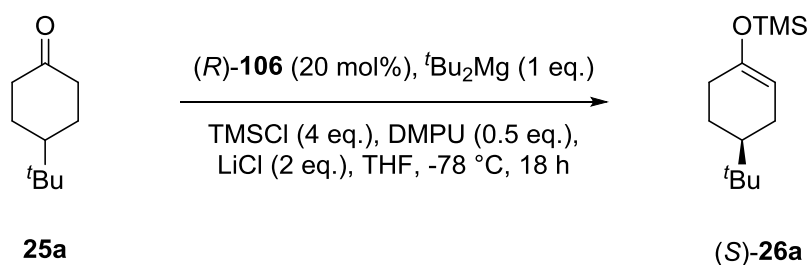


Figure 7.2

Unfortunately, when the reaction was carried out with this new amine similar results were obtained relative to initial efforts, despite the effect of different magnesium sources being investigated thoroughly (**Scheme 7.3**).⁸⁹ When magnesium bis-(di-*iso*-propylamide) was used as the achiral component a low yield of 27% and low e.r. of 52:48 was detected (entry 1 in **Table 7.3**). Using the analogue Hauser base, butylmagnesium amide offered an increase in the yield to 60%, but the e.r. of the product **26a** remained similar 53:47 (entry 2 in **Table 7.3**). Interestingly when the butyl group in the achiral magnesium source was changed to *tert*-butyl unit no reactivity was observed, possibly due to the hindered nature of the achiral base (entry 3 in **Table 7.3**). With an attempt to prepare a less sterically hindered base the chloride and bromide analogues were also tested (entries 4 and 5 in **Table 7.3**), although in these cases the products **26a** were obtained with a low 25% and 26% yield, but when *iso*-propylmagnesium chloride was used a high 80:20 e.r. was detected.



Scheme 7.3

Entry	Achiral base	Yield (%)	e.r. (<i>S</i>):(<i>R</i>)
1	$(i\text{Pr}_2\text{N})_2\text{Mg}$	27	52:48
2	$i\text{Pr}_2\text{NMg}^n\text{Bu}$	60	53:47
3	$i\text{Pr}_2\text{NMg}^t\text{Bu}$	-	-
4	$i\text{Pr}_2\text{NMgCl}$	25	80:20
5	$i\text{Pr}_2\text{NMgBr}$	26	58:42

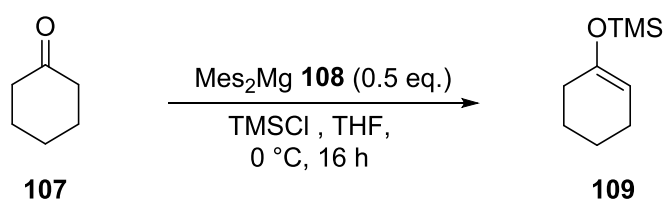
Table 7.3

Although a series of conditions were screened up to this point to develop an efficient catalytic deprotonation protocol, the identification of catalytic system, which affords the desired silyl enol ether product with high e.r. and yield remained elusive. Although at the expense of yield, a high e.r. (80:20) could be obtained (entry 4 in **Table 7.3**).

7.2 Carbon Centred Bases in Organic Synthesis

7.2.1 Synthesis of Functionalised Enolates

During the development of a catalytic protocol for the asymmetric deprotonation of prochiral substrates, the deprotonation ability of di-*tert*-butylmagnesium and bismesitylmagnesium in their own right were investigated. Surprisingly, these species turned out to be effective achiral bases and have subsequently been utilised in a series of new applications based on the suppressed nucleophilicity in these hindered reagents. An optimisation of the reaction parameters was carried out in the deprotonation of cyclohexanone **107** by bismesitylmagnesium **108** (Scheme 7.4).⁹⁴ Pleasingly, in the presence of 0.5 eq. di-mesitylmagnesium silyl enol ether **109** was obtained with a good 62% conversion (entry 1 in Table 7.4). The effect of salt additives was studied, with two eq. the lithium chloride the conversion was readily increased from 62 to 94% (entry 2 in Table 7.4). The amount of required electrophile was also reduced to 1 equivalent without any observable loss in the conversion (entry 3 in Table 7.4).

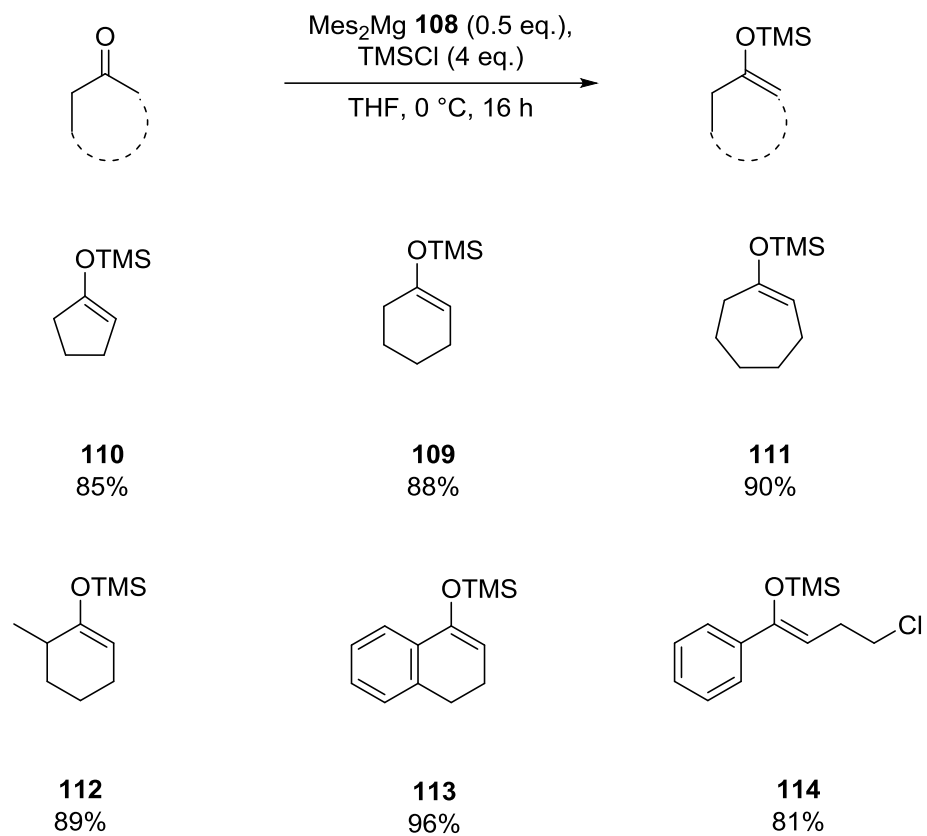


Scheme 7.4

Entry	LiCl (eq.)	TMSCl (eq.)	Conversion (%)
1	-	4	62
2	2	4	94
3	2	1	98

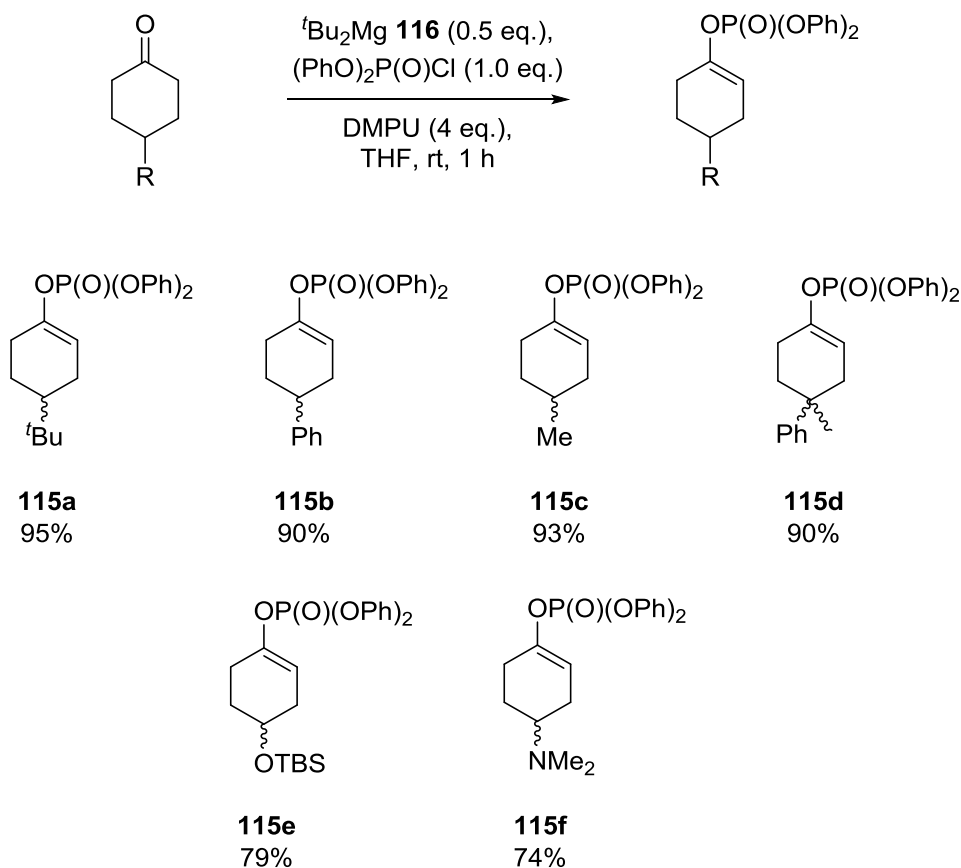
Table 7.4

Following these encouraging results, a series of cyclic substrates were investigated (Scheme 8.5). This protocol delivered the desired 5-7 membered cyclic silyl enol ethers **109-111** in high to excellent yields ranging from 85% to 90% (Scheme 7.5).⁹⁴ Interestingly, with 2-methylcyclohexan-1-one only the kinetic product **112** was observed and isolated with a good 89% yield. In addition, 3,4-dihydronaphthalen-1(2*H*)-one and 4-chloro-1-phenylbutan-1-one were also used as a substrates and the products **113** and **114** were obtained with high yields (96% and 81%), respectively.



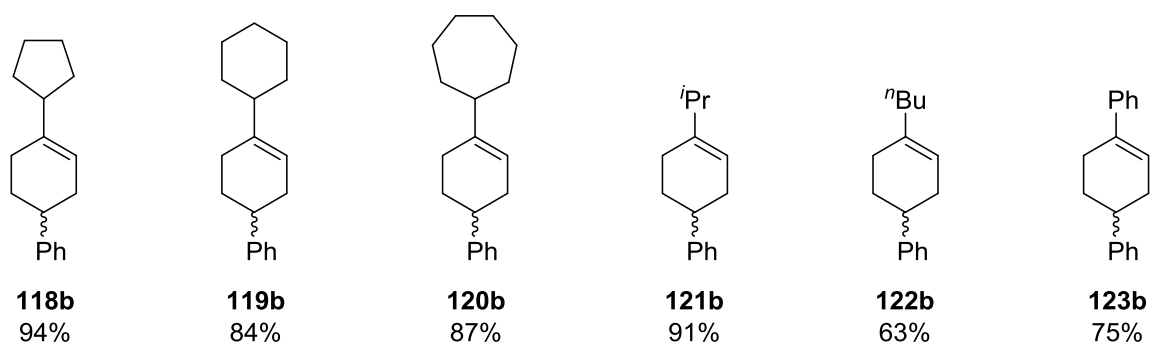
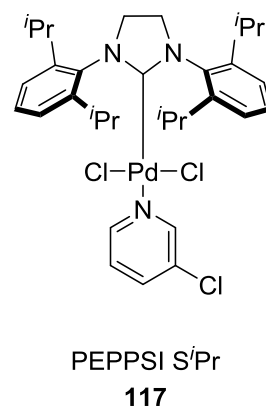
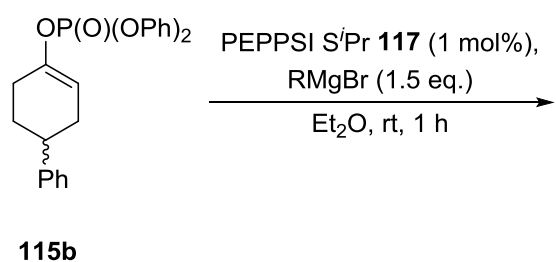
Scheme 7.5

More recently, carbon centred bases were successfully utilised in the synthesis of racemic enol phosphates **115** in the Kerr group.⁹⁵ In this manner, the deprotonation of 4-substituted cyclohexanones **25a-f** was achieved with di-*tert*-butylmagnesium **116** (**Scheme 7.6**). Indeed, only 0.5 eq. of the base was required and delivered a range of synthetically useful products **115a-f** in good to excellent yields (74-95%). Protected functional groups, such as a silyl protected alcohol **115e** and dimethyl amine **115f**, were also tolerated.



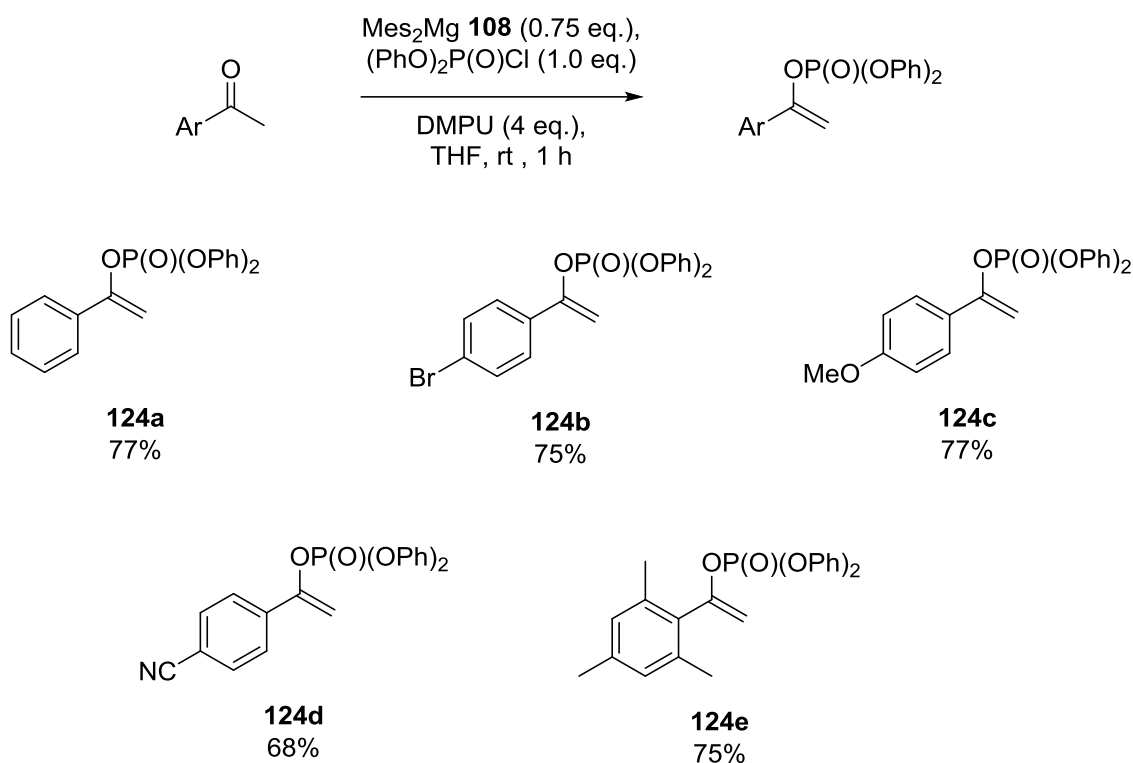
Scheme 7.6

The synthetic value of the racemic enol phosphate **115b** was demonstrated with a palladium catalysed Kumada coupling reaction (**Scheme 7.7**).⁹² The trisubstituted alkene products **118b-123b** were isolated in good to high yields (63–94%) after 1 h at room temperature by employing just 1 mol% of PEPPSI *S*ⁱPr catalyst **117**.



Scheme 7.7

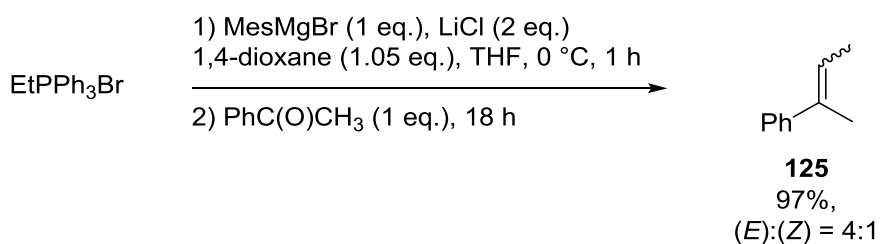
In addition to the above, aromatic aldehydes were also successfully reacted with dimesitylmagnesium **108** and the corresponding aromatic phosphoryl enol ethers **270a-e** were obtained in 68-77% yield (**Scheme 7.8**). Interestingly, a *para*-bromo substituent **270b** was tolerated and no halogen-magnesium exchange product was observed.



Scheme 7.8

7.2.2 Other Applications

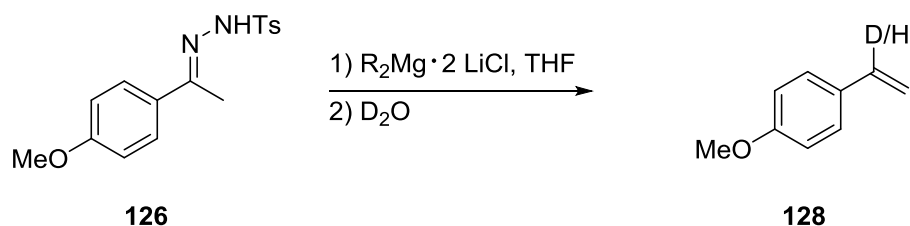
The applicability of carbon-centred bases has also been demonstrated by Kerr in the Wittig reaction of acetophenone (**Scheme 7.9**). The desired but-2-en-2-ylbenzene **125** was obtained with an excellent yield (97%) and (*E*):(*Z*)=4:1 ratio.⁹⁶



Scheme 7.9

In an attempt to further widen the scope of applicable transformations, carbon-centred bases were employed in the Shapiro reaction. Initially, tosylhydrazone **126** was reacted with various dialkylmagnesium complexes, and the intermediate carbanion was quenched with D_2O (**Scheme 7.10**).⁹⁷ With $(\text{TMP})_2\text{Mg}$ **127** (entry 1 in **Table 8.6**) the product **128** was isolated in a high yield 97%, although only 50% deuterium incorporation was observed in the benzylic position. The low deuterium incorporation was believed to be caused by the *in situ* generation of TMP-H , which can

also act as a proton source. When bismesitylmagnesium **108** was used at 0 °C (entry 2 in **Table 8.6**), a low 11 % yield was observed, which was increased to 69% with heating the reaction mixture to 40 °C (entry 3 in **Table 8.6**) and provided a high deuterium incorporation (92:8). The yield and selectivity were further elevated (entry 4 in **Table 8.6**) when 1.5 equivalent of bismesitylmagnesium **108** and 3 eq. lithium chloride were used. Di-*tert*-butylmagnesium **116** was also used as a base (entry 5 in **Scheme 7.10**), with the corresponding product **128** being isolated in a lower 58% yield but with similar selectivity D:H = 91:9.



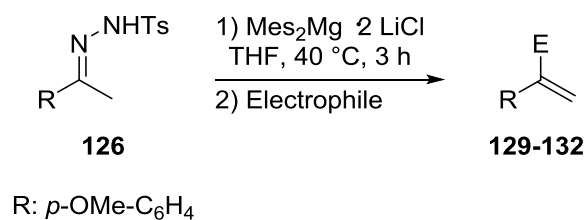
Scheme 7.10

Entry	Magnesium reagent	Conditions	Yield (%)	D:H
1	(TMP) ₂ Mg (127)	0 °C, 3 h	97	50:50
2	Mes ₂ Mg (108)	0 °C, 3 h	11	98:2
3	Mes ₂ Mg (108)	40 °C, 3 h	69	92:8
4 ^a	Mes ₂ Mg (108)	40 °C, 3 h	90	94:6
5 ^a	^t Bu ₂ Mg (116)	40 °C, 3 h	58	91:9

^a: 1.5 eq. of magnesium base and 3 eq. LiCl were added.

Table 7.5

The generality of the protocol was demonstrated by the use of several different electrophilic agents (**Scheme 7.11**).⁹⁷



Scheme 7.11

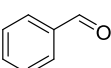
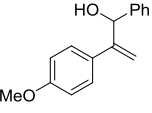
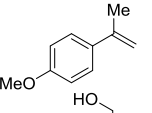
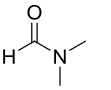
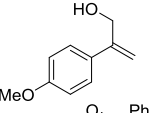
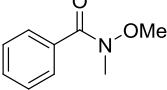
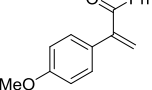
Entry	Electrophile	Quench conditions	Product	Yield (%)	E:H
1		-10 °C, 0.5 h		(129) 74	90:10
2	Me-I	0 °C, 1 h		(130) 81	93:7
3		0 °C, 1 h		(131) 65	90:10
4		40 °C, 0.5 h		(132) 72	97:3

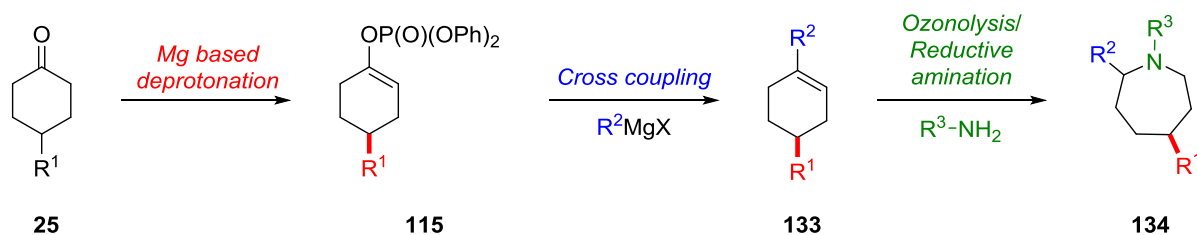
Table 7.6

The use of magnesium base reagents in organic synthesis has been extensively studied by the Kerr group in detail over the last decade. As a result a series of efficient protocols were published for the functionalization of simple molecular frameworks to prepare synthetically valuable intermediates. Efforts continually strive to produce convenient and practically accessible protocols of use to the synthetic chemistry community, therefore my project was focused on the incorporation and development of magnesium based strategies to prepare complex molecular structures.

8 Proposed Work

8.1 Synthesis of Chiral Azepanes

At the beginning of this research project we envisioned a synthetic sequence to prepare a series of sp^3 -rich azepanes from commercially available cyclohexanones using our magnesium based strategy, to prepare the starting enol phosphate in an efficient manner. Although azepanes are prevalent in medicinal chemistry and industry, to the best of our knowledge, a general and modular method of the synthesis of such azepanes is not reported (*vide infra*). The most commonly used strategies, for the preparation of such structures are either achieved by a ring expansion strategy⁹⁸ or through transition metal catalysed ring closing metathesis.⁹⁹ In both cases, highly functionalised starting materials are required, which are prepared through several steps, and enantioselective variants are only reported in a few cases with a highly limited substrate scope.^{100–102} Furthermore, ring closing metathesis techniques typically require expensive and elaborate catalysts in order to deliver the desired products. Therefore, we envisioned an operationally simple synthetic sequence for the preparation of sp^3 -rich azepanes using our magnesium-based deprotonation technology, as shown in **Scheme 8.1**.



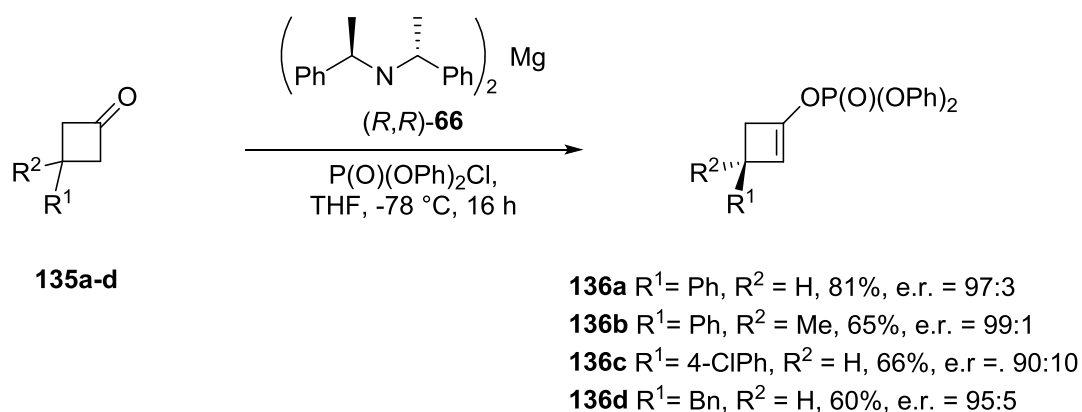
Scheme 8.1

The sequence starts with the magnesium-based deprotonation of cyclohexanones **25**, developed in the Kerr group.⁹² Using our asymmetric deprotonation strategy, the synthesis of the chiral enol phosphates **115** would be carried out prior to the products being exploited in a palladium-catalysed cross coupling reaction, to generate the corresponding trisubstituted alkenes **133**.¹¹⁸ At this stage, it was envisioned that the synthesis of the desired 7-membered rings **134** would be accomplished through a newly developed synthetic tool involving a telescoped ozonolysis/reductive amination sequence. Indeed, such a sequence would represent a highly accessible and practically efficient method for the preparation of these targets, whilst also decreasing the amount of waste generated during required work up and purification techniques as compared to a stepwise set of transformations.

This diverse protocol would create an ideal platform to prepare a wide range of otherwise synthetically challenging azepanes **134**, since the three different substituents on the 7-membered core could be implemented during different stages in the overall sequence. Therefore, our strategy would offer remarkable flexibility to fine tune molecular properties of this scaffold. In addition, the sequence could be directly implemented for the synthesis of chiral azepanes **134**, by using the magnesium mediated asymmetric deprotonation as the key chiral step in the sequence.

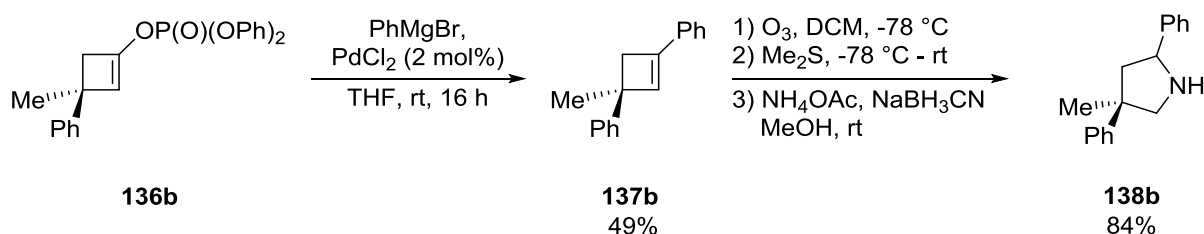
8.2 Asymmetric Deprotonation of Cyclobutanones

In addition to the above, recent and preliminary efforts within the group have described a reliable route for the asymmetric deprotonation of cyclobutanone substrates to deliver 4-membered chiral cyclic enol phosphates with good to high yields (60-81%) and good to excellent e.r. ranging from 90:10 to 99:1 **136a-d** (Scheme 8.2).¹⁰³



Scheme 8.2

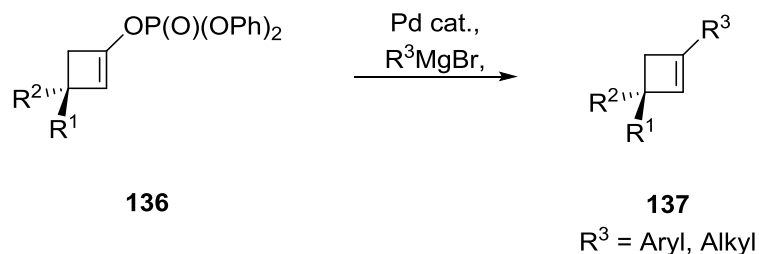
In a single example, chiral enol phosphate **137b** was then successfully coupled with an aryl Grignard reagent and the product **138b** was isolated in a moderate yield (Scheme 8.3). The corresponding product **138b** was further reacted through a one-pot ozonolysis/reductive amination sequence to afford a novel trisubstituted pyrrolidine **139b**. Although, the stereochemistry of final product was not determined, this route represents an elegant and short route for the synthesis of highly substituted chiral pyrrolidines.



Scheme 8.3

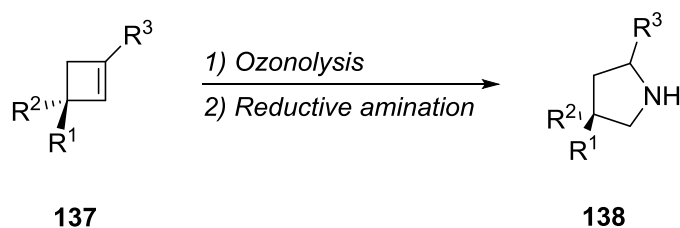
It was proposed at this stage, that after optimisation of the reaction condition for the cross coupling step, a series of substituted cyclobutanones of type **136** will be prepared. Thereafter a range of electronically and sterically different magnesium reagents to prepare a series of novel

enantiomerically enriched trisubstituted alkenes **137** (Scheme 8.4). Moreover, the scope of the cross coupling, in respect of the Grignard coupling partner will be extended for alkyl Grignard (*tert*-butyl-, methylmagnesium bromide) reagents (Scheme 8.4).



Scheme 8.4

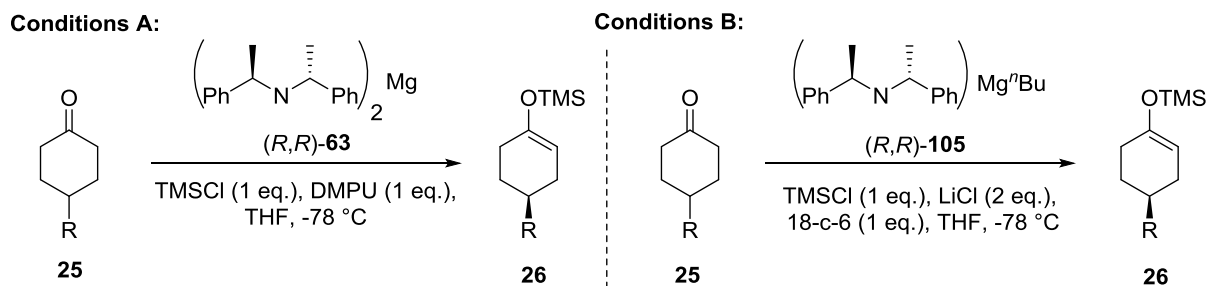
Once a range of such species is in hand, attention will focus on the optimisation of the one-pot ozonolysis/reductive amination sequence to further elaborate the cyclobutene structures and prepare synthetically useful, and optically pure, heterocyclic motifs such as **138** (Scheme 8.5).



Scheme 8.5

8.3 Structural Analysis of the Base by NMR spectroscopy

Previously in the Kerr group both THF and hexane were successfully used in the formation of magnesium bisamides, such as (*R,R*)-**63** and (*R,R*)-**105**.^{79,89,91} Interestingly during the development of more effective mixed magnesium bases, an alkylmagnesium amide (*R,R*)-**105** was developed. In the asymmetric deprotonation of 4-substituted cyclohexanones **25**, and identical results were obtained with the corresponding bisamide (*R,R*)-**195**, in comparison with the corresponding mixed alkylmagnesium amide (Table 8.1).⁹²



Scheme 8.6

Entry	R group	Conditions	Conversion (%)	e.r. (S):(R)
1	^t Bu	A	93	93:7
		B	93	95:5
2	ⁱ Pr	A	96	93:7
		B	96	98:2
3	ⁿ Pr	A	92	94:6
		B	95	94:6
4	Me	A	96	95:5
		B	99	92:8
5	OTBDMS	A	91	92:8*
		B	87	91:9*

* Determined by optical rotation

Table 8.1

Therefore, the question arose as to whether a different or an identical magnesium species is, responsible for the observed reactivity and selectivity in these two cases. Subsequently, a detailed ¹H NMR spectroscopic investigation of the formation of magnesium amides was proposed to identify the reactive chiral base in solution. Finally, as part of this work, a DOSY experiment was also envisioned to determine the aggregation state of the active organomagnesium base. In addition, as part of this project, we envisioned to test a series of frequently added additives with the standard conditions to determine their role in our asymmetric deprotonation.

9 Results and Discussion

9.1 Synthesis of Chiral sp^3 -rich Azepanes

9.1.1 Introduction

Recently, Lovering *et al.* reported that the proportion of sp^3 -rich carbon atoms in an orally active drug candidate directly correlates with their success rate in clinical trials.^{104,105} As a result, there is an enormous demand for the generation of simple sp^3 -rich fragments with reactive functionalities from readily available starting materials. Interestingly, 7-membered rings with a *N*-heteroatom have been widely used as biologically active medicine as shown in Figure 9.1.

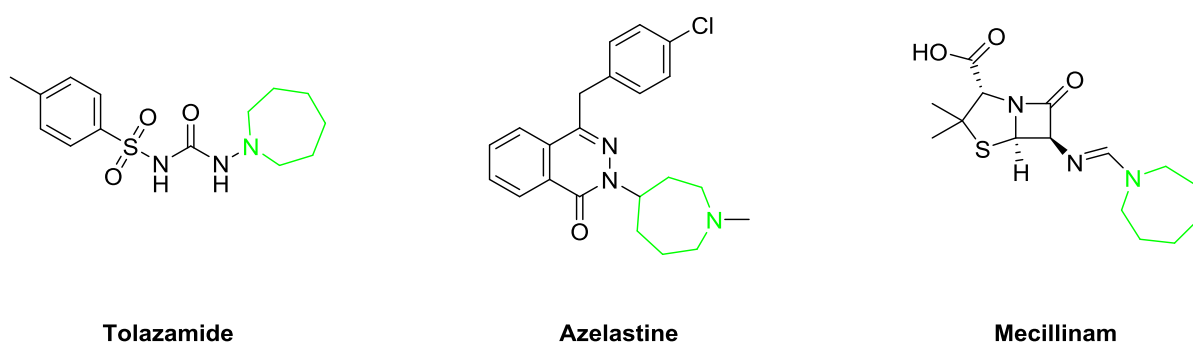
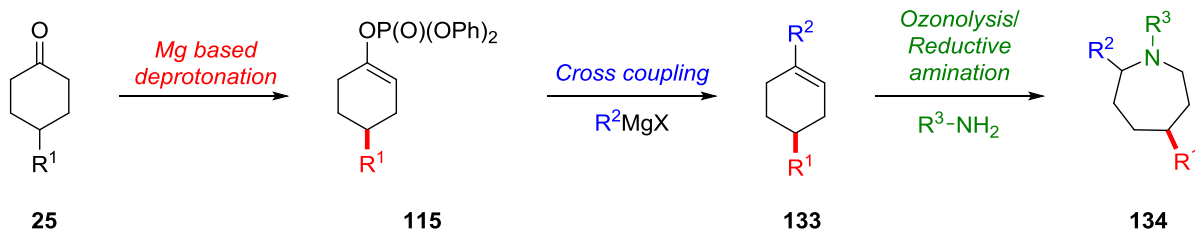


Figure 9.1

Tolozamide is an oral blood glucose lowering drug, used for the treatment of type 2 diabetes,¹⁰⁶ whilst azelastine is a H1-histamine antagonist used in the therapy of rhinitis.^{107,108} A further example is mecillinim, which is an extended spectrum penicillin antibiotic used in bladder and kidney infections.^{109,110} As mentioned previously, we envisioned an operationally simple and highly flexible synthetic sequence for the preparation of sp^3 -rich azepanes using our magnesium-based deprotonation as the key step (**Scheme 8.1**).



Scheme 9.1

First, we investigated 3D properties of our target molecule **134** computationally in order to validate our target from a medicinal-chemistry perspective.

9.1.2 Computational Analysis of the 3D Properties of the Azepane Core

In order to assess the lead-likeness and 3D properties of the targeted 7-membered azepane scaffold, the Llama software was used.¹¹¹ In this program, the target structure is decorated at its reactive groups by well known reactions. In this way, a virtual library is created and the 3D properties of these molecules can be analysed. When both diastereomers of 2,5-dimethylazepane **139** (Figure 9.2) were decorated with the Llama software, a library of 52 products was created.

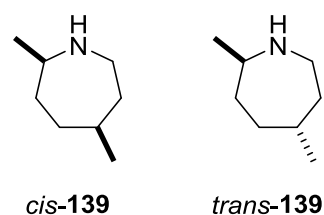


Figure 9.2

Analysis of these molecules revealed that they possess a high likelihood to be lead like candidates in drug discovery projects (Figure 10.14).

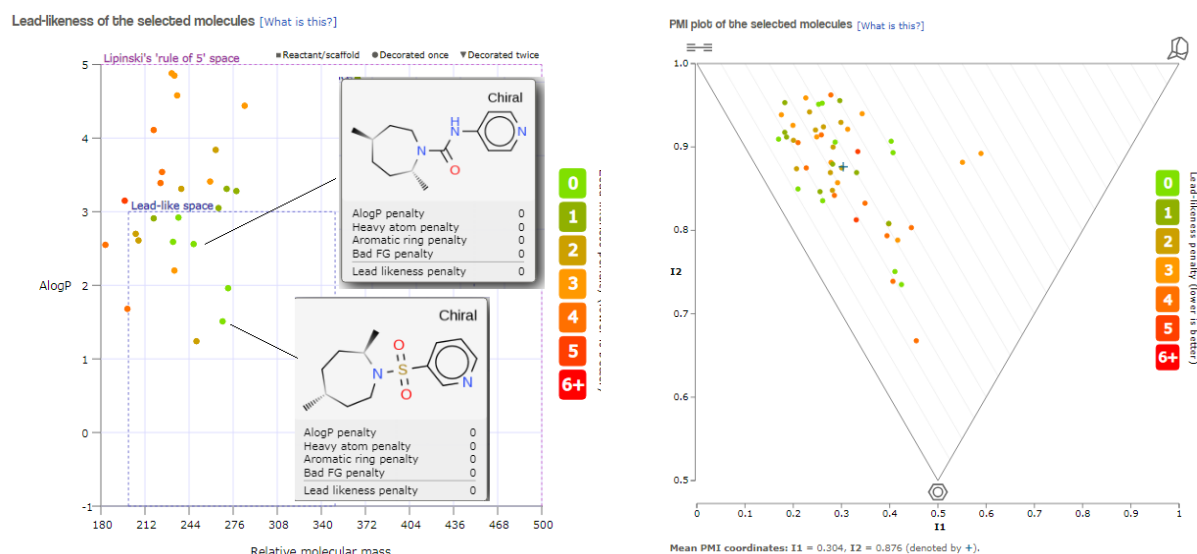
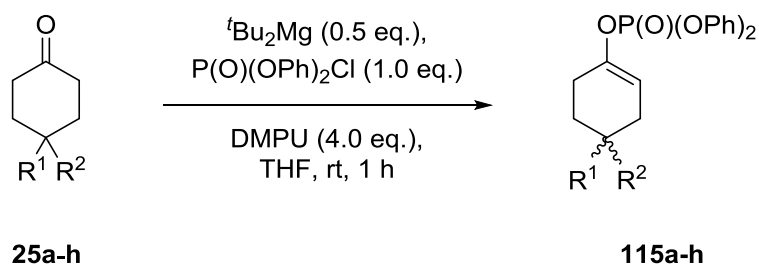


Figure 9.3

A high proportion of the library 21% (11 molecules out of 52) occupies the lead-like space based up on the Lipinski's rules and they have a low lead likeness penalty (Left graph, Figure 9.3). In addition, when the 3D properties of these molecules were analysed by the creation of the PMI (Principal moments of inertia) plot, a high degree of 3D character was observed and the centre point of the library is far away from the flat-linear plane (Right graph, 9.3). Therefore, following the validation of our target scaffold our attention turned towards the preparation of these molecules.

9.1.3 Synthesis of Racemic Enol Phosphates

The synthetic sequence towards the preparation of 7-membered azepanes started with the synthesis of racemic enol phosphates of type **115**. Recently, the Kerr group reported a very mild and highly efficient protocol for the preparation of racemic enol phosphates.¹¹² The desired products can be obtained after just 1 h in the presence of a non-nucleophilic base, such as di-*tert*-butyl magnesium, in good to excellent yields 62-90%. As such, this method was used for the preparation of a range of enol phosphates **115a-h** for further manipulation (**Scheme 10.65**). Firstly, the 4-*tert*-butyl- and 4-phenyl-substituted enol phosphates **115a** and **115b** were prepared. In both cases, the desired products **115a** and **115b** were obtained in a good 71% and 80% yield (entry 1 and entry 2 in **Table 9.1**), respectively. To investigate the effect of the substituent size on the asymmetric deprotonation step, substrates with smaller alkyl groups at the 4-position were also targeted. Therefore, the 4-propyl- **115g** and 4-methyl-substituted **115d** analogues were also targeted and, in both cases, the desired products were isolated in excellent yields; 88% for **115g** and 90% for **115d** (entry 3 and entry 4 in **Table 9.1**). Thereafter, a substrate with a quaternary stereocenter **115e** (entry 5 in **Table 9.1**) was synthesised in a similarly good 81% yield. Finally, substrates **115e,f-h** with additional heteroatoms were prepared. In this way, a *tert*-butyldimethylsilyl protected alcohol **115e** (entry 6 in **Table 9.1**), dimethyl amine **115f** (entry 7 in **Table 9.1**) and acetal **115h** (entry 8 in **Table 9.1**) analogues were isolated in 62%, 86% and 73% yields.



Scheme 9.2

Entry	Compound	R ¹	R ²	Yield(%)
1	115a	^t Bu	H	71
2	115b	Ph	H	80
3	115g	ⁿ Pr	H	88
4	115c	Me	H	90
5	115d	Ph	Me	81
6	115e	OTBDMS	H	62
7	115f	NMe ₂	H	86
8	115h	-O-CH ₂ CH ₂ -O-		73

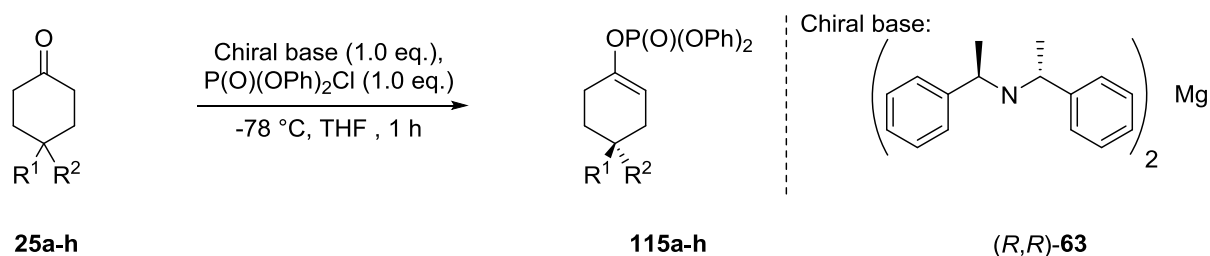
Table 9.1

With the racemic enol phosphates **115a-h** in hand, our subsequent efforts focused on the preparation of enantio-enriched derivatives before turning to the cross-coupling reaction that would ultimately provide starting substrates for our key ozonolysis/reductive amination procedure. Indeed, chiral HPLC analysis methods could be established at the enol phosphate stage for most compounds (see experimental section for full details), and we anticipated that we would be able to establish the method for the remainder of the compounds post cross-coupling.

9.1.4 Synthesis of Chiral Enol Phosphates

As detailed in the introductory section, our research team has had a long standing interest in the development and application of novel chiral magnesium centred amide bases.^{81,82,91,92} These organometallic reagents offer a series of advantages over their lithium analogues, these reactants show a simpler aggregation state, they have an increased thermal stability and the bifunctional nature of magnesium allows to have a spectator ligand on the magnesium centre.⁶⁶ Originally, these bases were utilised for the preparation of chiral silyl enol ethers,^{79,82,91} although, more recently, the protocol has been successfully expanded for the preparation of enantiomerically enriched enol phosphates.⁹² As part of this programme of work towards the ultimate preparation of desirable azepane structures, a range of chiral enol phosphates **115** were prepared *via* the use of previously optimised conditions (**Scheme 10.66**).⁹² When the 4-phenyl and 4-*tert*-butyl substituted ketones were used as the substrates, the target enol phosphates **115b** and **115a** were isolated in good yields 80% and 76% and with outstanding enantioselectivities of 93:7 and 99:1 (entry 1 and entry 2 in **Table 9.2**). Moving to the *n*-propyl and methyl derivatives **115g** and **115d**, which were liquid substances stored over molecular sieves prior to the reaction, high yields were obtained 90% and 93% (entry 3 and entry 4 in **Table 9.2**), but the products **115g** and **115d** were isolated with low enantioselectivity

(the enantioselectivity was determined after a cross coupling reaction with phenylmagnesium bromide, entry 3 and 4 in **Table 9.7**). Fortunately, upon re-distilling and storing these starting substrates under argon, and in the absence of any molecular sieves, the reactions afforded the desired products **115g** and **115d** with high enantiomeric ratios of 91:9 and 84:16 and in excellent yields 97% and 90% (entry 5 and entry 6 in **Table 9.7**). From this point forward, the asymmetric deprotonation of other liquid substrates was carried out using this modification. Interestingly, with the alkyl substituents at the 4-position, the observed enantioselectivity decreased in the following order: $t\text{Bu} > \text{Pr} > \text{Me}$, possibly due to the decreased capacity of the smaller groups to effectively lock the conformation of the starting cyclohexanones. Having said this, the lowest ratio obtained in this study related to the 4-methyl derivative **115d**, which was still isolated with a very good 84:16 enantiomeric ratio (entry 6 in **Table 9.7**). When the 4,4'-disubstituted cyclohexanone **25d** was tested, the desired enol phosphate **115d** was obtained in a high yield (93%) and good e.r. of 86:14 (entry 7 in **Table 9.2**). This shows that our system is capable of generating what would otherwise be a synthetically challenging quaternary carbon stereocentre. When a bulky silyl protecting group was applied, the desired product **115e** was obtained with a good yield 74% (entry 8 in **Table 9.2**), but the individual enantiomers **115e** were not separable on chiral HPLC. Finally, when a tertiary amine **25f** was incorporated in the structure, the desired product **115f** was obtained in a good yield (86%), although determination of the enantiomeric ratio was not possible by chiral HPLC (entry 8 in **Table 9.2**).



Scheme 9.3

Entry	Compound	R ¹	R ²	Yield(%)	E.r.
1	115a	^t Bu	H	80	93:7
2	115b	Ph	H	76	99:1
3 ^a	115g	ⁿ Pr	H	90	51:49 ^c
4 ^a	115c	Me	H	93	52:48 ^c
5 ^b	115g	ⁿ Pr	H	97	91:9 ^c
6 ^b	115c	Me	H	90	84:16 ^c
7	115d	Ph	Me	93	86:14
8	115e	OTBDMS	H	74	- ^d
9	115f	NMe ₂	H	86	- ^d

^a:Substrates were stored over molecular sieves prior to the reaction.

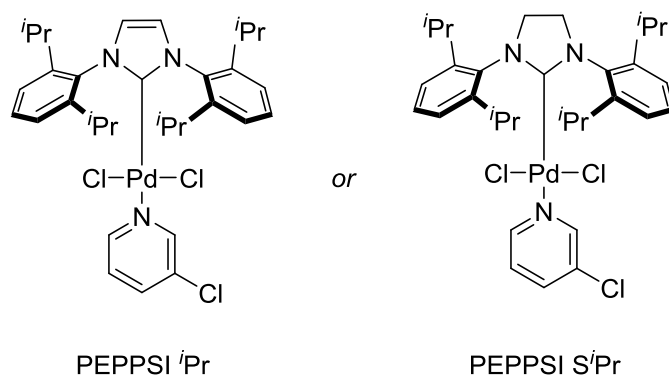
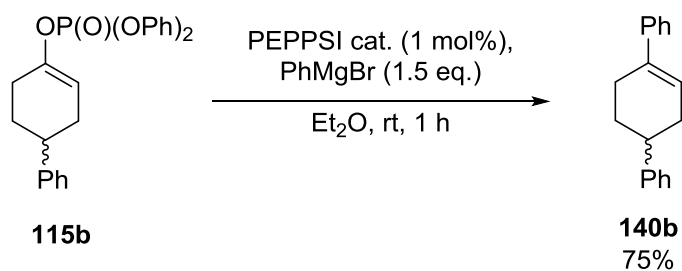
^b:Freshly distilled substrates were used, with no contact being made with molecular sieves. c: E.r. was determine after cross coupling with phenylmagnesium bromide. ^d:Enantiomers were not separable on chiral HPLC.

Table 9.2

After the successful preparation of racemic and chiral enol phosphates **115** we turned our attention towards the optimisation of the palladium catalysed Kumada cross coupling.

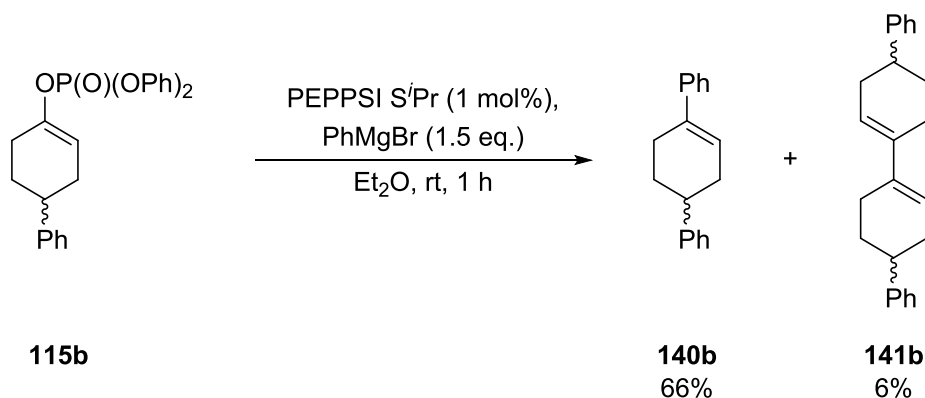
9.1.5 Cross Coupling

At this stage, the application of a Kumada cross coupling reaction was targeted to prepare the desired trisubstituted cyclic alkenes of type **133**. Based upon preliminary results from our group, the palladium-catalysed cross-coupling of enol phosphates **115** with phenylmagnesium bromide was a viable strategy for the synthesis of cyclic trisubstituted alkenes.⁹² When diphenyl (1,2,3,6-tetrahydro-[1,1'-biphenyl]-4-yl) phosphate **115b** was reacted with phenylmagnesium bromide, the product **140b** was obtained in a high yield 75% (**Scheme 9.4**).⁹²



Scheme 9.4

At the outset, the developing conditions from our laboratory were tested (**Scheme 9.5**). Indeed, the desired product **140b** was isolated in a lower but still good yield 66%, however, a low amount of the homocoupled enol phosphate **141b** 6% was obtained. Indeed, it was not a trivial process to separate the desired product **140b** from compound **141b**.

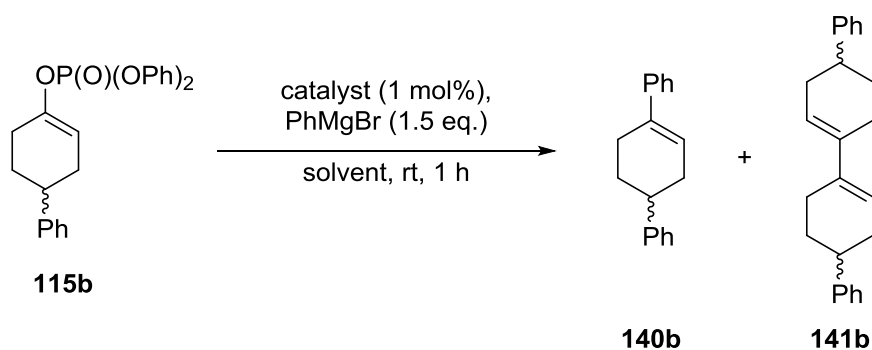


Scheme 9.5

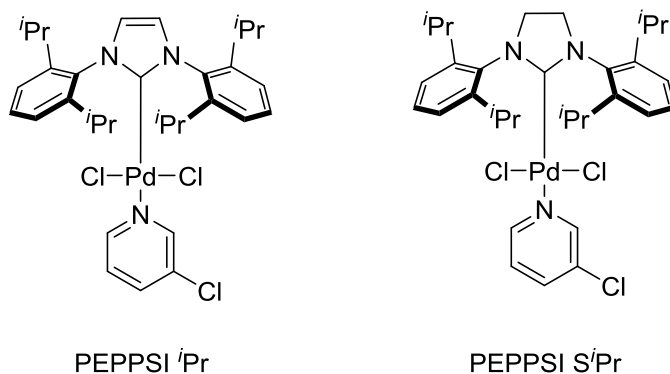
In an effort to improve the overall efficiency of the key cross coupling reaction, and to eliminate the formation of the undesired homocoupled by-product **141b**, our efforts focused on the optimisation of the reaction conditions.

9.1.6 Development of a New Protocol

At this stage, a detailed optimisation of the reaction parameters was carried out in order to further improve the yield towards **140b** (Scheme 9.6). Previous knowledge from within our laboratory highlighted that the two important factors in such a reaction would be the catalyst and the solvent. As such, a number of catalysts were tested and in varying solvents as described below in Scheme 9.6. In every occasion, the undesired homocoupled by-product **141b** was detected. Whilst low amounts of this was formed, it resulted in the overall purification of the desired product being non-trivial. Initially, when PEPPSI *i*Pr was used (entry 1 in Table 9.3), the desired product **140b** was isolated in a 60% yield with 8% of **141b** also being obtained. The reaction was also performed with PEPPSI *S*Pr (entry 2 in Table 9.3), since this catalyst was also successfully reported in the cross coupling of alkyl Grignard reagents and enol phosphates.⁹² A similar yield was obtained (64%) towards the desired product **140b**, with a slightly lower amount of the undesired by-product **141b** being detected (6%). Since a similar cross coupling protocol with was also reported by Skrydstrup *et al.*¹¹³ for the functionalisation of achiral enol phosphates with a palladium(II) chloride under glovebox conditions, this protocol was also tested. Unfortunately, in this case (entry 3 in Table 9.3), **140b** was obtained with lower yield (34%), in comparison with the previous runs with the PEPPSI catalysts (*cf.* entries 1-3 in Table 9.3). The effect of the solvent was also investigated (entry 4 in Table 9.3), whereby the best performing catalyst PEPPSi *S*Pr was used with THF as the solvent. In this case, whilst an improvement on the Skrydstrup conditions was detected, a significantly lower reactivity towards the desired product **140b** was detected (44%).



PEPPSI catalyst:



Scheme 9.6

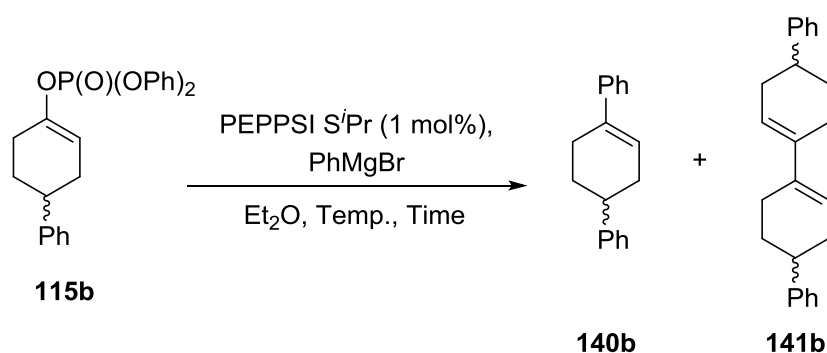
Entry	Catalyst	Solvent	Yield of 140b (%)	Yield of 141b (%)
1	PEPPSI <i>i</i> Pr	Et ₂ O	60	8
2	PEPPSI <i>S'</i> Pr	Et ₂ O	64	6
3*	PdCl ₂	THF	34	3
4	PEPPSI <i>S'</i> Pr	THF	44	2

*: 5 mol% catalyst was used and the reaction was stirred for 24 h.

Table 9.3

Deciding to move forward with PEPPSI *S'*Pr as the catalyst and Et₂O as the solvent, we next investigated a range of varying reaction conditions. The results of these experiments are summarised in **Table 9.4**. When the reaction was performed at 0 °C (entry 1 in **Table 9.4**), the product **140b** was observed with a low 20% yield and a significant amount of unreacted starting material **115b** was detected. Indeed, when the temperature of the reaction was increased to 40 °C (entry 2 in **Table 9.4**), the yield increased to 63%, however, the corresponding homocoupled enol phosphate **141b** was also observed in increased amounts 13%. In an attempt to avoid the formation of the undesired homocoupled byproduct **141b** the reaction was also carried out under microwave conditions (entry 3 in **Table 9.4**) and, although the desired product **140b** was detected with a good

66% conversion, formation of other by-products were also detected. In a further effort to boost the yield, the amount of Grignard reagent was increased to facilitate the formation of the catalytically active palladium(0) catalyst before the addition of the electrophile. However, when phenylmagnesium bromide was used in 3 eq. (entry 4 in **Table 9.4**) the desired product **140b** was obtained with a similar yield as obtained thus far of 63% and the byproduct **141b** was also isolated with 10% yield. Further considerations related to the addition time of the reagents. In order to avoid any side reaction with the Grignard reagent, the enol phosphate **115b** was added last over 1 h (see experimental for full details). Unfortunately, the reaction saw the typical, moderate 66% conversion to product **140b** with a significant (16%) conversion to the undesired homocoupled product **141b** (entry 5 **Table 9.4**). Subsequently, the Grignard reagent was added in a slow fashion over 1 h to the mixture of all other reagents (entry 6 in **Table 9.4**). To our delight, the desired coupled product **140b** was observed with an excellent 82% conversion and minimal amounts of the homocoupled enol phosphate **141b** was detected (2%).



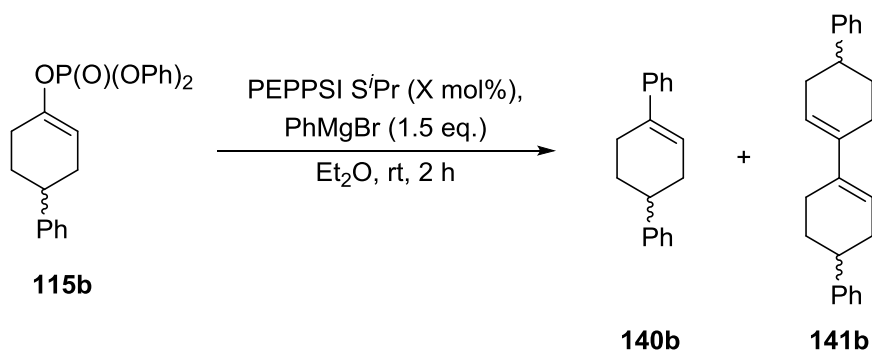
Scheme 9.7

Entry	PhMgBr (eq.)	Reaction conditions	Yield of 140b (%)	Yield of 141b (%)
1	1.5	0 °C, 1 h	20	3
2	1.5	40 °C, 1 h	63	13
3	1.5	μ w irradiation, 80 °C, 15 min	50	5
4	3	0 °C, 1 h	63	10
5 ^a	1.5	rt, 1 h	66	16
6 ^b	1.5	rt, 1 h	82	2

^aSlow addition of the substrate last over 1 h; ^bSlow addition of the Grignard reagent over 1 h

Table 9.4

Following this promising result, our attention turned towards the investigation of the effect of catalyst loading. The results are summarised in **Table 9.5**. When 0.5 mol% catalyst loading was used (entry 1 in **Table 9.5**), a significant decrease in the reactivity was observed. The desired product **140b** was only obtained with a 44% yield and significant amount of unreacted starting material was detected. However, when the catalyst loading was increased to 5 mol% (entry 2 in **Table 9.5**) the product **140b** was observed with an excellent 87% yield without any detectable by-product **141b** formation.



Scheme 9.8

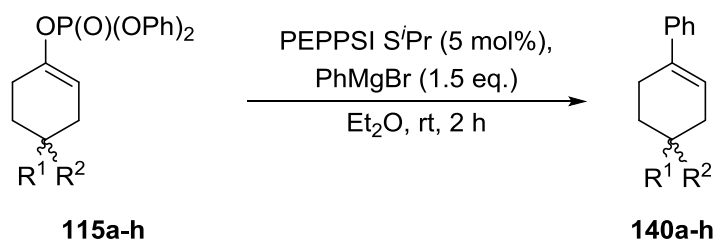
Entry	Catalyst loading (mol%)	Yield of 140b (%)	Yield of 141b (%)
1	0.5	44	4
2	5	87	-

Table 9.5

Having reached an excellent system whereby the desired material **140b** was obtained in high yield, and as the sole product, we looked to translate this protocol to the range of enol phosphate compounds **115** previously prepared.

9.1.7 Substrate Scope for the Cross Coupling with Phenylmagnesium Bromide

With the newly optimised conditions in hand, these were applied using the previously prepared racemic enol phosphates of type **115** to deliver the desired cross coupled products (**Scheme 10.72**). Pleasingly, such substrates were successfully utilised as the electrophilic coupling partners in our newly developed, operationally simple and extremely mild, palladium catalysed Kumada reaction. The substrate scope is summarised in **Table 9.6**. As described above, the *tert*-butyl substituted enol phosphate **115a** (entry 1 **Table 9.6**) delivered the corresponding product **140a** in a high 88% yield after isolation. Additionally, the 4-*n*-propyl- **140g** and 4-methyl **140d** substituted analogues were also prepared in an identical fashion (entry 2 and entry 3 in **Table 9.6**), and in good to excellent yields of 87% and 65%. In the case of the methyl substituted enol phosphate **115c** (entry 3 in **Table 9.6**), full conversion towards the desired product **140c** was observed, however, due to its low molar mass, the molecule was volatile and consequently some material was lost on isolation. The disubstituted analogue **140d** (entry 4 in **Table 9.6**) was also successfully isolated in an excellent 95% yield. Furthermore, and to our delight, when oxygen and nitrogen heteroatoms were included in the structure, the desired products **140e**, **140f** and **140h** were isolated in very good yields; 88%, 82% and 75%, respectively (entries 5-7 in **Table 9.6**). Such examples demonstrated that our cross coupling conditions are compatible with important functional groups, and the products can be obtained in good to excellent yields without poisoning the palladium catalyst.



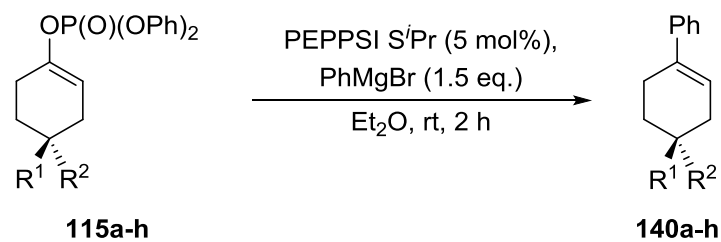
Scheme 9.9

Entry	Product	R ¹ group	R ² group	Yield(%)
1	140a	^t Bu	H	88
2	140g	ⁿ Pr	H	87
3	140c	Me	H	65
4	140d	Ph	Me	95
5	140e	OTBDMS	H	88
6	140f	NMe ₂	H	82
7	140h	-O-CH ₂ CH ₂ -O-		75

Table 9.6

With the racemic substrates in hand, and chiral HPLC methods established for downstream analysis, we targeted the preparation of the enantiomerically enriched cyclic alkenes under identical conditions (**Table 9.7**). In general, and as expected, employing our enantioenriched enol phosphates in the cross coupling reaction resulted in similarly high yields as compared to the racemic counterparts. Pleasingly, the phenyl substituted product **140b** was obtained in an outstanding 96% yield and with a 99:1 enantiomeric ratio, as determined *via* the previously described magnesium amide-based deprotonation reaction (entry 1 in **Table 9.7**). The *tert*-butyl analogue **140a** was also delivered in high yield and it was confirmed that no racemisation had occurred under the cross coupling conditions, with the 93:7 enantiomeric ratio being retained from the starting enol phosphate (entry 2 in **Table 9.7**). When the starting ketones **25g** and **25c** were stored over molecular sieves the the cross coupling products were obtained with high yields of 90% and 92% but with a low e.r. (entry 3 and 4 in **Table 9.7**). However when these substrates were freshly distilled and stored under argon the product **140g** was isolated in an excellent 90% yield and high 91:9 e.r (entry 5 in **Table 9.7**). Similarly, the methyl substituted analogue **140c**, was delivered in an excellent 92% yield and with a very good 84:16 ratio (entry 6 in **Table 9.7**). During the preparation of the chiral variant **140c**, the standard workup protocol was modified and extra care was taken to isolate this low boiling oil by setting the temperature of the rotavapor bath to 30 °C and the pressure to 150 mbar. Subsequently, the 4-phenyl-4'-methyl substituted cross coupling product **140d** as well as the heteroatom containing products **140e** and **140f** were all prepared efficiently and in high yields 94%, 90% and 80% (entries 5-7 in **Table 9.7**). It should be noted that it was still not possible to determine

the enantiomeric ratio of the dimethyl amine derivative **140f** via chiral HPLC analysis, despite a number of columns being tested.



Scheme 9.10

Entry	Product	R ¹ group	R ² group	Yield(%)	E.r. of 140	E.r. of 115
1	140b	Ph	H	96	99:1	99:1
2	140a	^t Bu	H	80	93:7	93:7
3 ^a	140g	ⁿ Pr	H	90	51:49	- ^c
4 ^a	140c	Me	H	92	52:48	- ^c
5 ^b	140g	ⁿ Pr	H	91	91:9	- ^c
6 ^b	140c	Me	H	93	84:16	- ^c
7	140d	Ph	Me	94	86:14	86:14
8 ^b	140e	OTBDMS	H	90	95:5	- ^c
9 ^b	140f	NMe ₂	H	80	-	- ^c

^a:Substrates were stored over molecular sieves prior to the reaction.

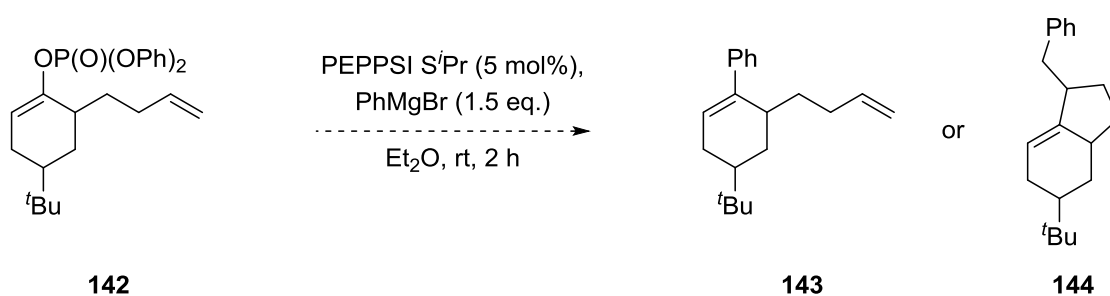
^b:Freshly distilled substrates were used, with no contact being made with molecular sieves.^c: Enantiomers were unseparable on chiral HPLC.

Table 9.7

At this stage in the project, we had established conditions for the key asymmetric deprotonation step to prepare a range of chiral enol phosphate **115**, as well as the subsequent cross coupling for optimised and a new protocol was developed to obtain the desired cyclic alkenes **140** with high yields. Indeed, we now had an array of substrates that were primed for our ozonolysis/reductive amination sequence that would ultimately lead to the targeted sp³ rich azepanes. Having said this, we were intrigued to explore further aspects of the cross coupling reaction before moving forward, in order to postulate for the formation of the homocoupled enol phosphate **141**.

9.1.8 Mechanistic Insight in the Formation of the Homocoupled Enol Phosphate

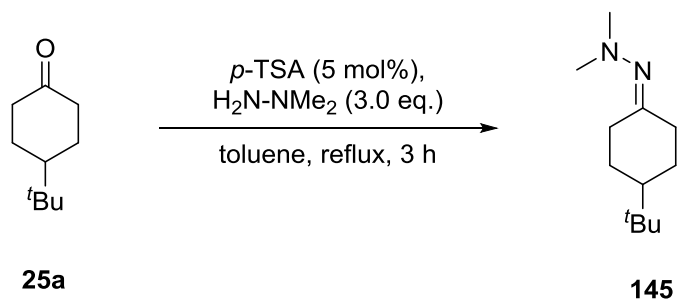
As mentioned above, we were interested to further explore the cross coupling reaction in an effort to explain the formation of the undesired homocoupled byproduct **141**. A survey of the literature was carried out and it was revealed that, under similar conditions, the formation of homocoupled products had been previously reported.¹¹³ In order to create a rational mechanistic proposal for the formation of this somewhat unexpected product, we proposed to perform the reaction with a molecular probe **142** (Scheme 9.11).



Scheme 9.11

The structure of the targeted probe **142** contained a pendant alkene group and subjecting this substrate to the reaction conditions would answer the essential question: does the coupling reaction proceed through a two electron pathway or single electron transfer mechanism? Indeed, both of these mechanisms have been reported for Kumada couplings in the presence of the PEPPSI catalyst.^{114,115} If a single electron transfer mechanism was in place, one would expect rapid cyclisation to the bicyclic product **144**, while if the reaction proceeds through a two electron pathway only **143** will be detected.

Preparation of substrate **142** started with the condensation of 4-(*tert*-butyl)-cyclohexanone **25a** and dimethylhydrazine under acidic conditions on a 1 mmol scale (Scheme 10.75). The corresponding hydrazone **144** was isolated in a good 62% yield (entry 1 in Table 9.8).¹¹⁶ When the reaction was scaled up to 3 mmol, the product **145** was obtained with a slightly higher 66% yield (entry 2 in Table 9.8).

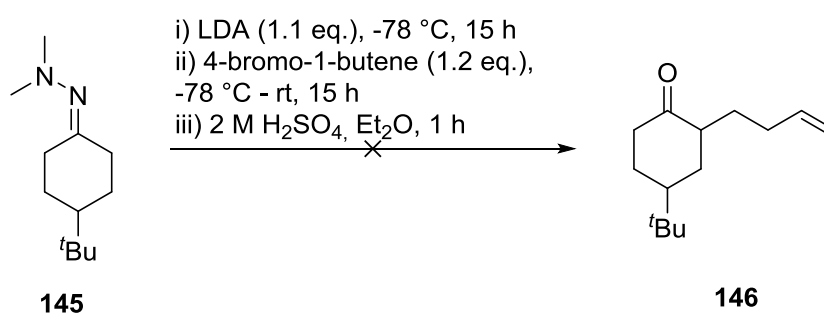


Scheme 9.12

Entry	Scale (mmol)	Yield (%)
1	1	62
2	3	66

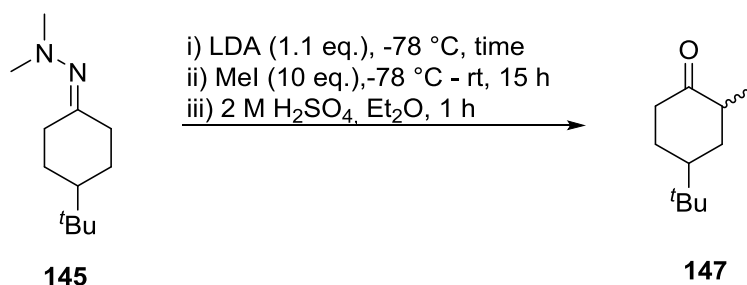
Table 9.8

With hydrazone **145** in hand, α -alkylation was attempted with 4-bromo-1-butene, using LDA as base and perform the alkylation with 4-bromo-1-butene. Unfortunately, the desired product **146** was not observed in the ^1H NMR spectrum of the crude reaction mixture and 87% of the starting material **25a** was recovered (Scheme 9.13).



Scheme 9.13

At this stage, it was not clear whether the failure of the reaction was caused by insufficient deprotonation of the hydrazone or, indeed, due to the problems with the electrophile employed. To explore, the reaction was attempted using the simpler methyl iodide reagent and the time allowed for deprotonation of the hydrazone was explored (Table 10.25). Unfortunately, the desired product **147** was not observed in any case, even after prolonged 20 h reaction time prior to addition of the electrophile.

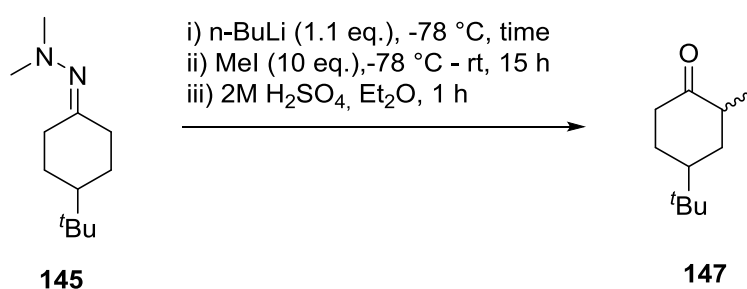


Scheme 9.14

Entry	Reaction time (h)	Conv. towards 147 (%)	Rec. SM (%)
1	1	-	99
2	2	-	98
3	4	-	99
4	20	-	97

Table 9.9

Following this, a stronger base, n-butyllithium was used at -78 °C, but even after 8 hours only the product from hydrolysis of the starting hydrazone **145** was present in the reaction mixture (**Scheme 10.78**).

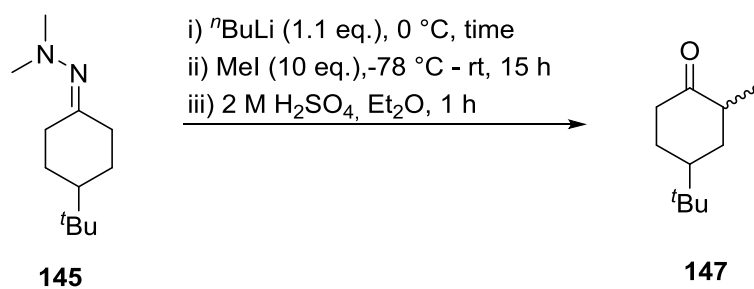


Scheme 9.15

Entry	Reaction time (h)	Conv. towards 299 (%)	Rec. SM (%)
1	1	-	99
2	2	-	99
3	4	-	99
4	8	-	99

Table 9.10

At this stage, we attributed the low reactivity with the hindrance of the α -centre, therefore the deprotonation stage of this overall reaction sequence was attempted at the elevated temperature of 0 °C in an attempt to boost reactivity (**Scheme 9.16**). Since at this stage we wanted to maximise the conversion towards product **147**, therefore the d.r. is not reported. Pleasingly, when the reaction was stirred at 0 °C for 1 h, the desired product **147** was observed with a good 60% conversion (entry 1 in **Table 9.11**). Increasing the reaction time to 2 h, caused an appreciable increase in the conversion to 73% (entry in **Table 9.11**), whilst increasing further showed no significant effect (entry 3 in **Table 9.11**).

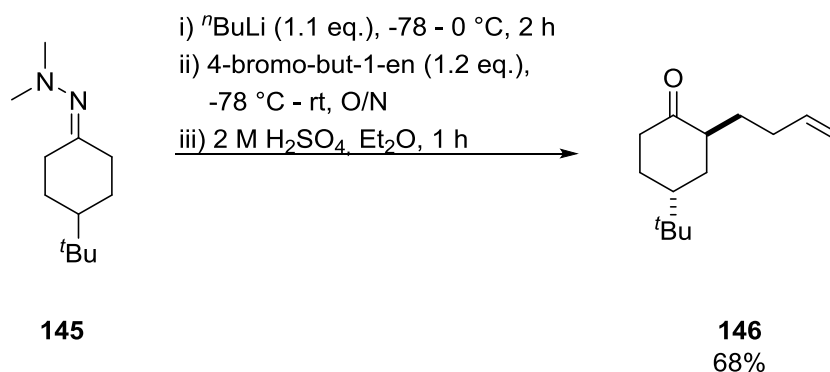


Scheme 9.16

Entry	Reaction time (h)	Conv. towards 147 (%)
1	1	60
2	2	73
3	4	62

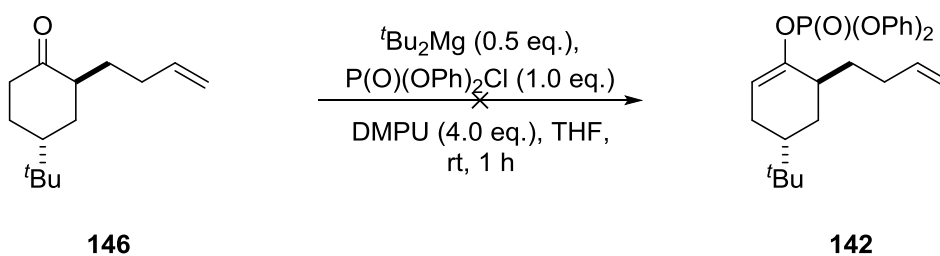
Table 9.11

As such, we considered the use of n-butyl lithium at 0 °C for 2 h optimal and we then turned to employing our desired electrophile, 4-bromo-but-1-ene (Scheme 9.17). To our delight, the desired product **146** was isolated in an appreciable 68% yield as a single diastereomer.



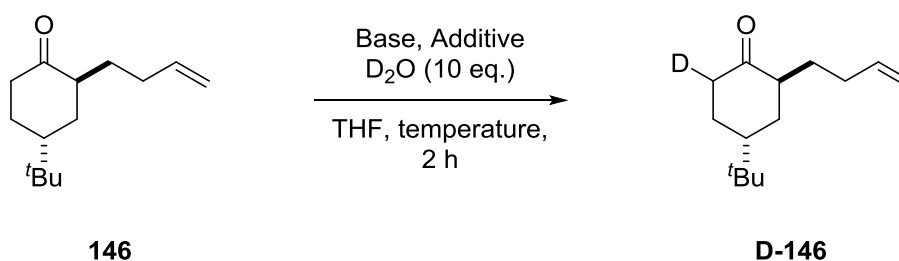
Scheme 9.17

Subsequently, the formation of the enol phosphate **142** was attempted using our previously reported conditions (Scheme 9.18).⁹⁵ Surprisingly, in this case, formation of the desired product was not detected at all, and the starting material **298** was recovered quantitatively.



Scheme 9.18

In relation to the above, we rationalised the observed lack of reactivity with the sterically hindered nature of the acidic α -hydrogen in **146** and the base. Indeed, our reported conditions had not been used before for α -substituted ketones. As such, to monitor whether the deprotonation process was occurring at all, D_2O was used as the electrophile and the reaction was examined using ${}^1\text{H}$ NMR spectroscopy (Scheme 9.19). At the same time, we explored the nature of the base and the additive present in the overall system. When the reaction was performed with di-*tert*-butylmagnesium under our standard conditions, deuterium incorporation into the α -position was not observed (entry 1 in Table 9.12). In an attempt to increase the kinetic basicity of the base, *via* the *in situ* formation of an ate complex,¹¹⁷ the reaction was attempted in the presence of lithium chloride (entry 2 in Table 9.12). Again, deuterium incorporation was not observed, even when the reaction temperature was increased to reflux (entry 3 in Table 9.12). When exploring alternative magnesium base reagents, the sterically less hindered Grignard analogue ${}^t\text{BuMgCl}$ offered no reactivity at 0 °C or rt (entry 4 and entry 5 in Table 9.12). However, we were extremely pleased to realise that the use of the less hindered magnesium species bismesitylmagnesium, a reagent whose use in similar deprotonation systems had been developed within our laboratory, delivered the desired product **D-146** with excellent deuterium incorporation of >99% (entry 6 in Table 9.12).

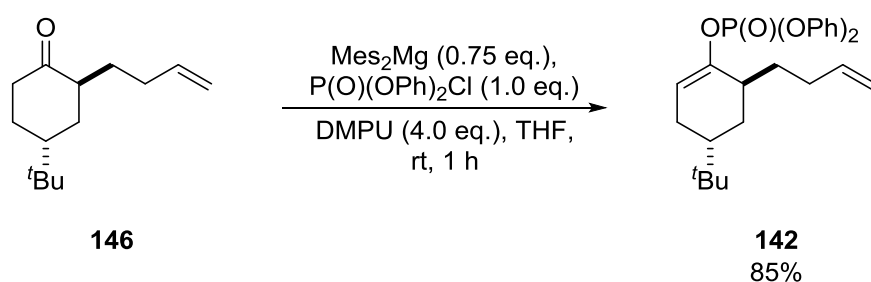


Scheme 9.19

Entry	Base (eq.)	Additive	Temp. (°C)	D incorporation (%)
1	^t Bu ₂ Mg (0.5)	DMPU (4.0 eq)	rt	0
2	^t Bu ₂ Mg (0.5)	LiCl (10.0 eq.)	rt	0
3	^t Bu ₂ Mg (0.5)	LiCl (10.0 eq.)	reflux	0
4	^t BuMgCl (1.0)	LiCl (10.0 eq.)	0	0
5	^t BuMgCl (1.0)	LiCl (10.0 eq.)	rt	0
6	Mes ₂ Mg (0.5)	DMPU (4.0 eq)	rt	>99

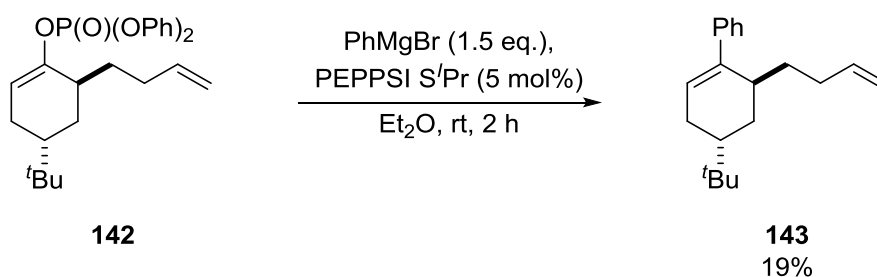
Table 9.12

Accordingly, when the formation of the enol phosphate **142** was attempted with these optimised conditions, to our delight, the desired product **142** was obtained with a high 85% yield (**Scheme 9.20**).



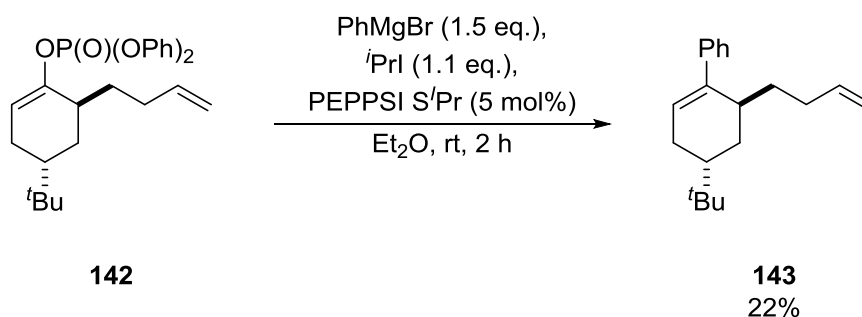
Scheme 9.20

With the target molecular probe in hand **142**, we were able to investigate the mechanism of the cross coupling reaction. As such, we employed **142** in the standard reaction protocol and isolated the coupling product **143** in a low 19% yield, (**Scheme 9.21**).



Scheme 9.21

The reaction was also performed in the presence of *iso*-propyl iodide, which is a common radical initiator in Kumada type couplings. In this case, the product **143** was obtained with a similar 22% yield (Scheme 9.23).



Scheme 9.22

Importantly, in the ^1H NMR spectrum of these experiments, signals associated with any cyclised product, such as that corresponding **144**, were not detected. This indicated that the reaction proceeded through a two electron pathway. Based up on these observations, a catalytic cycle for the formation of the homocoupled enol phosphate was suggested (Figure 9.4).

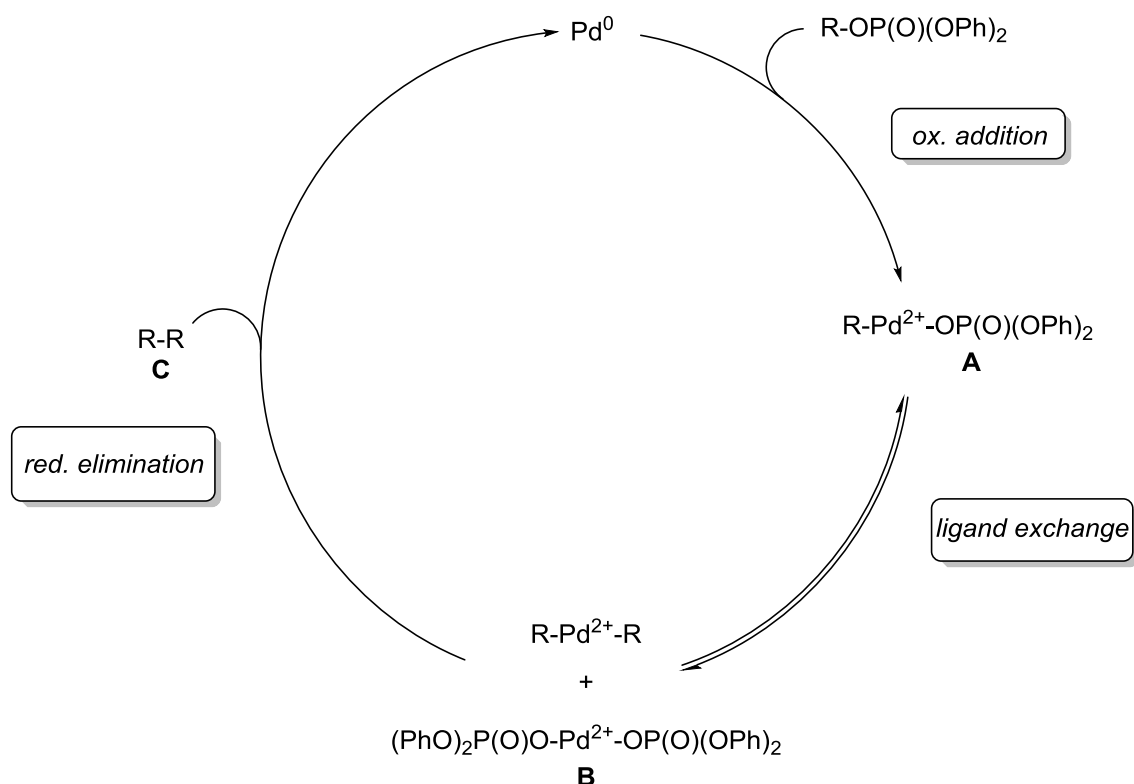
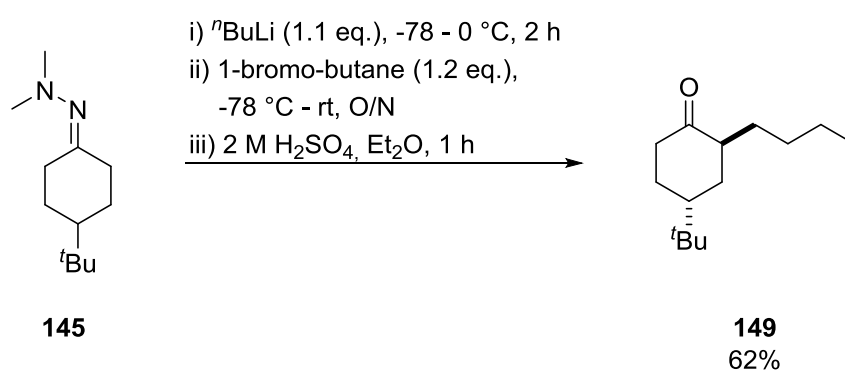


Figure 9.4

The cycle starts with the oxidative addition of the enol phosphate substrate to form **A**, this step is followed by a ligand exchange step between two palladium species, which could lead to the

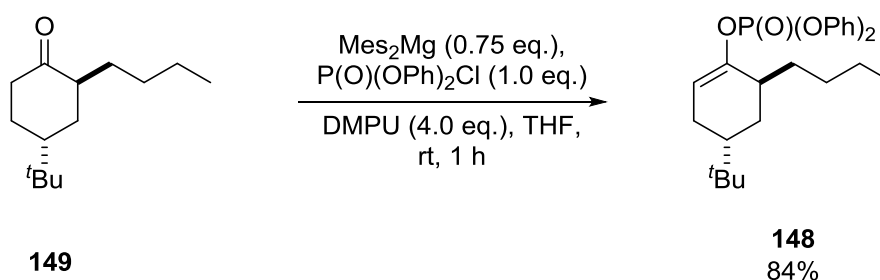
formation of Pd(II) phosphate **B**. At this point, reductive elimination would give rise to the observed homocoupled product **C** and regenerate the catalytically active species. In addition to this, if the Grignard reagent is present in excess, rapid transmetallation could push the equilibrium towards the formation Pd(0), which could explain why slow addition of the Grignard reagent required in order to synthesize the desired cross coupled in high yield.

As shown above, the reactivity of substrate **146** under the standard coupling conditions (with and without the additive) was significantly lower than the typical monosubstituted analogues **115** previously prepared. We attributed this reactivity difference to the sterically hindered environment that would result between the α -substituted ketone and the relatively large phosphonate electrophile. Consequently, the formation of a similar enol phosphate **148**, without the alkene group, was targeted via the same synthetic route described previously (**Scheme 9.23**). When alkylation was carried out with 1-bromo-butane, the product **149** was isolated in a good 62% yield.



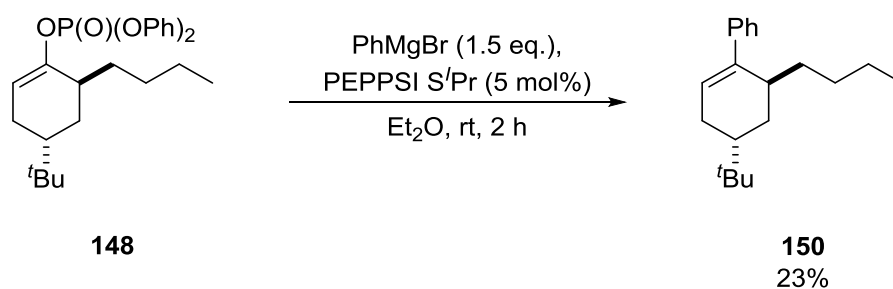
Scheme 9.23

Subsequently, the corresponding enol phosphate **148** was isolated in a high 84% yield using our optimised conditions with bismesitylmagnesium (**Scheme 9.24**).



Scheme 9.24

However, when the cross coupling reaction was carried out, again, a poor yield of the product **150** was obtained. This indicated that steric hindrance of the electrophile is likely responsible for the observed low yield (**Scheme 9.25**).

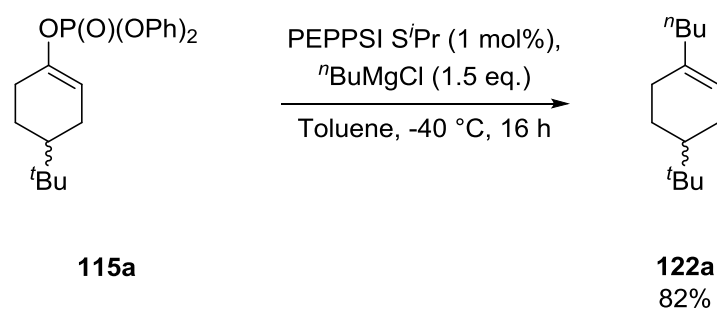


Scheme 9.25

Despite the low yielding result in relation to product **150**, our efforts turned to expand the cross coupling substrate scope with traditionally more challenging alkyl Grignard reagent partners. This would complement our array of phenyl-substituted compounds and provide a more diverse range of starting substrates for the key ozonolysis/reductive amination sequence that will ultimately deliver a range of highly desirable sp^3 -rich azepane structures.

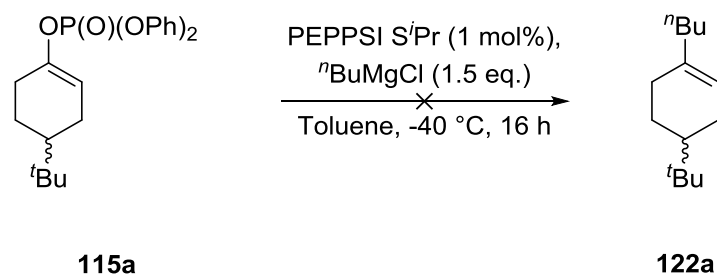
9.1.9 Extension of the Substrate Scope: Secondary Alkyl Grignard Reagents

Alkyl Grignard reagents are well known to be more challenging nucleophilic coupling partners due to their ability to undergo β -hydride elimination readily.¹¹⁸ Within our research group, very preliminary results in this area have shown *n*-butylmagnesium chloride to react successfully with enol phosphate **115a** (Scheme 9.26).⁹² Indeed, only 1 mol% of palladium catalyst was used and the desired product **122a** was isolated with a high 82% yield.



Scheme 9.26

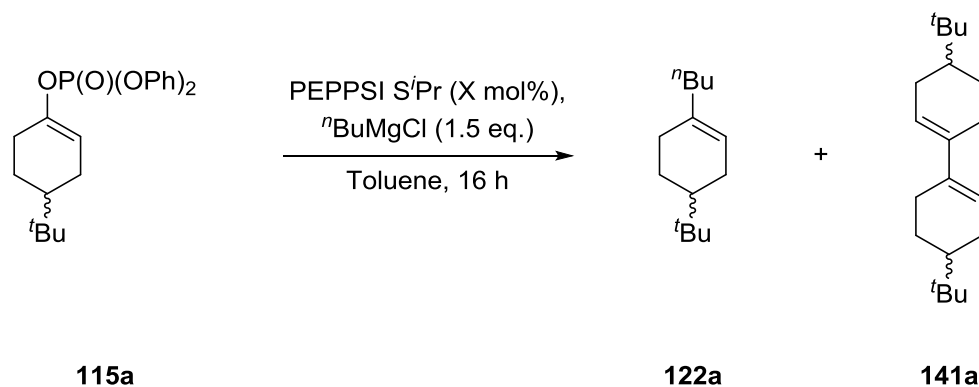
In an effort to build on this result, we first started our investigations with the replication of this reaction (Scheme 9.27). Surprisingly, when the reaction was performed under identical conditions no conversion towards the desired product **122a** was detected and the starting material **115a** was recovered in 96% yield.



Scheme 9.27

As such, it was decided that a re-investigation of this overall system was required. Initially keeping toluene as the reaction solvent for these studies, a series of changes in reaction temperature and catalyst loading were explored and the results are summarised in **Table 9.13**. In an attempt to increase the conversion, the amount of catalyst was increased from the very low 1 mol% to 7.5 mol% (entry 1 in **Table 9.13**). In this regard, only a minimal amount (<5%) of the desired product **122a** was observed. Indeed, it was envisioned that the low performance of the catalyst was due to the very low reaction temperature applied. Accordingly, and keeping at 1 mol% catalyst loading, we increased the reaction temperature to 0 °C (entry 2 in **Table 9.13**). Pleasingly, this resulted in the desired product **122a** being detected with a significantly higher (25%) conversion, although low amount of the homocoupled product **305a** was also observed. When the reaction was performed at even higher temperature (rt, entry 3 in **Table 9.13**), the cross coupled product **122a** was detected with a further increase to 38% conversion, but the undesired homocoupled enol phosphate **141a** was also detected in a relatively high ratio of 11%. One should note that the separation of the desired and undesired products was not trivial. Therefore, the reaction temperature was kept at 0 °C for further experiments and further explored the catalyst loading. Increasing from 1% to 2% (entry 4 in **Table 9.13**) further improved the reaction efficiency, however, it should be noted that when this reaction was repeated using the same vessel, varying, and often low, results were obtained (entry 5 in **Table 9.13**). At this point, it was considered that left over palladium in the glassware could catalyse the decomposition of the active palladium catalyst and prevent catalyst turnover. As such, in further experiments, the glassware was washed with *aqua regia* in order to remove any leftover palladium from the vessel (see experimental section for further details). To our delight, relatively good conversion was retained (entry 6 in **Table 9.13**). In addition to this, more polar, ethereal, solvents were also used as reaction medium (entry 8 and entry 9 in **Table 9.13**) but the desired product **122a** was obtained in a significantly lower 10% conversion with Et₂O and not at all with THF. The final two attempts in this optimisation process looked at the use of freshly prepared Grignard reagent as opposed to the commercial source. In fact, this proved very successful with a very good 71% conversion obtained when employing just 2 mol% of the catalyst (entry 10 in **Table 9.13**).

Indeed, in this case, we were also motivated to see that none of the undesired homocoupled product **141a** was present. Furthermore, when the catalyst loading was increased to 3 mol% (entry 11 in **Table 9.13**) the coupling product **122a** was obtained with an even higher 87% conversion, and no starting material **115a** or homocoupled product **141a** signals were observed upon analysis of the ^1H NMR spectrum of the crude reaction mixture.



Scheme 9.28

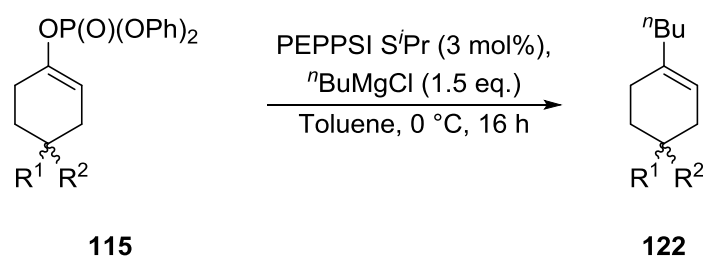
Entry	Temperature (°C)	Catalyst loading (mol%)	Unreacted 115a (%)	Product 122a (%)	Product 141a (%)
1	-40	7.5	95	<5	-
2	0	1	68	25	6
3	rt	1	51	38	11
4	0	2	44	44	8
5	0	2	74	21	4
6 ^a	0	2	56	40	4
7 ^{a,b}	0	2	58	38	4
8 ^{a,c}	0	2	90	10	-
9 ^{a,d}	0	2	-	-	-
10 ^{a,e}	0	2	29	71	-
11 ^{a,e}	0	3	-	87	-

^a: Glassware was washed with *aqua regia*, ^b: Dist. toluene was used as solvent, ^c: Diethyl ether was used as solvent, ^d: THF was used as solvent, ^e: Instead of commercial Grignard freshly prepared Grignard was used.

Table 9.13

With this newly established procedure in place for the coupling of our enol phosphate compounds with alkyl Grignard reagents, the substrate scope was tested using the range of enol phosphates **115** previously prepared (**Table 9.14**). As standard, all of these reactions were carried out initially using racemic starting materials with the ultimate aim of translating this to the asymmetric variant downstream (*vide infra*). When the phenyl substituted analogue **115b** was applied, we were pleased

to obtain the desired product **122b** in an impressive 80% yield (entry 1 in **Table 9.14**). Whilst the smaller 4-methyl substituted enol phosphate **115c** showed a good conversion, the coupled product **122c** was isolated in only 40% yield (entry 2 in **Table 9.14**). Indeed, and as mentioned previously, the volatile nature of the molecule rendered the isolation somewhat difficult. Finally, two disubstituted analogues were utilised as starting materials (entry 3 and entry 4 in **Table 9.14**). In both cases, the products **122d** and **122h** were obtained in good yields, 63% and 70%, respectively. It should be noted that, for this set of products, analysis by chiral HPLC was not possible at this stage, however, our enantio-enriched products were assessed in the previous step, i.e. at the enol phosphate stage, and we did not expect racemisation to occur during cross coupling conditions.

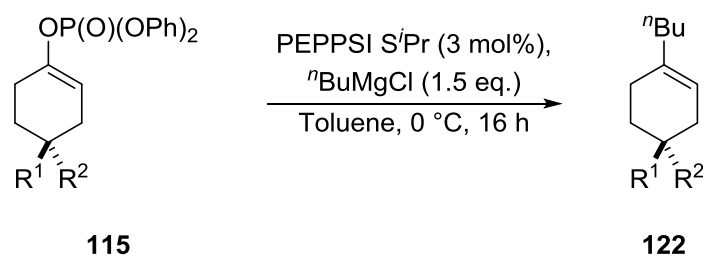


Scheme 9.29

Entry	Compound	R ¹ group	R ² group	Yield(%)
1	122b	Ph	H	80
2	122c	Me	H	40
3	122d	Ph	Me	63
4	122h	-OCH ₂ CH ₂ O-		70

Table 9.14

With the racemic compounds **122a-d** and **122h** in hand, attention turned towards the preparation of enantiomerically enriched coupling products **122**. As such, the previously prepared enantiomerically enriched enol phosphates **115** were subjected to the developed cross coupling protocol with similar results being obtained as compared to the racemic counterparts (*cf.* **Table 9.14** and **Table 9.15**). The enantiomers of the products **122** were not separable on chiral HPLC.

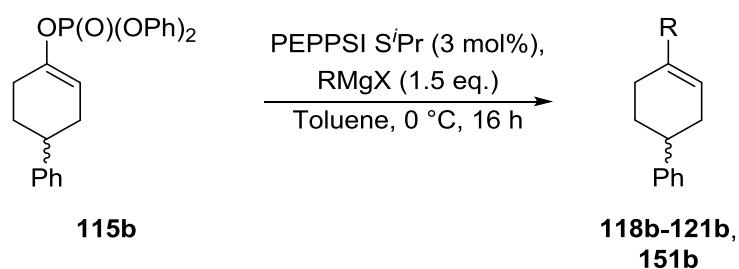


Scheme 9.30

Entry	Starting material (e.r.)	R ¹ group	R ² group	Yield(%)
1	115a (95:5)	^t Bu	H	88
2	115b (99:1)	Ph	H	76
3	115c (84:16)	Me	H	43
4	115d (86:14)	Ph	Me	62

Table 9.15

At this stage, a range of compounds had been prepared which derived from the cross coupling of either PhMgBr or *n*-BuMgCl. To further widen the range of compounds available to probe the synthetic sequence towards the azepane targets, further synthetic work focused on the application of secondary alkyl Grignard reagents in our optimised conditions (Table 9.16). When *iso*-propylmagnesium chloride was used as a coupling partner (entry 1 in Table 9.16), the desired product **121b** was isolated with a high 79% yield. Switching the halogen atom from chlorine to bromine (entry 2 in Table 9.16) had a negligible influence on the reaction outcome, and the desired product **121b** was isolated in an almost identical 80% yield. For the remainder of the substrate scope, alkylmagnesium bromide reagents were used due to the availability of the starting alkylbromides in our laboratory. The optimised conditions were also successfully expanded for the cross coupling of secondary cyclic alkenes. Indeed, the Kumada coupling reaction is frequently used in drug discovery projects.¹¹⁹ Furthermore, the preparation of such structures can significantly enhance the 3D character of candidate molecules, which is one of the key parameters during lead optimisation in the pharmaceutical industry.^{104,105} When cyclopentylmagnesium bromide was employed, **118b** was isolated in a high 84% yield (entry 3 in Table 9.16). Larger Grignard reagents were also coupled under these conditions, as demonstrated by the 6- and 7-membered variants (entry 4 and entry 5 in Table 9.16), whereby the products **119b** and **120b** were obtained in 90% and 78% yield, respectively. Coupling with a smaller Grignard reagent, namely cyclopropylmagnesium bromide, was successful however the reaction temperature required elevation to rt and the catalyst loading was also increased to 6 mol% (entry 6 in Table 9.16). Under these conditions, the desired product **151b** was isolated in a moderate 43% yield.



Scheme 9.31

Entry	Compound	R group	X group	Yield(%)
1	121b	ⁱ Pr	Cl	79
2	121b	ⁱ Pr	Br	80
3	118b	^c Pentyl	Br	84
4	119b	^c Hexyl	Br	90
5	120b	^c Heptyl	Br	78
6 ^a	151b	^c Propyl	Br	43

^a6 mol% catalyst was used and the reaction was performed at rt.

Table 9.16

The cross coupling of enantiomerically enriched enol phosphates with alkyl Grignard reagents was not carried out due to the lack of time and our attention was focused on the development of the ozonolysis-reductive amination steps of the sequence.

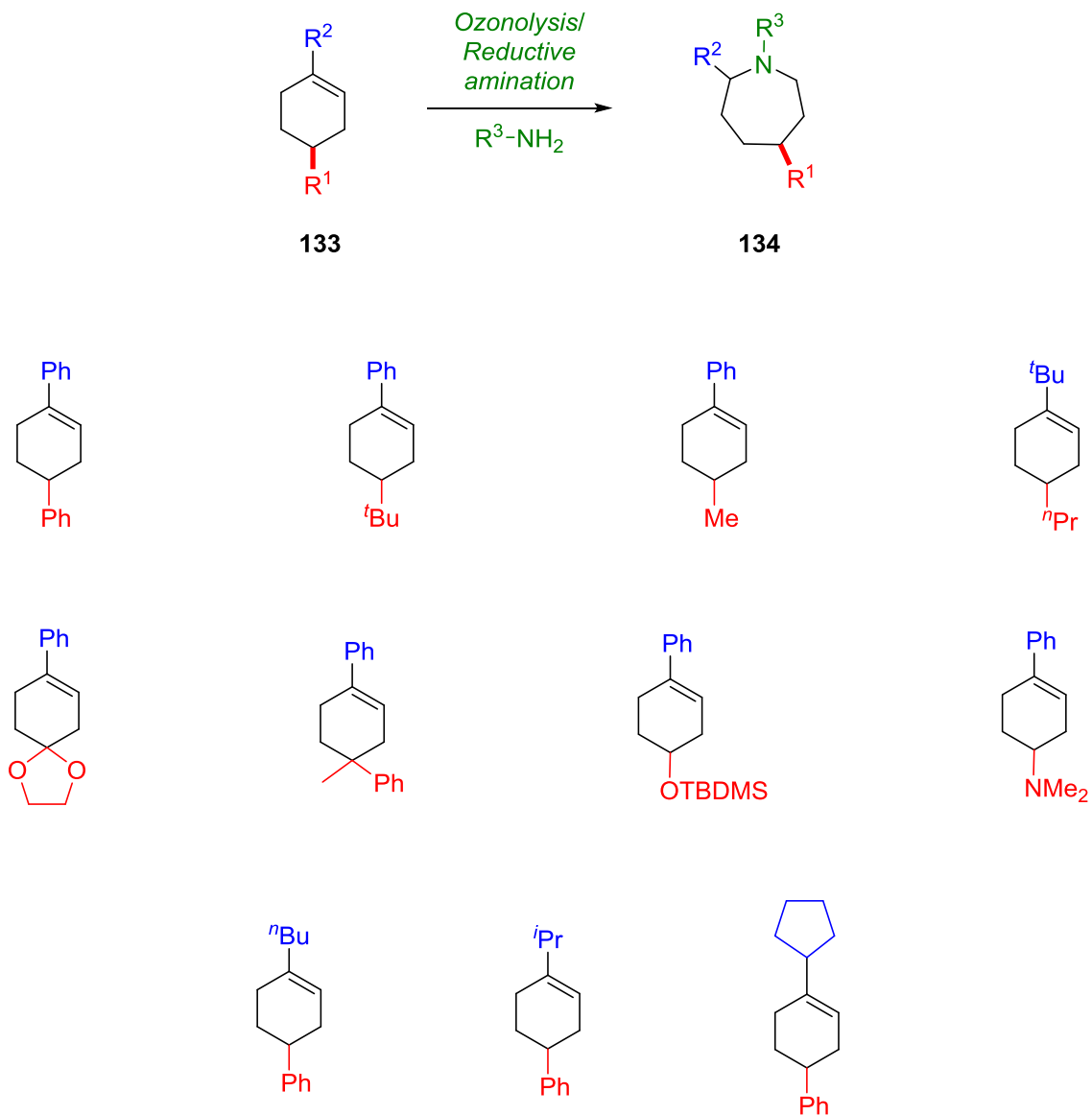
9.1.10 Summary for the Cross Coupling

With regards to the development of the above described cross coupling chemistry, at the outset, synthetic efforts concentrated on reacting our prepared enol phosphate structures of type **115** with phenylmagnesium bromide. Using 4-*tert*-butyl cyclohexanones **25a** as the standard starting substrate, the previously reported conditions delivered the desired coupled product in a significantly lower yield and a long purification step was required due to the formation of a homocoupled enol phosphate byproduct. As such, optimisation of the reaction conditions was successfully carried out, which ultimately delivered the desired product in a very high yield and without the detection of the undesired coupling product. With these newly developed conditions in hand, a series of racemic and enantiomerically enriched enol phosphates of type **115** were readily used as electrophiles in a highly efficient and mild coupling reaction with phenylmagnesium bromide.

Additionally, a mechanistic investigation of the reaction was also carried out using a carefully designed substrate **142** that would provide insight into the nature of the mechanism (radical-based or otherwise). This substrate was successfully synthesised through a three-step sequence and provided valuable information about the mechanism of the Kumada coupling. Ultimately, we believe that the process does not follow a single electron transfer mechanism.

With these results in hand, we focused our efforts on further expanding the substrate scope of the coupling reaction to primary and, more challenging, secondary alkyl Grignard reagents. This new method development neatly delivered a set of compounds that are primed to eventually deliver a

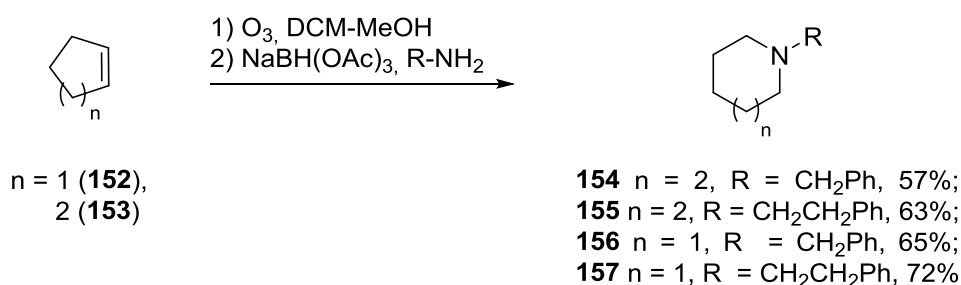
set of pharmaceutically interesting azepane structures *via* our proposed ozonolysis and reductive amination sequence. shows the array of substrates that have been prepared (**Scheme 9.32**).



Scheme 9.32

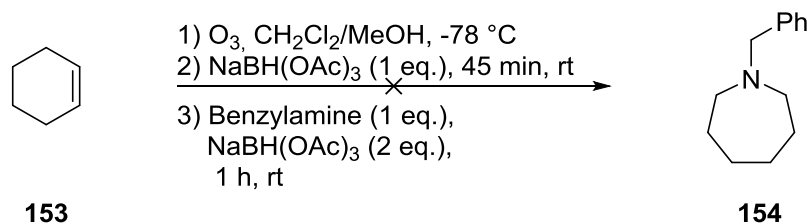
9.1.11 Ozonolysis-Reductive Amination

With the cross coupled products in hand, we focused our synthetic efforts on the development of an ozonolysis/reductive amination sequence for the synthesis of enantiomerically enriched azepanes. Indeed, a similar reaction has been reported in the literature, whereby a small series of piperidine and azepane structures have been prepared from cyclopentene and cyclohexene, respectively.¹²⁰ The structures were obtained in moderate to good yields 57-72% (**Scheme 9.33**). It was noted that a limited number of starting alkenes were tested and only alkyl amines had been explored in the reductive amination step, therefore, the products **154-157** obtained were relatively simple.



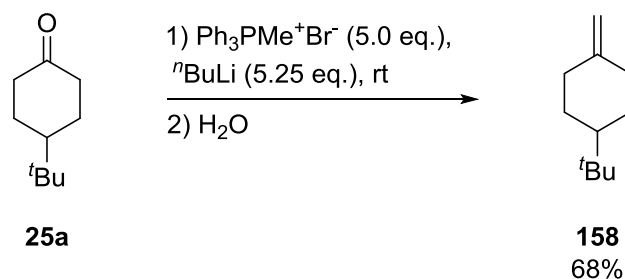
Scheme 9.33

At the outset, and to grasp the reaction procedure, cyclohexene **153** was employed in this one pot ozonolysis/reductive amination sequence. Following the literature publication,¹²⁰ in our hands, only decomposition products were detected on analysis of the crude ¹H NMR spectrum (**Scheme 9.34**).



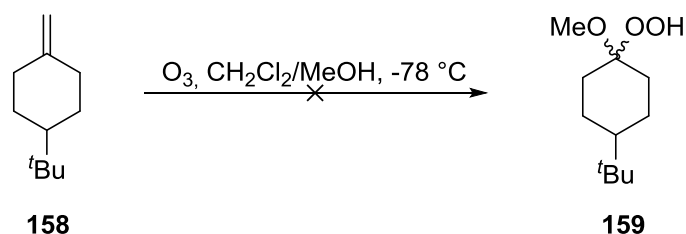
Scheme 9.34

In an attempt to investigate the failure of this reaction, the ozonolysis and reductive amination steps were investigated independently. First, the ozonolysis was attempted with an alternative reported substrate **25a** to prepare a stable alkylperoxide, 1-(*tert*-butyl)-4-methylenecyclohexane **158**, which was prepared by a Wittig reaction in a good 68% yield (**Scheme 9.35**).¹²¹



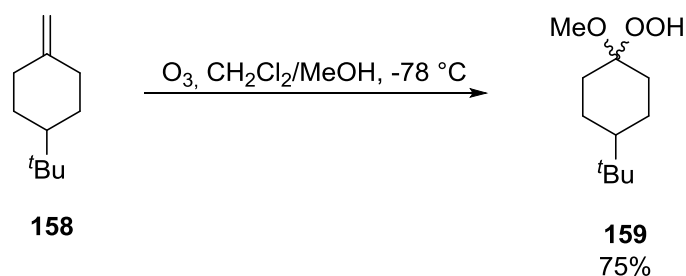
Scheme 9.35

When the ozonolysis was first carried out with **158**, only decomposition products were detected (Scheme 9.36). At this point, we reasoned that even if the desired product **159** was formed, it is likely decomposed under the ozonolysis conditions.



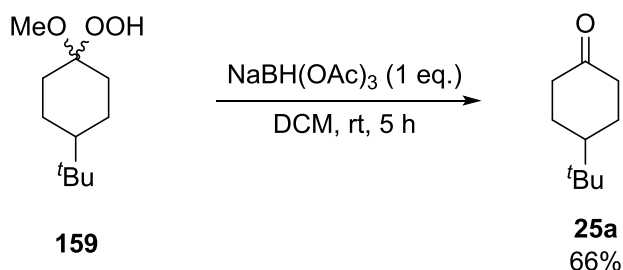
Scheme 9.36

Therefore, extra care was taken to ensure that the ozone flux was immediately stopped after the appearance of the blue colour (unreacted ozone). Any prolonged reaction time was found to be detrimental for a successful reaction. In addition to this, a high stream of oxygen was used to remove the traces of ozone from the solution as soon as possible, in order to prevent the formation of highly oxidised by-products (Scheme 9.37).¹²² With these new conditions, the product **159** was obtained in a high 75% yield, similar to the reported value in the literature (74%).¹²⁰



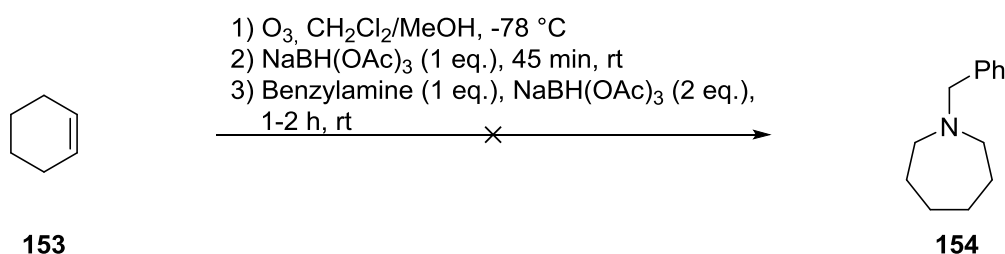
Scheme 9.37

Subsequently, substrate **159** was subjected to the reduction and, as anticipated, ketone **25a** was obtained in a good 66% yield, indicating that the reduction step was also successful (Scheme 9.38).



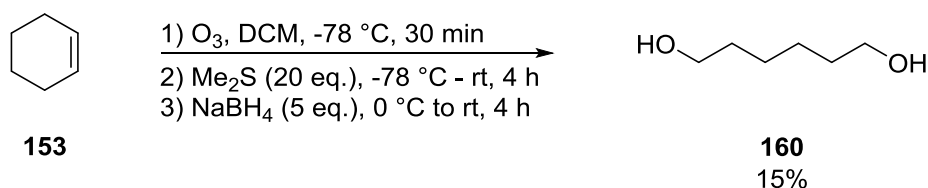
Scheme 9.38

With these encouraging results in hand, we employed these modified ozonolysis conditions with cyclohexene **153**. Unfortunately, no desired product **154** peaks were observed in the ^1H NMR spectrum of the crude mixture (**Scheme 9.39**).



Scheme 9.39

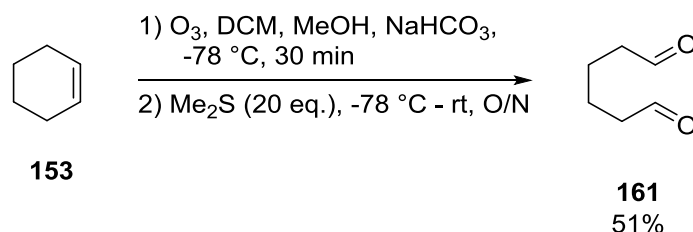
In addition, in attempt to validate our ozonolysis conditions the crude mixture was analysed by ^1H NMR and a no starting material **153** was observed. Although, when the crude mixture was added to a solution of sodium borohydride after quenching the reaction with dimethyl sulfide, the expected diol product **160** (15%) was isolated with a low 15% yield (**Scheme 9.40**), indicating that the aldehyde or the peroxide intermediate is not stable under the reaction conditions.



Scheme 9.40

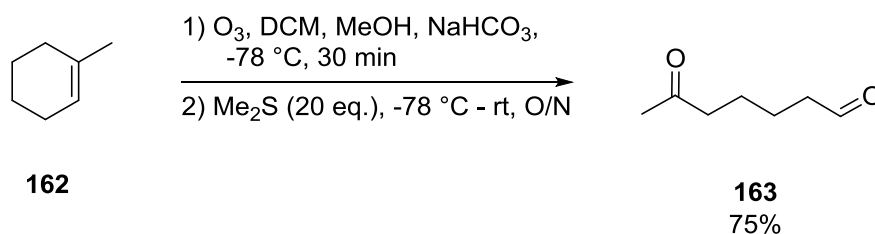
At this point, a systemic search for alternative ozonolysis conditions was performed, and it was found that the Schreiber group had reported an alternative protocol for the ozonolysis of cyclic substrates, whereby sodium bicarbonate was added to buffer the pH of the solution and likely aid the formation of the hemiacetal adduct in methanol.¹²³ It was suggested that the addition of sodium bicarbonate is essential since the aldehyde-alkoxy hydroperoxide, produced after the ozonolysis step, often forms oligomers and decomposed before the reductive amination step.¹²³ As such, it

was decided that, quenching the peroxy aldehyde in situ would afford the dialdehyde **161**, would be targeted, given that it is likely to be a more stable than the peroxy intermediate. Therefore, after the completion of the ozonolysis step, dimethyl sulfide was added to quench the formed alkoxy hydroperoxide immediately. To our delight, following this protocol resulted in the dialdehyde **161** being obtained in a significantly higher 51% yield (**Scheme 9.41**).



Scheme 9.41

Thereafter, and in an attempt to conserve stocks of the previously prepared cross coupled products whilst scoping out the reaction conditions, a structurally similar trisubstituted cycloalkene **162** was employed in the developing ozonolysis reaction (**Scheme 10.105**). In this case, desired keto-aldehyde **163** was obtained with an even higher 75% yield (entry 1 in **Table 9.17**). The reaction was then successfully performed at an elevated scale and the product **163** was isolated in an improved 83% yield (entry 2 in **Table 9.17**).

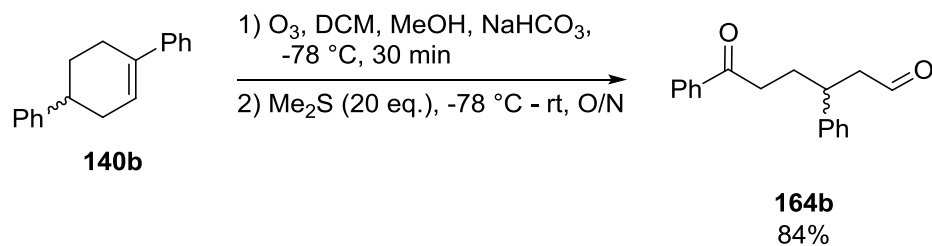


Scheme 9.42

Entry	Scale (mmol)	Yield (%)
1	1	75
2	3	83

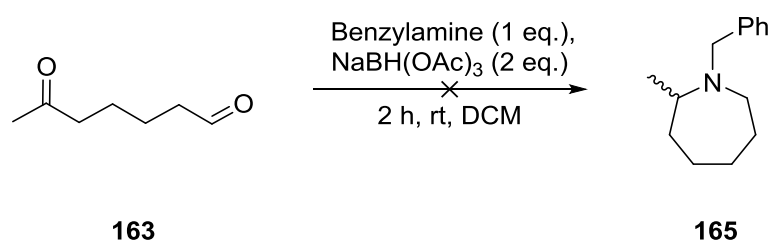
Table 9.17

Given the success above, we then looked to apply one of our previously prepared (racemic) cross coupled products. In this regard, substrate **140b** was reacted and, pleasingly, the desired product **164b** was obtained in a similarly high 84% yield (**Scheme 9.43**).



Scheme 9.43

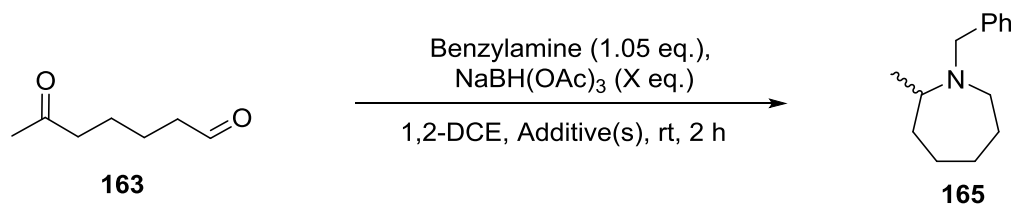
Next, the reductive amination step was examined using previously prepared, model, substrate **163**. Under the originally reported conditions,¹²⁰ none of the desired product **165** was observed upon analysis of the ¹H NMR spectrum (Scheme 9.44).



Scheme 9.44

Therefore, further optimisation of the reductive amination reaction conditions was performed. Upon reviewing the literature, a recent review¹²⁴ showed 1,2-DCE as a superior solvent for this reaction, and attributed this to the fact that highly nucleophilic amines can react with DCM.¹²⁵ In addition to the solvent, we also envisioned that the pH of the solution would dramatically influence the overall reaction pathway. It has been noted that, under standard conditions, if one equivalent of organic acid is added, the rate of the reductive amination drastically increases with ketones.¹²⁴ Accordingly, our subsequent reactions probed the effect of pH *via* the addition of acetic acid and/or the effect of utilising sodium acetate as a buffer additive. Our results, using 1,2-DCE as the solvent, are summarised in **Table 9.18**. Interestingly, when the reaction was performed in 1,2-DCE instead of DCM, in the absence of any additive, the desired product **165** was detected with a 22% conversion (entry 1 in **Table 9.18**). When 1 eq. of sodium acetate and 1 eq. of acetic acid was added, the product **165** was obtained in a similar 18% conversion (entry 2 in **Table 9.18**). Indeed, when these additives were added individually (entry 3 and entry 4 in **Table 9.18**), the product azepane **165** was not observed at all, and, in both cases, decomposition of the starting material **163** was detected. Thereafter, the quantity of reducing agent, NaBH(OAc)₃ probed; increasing to 2.8 eq. resulted in a significant increase in the conversion 44% (entry 5 in **Table 9.18**), however, increasing further did not further elevate the efficiency for the reaction, and the product **165** was observed with an almost identical 43% conversion (entry 6 in **Table 9.18**). Finally, the amount of benzylamine was also

doubled, to 2.10 eq., in an attempt to further increase the conversion, however, the desired product **165** was obtained, again, with a similar 46% conversion (entry 7 **Table 9.18**).



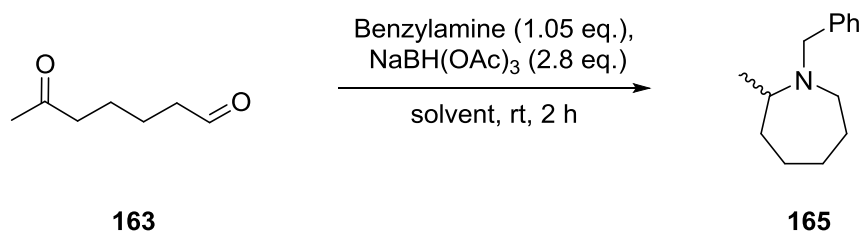
Scheme 9.45

Entry	NaBH(OAc) ₃ (eq.)	Additive(s) (eq.)	Conversion (%)
1	1.4	-	22
2	1.4	AcOH (1), NaOAc (1)	18
3	1.4	AcOH (1)	-
4	1.4	NaOAc (1)	-
5	2.8	-	44
6	4.2	-	43
7^a	2.8	-	46

^a2.10 eq. benzylamine was used instead of 1.05.eq.

Table 9.18

Given that switching the solvent from DCM to 1,2-DCE had a positive impact on the reaction outcome, a series of alternative polar solvents were explored for our novel reductive amination step (**Table 9.19**). When the reaction was carried out in THF, with the aim to potentially facilitate the formation of polar intermediates, a lower conversion of 28% was detected (entry 1 in **Table 9.19**). It is likely that the conversion was affected by the solubility of the reducing agent; in this case, a solid-liquid biphasic mixture was obtained at the end of the reaction. Thereafter, alternative polar solvents, such as EtOAc, DMC and IPA were also explored (entries 2-4 in **Table 9.19**), however, the desired product **165** was obtained with low conversion in every case. Finally, when CPME was used as the reaction medium, we were extremely pleased to find that a substantially higher conversion of 70% was observed towards the desired azepane product **165** (entry 5 in **Table 9.19**). It could be reasoned that the immiscibility of water in CPME was favourable in terms of driving the required imine formation as part of the overall process. After isolation and workup, the product **165** was obtained with a high 71% yield.



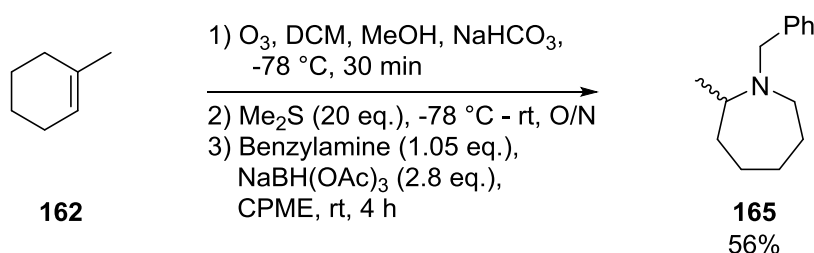
Scheme 9.46

Entry	Solvent	Conversion (%)
1	THF	28
2	EtOAc	10
3	DMC	<5
4	IPA	<5
5	CPME	70 (71) ^a

^aisolated yield

Table 9.19

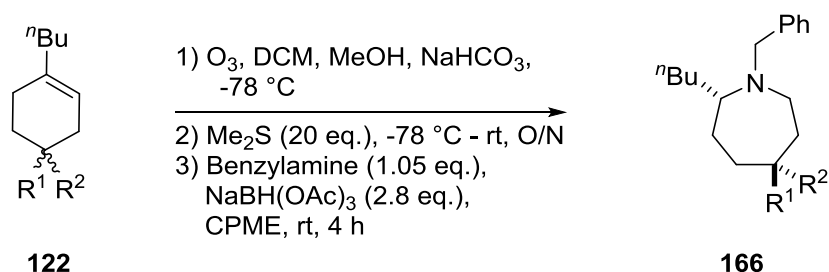
Finally, when the ozonolysis/reductive amination sequence was carried out in the intended telescoped fashion, without the isolation of aldehyde intermediate **163**, we were delighted to obtain the product **165** in a 56% yield (Scheme 9.47).



Scheme 9.47

Turning to a set of our prepared alkenes **122** (obtained *via* enol phosphate formation and subsequent, alkyl, cross coupling reaction), we applied the optimised reaction conditions as described above (Table 9.20). Across the board, yields in the range of 45-54% were achieved over this multi-step but telescoped procedure. When the *tert*-butyl-substituted substrate **166a** was employed (entry 1 in Table 9.20), to our delight, the desired azepane **166a** was obtained with a good 50%. Importantly, only one diastereomer was detected after the reaction, and the relative stereochemistry of the product was realised after debenylation and *via* 2D NMR techniques (*vide infra*). Altering the substituent at the 4-position for an aryl group, as in **122b**, had a minor impact on the reaction outcome and the target 7-membered heterocycle **166b** was isolated with a similar 54% yield (entry 2 in Table 9.20). Smaller substituents are also tolerated, as shown with the 4-methyl-substituted analogue **166c** (entry 3 in Table 9.20), albeit with a slightly reduced reaction yield to

45%. We also demonstrated that quaternary stereocenters can also be included in the structure (entry 5 in **Table 9.20**) and that the product **166d** was obtained in a 54% yield. Finally, the ketal functionality was tolerated in the sequence (entry 5 in **Table 9.20**) and the desired product **166h** was isolated in a good 52%.

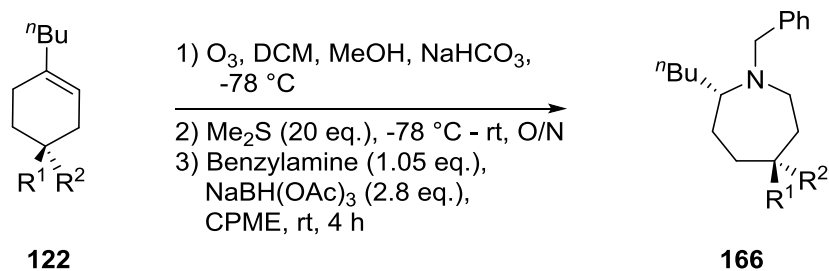


Scheme 9.48

Entry	Product	R ¹ group	R ² group	Yield(%)
1	166a	^t Bu	H	50
2	166b	Ph	H	54
3	166c	Me	H	45
4	166d	Ph	Me	54
5	166h	-OCH ₂ CH ₂ O-		52

Table 9.20

The above reactions used racemic starting materials **122**. Indeed, the ultimate aim was to generate optically active azepane structures **166**, and, therefore, attention turned towards employing our previously prepared enantiomerically-enriched cross coupling substrates **122**. (**Table 9.21**). In general, similar yields were obtained as compared to the racemic reactions (*cf.* **Table 9.20** and **Table 9.21**). Again, when the chiral 4-phenyl-substituted alkene **122a** was used as a starting material (entry 1 in **Table 9.21**), the target azepane **166a** was obtained in a good 51% yield and a high e.r. of 93:7. Indeed, we were delighted to see that the enantiomeric ratio was retained from the enol phosphate stage, i.e. no racemisation occurred during the full reaction sequence. The 4-phenyl-substituted molecule **166b** was also successfully prepared with a 53% yield being obtained and an excellent 99:1 e.r. (entry 2 in **Table 9.21**). The smaller methyl variant **166c** was also isolated, albeit with a slightly lower 48 % yield as compared to the racemic reaction, but with high e.r. 82:18 (entry 3 in **Table 9.21**). Finally, the quaternary stereocenter **166d** was also implemented in the structure with a 87:13 e.r. and 54% yield (entry 4 in **Table 9.21**).

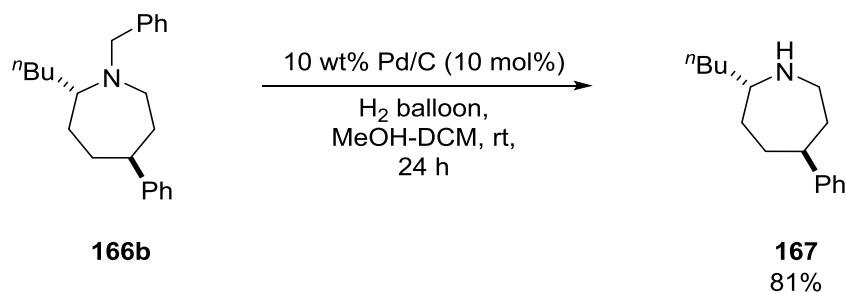


Scheme 9.49

Entry	Product	R ¹ group	R ² group	Yield(%)	E.r. of product 166	E.r. of enol phosphate 166
1	166a	^t Bu	H	51	93:7	93:7
2	166b	Ph	H	53	99:1	99:1
3	166c	Me	H	48	82:18	84:16
4	166d	Ph	Me	54	87:13	86:14

Table 9.21

Thereafter, deprotection of the benzyl group was carried out under extremely mild conditions to deliver the targeted core azepane **167**, functionalised at the 2- and 5-positions (Scheme 9.50).¹²⁶



Scheme 9.50

The relative stereochemistry of **167** was determined by 2D NMR spectroscopic experiments to be that shown in Figure 9.5. Indeed a strong nOe was observed between the α -CH and one of the α -CH₂ hydrogen at 2.73 and 3.20 ppm, respectively (red protons in Figure 10.16) and no correlation was detected between the benzylic hydrogen at 2.68 ppm and the same α -CH₂ hydrogen at 3.20 ppm. As such, the relative stereochemistry of the prepared azepane **167** was assigned tentatively as *trans*.

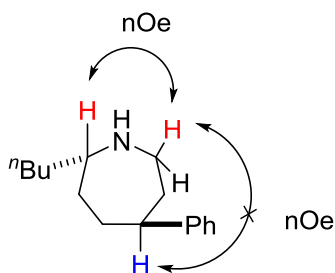
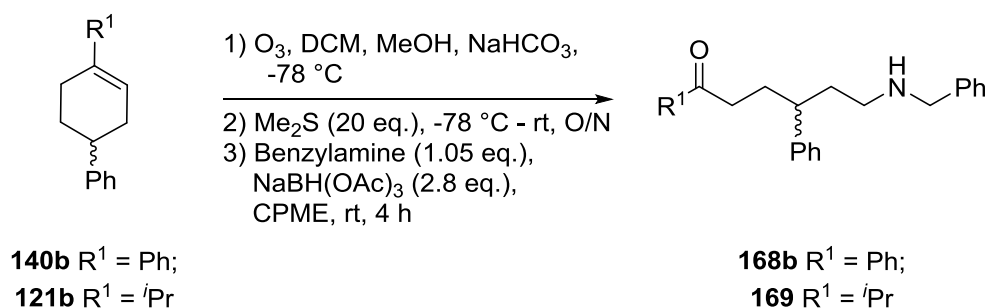


Figure 9.5

Having successfully prepared a series of enantiomerically enriched azepane structures derived from the *n*-butyl containing alkenes of type **122**, we continued towards the synthesis of additional azepane structures using the remaining phenyl and secondary alkyl cross coupling products. This would diversify the range of azepane structures attainable *via* this practically accessible method.

9.1.12 Further Azepane Targets

As mentioned above, attention next turned towards the expansion of the substrate scope to deliver a further array of chiral azepane structures. In this regard, both the phenyl-substituted alkene **291b** and a the *iso*-propyl derivative **304** were subjected to the telescoped ozonolysis-reductive amination conditions (**Table 9.22**). In both cases, the corresponding ring opened products (**327b** and **328**) were isolated in moderate yields (entry 1 and entry 2 in **Table 9.22**). It was clear that such compounds had derived from initial ozonolysis followed by the first reductive amination step, with the second reductive amination to cyclise the molecule not occurring.



Scheme 9.51

Entry	Product	R ¹ group	Yield(%)
1	168b	Ph	52
2	169	<i>i</i> Pr	59

Table 9.22

Although these substrates were originally not targeted, a literature search revealed that such ϵ -amino ketone compounds have previously been reported as important motifs in the study of biological systems (Figure 9.6).^{127,128}

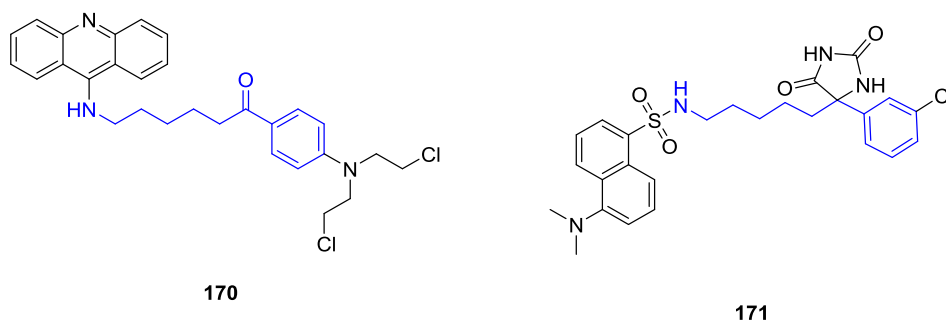
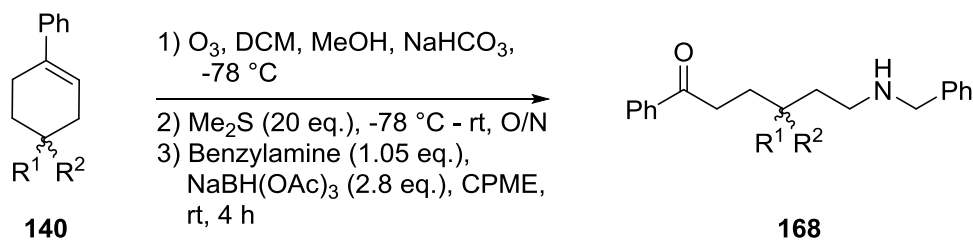


Figure 9.6

Molecule **170** was reported as a potent DNA directed alkylating agent of cancer cell lines,¹²⁷ while molecule **171** was reported as a fluorescent analogue of phenytoin and reported as a neurotic pain inhibitor.¹²⁸ Synthetically, several steps were required to prepare the corresponding targets **170** and **171**, with some of these being very low yielding. In relation to that above, we believe that our tandem ozonolysis/reductive amination sequence offers a significant advantage for the preparation of these type of molecules. Indeed, our process is an incredibly short sequence, with only one chromatographic isolation required when starting from the cyclic alkene stage. Furthermore, with our novel strategy, the preparation of chiral analogues is also readily achievable. Indeed, regarding the previous strategies, the preparation of chiral analogues was unreported.

Based on this, using our series of (racemic) phenyl-substituted alkene starting substrates **140**, a library of differentially substituted ϵ -amino ketones **168** were synthesised using our methodology (Table 9.23). Across the board, moderate to good yields (44-60%) of the desired ϵ -amino ketones **168** were achieved. A range of alkyl substituents **168a**, **168g** and **168c** were tolerated, providing yields in the region of 53-58% (entries 1-3 in Table 9.23). Quaternary centres can also be included in the structure, as shown with substrate **140d**, where the more heavily substituted product **168d** was isolated in a good 59% yield (entry 4 in Table 9.23). Oxygen heteroatoms are also accepted, as shown in entry 5 in Table 9.23 where the silyl protected product **168e** was obtained with a slightly lower 44%. Finally, the desired product **168h** was isolated with a good 60% yield (entry 6 in Table

9.23). Notably, products such as **168e** and **168h** would also allow for further diversification using the heteroatom as a functional handle.

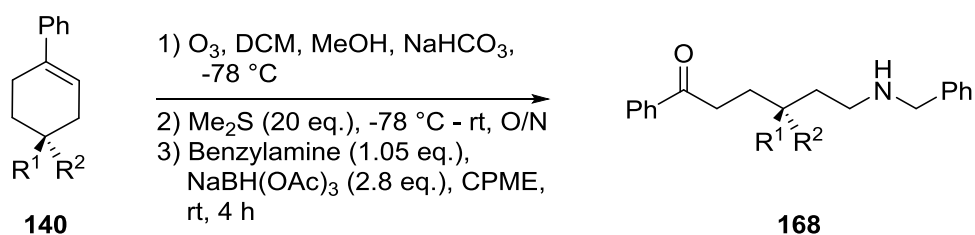


Scheme 9.52

Entry	Product	R ¹ group	R ² group	Yield(%)
1	168a	^t Bu	H	54
2	168g	ⁿ Pr	H	53
3	168c	Me	H	58
4	168d	Ph	Me	59
5	168e	OTBDMS	H	44
6	168h	-OCH ₂ CH ₂ O-		60

Table 9.23

In relation to the above, we also employed our enantiomerically enriched substrates **140** in this process, delivering a range of optically active ϵ -amino ketones **168** as shown in **Table 9.24**. When chiral substrate **140a** was applied, the desired product **168a** was isolated in a similar 52% yield as compared with the racemic counterpart, and with an excellent 94:6 e.r. (entry 1 in **Table 9.24**). With the phenyl substituted cyclic alkene **140b**, the desired product **168b** was isolated with a moderate 54% yield and outstanding 99:1 e.r (entry 2 in **Table 9.24**). The smaller alkyl variants **140g** and **140c** (entry 3 and entry 4 in **Table 9.24**) also delivered their corresponding ϵ -amino ketones **168g** and **168c** in an efficient manner, as did the substrate bearing a quaterner stereocenter **140d** (entry 5 in **Table 9.24**) Finally, when the silyl protected analogue was used, **168e**, as observed with the racemic analogue, the yield obtained was slightly lower at 42% yield, however, a high 95:5 e.r. was retained (entry 6 in **Table 9.24**). It is important to note that, in every case, the e.r. of the ϵ -amino ketone products **168** were in alignment with initial chiral enol phosphate starting material **115** prepared *via* the asymmetric deprotonation with chiral magnesium amide base (*R,R*)-**63** (*vide supra*).

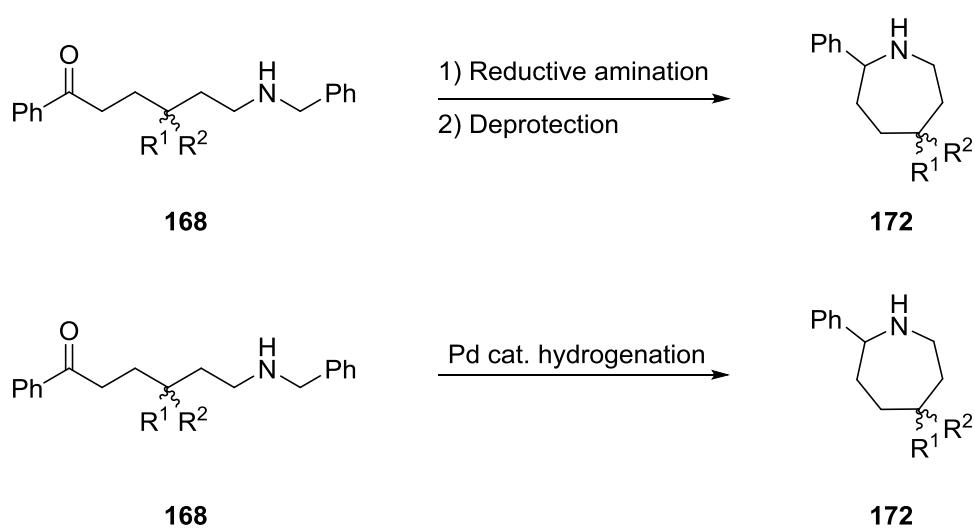


Scheme 9.53

Entry	Product	R ¹ group	R ² group	Yield(%)	E.r. of product 168	E.r. of 140
1	168a	^t Bu	H	52	94:6	93:7
2	168b	Ph	H	54	99:1	99:1
3	168g	ⁿ Pr	H	54	90:10	91:9
4	168c	Me	H	61	86:14	84:16
5	168d	Ph	Me	60	88:12	86:14
6	168e	OTBDMS	H	42	97:3	95:5

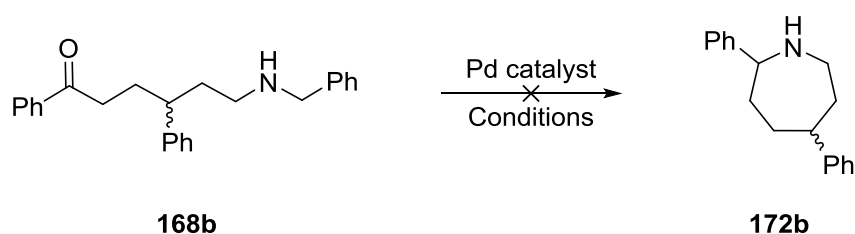
Table 9.24

Whilst we have described that such ε-amino ketones are intriguing and biologically useful compounds in their own right, we returned to focus on our original aim, which was to obtain a series of azepane structures. In relation to this, two alternative strategies were envisioned to obtain the desired 7-membered cyclic amines of type **172**; (i) direct, intramolecular, reductive amination of the ε-amino ketones, followed by a separate debenzoylation step or (ii) exploring a palladium catalysed debenzoylation, followed an *in situ* ring closure (Scheme 9.54).



Scheme 9.54

Since the latter sequence had the potential to deliver the desired targets in just one step, efforts were initially focused on exploring palladium catalysed hydrogenation methods (**Table 9.25**). When palladium on charcoal and a hydrogen balloon were used, we were disappointed to detect no product formation, and, in fact, the starting material **168b** was recovered in a 95% yield (entry 1 in **Table 10.41**). Thereafter, the more active Pearlman's catalyst was used, which has been previously reported for the debenzoylation of acyclic secondary amines.¹²⁹ Unfortunately, in our case, with even this more reactive catalyst, the desired product **172b** was not detected and decomposition of the starting material **168b** occurred (entry 2 in **Table 10.41**). Finally, the reaction temperature was increased to reflux and, due to safety reasons, the hydrogen source was changed to ammonium formate (entry 3 in **Table 10.41**).¹³⁰ Disappointingly, the desired product **172b** was, again, not observed.



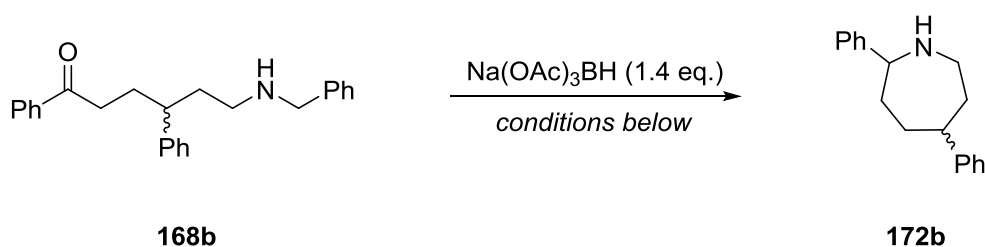
Scheme 9.55

Entry	Pd catalyst	Hydrogen source	Conditions	Recovered SM (%)	Comment(s)
1	Pd/C (10 mol%)	H ₂ balloon	MeOH-DCM, rt, 1 d	95	-
2	Pd(OH) ₂ (30 mol%)	H ₂ balloon	THF- <i>i</i> -PrOH, rt, 1 d	-	Decomposition was detected
3	Pd/C (16 mol%)	NH ₄ HCO ₂ (5.0 eq.)	MeOH, reflux, 90 min	46	Decomposition was detected

Table 9.25

Due to the encountered difficulties, our attention turned towards the reductive amination/debenzoylation strategy, since it has been reported with less hindered primary amines, such as benzylamine, for the synthesis of 6-¹³¹ and 7-membered^{132,133} nitrogen containing heterocycles. Furthermore, we were also confident that we could successfully remove the benzyl protecting group post reductive amination, given that this had previously worked effectively on a similar substrate (*vide supra*). As such, a range of conditions involving sodium triacetoxyborohydride as the reducing agent were explored and are summarised in **Table 9.26**. First, it was envisaged that the second ring closing reductive amination could be achieved through the use of higher temperatures, since both the reacting sites in our substrate were sterically hindered. However, when

the reaction was carried out in refluxing toluene (entry 1 in **Table 9.26**), the desired product **172b** was not detected and the unreacted starting material **168b** was returned in 95% yield. Since the solubility of the reducing agent is limited in toluene, the reaction was performed in CPME, which was successfully employed as the solvent in our initial reductive amination examples (*c.f.* **Tables 10.36 and 10.37**). Unfortunately, with even this solvent mostly unreacted starting material **168b** was obtained (entry 2 in **Table 9.26**). In an effort to increase the overall reactivity of this substrate, 1 eq. of acetic acid was added, although a similar reaction profile was observed (entry 3 in **Table 9.26**). In a further attempt to force the initial imine formation, molecular sieves were added to the reaction mixture, however, again, only starting material **168b** was obtained (entry 4 in **Table 9.26**). Further efforts included employing the use of microwave heating, however, when the reaction was heated to 120 °C for 2 h, none of the desired product **172b** peaks were observed and, in fact, degradation of the starting material **168b** had occurred with only 40% being returned on this occasion (entry 5 in **Table 9.26**). At this stage, a literature survey was carried out and it was realised that a series of additives had been reported to facilitate the reductive amination of sterically hindered amines. In this regard, Alexakis' method was used,¹³⁴ whereby titanium *iso*-propoxide is used in excess and in a solvent free environment (entry 6 in **Table 9.26**). Unfortunately, the desired product **172b** was not detected. Nonetheless, we attempted to modify Alexakis' protocol by repeating this reaction in the presence of CPME as the reaction medium, but to no product **172b** formation was detected (entry 7 in **Table 9.26**). Alternative Lewis acids such as nickel(II) chloride and zinc(II) chloride were also tried as additives based upon literature precedents.^{135,136} In these cases, the desired product **172b** was not observed (entry 8 and entry 9 in **Table 9.26**). Finally, Hartley *et al.* reported alternative reductive amination conditions for the synthesis of piperidine alkaloids.¹³⁷ In this system, TMSCl was added as a drying agent to react with the by-product water. Unfortunately, following this procedure on our molecule had no effect (entry 10 in **Table 9.26**).

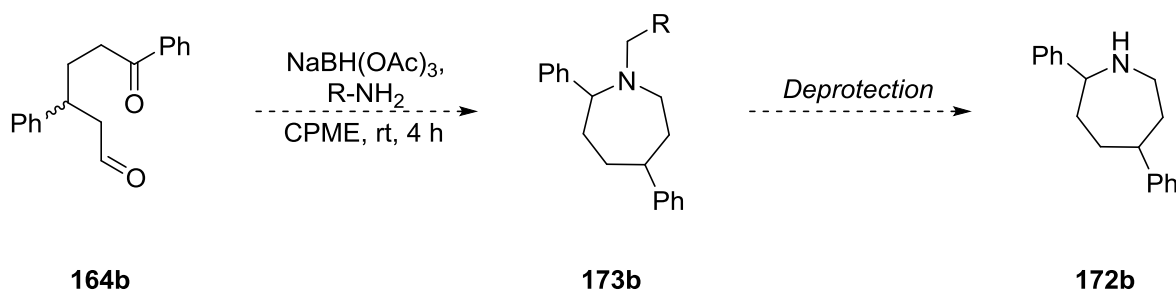


Scheme 9.56

Entry	Conditions	Unreacted 168b (%)	Product 172b (%)
1	toluene, reflux, O/N	95	-
2	CPME, reflux, O/N	80	-
3	CPME, reflux, O/N, AcOH (1.0 eq.)	90	-
4	CPME, reflux, O/N, AcOH (1.0 eq.), 4 Å mol. sieves	95	-
5	CPME, μ w, 120 °C, 2 h	40	-
6	Ti(O ⁱ Pr) ₄ (3.03 eq), 110 °C, O/N	90	-
7	Ti(O ⁱ Pr) ₄ (3.03 eq), CPME, reflux, O/N	95	-
8	ZnCl ₂ (3.03 eq), CPME, reflux, O/N	-	-
9	NiCl ₂ *6 H ₂ O (3.03 eq), CPME, reflux, O/N	95	-
10	i) TMSCl (5.0 eq.), DCM, rt, O/N ii) NaBH(OAc) ₃ (2.8 eq.), DCM, rt, 36 h	60	-

Table 9.26

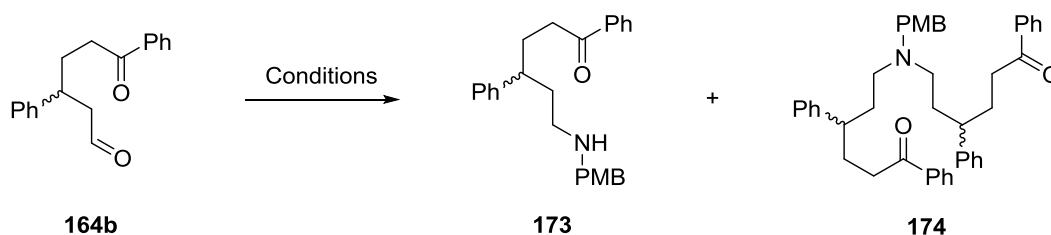
In the absence of alternative reductive amination conditions, focus was returned to the products from the ozonolysis reactions and it was envisioned that switching the amine component in the subsequent step could help prepare the required azepane product **173b**. Indeed, the amine was a flexible component at this stage, with our objective to ultimately deprotect the nitrogen to reveal the free azepene core (**Scheme 9.57**).



Scheme 9.57

As such, *para*-methoxybenzylamine (PMB amine) was considered as an alternative amine, due to the number of reported strategies to successfully remove the electron rich aryl ring through acidic or SET conditions (**Table 9.27**). Indeed, it was hoped that this would then allow for more fruitful results in terms of achieving the removal of the PMB group and subsequent *in situ* cyclisation to the azepane. When our previously optimised conditions were used with *para*-methoxybenzylamine, we anticipated that we could obtain a mixture of products; including, although somewhat unlikely, the fully cyclised and ultimately desired azepane (*via* a second, intramolecular, reductive amination), and the ϵ -amino ketone product. In reality, the ϵ -amino ketone product **173** was isolated in a low 31% yield, alongside the bis-alkylated product **174** in a significant 19% yield, which derived from a second, intermolecular, reductive amination procedure (entry 1 in **Table 9.27**). Due to the observed

low yield of the ϵ -amino ketone **173**, and based on a further literature search,^{138,139} NaCNBH₃ was applied in place of Na(OAc)₃BH. When the reaction was attempted in the presence of zinc(II) chloride (entry 2 in **Table 9.27**), the ϵ -amino ketone product **173** was obtained in an improved 40% yield. Pleasingly, the yield was improved further when the reaction was carried out under acidic conditions (entry 3 in **Table 9.27**).¹³⁸ Indeed, in the latter two cases, none of the unwanted bis-alkylated product **174** was observed.

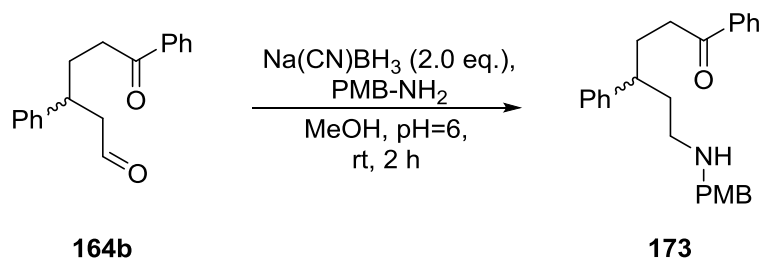


Scheme 9.58

Entry	Conditions	Yield of 173 (%)	Yield of 174 (%)
1	NH ₂ -PMB (1.05 eq.), Na(OAc) ₃ BH (2.80 eq.), CPME, rt, 4 h	31	19, d.r = 1:1
2	NH ₂ -PMB (2.0 eq.), Na(CN)BH ₃ (2.0 eq.), ZnCl ₂ (0.5 eq.), MeOH, rt, 15 h	40	-
3	NH ₂ -PMB (1.0 eq.), Na(CN)BH ₃ (2.0 eq.), Glacial acetic acid (pH = 6), MeOH, rt, 15 h	54	-

Table 9.27

Following on from the above studies, and using the Na(CN)BH₃ conditions shown in entry 3 in **Table 9.27**, a detailed DoE study was performed in an attempt to further improve the yield towards the ϵ -amino ketone product **173**. The decision to use a DoE approach was based on the fact that it was trivial to assess the conversion level *via* analysis of the ¹H NMR spectrum. This would allow the range of reactions dictated by the DoE to be carried out and analysed quickly. At the beginning of the optimisation, the key parameters were identified as the addition time of the substrate **164b**, the volume of methanol, and the number of equivalents of the amine nucleophile. The reaction outcomes are summarised in **Table 9.28**.



Scheme 9.59

Run	A: Addition time of substrate (h)	B: MeOH volume (mL)	C: Equivalents of amine (eq.)	Conversion 173 (%)
1	1.25	2	5	50
2	1.25	2	5	54
3	2	1	7	48
4	2	4	7	39
5	1.25	2	5	50
6	0.5	4	7	71
7	2	4	3	59
8	0.5	1	3	54
9	2	1	3	40
10	0.5	1	7	65
11	0.5	4	3	68

Table 9.28

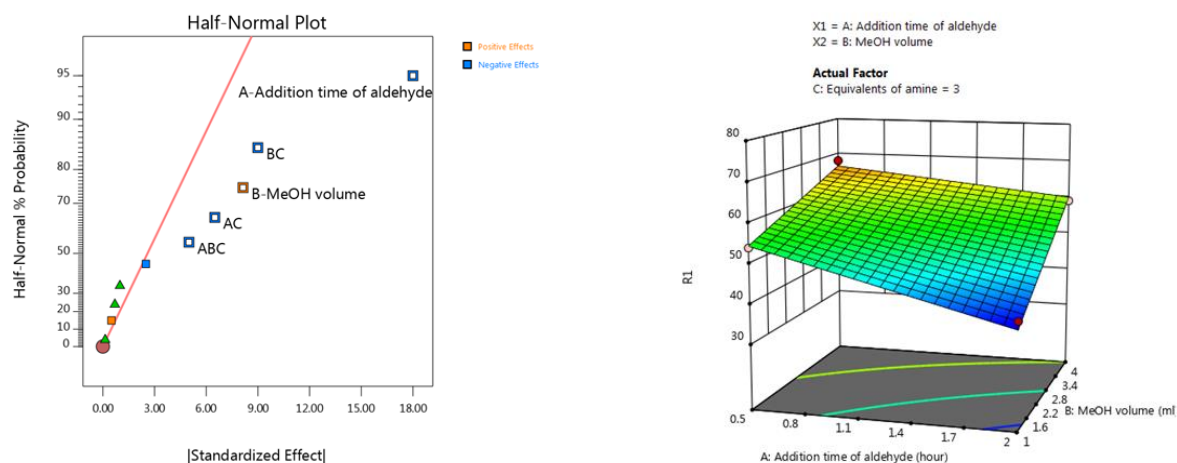
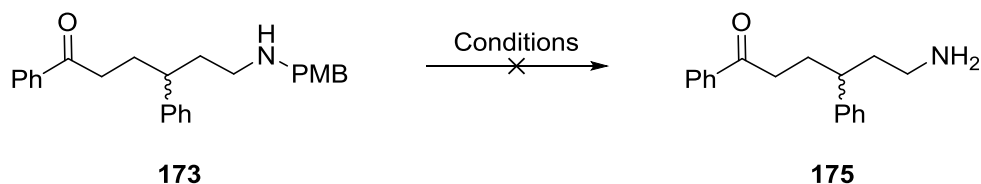


Figure 9.7

As shown in entries 1, 2 and 5 in , the product **173** was obtained with similar conversions when the reaction was performed under identical conditions 50%, 54% and 50%. In general, higher equivalents of the amine did not improve the yield and it has shown to have a minimal impact on the reaction outcome therefore for the preparation of 3D plot this variant was chosen to set constant (right side on **Figure 9.7**). Analysis of the half normal pot revealed that the addition time of the aldehyde is the most important parameter, possibly due to the rapid decomposition of the keto-aldehyde **164b**, therefore the highest yields were observed when the substrate was added quickly 54-71% (entry 6, 8, 9 and 10 in. Interestingly, the volume of methanol has also had positive impact on the yield, possibly because at lower concentrations formation of by-product **174** is unfavoured. With the optimised conditions in hand we manage to isolate the desired product **173** in a good 71% yield with out any detectable by-product **174**. With a high 71% yield obtained for key intermediate **173**, attempts to reveal the free amine **175** were performed. Researching the literature revealed two common methods for the removal of the electron rich benzyl group; (i) the use of strong acids,^{140–143} and (ii) the use of single electron reductants.¹⁴⁴ Due to the availability of reagents, initial attempts looked at the acidic conditions (**Table 9.29**).



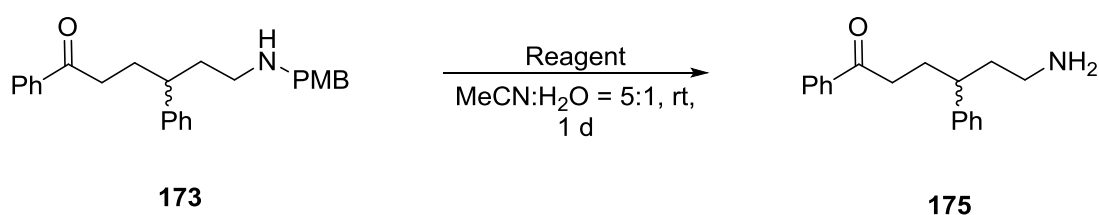
Scheme 9.60

Entry	Conditions	Yield of 175 (%)	Recovered 173 (%)
1	TFA (5.0 eq.), DCM, rt, 24 h	-	100
2	Triflic acid (3.0 eq.), TFA, rt, 4 h	-	100
3	TFA (5.0 eq.), reflux, 4 h	-	100
4	TFA (5.0 eq.), microwave heating, 120 °C, 10 min	-	100

Table 9.29

In the first instance, the reaction was carried out at room temperature using trifluoroacetic acid (TFA), however, after 24 h, the starting material **173** recovered quantitatively (entry 1 in **Table 9.29**).¹⁴³ Thereafter, the stronger triflic acid was used but similar results were obtained (entry 2 in **Table 9.29**).¹⁴¹ Following this, and in an attempt to force some reactivity, the substrate **173** was reacted with trifluoroacetic acid under refluxing conditions (entry 3 in **Table 9.29**).¹⁴⁰ Once again, the desired product **175** was not detected. In a final attempt, microwave irradiation was used, whereby the reaction temperature was further increased to 120 °C, but to no desired product **175** formation was detected.¹⁴²

Despite these results, we continued our efforts by considering single electron methods. In this respect, both ceric(IV) ammonium nitrate (CAN) and 2,3-dichloro-5,6-dicyano-1,4-benzoquinone (DDQ) have been reported for the selective deprotection of aliphatic amines.¹⁴⁴ Frustratingly, when our particular substrate **173** was exposed either of these reagents none of the desired product **175** was obtained (**Table 9.30**). Whilst the reaction with CAN returned the starting material in full, the DDQ protocol completely decomposed the starting ϵ -amino ketone **173**.



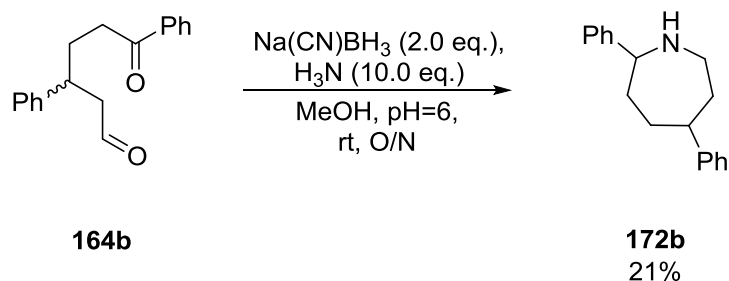
Scheme 9.61

Entry	Reagent	Yield of product (%)	Recovered 173 (%)
1	CAN (2.1 eq.)	-	100
2	DDQ (1.2 eq.)	-	-

Table 9.30

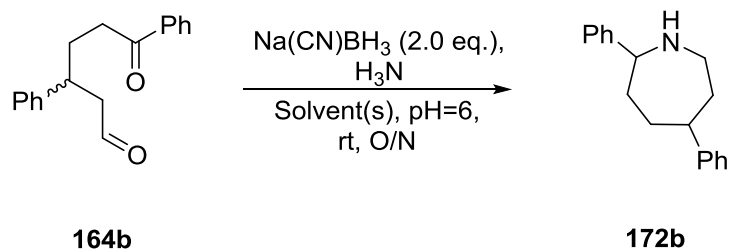
Due to the observed difficulties, we envisioned an alternative strategy for the preparation of the core azepane structure, whereby instead of employing 4-methoxybenzylamine in the reductive

amination process, ammonia could be used as a nitrogen source. Indeed, this would potentially lead to direct formation of the desired unprotected 7-membered heterocycle. As such, the reaction was carried out in the presence of ammonia and we were delighted to isolate the desired product **172b** as a single diastereomer, albeit in 21% yield (**Scheme 10.124**).



Scheme 9.62

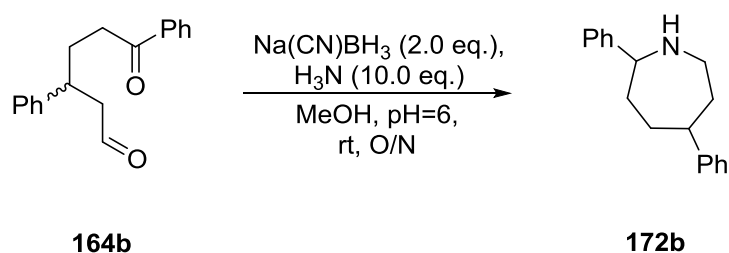
With this promising result, we looked to further probe the reaction conditions in an effort to enhance the isolated yield of the target azepane **172b**. Optimisation included changes in solvent, equivalents of ammonia, and attention to the rate of addition of the substrate **164b** (**Table 9.31**). First the solvent for the reaction was changed (used for dissolve the reducing agent and ammonia, to this solution the solution of the aldehyde **164b** was added) and a series of commonly used polar solvents were tried. When MeOH was replaced by CPME (entry 1 in **Table 9.31**), the desired product **172b** was obtained with 24%. Switching to a polar halogenated solvent DCE had a minor impact on the reaction outcome and the product **172b** was detected with a 25% conversion (entry 2 in **Table 9.31**). When THF was used as solvent for the reducing agent the product **172b** was obtained with a low 13% conversion (entry 3 in **Table 9.31**). Although when we switched to DCM the desired heterocycle **172b** was observed with a higher 35% conversion (entry 4 in **Table 9.31**). Therefore we also attempted to change the solvent of the starting substrate **164b** to DCM but in this case the conversion decreased significantly to 14% (entry 5 in **Table 9.31**). At this point the amount of ammonia was also decreased to 5 eq. and the product **172b** was obtained with a similar 34 % conversion (entry 6 in **Table 9.31**). In an attempt to increase the conversion we tried to add the solution of the substrate **164b** in a controlled manner. When the solution of the aldehyde-ketone **164b** was added over 15 min a lower conversion was obtained 20% (entry 7 in **Table 9.31**). While adding the solution slowly also decreased the conversion to 15% (entry 8 in **Table 9.31**).



Entry	NH ₃ (eq.)	Reaction solvent	Solvent to dissolve 164b	Comment	Conv. (%)*
1	10	CPME	MeOH	-	24
2	10	DCE	MeOH	-	25
3	10	THF	MeOH	-	13
4	10	DCM	MeOH	-	35
5	10	DCM	DCM	-	14
6	5	DCM	MeOH	-	34
7	5	DCM	MeOH	aldehyde added over 15 min	20
8	5	DCM	MeOH	aldehyde added over 1 h	15

Table 9.31

After these experiments, and given that we had increasing solubility concerns with Na(CN)BH₃ in DCM, we looked to alternative borohydride reagents (Table 9.32). When sodium triacetoxy borohydride was used, the desired product **172b** was detected with a low 9% conversion (entry 1 in Table 9.32). In addition to this, the reductive amination sequence was attempted using a tertiary amine salt (entry 2 in Table 9.32), however, under these conditions, the desired product **332** was not formed at all.

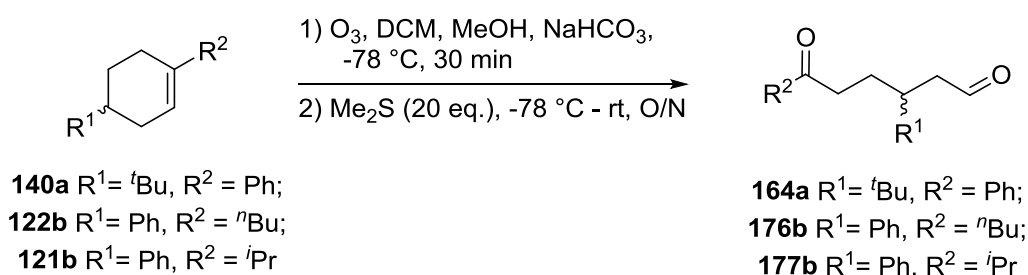


Scheme 9.63

Entry	Comment	Conv.(%)*
1	Na(OAc) ₃ BH	9
2	Bu ₄ N ⁺ BH ₄ ⁻	-

Table 9.32

Due to time constraints, at this stage in the project, we decided to take our optimal conditions thus far and create a substrate scope for this reductive aminocyclisation. Indeed, this included initial ozonolysis of our previously prepared alkenes to generate dicarbonyl intermediates, followed by a double reductive amination step to deliver the targeted azepane motif. More specifically, when the *tert*-butyl-substituted alkene **140a** was used as a substrate in the ozonolysis step the product **164a** was isolated in a high 75% yield (entry 1 in **Table 9.33**). Pleasingly, when the primary and secondary alkyl cross coupled substrates **122b** and **121b** were ozonised (entry 2 and entry 3 in **Table 9.33**), the desired products **176b** and **177b** were delivered in a high 81% and outstanding 99% yield, respectively.

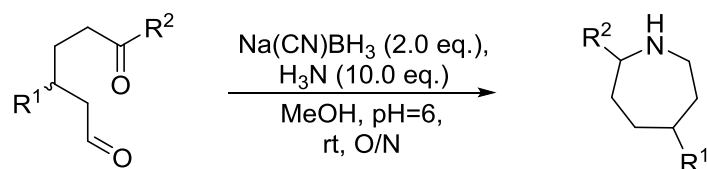


Scheme 9.64

Entry	Product	R ¹ group	R ² group	Yield (%)
1	164a	<i>t</i> Bu	Ph	75
2	176b	Ph	<i>n</i> Bu	81
3	177b	Ph	<i>i</i> Pr	99

Table 9.33

With these substrates in hand, the one pot double reductive amination sequence was performed under our optimal conditions (**Table 10.50**).



164a R¹ = *t*Bu, R² = Ph;

176b R¹ = Ph, R² = *n*Bu;

177b R¹ = Ph, R² = *i*Pr

178 R¹ = *t*Bu, R² = Ph;

179 R¹ = Ph, R² = *n*Bu;

180 R¹ = Ph, R² = *i*Pr

Scheme 9.65

Entry	Product	R ¹ group	R ² group	Yield (%)
1	178	<i>t</i> Bu	Ph	27
2	179	Ph	<i>n</i> Bu	32
3	180	Ph	<i>i</i> Pr	31

Table 9.34

In this regard, we were very pleased to obtain a further set of final azepane targets **178-180**. Whilst the yields were low (as somewhat expected), we had nonetheless effectively demonstrated that our overall synthetic sequence, starting from trivial cyclohexanone structures, represented a practically accessible and flexible method for the formation of intriguing heterocyclic motifs.

9.1.13 Summary and Future Work

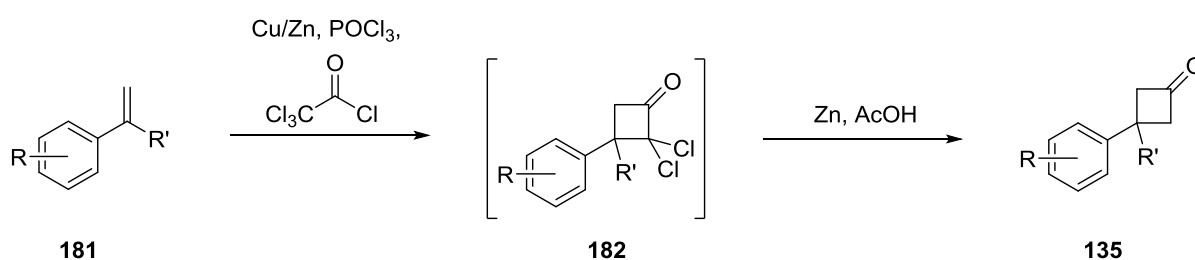
In the second part of this chapter the synthesis of chiral azepanes was described. First, a palladium catalysed Kumada cross coupling method with arylmagnesium bromides was reoptimised to prepare a series of trisubstituted cyclic alkenes **140** with high yields (74-97%) and the enantioselective enol phosphates **115** were also successfully utilised as substrates. In the future we would like to investigate the impact of the electronic nature of the aryl Grignard reagent for the reaction outcome. Therefore a series of differently substituted aryl Grignard reagent with electron donating and withdrawing groups will be used in this novel cross coupling reaction. In an attempt to rationalise the formation of the homocoupled enol phosphate **141** we also successfully synthesized a molecular probe **142** and show evidence that the reaction proceeds through a two electron pathway. The substrate scope of this novel cross coupling step was also extended for primary- and secondary alkyl Grignard reagents and the desired products **118b-121b** and **151b** were isolated with good to excellent yields. Thereafter the synthesis of the target protected azepanes **166** was readily achieved through an ozonolysis-reductive amination sequence with moderate yields 45-54%. Although when the R² position was sterically hindered (R²= Ph, ⁱPr) the second ring closing reductive amination step did not occur. In these cases although these substrates **168b** and **169** were originally not targeted, a literature search revealed that they are used as tags to attach fluorescent probes to biologically active structures^{127,128} and therefore a series of these novel amino ketones **168** were prepared in moderate to good yields (44-60%) in an enantiomerically enriched fashion with good enantiomer ratios (88:12-99:1). Finally the synthesis of the free azepanes **178-180** were also achieved under different sets of reductive amination conditions with these challenging substrates. Although optimisation of the reaction conditions is required, to further improve the yield in this novel reductive aminocyclisation. With the optimised conditions in hand a series of amines with different electronic nature will be used as a nucleophilic partner in this novel reductive amination sequence.

9.2 Towards the Synthesis of Chiral Pyrrolidines

As described in the above sections, recent efforts within the Kerr research team have focused on the preparation of chiral phosphoryl enol ethers and their further manipulation to prepare highly-functionalised, enantiomerically-enriched cyclic systems. As part of this, the asymmetric deprotonation of cyclobutanone substrates **135** has previously been reported by the Kerr group, with one example being further manipulated, *via* a cross-coupling and ring opening sequence, to a desirable chiral pyrrolidine motif **138b** (*vide supra*).¹⁰³ In an effort to determine the full capacity of this overall process, and deliver a range of desirable and enantiomerically-enriched pyrrolidine compounds **138**, a library of cyclobutanone substrates **135** were required.

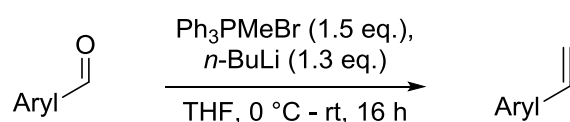
9.2.1 Synthesis of Cyclobutanones

The preparation of cyclobutanones of type **135** was envisaged using a reported two-step cycloaddition and reduction sequence (**Scheme 9.66**).¹⁰³



Scheme 9.66

Whilst a range of styrenes were available in our laboratory or commercially, two further starting styrenes were prepared *via* a standard Wittig reaction.^{103,145} The 4-chloro-derivative **135c** was prepared on varying scales (20 mmol and 40 mmol) in moderate to good yields (44-63%) (entries 1 and 2 in **Table 9.35**), whilst the 2-naphthalene analogue **135e** was obtained with a high 86% yield using the same reaction conditions (entry 3 in **Table 9.35**).

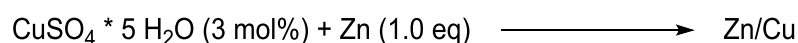


Scheme 9.67

Entry	Product	Aryl group	Scale (mmol)	Yield (%)
1	181c	4-Chlorophenyl	20	44
2	181c	4-Chlorophenyl	40	63
3	181e	2-Naphthyl	43	86

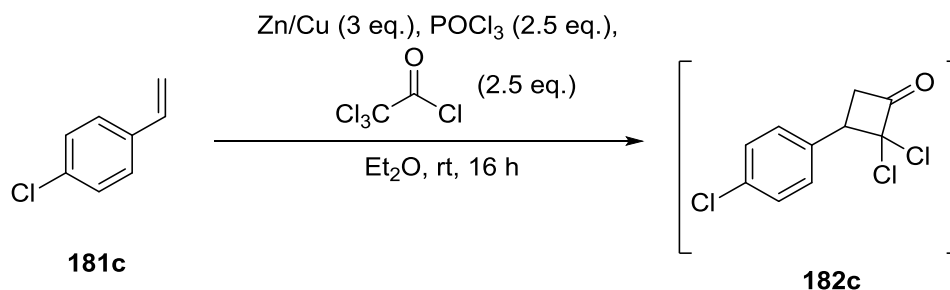
Table 9.35

With these compounds in hand, the [2+2] cycloaddition reaction was considered. In relation to this, the requisite zinc-copper couple was prepared by mixing zinc dust and copper(II) sulfate (**Scheme 9.68**).



Scheme 9.68

When this reagent was employed in the [2+2] cycloaddition reaction of styrene substrate **181c** and *in situ* prepared dichloroketene, we were pleased to obtain an improved overall yield of the desired cyclobutanone compound as compared with the previous results.¹⁰³ Firstly, the reaction was carried out on a 3 mmol small scale with 1-chloro-4-vinylbenzene **181c** and moderate conversion of 43% to the dichlorocyclobutanone **182c** was observed (entry 1 in **Table 9.36**). When the reaction was repeated on a larger, 20 mmol scale, to our delight the product **182c** was obtained with 63% conversion (entry 2 in **Table 9.36**), which is higher than the previously reported (56% conversion).¹⁰³

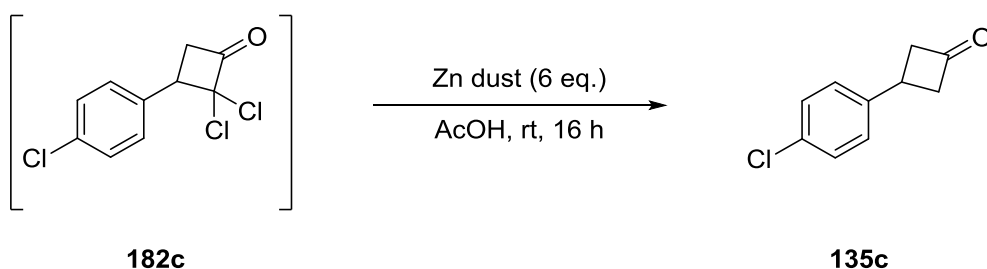


Scheme 9.69

Entry	Scale (mmol)	Conv. (%)
1	3	43
2	20	63

Table 9.36

Subsequently, the reduction of the dichlorocyclobutanone **182c** intermediate was carried out using the crude material from the reactions described above. On a small scale, the desired product **135c** was isolated in a moderate 37% yield (entry 1 in **Table 9.37**). To our delight, when the reaction was repeated on a larger scale, a significantly higher 78% yield was achieved (entry 2 in **Table 9.37**).

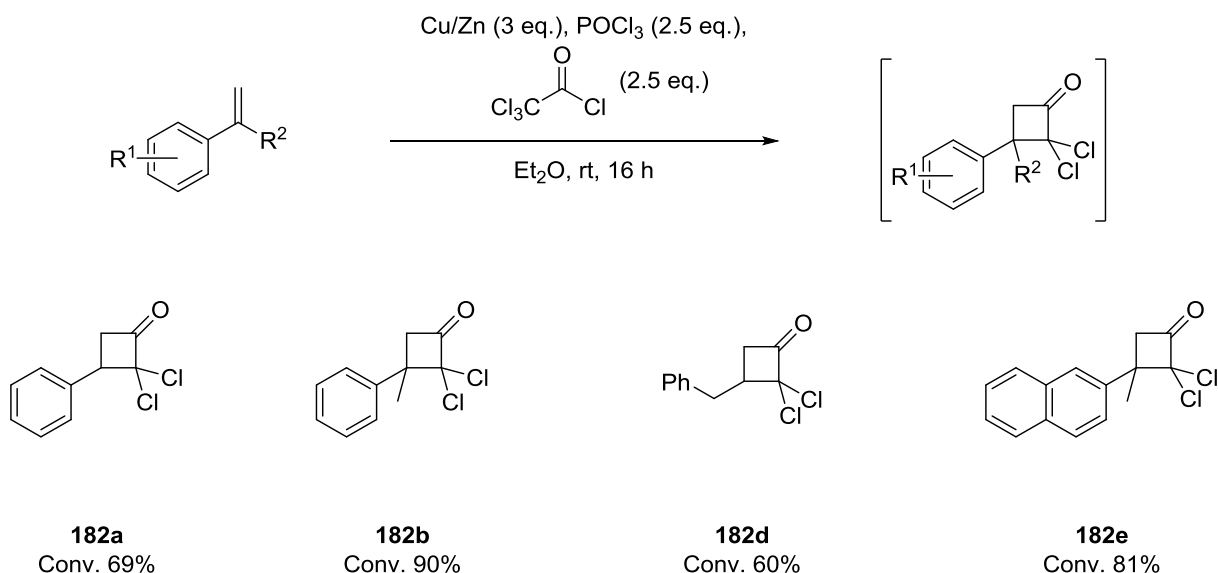


Scheme 9.70

Entry	Scale (mmol)	Yield (%)
1	3	37
2	20	78

Table 9.37

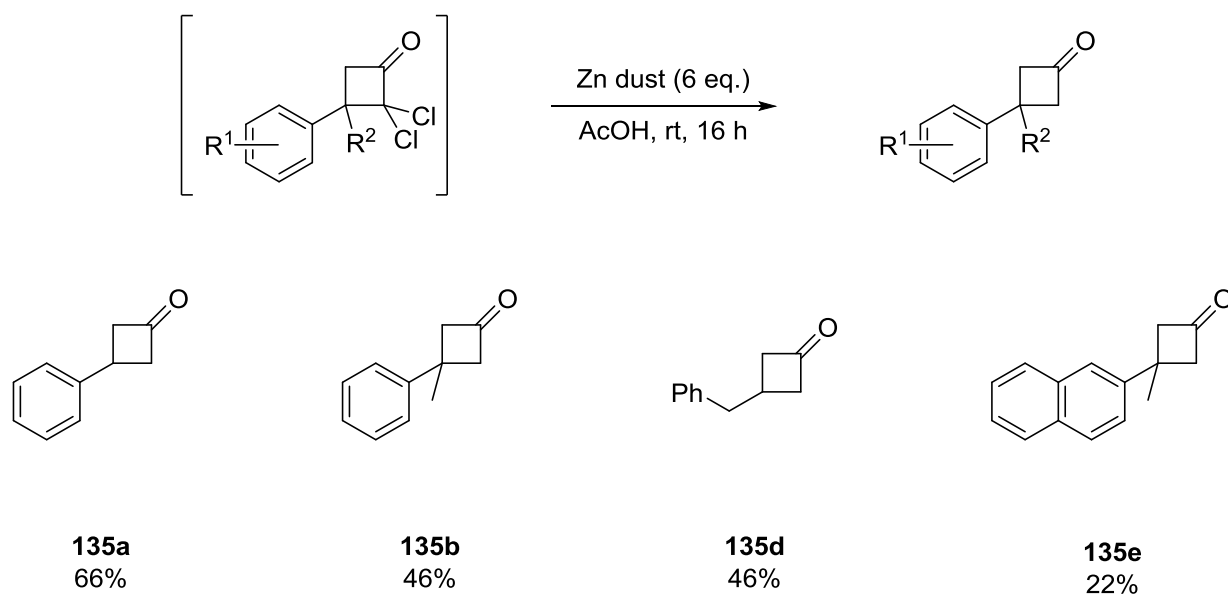
After successfully reproducing, and improving on, the previously reported results, the sequence was then carried out with a series available styrenes **181a-e**, including the prepared naphthalene derivative **181e**, to deliver a range of 3-substituted and 3,3'-disubstituted cyclobutanones **182a-e**. Indeed, the dichlorocyclobutanone intermediates were prepared first with generally good conversions (**Scheme 9.71**). In general, with 3,3'-disubstituted styrenes, a higher conversion towards the desired intermediates **182b** and **182e** was observed (81-90%), while the conversions were slightly lower than this with the 3-substituted substrates **182a**, **182c** and **182d** (60-69%).



Scheme 9.71

In the following step, the reduction of dichlorocyclobutanone intermediates **182** was carried with 6 eq. of zinc dust in acetic acid (**Scheme 9.72**). Overall, the corresponding products were obtained in

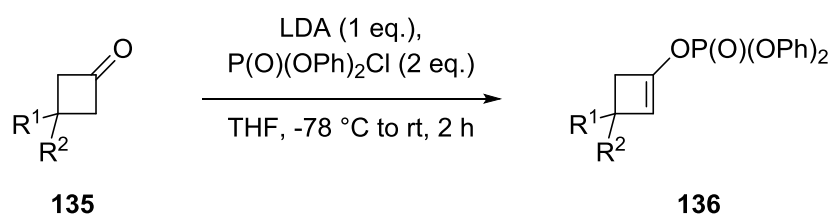
moderate to good yields (46-78%), with the exception of naphthyl-substituted cyclobutanone **135e**, which was isolated in a low 22% yield.



Scheme 9.72

9.2.2 Synthesis of Racemic Enol Phosphates

Having prepared a range of cyclobutanones **135a-e**, the syntheses of the racemic enol phosphate compounds **136a-e** was carried out to obtain reference samples for the downstream chiral HPLC analysis (Scheme 9.73). As such, reaction with LDA at $-78\text{ }^{\circ}\text{C}$, followed by addition of diphenylphosphoryl chloride, allowed access to the desired structures **136** (Table 9.38). When the reaction was carried out on a small scale (entry 1 in Table 9.38), the product **136a** was isolated in a high 80% yield. However, further reactions that were carried out on a 2 mmol scale delivered the corresponding products **136a-c,e** in slightly lower yields of 62-67% (entries 2-5 in Table 9.38).



Scheme 9.73

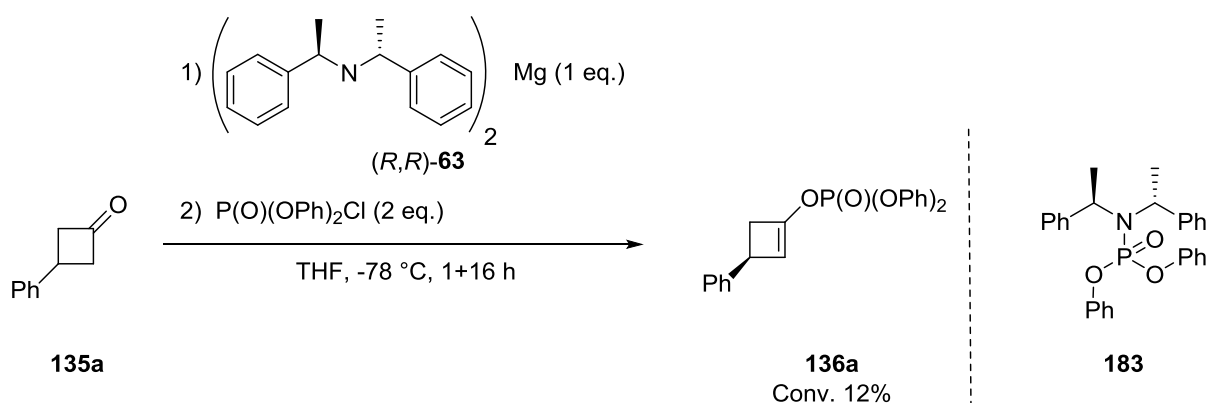
Entry	Compound	R ¹ group	R ² group	Yield(%)
1	136a	Ph	H	80*
2	136a	Ph	H	64
3	136b	Ph	Me	67
4	136d	Bn	H	69
5	136e	Naphthyl	Me	62

*: Reaction was carried out on an 1.0 mmol scale.

Table 9.38

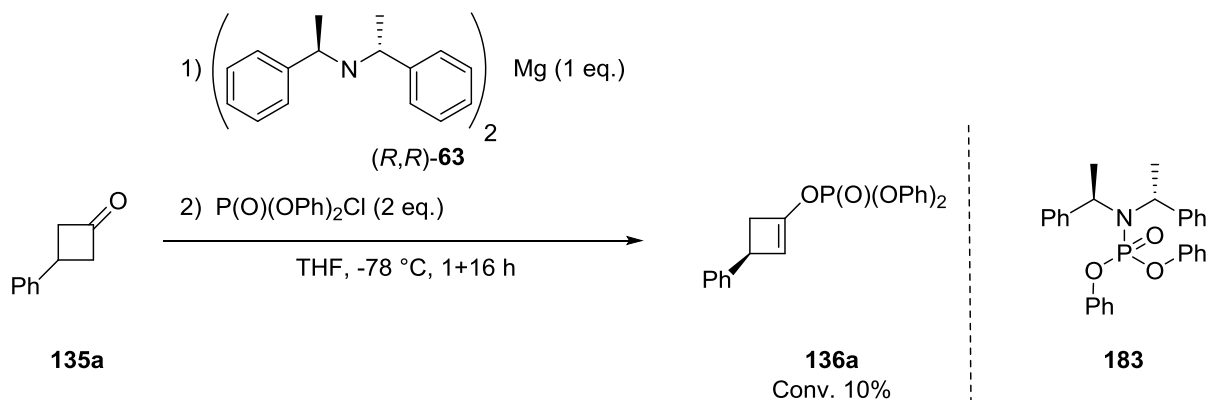
9.2.3 Asymmetric Deprotonation of Cyclobutanones

Following the analysis of the racemic transformation, the asymmetric deprotonation with *C*₂-symmetric magnesium bisamide (*R,R*)-**63** was carried out, initially with 3-phenylcyclobutanone **135a**. When the reaction was first attempted, a low 12% conversion towards the desired product **136a** was observed (**Scheme 9.74**). Moreover, during column chromatography, the desired product co-eluted with by-product **183**, the nucleophilic substitution product between the electrophile and the magnesium amide species. The enantiomeric ratio was not determined in this case.



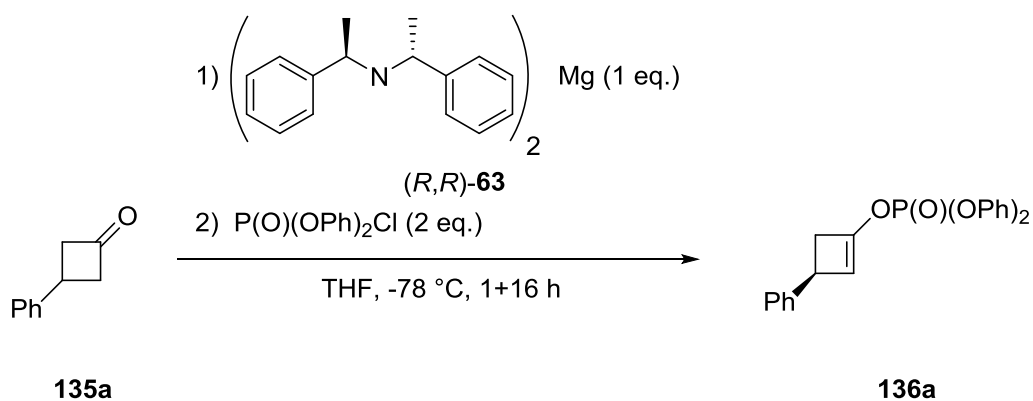
Scheme 9.74

At this stage, the reaction was repeated using a fresh supply of di-*n*-butylmagnesium (**Scheme 9.75**). However, similar results were obtained, whereby the product **136a** was detected in a low 10% conversion, and as an inseparable mixture with by-product **183** (**Scheme 9.75**).



Scheme 9.75

Subsequently, the electrophile was added at -78 °C and to our delight a substantially higher conversion (75%) and yield (57%) was obtained, albeit with a lower e.r. (59:41) (entry 1 in **Table 9.39**), in comparison with the previously reported 97:3 result from our laboratories. When the reaction was repeated, a similarly moderate yield of 55% and low enantiomeric ratio of 55:45 was obtained (entry 2 in **Table 9.39**).

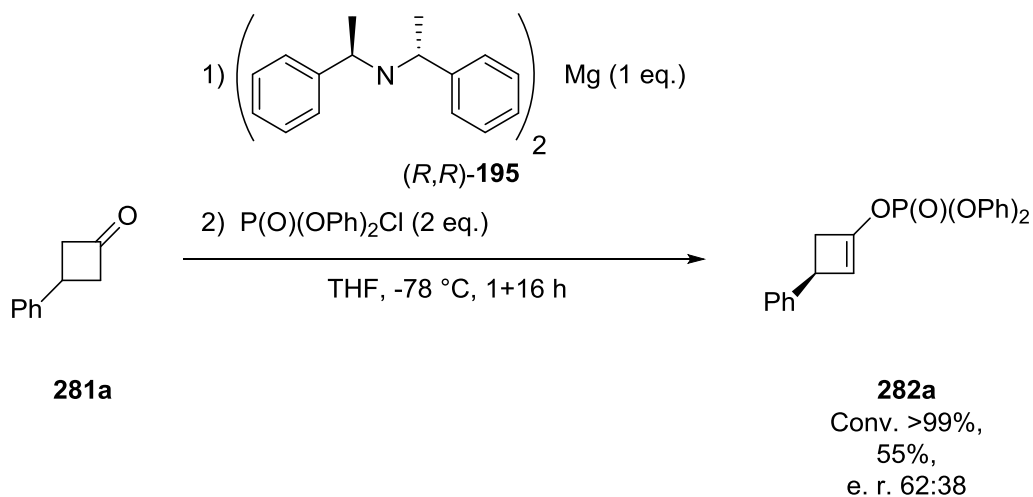


Scheme 9.76

Entry	Conversion (%)	Yield (%)	e.r.
1	75	57	59:41
2	73	55	55:45

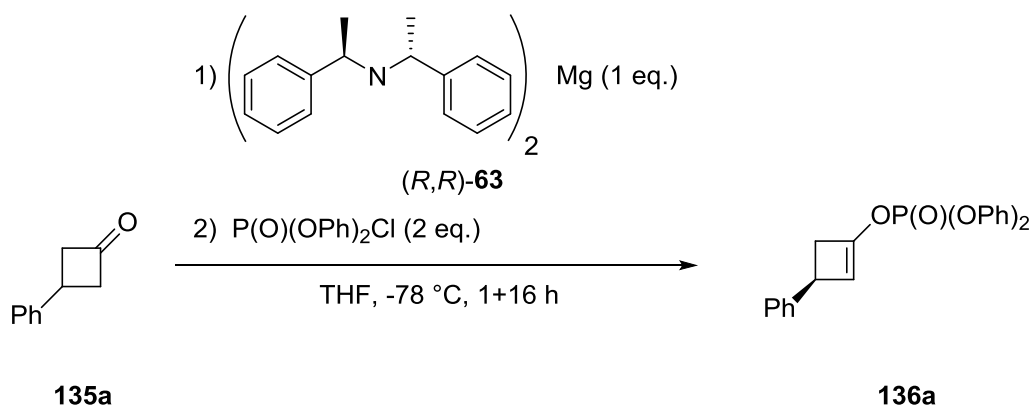
Table 9.39

In an effort to improve the yield, the quench procedure was modified. Specifically, methanol was employed, to quench the reaction in place of the standard saturated sodium bicarbonate solution. However, a similar enantiomeric ratio (62:38), and yield (55%) was obtained (**Scheme 9.77**).



Scheme 9.77

Finally, the base **(R,R)-63** was prepared in hexane instead of THF, which was a common solvent previously used in our group for the asymmetric deprotonation of cyclohexanones,⁷⁸ however, a comparable e. r. of 66:34, with a lower yield of 47%, was obtained (entry 1 in **Table 9.40**). This experiment was repeated to assess the reproducibility of the protocol, however, similar results were observed and the product **136a** was obtained with 52% yield and 62:38 e.r. (entry 2 in **Table 9.40**).

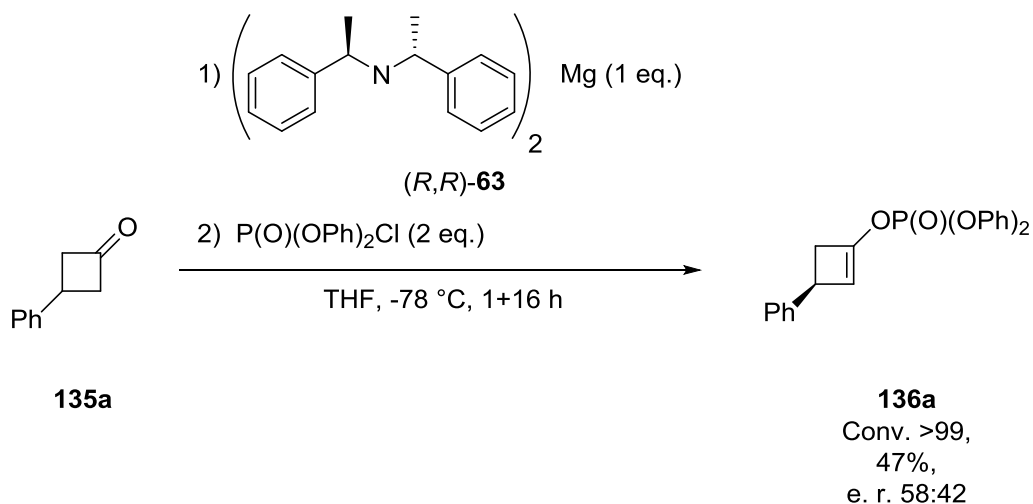


Scheme 9.78

Entry	Conversion (%)	Yield (%)	e.r.
1	>99	47	66:34
2	>99	52	62:38

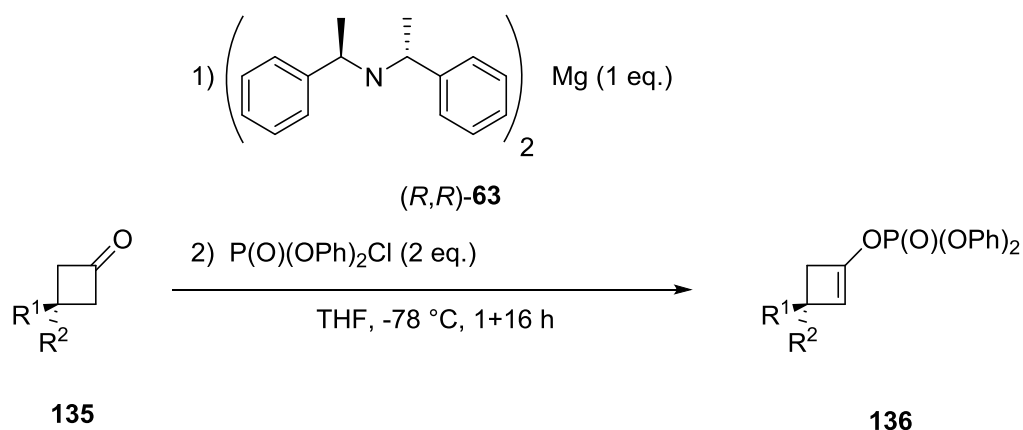
Table 9.40

Given that these reactions were not delivering the high enantiomeric ratios disclosed previously in our laboratories further efforts concentrated on ensuring that the reagents used were of sufficient purity, and free from any moisture or additive that could affect the overall transformation. As such, the starting material **135a** was re-distilled and stored in a flame-dried flask, this time without 4 Å molecular sieves, to avoid possible contamination from the drying agent. Frustratingly, a similarly poor yield of 47% and e.r. of 58:42 was obtained (**Scheme 9.79**).



Scheme 9.79

The enantioselective deprotonation was also attempted with three alternative substrates **135b**, **135d** and **135e** to further explore the unexpected results obtained thus far. In comparison with the previously reported results, low enantiomeric ratios in the range of 57:43-59:41 and low to moderate yields (38-44%) were observed in these reactions (entries 1-3 in **Table 10.11**).

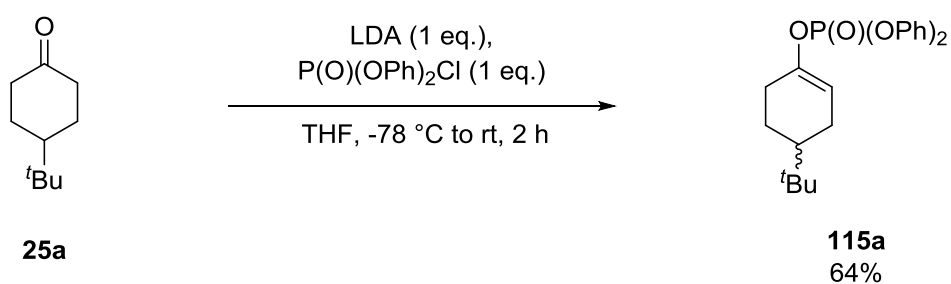


Scheme 9.80

Entry	Product	R ¹	R ²	Yield (%)	e.r.
1	136b	Ph	Me	44	57:43
2	136d	Bn	H	44	59:41
3	136e	Naphthyl	Me	38	59:41

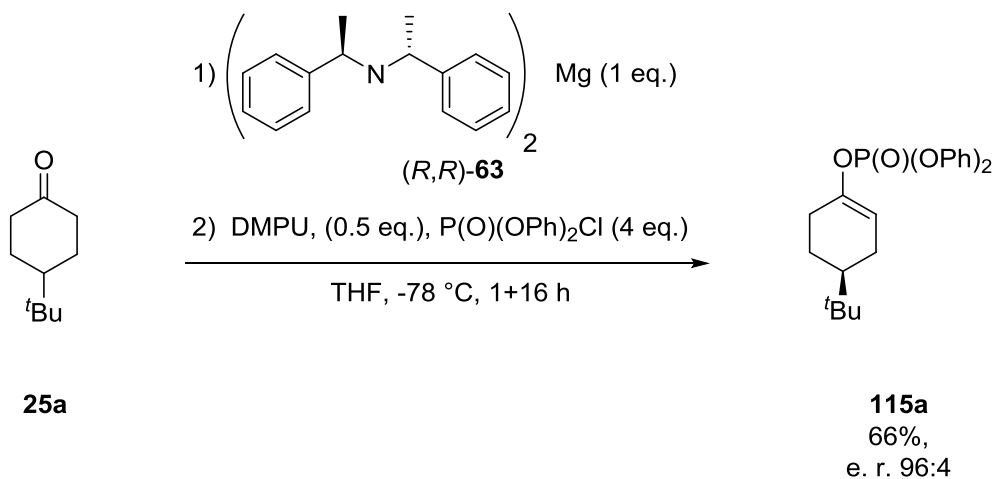
Table 9.41

In order to, assess whether the base or the substrate was responsible for the observed low enantioselectivity, we envisaged employing the exact same batch of base (*R,R*)-**63** in the asymmetric deprotonation of both 4-*tert*-butylcyclohexanone **25a** and 3-phenyl-cyclobutanone **135a** substrates. As such, to allow chiral HPLC analysis, the racemic enol phosphate **115a** was prepared using LDA in a good 64% yield (**Scheme 9.81**).

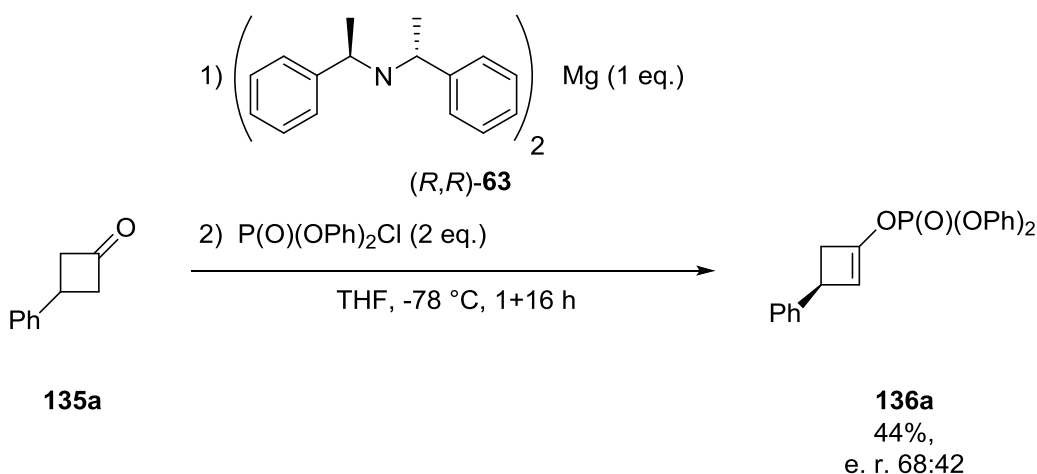


Scheme 9.81

Subsequently, the enantioselective deprotonation of the two different cyclic systems **25a** and **135a** were tested using the same batch of chiral magnesium amide (*R,R*)-**63** (**Scheme 9.82** and **Scheme 9.83**).



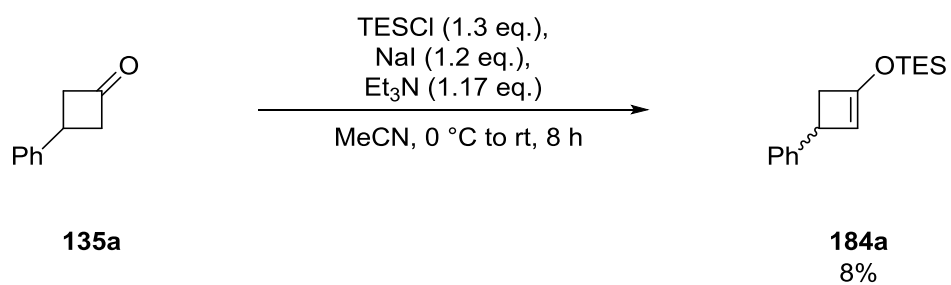
Scheme 9.82



Scheme 9.83

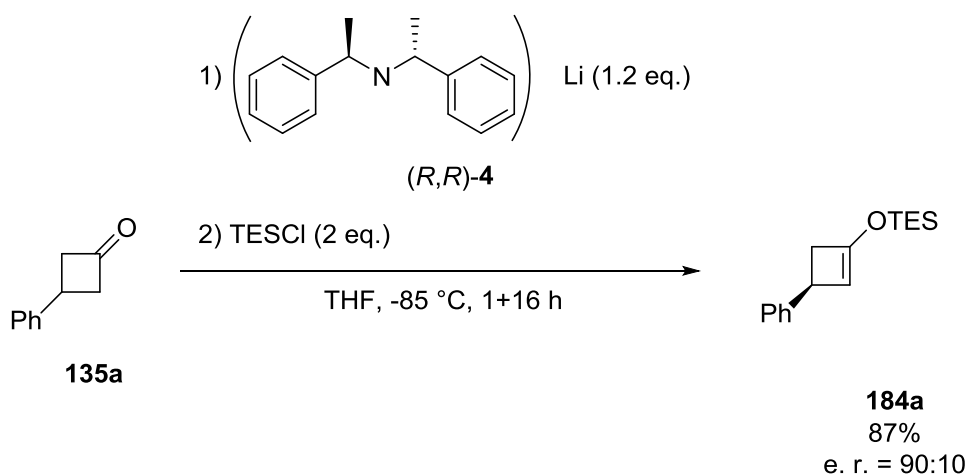
With the 6-membered ketone **25a**, using conditions reported by our group,⁹² a good yield of 66% and an excellent enantiomeric ratio of 96:4 was obtained (**Scheme 9.82**). In contrast, the reaction of 3-phenyl-cyclobutanone **135a** delivered a significantly lower enantiomeric induction (e. r. = 68:42) with a moderate 44% yield (**Scheme 9.83**). This result proved that the lower levels of enantioinduction were not due to issues with the preparation of the base (*R,R*)-**63**.

In addition to the above, the original protocol reported by Honda and co-workers⁵² that showed the preparation of enantio-enriched silyl enol ethers were repeated. Again, the racemic product **184a** was prepared first to allow determination of the e.r. by chiral HPLC (**Scheme 9.84**).



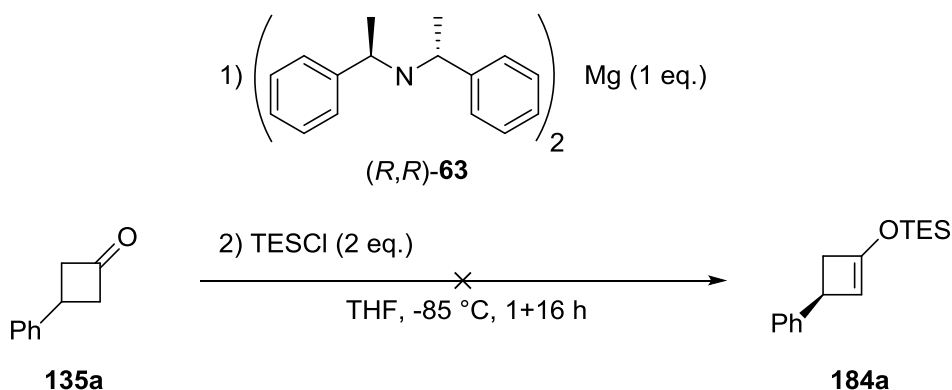
Scheme 9.84

Thereafter, the asymmetric deprotonation was carried out with the chiral lithium amide base (*R,R*)-**4** and the product **184a** was isolated in a high 87% yield and with an excellent 90:10 e.r. (Scheme 9.85). This result demonstrated that the low level of enantiomeric induction with the chiral magnesium base (*R,R*)-**63** are not due to issues with the purity of substrate **135a**.



Scheme 9.85

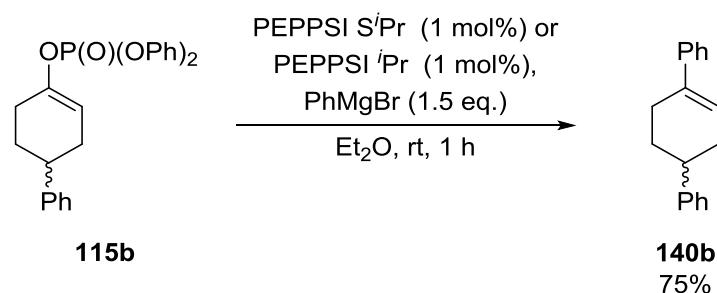
Furthermore, when the magnesium bisamide (*R,R*)-**63** was used, the corresponding silyl enol ether **184a** was not detected (Scheme 9.86).



Scheme 9.86

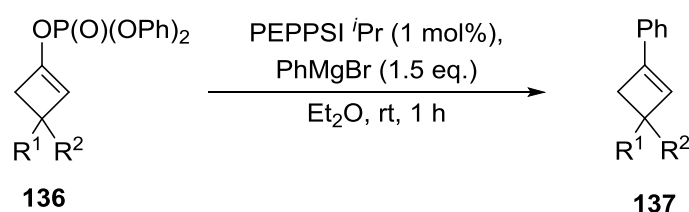
Given the issues when attempting to reproduce the high enantiomeric ratios previously described, we began to recognise that there could have been a misassignment in the chiral HPLC analysis at the outset. To confirm the exact enantiomeric ratio of our current transformations, it was decided to derivatise the chiral enol phosphate products **136** and to re-assess.

In relation to this, a palladium-catalysed Kumada cross coupling reaction had recently been established in our group as a robust and practically accessible method, for the functionalisation of enol phosphates such as **115b** (Scheme 9.87).⁹²



Scheme 9.87

As such, this transformation was regarded as ideal to apply to our prepared 4-membered cyclic enol phosphate products **136**, to truly determine the enantiomeric ratios. Indeed, these reactions were first carried out using the racemic starting substrates **136** in order to obtain references for the chiral HPLC analysis (Scheme 9.88). Pleasingly, in the case of monosubstituted cyclobutenes **136a** and **136d**, the products **137a** and **137d** were obtained in an excellent yield (entry 1 and entry 3 in Table 9.42). With disubstituted cyclobutene **136b**, the product **137b** was obtained in a decreased but still good 66% yield (entry 2 in Table 9.42).

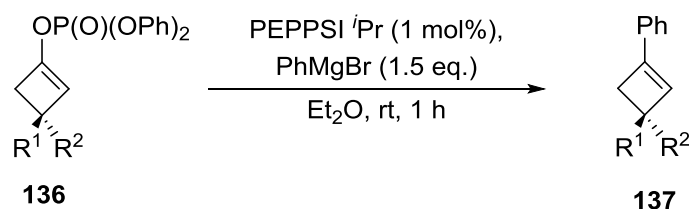


Scheme 9.88

Entry	Product	R substituent	R' substituent	Yield (%)
1	137a	Ph	H	82
2	137b	Ph	Me	66
3	137d	Bn	H	99

Table 9.42

Obtaining these samples, allowed an adequate chiral HPLC analysis method to be established. With the racemic samples in hand, the cross coupling of the corresponding chiral substrates was also achieved (**Scheme 9.89**).

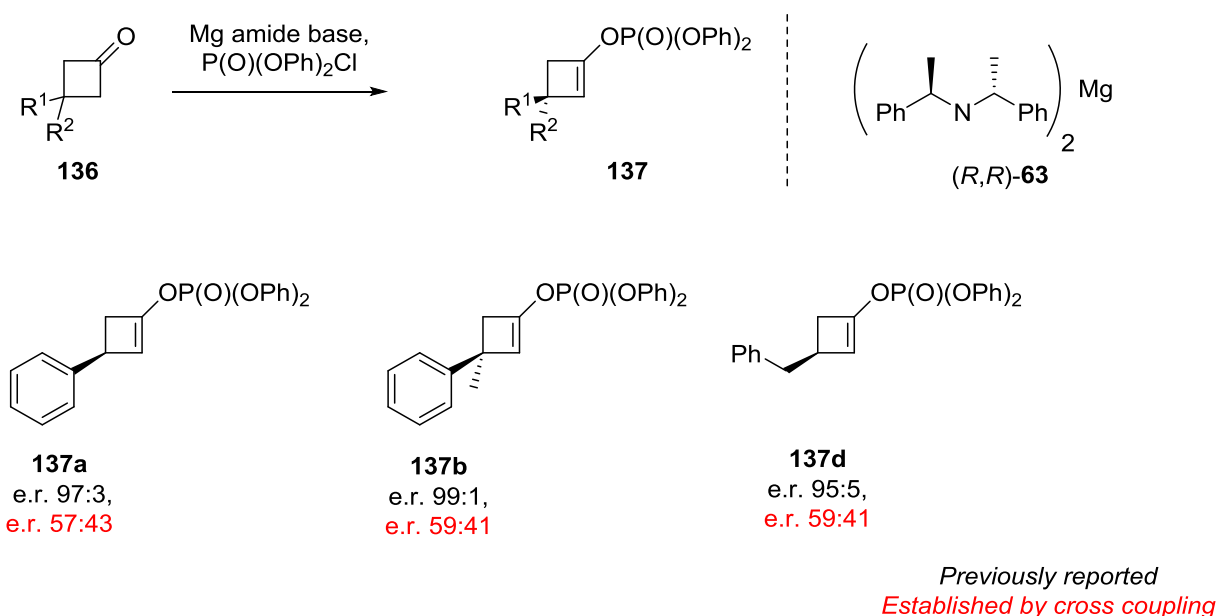


Scheme 9.89

Entry	Product	R ¹	R ²	Yield (%)	e.r.
1	137a	Ph	H	76	59:41
2	137b	Ph	Me	58	58:42
3	137d	Bn	H	96	58:42

Table 9.43

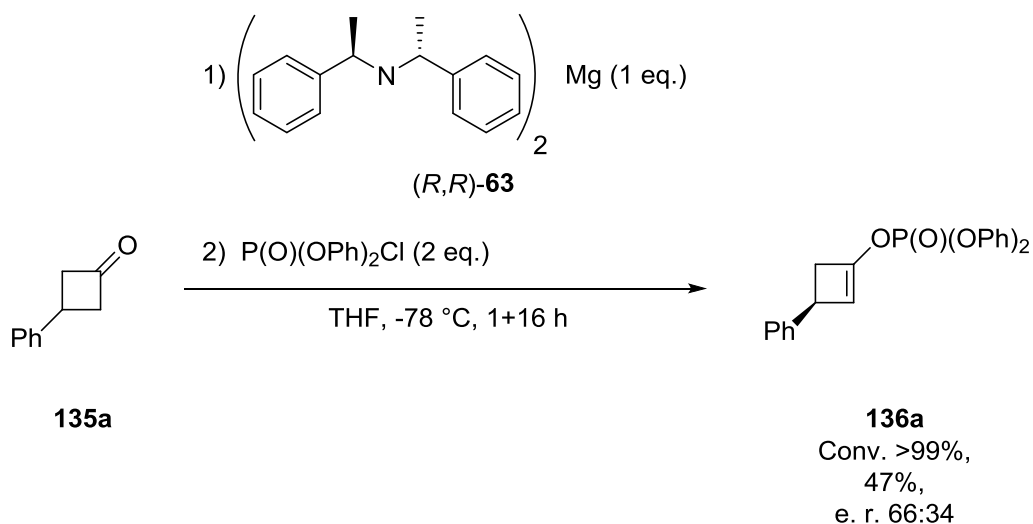
The chiral analysis of the enantiomerically enriched products revealed that there had, indeed, been a mis-assignment of the e.r. and that the lower levels, as reported from this package of work, were upheld. A summary of the previously reported and actual enantiomeric ratios for **137a**, **137b** and **137d** are shown in **Scheme 9.90**.



Scheme 9.90

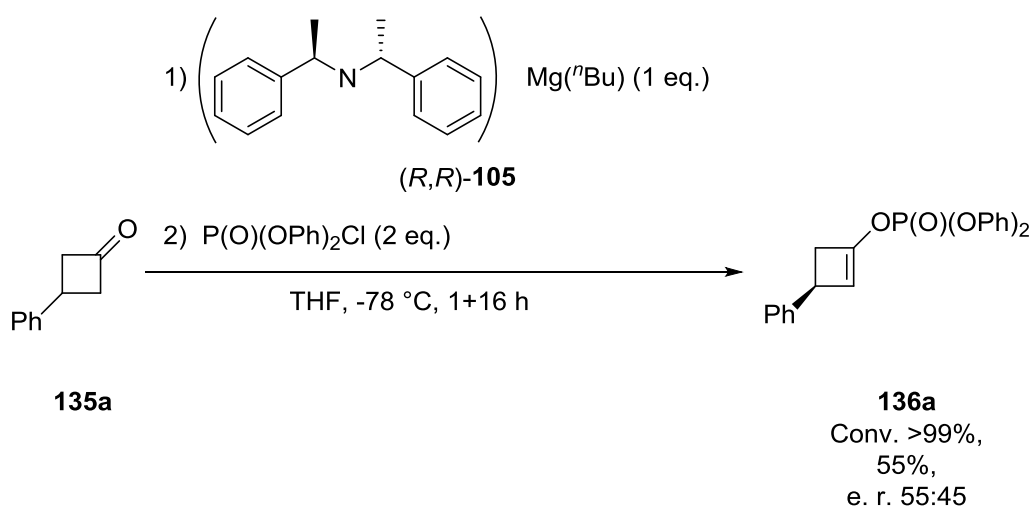
With these results in hand, it was clear that magnesium bisamide species (*R,R*)-**63** only induced a moderate level of asymmetry in this overall transformation. As such, a series of experiments were

conducted with the aim to developing a more efficient system. Firstly, the magnesium amide (*R,R*)-**63** was prepared in hexane, instead of THF. In this case, whilst a slightly higher enantiomeric ratio was observed (66:34), the product **136a** was obtained in a similar moderate yield of 47% (**Scheme 9.91**).



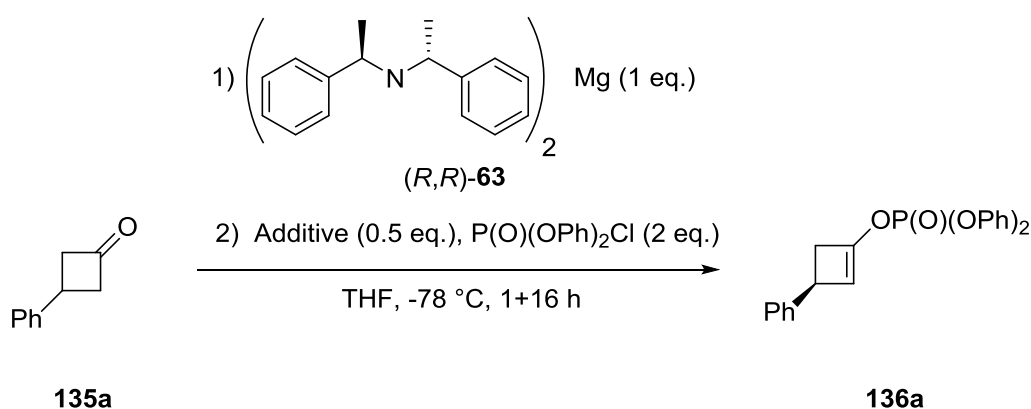
Scheme 9.91

In addition to the above, the mixed alkylmagnesium amide (*R,R*)-**105** was explored (**Scheme 10.48**). Indeed, such a base has been shown to be an effective base in our group in the asymmetric deprotonation of 4-*tert*-butylcyclohexanone **25a** and provided the desired silyl enolate product **26a** with similar e.r. value of 94:6, in comparison, with the magnesium bisamide (*R,R*)-**63** base mediated deprotonation (e.r. =94:6) (**Scheme 9.107**). When the mixed alkylmagnesium amine (*R,R*)-**105** was used the product **136a** was obtained with a moderate yield (55%), but the e.r. decreased to 55:45.



Scheme 9.92

Unfortunately, none of these amended conditions showed a significant improvement on the enantiomeric ratio of the product **136a**, although the yield was slightly higher in both cases. In a final attempt, different Lewis basic additives were also studied, such as TMEDA and DMPU, to stabilise and deaggregate the chiral magnesium base (*R,R*)-**63**. The beneficial effect of DMPU was previously reported in the asymmetric deprotonation of cyclohexanones **25a** (Scheme 9.93).⁸¹ In the case of DMPU, a slightly higher yield (62%) was obtained but the enantioselectivity of the process remained low e.r. of 55:45 (entry 1 in Table 9.44). Unfortunately, the use of TMEDA also delivered the product **136a** with significantly lower yield of 35% and the observed enantioselectivity only slightly increased to 62:38. (entry 2 in Table 9.44).



Scheme 9.93

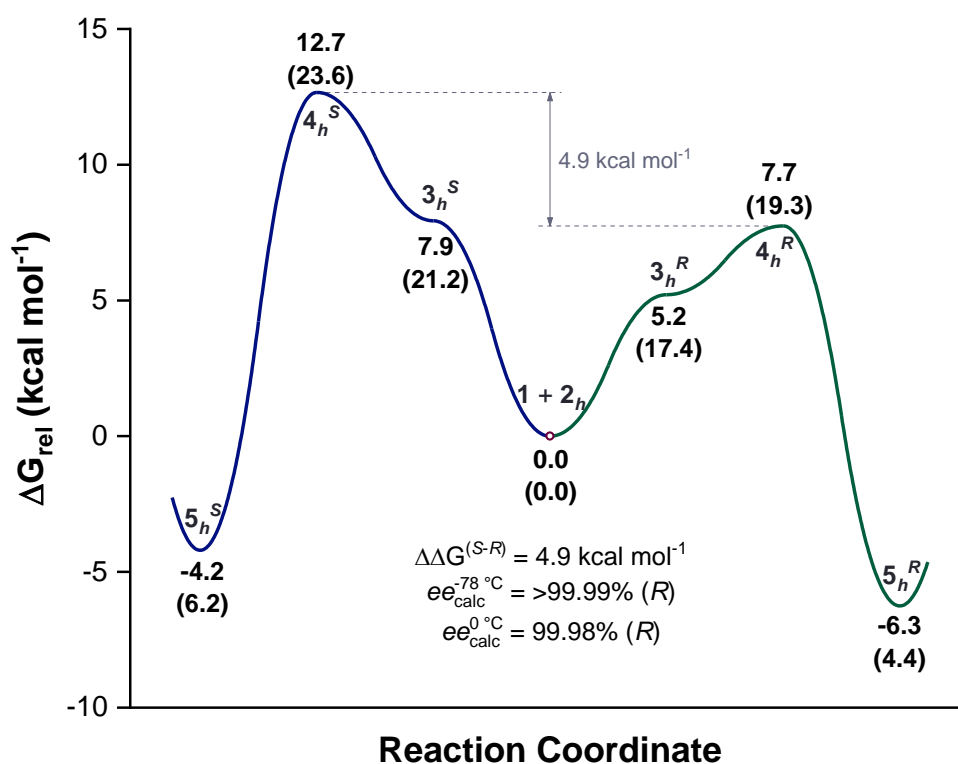
Entry	Additive	Yield (%)	e.r.
1	DMPU	62	55:45
2	TMEDA	35	62:38

Table 9.44

In summary, during this project a series of experiment were conducted to extend the scope of our asymmetric deprotonation protocol with a series of chiral magnesium bases developed in our group. It has been shown that, although these bases are efficient with 4-substituted cyclohexanones **25** as substrates, only significantly lower enantioselectivities can be obtained in the asymmetric deprotonation of cyclobutanones **135**. Although the preparation of these molecules would allow us to develop a series of chiral pyrrolidines **138**, which are difficult to obtain with other strategies. Therefore based on the Kerr group's growing expertise in theoretical design of reagents for organic synthesis, we focused our attention on exploring this reaction *in silico* with the aim to propose an efficient base for the deprotonation of cyclobutanones **135**.

9.2.4 Towards a Novel Amine Structure

At this stage due to the low enantioselectivity observed in the enantioselective deprotonation of cyclobutanones, a series of computational investigations were carried out. With the aim to identify a novel and synthetically achievable mixed alkylmagnesium amide, which could afford the corresponding phosphoryl enol ethers with high enantiomeric ratios. The computational experiments were carried out and the potential energy surfaces were created by Renan Zorzatto. First, a known substrate 4-phenyl cyclohexanone **25b** was calculated with a mixed base structure (*R,R*)-**63** in order to establish the used computational method. The results of this computational experiment are summarised below (Figure 9.8).



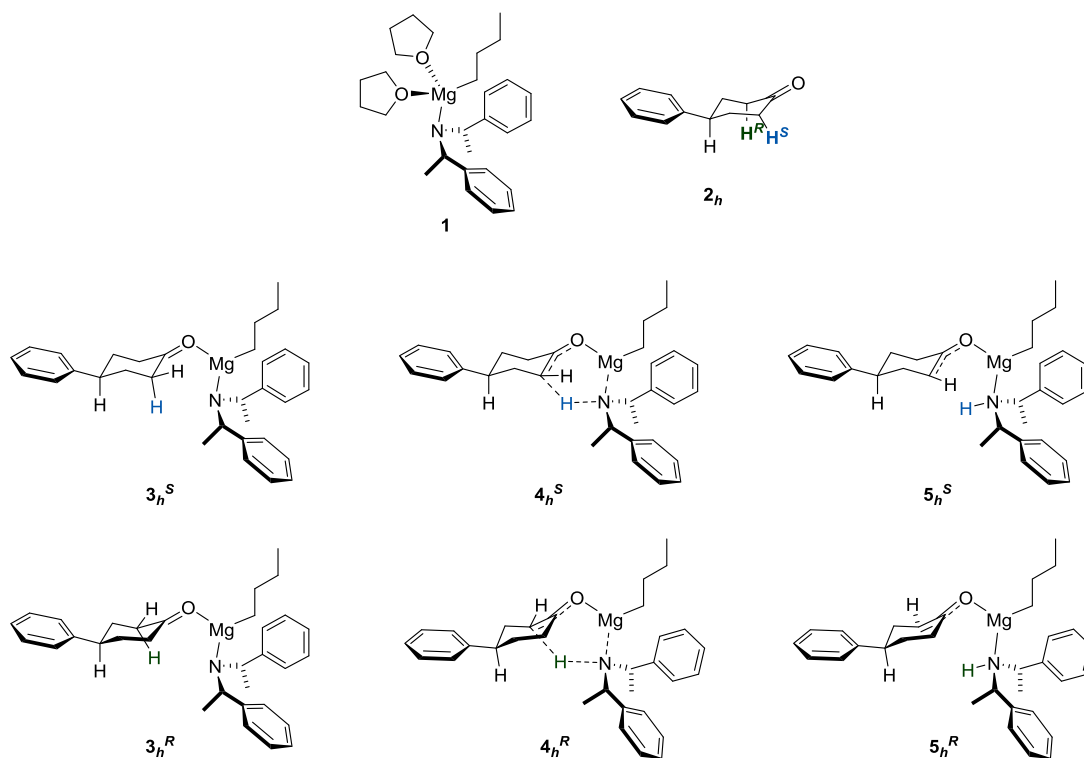
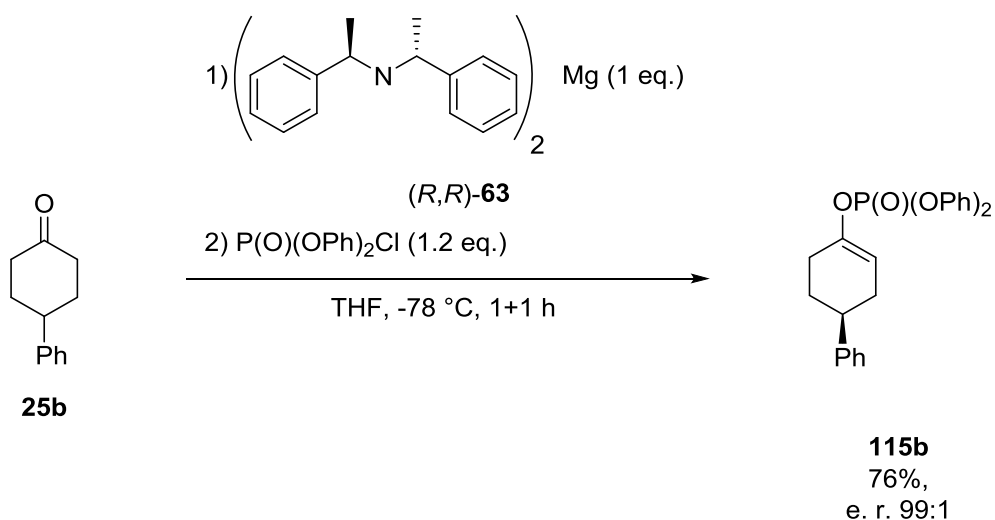


Figure 9.8

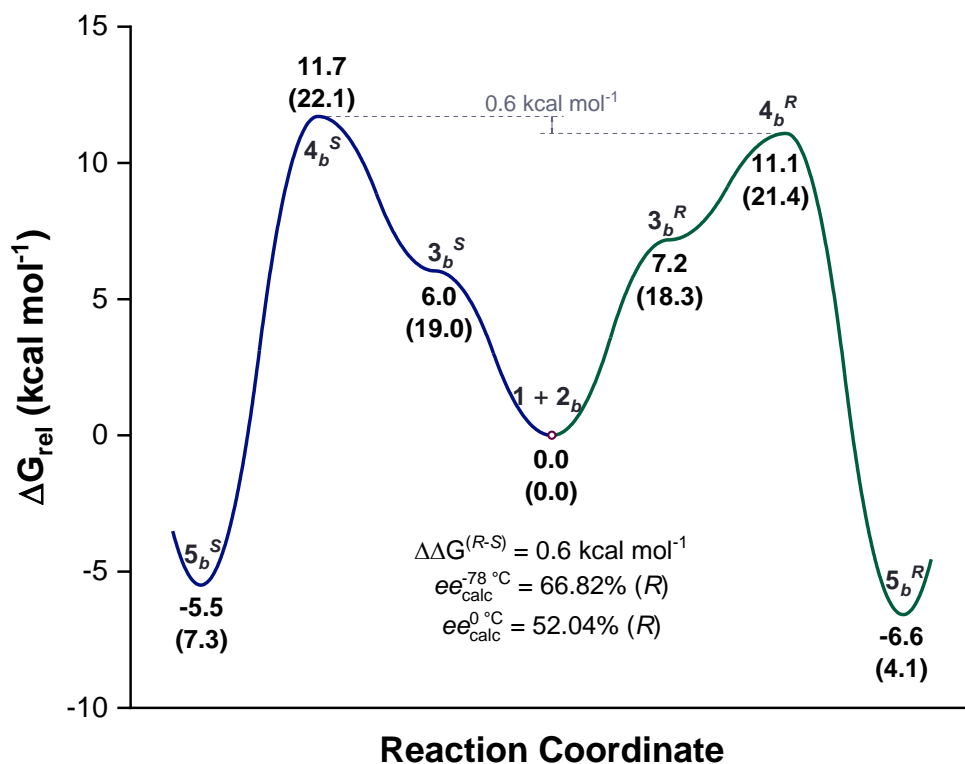
The values quoted refer to the Gibbs free energy of the optimised structure and one molecule of THF was omitted from structures 3-5 for clarity

Starting from ketone **2_h** and ligand **1**, two different deprotonation pathways were envisioned through the removal of the pro-(*S*) or pro-(*R*) acidic protons. In both cases the reaction started with the decoordination of a molecule of THF and the coordination of the conformationally locked substrate. The PES analysis showed that this elementary step is readily achievable through a relatively small energy barrier (2.7 kcal/mol and 0.0 kcal/mol on both pathways). Thereafter the base could remove either the pro-(*S*) (blue hydrogen, left side on **Figure 9.8**) or pro-(*R*) (green hydrogen, right side on **Figure 9.8**) axial proton leading to the corresponding enolate. When the energy profile leading to the pro-(*S*) product was calculated, a 7.2 kcal/mol barrier was observed which is significantly higher (by 4.9 kcal/mol) than the corresponding energy barrier with the analogous pathway leading to the (*R*)-enolate 2.5 kcal/mol. Therefore a good enantiomeric ratio was predicted for the asymmetric deprotonation of 4-phenylcyclobutanone **25b** with the mixed alkyl magnesium amide. Importantly a similarly high ee was obtained when the reaction was carried out under the standard deprotonation conditions and the product **115b** was obtained in a good yield of 76% and high e.r. of 99:1..



Scheme 9.94

In the case of 4-phenylcyclobutanone **135a**, the observed low enantioselectivity was assumed to be caused by the small energy difference between the removal of the *pseudo*-axial and *pseudo*-equatorial hydrogens. Therefore, the energetics of these pathways were calculated with the benchmark mixed alkylmagnesium amide structure **1** (Figure 9.9).



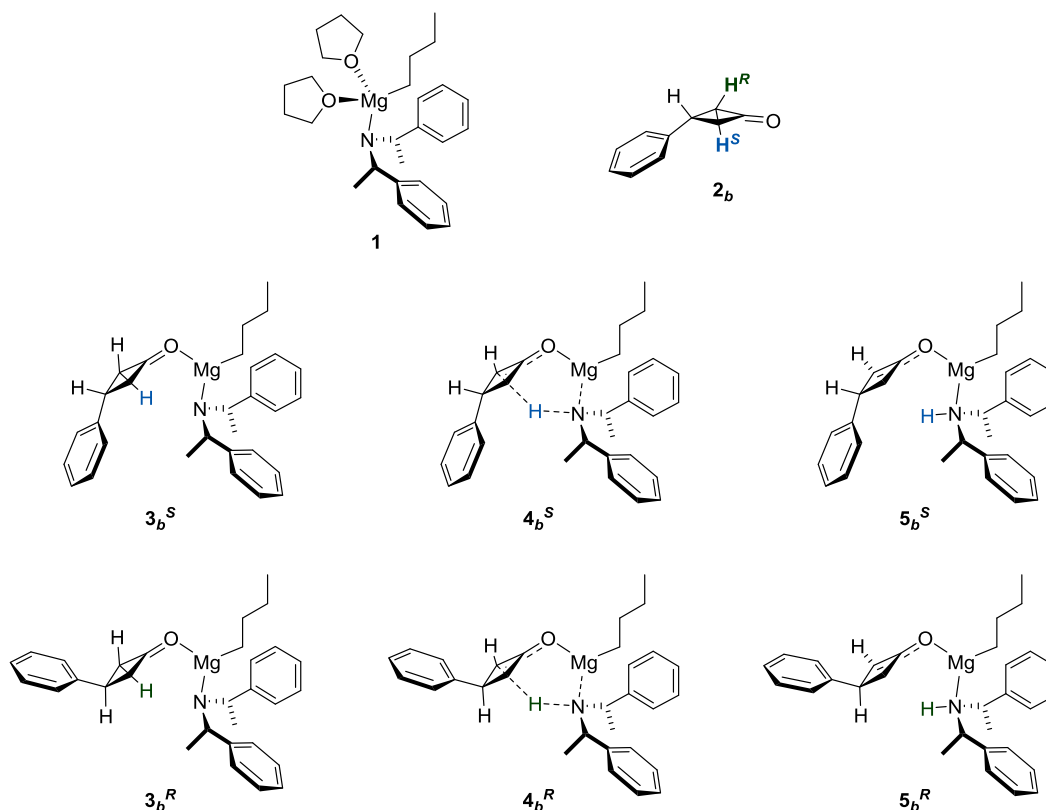


Figure 9.9

The values quoted refer to the Gibbs free energy of the optimised structure and one molecule of THF was emitted from structures 3-5 for clarity

Again, in parallel with the 4-phenylcyclohexanone **25b** case, the reaction started with the replacement of one molecule of coordinated THF, which step which was slightly endergonic by 1.9 and 0.8 kcal/mol in both cases for 3_b^S and 3_b^R for the diastereomeric complexes. This was followed by the removal of the acidic hydrogen atom by the amide. In this case, a low energy difference 0.6 kcal/mol was observed between the removal of the *pseudo*-axial proton (blue hydrogen, left side on **Figure 9.9**) and the removal of the *pseudo*-equatorial proton (green hydrogen, right side **Figure 9.9**). Therefore, a sterically more demanding novel amine structure would be able to create an extended, tighter chiral pocket which would be able to discriminate effectively between the two diastereotopic faces of the cyclobutanone..

Due to the lack of reported protocols in the literature for the asymmetric deprotonation of cyclobutanones **135** with alternative amide bases, our research focused on the asymmetric deprotonation with higher membered rings, where a similar small energy difference between the removal of the *pseudo*-axial and -equatorial hydrogens are expected to translate well to the cyclobutanone system the cyclobutanone system. To our delight, benzhydryl ligands were successfully used in asymmetric deprotonation reactions of tropinone and granatanone.^{146,147} In addition, these ligands were also synthetically accessible through short sequences and were highly

modular.^{146,147} When a novel sterically more hindered mixed alkyl magnesium amide structure was calculated with sterically demanding CF₃ groups in the *meta*- position of the aryl rings, the deprotonation event which leads to the formation of the corresponding enolates was predicted to occur with high enantiodiscrimination *in silico*. In this case, all of the four possible diastereomeric transition states were calculated to ensure the formation of the desired product would proceed with high enantioselectivity (**Figure 9.10**).

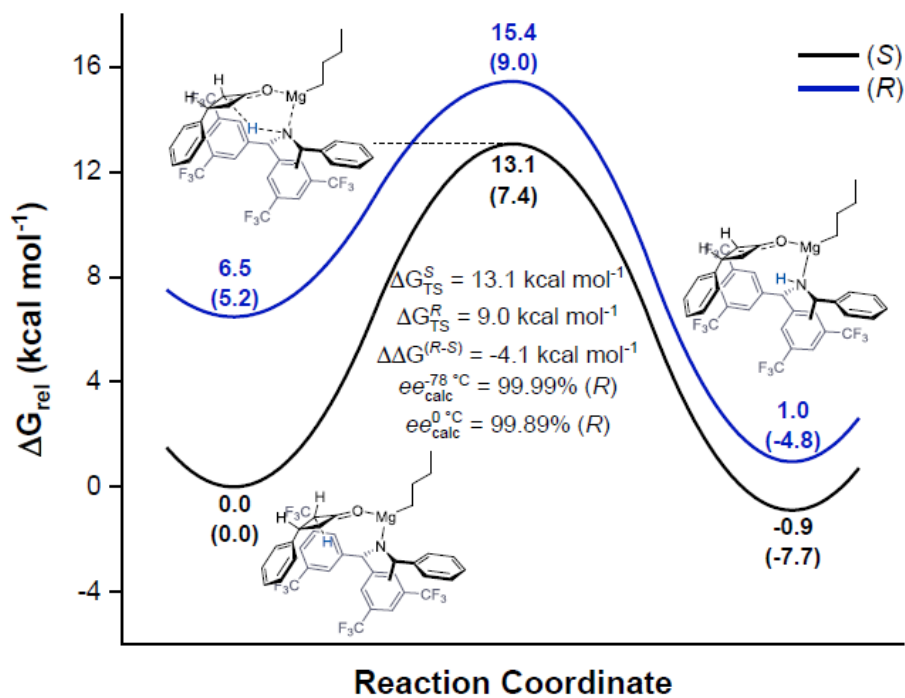


Figure 9.10

First, the energy profile for the removal of the *syn*-hydrogen atoms with respect to the phenyl substituent were evaluated. In this case, a good selectivity towards the (*R*)-enolate was predicted, clearly indicating the the capability of this novel alkylmagnesium amide to distinguish between the *syn*-(*R*)- and *syn*-(*S*)-hydrogens. At this stage the inability to obtain the desired enolate with a high e.r. was attributed to the low energy difference between the removal of *syn*- and *anti*- hydrogen atoms (with respect to the phenyl group). Therefore the energy barriers for the removal of the *anti*-hydrogen atoms were also calculated, and significant energy difference between the two transition states of 2.5 kcal/mol was observed in favour of the (*R*)-enolate (**Figure 9.11**).

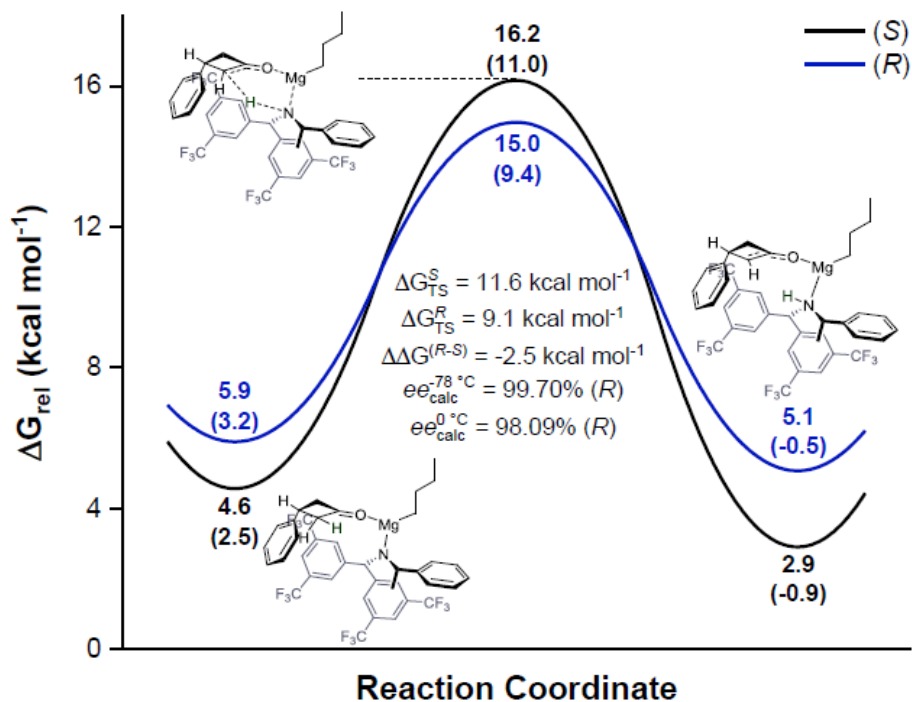


Figure 9.11

Finally, since equilibration of the different coordination modes can occur in the reaction medium, the energy profile of all possible pathways were re-evaluated and the ee was calculated with the two lowest activation energies (Table 9.45).

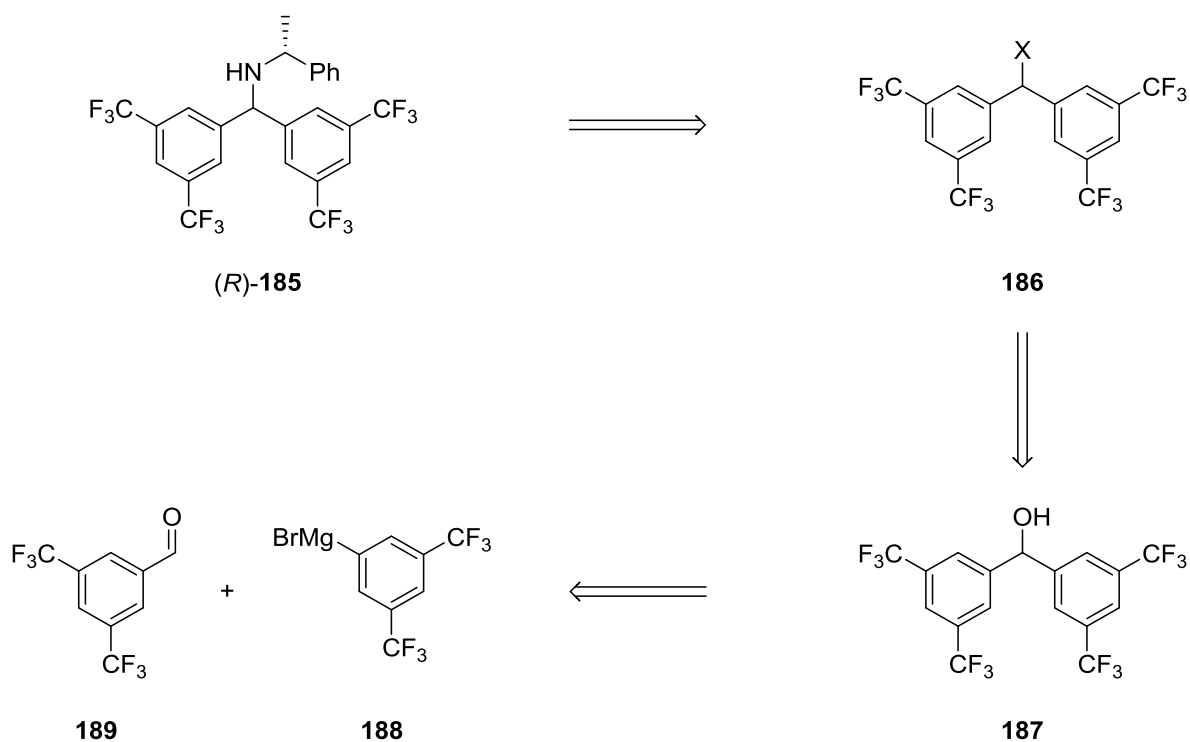
Parameter	H ^(S) _{syn}		H ^(R) _{syn}		H ^(S) _{anti}		H ^(R) _{anti}	
	Adduct	TS	Adduct	TS	Adduct	TS	Adduct	TS
ΔG_{rel} (kcal mol ⁻¹)	0.0	13.1	6.5	15.4	4.6	16.2	5.9	15.0
ΔH_{rel} (kcal mol ⁻¹)	0.0	7.5	5.2	9.0	2.5	11.0	3.2	9.4
$\Delta\Delta G^{(\text{S-R})}$		-1.91						
$ee^{-78\text{ }^\circ\text{C}}$ (%)		98.55						
$ee^{0\text{ }^\circ\text{C}}$ (%)		94.23						

Table 9.45

Even in this case a high ee was predicted, therefore, our efforts were focused on the synthesis of this novel magnesium base.

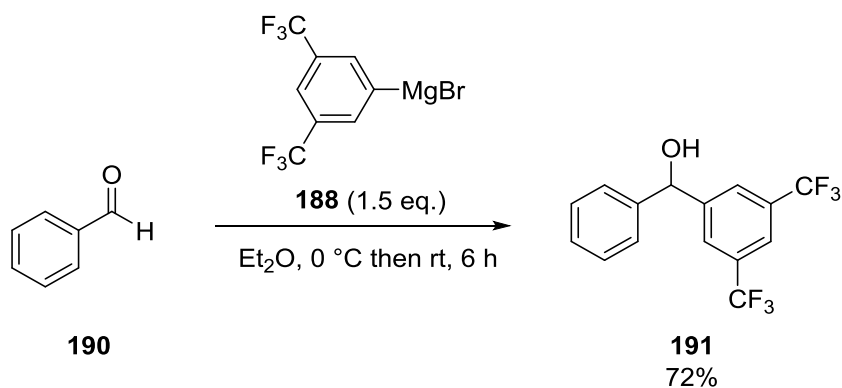
9.2.5 Synthesis of the Novel Amine

The synthesis of novel amine structure (*R*)-**185** was envisaged through the sequence described in **Scheme 9.95**. Final installation of the chiral amine arm would be carried out *via* a nucleophilic displacement reaction of a suitable leaving group. The ultimate starting materials would be an aldehyde and Grignard reagent.



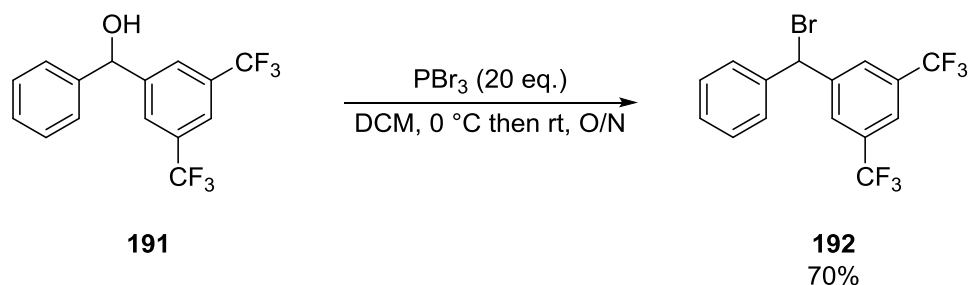
Scheme 9.95

Due to the cost of the required 3,5-substituted benzaldehyde starting material **189**, the reaction sequence was first optimised with benzaldehyde **190**. Indeed, the direct addition was carried out based upon literature conditions,¹⁴⁸ and, pleasingly, the desired alcohol **191** was obtained in a high 72% yield. (**Scheme 9.96**).



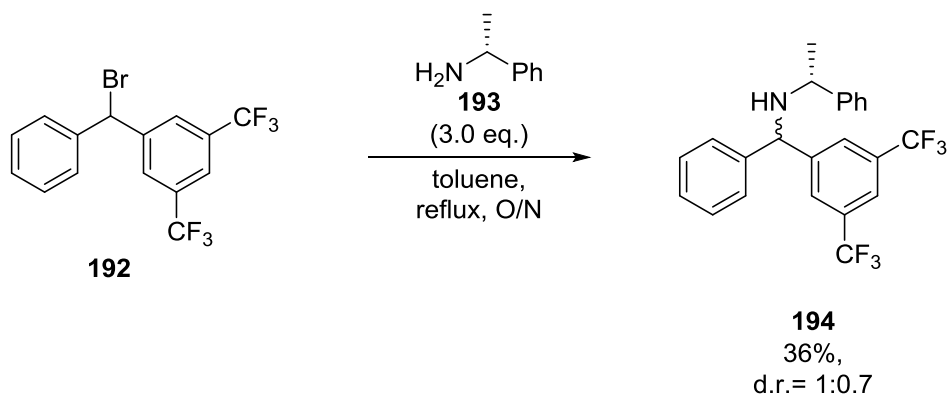
Scheme 9.96

Thereafter a bromination reaction was carried out with phosphorous(III) tribromide, delivering the corresponding product **192** in a good 70% yield. (Scheme 9.97).¹⁴⁸



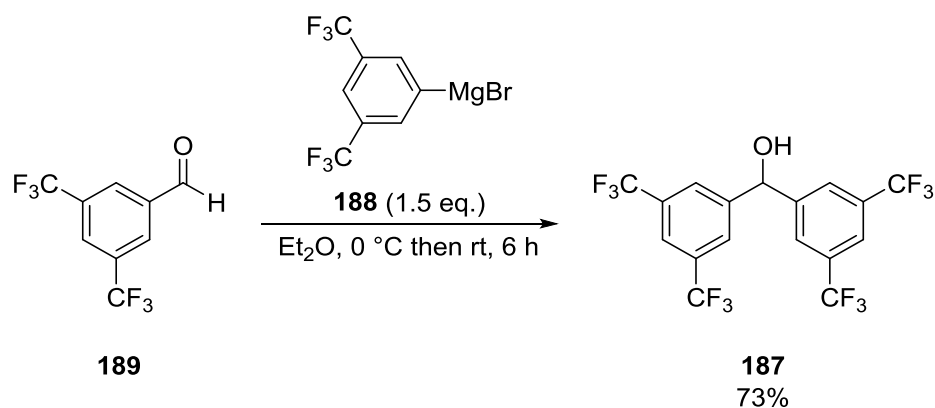
Scheme 9.97

Finally, nucleophilic substitution with (*R*)-1-phenylethylamine **193** was carried out under refluxing conditions in toluene. The desired amine product **194** was obtained in a moderate yield of 36% with a 1:0.7 d.r. (Scheme 9.98).



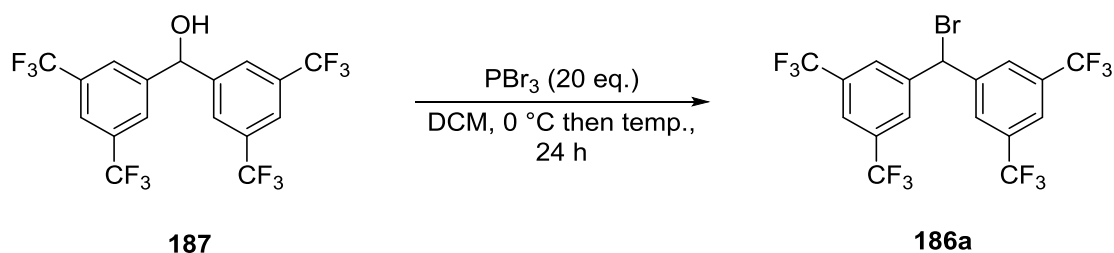
Scheme 9.98

With the established method in hand, the same conditions were applied to prepare the desired analogue, bis(3,5-bis(trifluoromethyl)phenyl)methanol **187** (Scheme 9.99). Indeed, we were pleased to obtain **187** in a similar 73% yield.



Scheme 9.99

Thereafter, bromination was attempted (**Scheme 9.100**). After 24 h at rt, only starting material **187** was observed, therefore, after a work-up procedure, the crude mixture was resubjected, using further quantities of PBr_3 , and refluxed for a further 24 hours. Whilst a series of new peaks were detected using TLC analysis, during isolation, the desired product **186a** decomposed on silica.

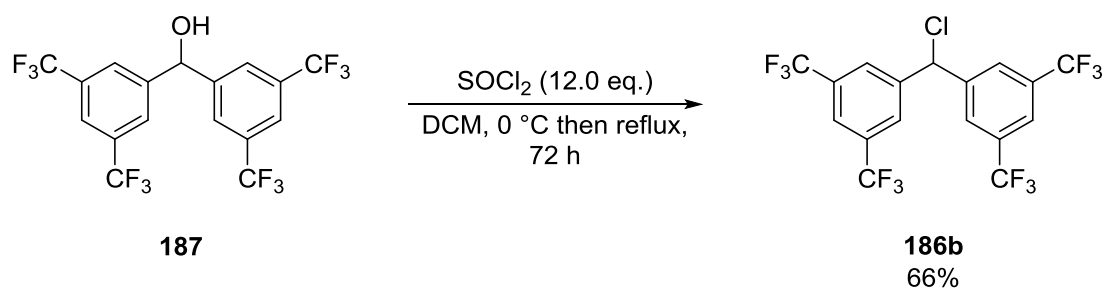


Scheme 9.100

Entry	Temp. (°C)	Comment
1	rt	Only SM
2	reflux	Decomposition

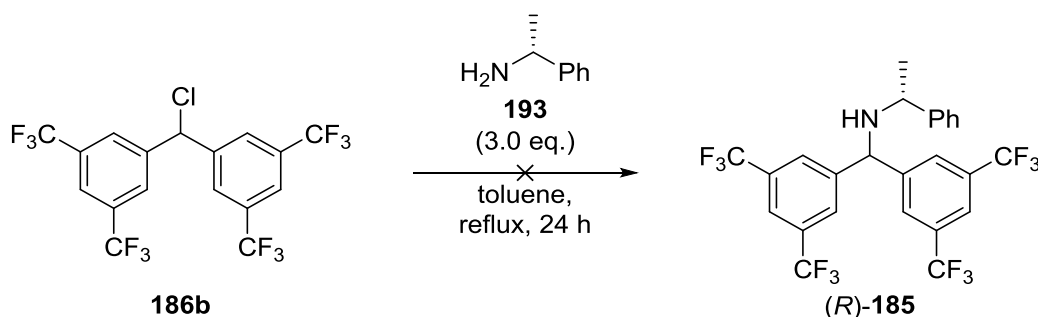
Table 9.46

At this stage, alternative leaving groups were considered, including chloro-, tosyl-, and mesityl derivatives in place of the bromo compound **186a**. As such, the chlorination of **187** was attempted with thionyl chloride as shown in **Scheme 9.101**.¹⁴⁸ To our delight, the desired chlorinated product **186b** was isolated in a good 66% yield after recrystallisation from petroleum ether.



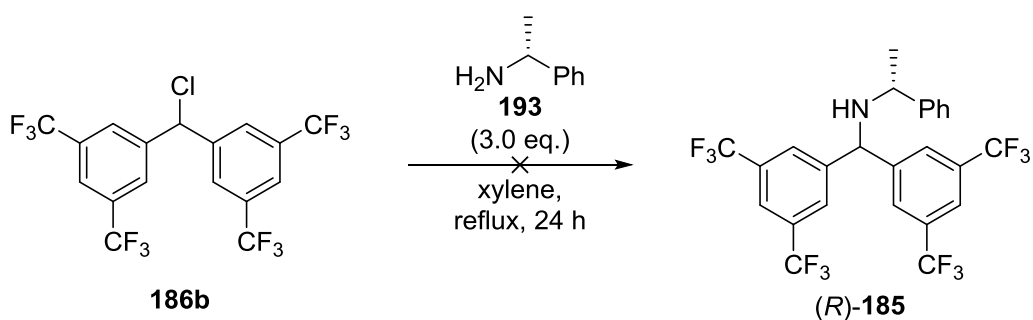
Scheme 9.101

Subsequently, nucleophilic substitution was carried out in an effort to deliver the desired final amine target (*R*)-**185** (Scheme 9.102). Unfortunately, under refluxing conditions for 24 h, only starting material **186b** was detected in the crude ^1H NMR spectrum.



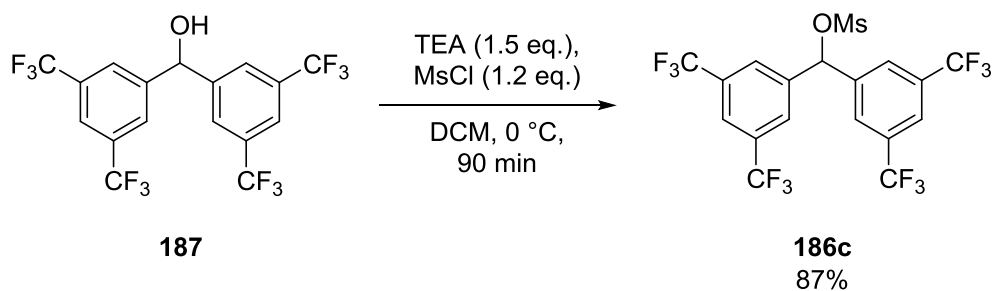
Scheme 9.102

Indeed, this is possibly due to the increased stability of the carbon-chlorine bond. Employing harsher conditions, *via* the use of the higher boiling solvent xylene, also did not yield the desired product (*R*)-**185** (Scheme 9.103).



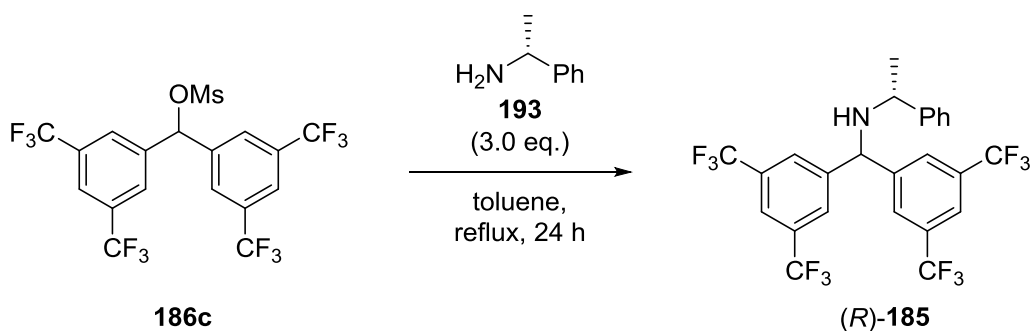
Scheme 9.103

Due to these observed difficulties, our attention turned to alternative, but still reactive, leaving groups, which could be easily prepared from the corresponding secondary alcohol **187**. In this manner, the analogous mesylate **186c** was prepared using literature conditions (Scheme 9.104).¹⁴⁸ The corresponding mesylate **186c** was obtained in an excellent 87% yield in the presence of 1.5 eq. triethylamine and 1.2. eq. mesyl chloride.



Scheme 9.104

The final nucleophilic substitution step was attempted with the mesylate starting material **307** (entry 1 in **Table 9.47**). When toluene was used as a solvent the desired product peaks **185** were not observed in the crude ^1H NMR spectrum. As such, the reaction was performed at higher temperatures, using xylene as the reaction medium, and for an extended time period 72 h. In this case the desired product (*R*)-**185** was obtained with a low 16% yield (entry 2 in **Table 9.47**).



Scheme 9.105

Entry	Solvent	Reaction time	Yield (%)
1	toluene	24 h	-
2	xylene	72 h	16

Table 9.47

At this stage due to the low yielding last step and the lack of time we focused our synthetic endeavours on the preparation of chiral azepanes through *via* enantiomerically enriched 6-membered cyclic enol phosphates, which project was carried out parallel with the asymmetric deprotonation of cyclobutanones.

9.2.6 Summary and Future Work

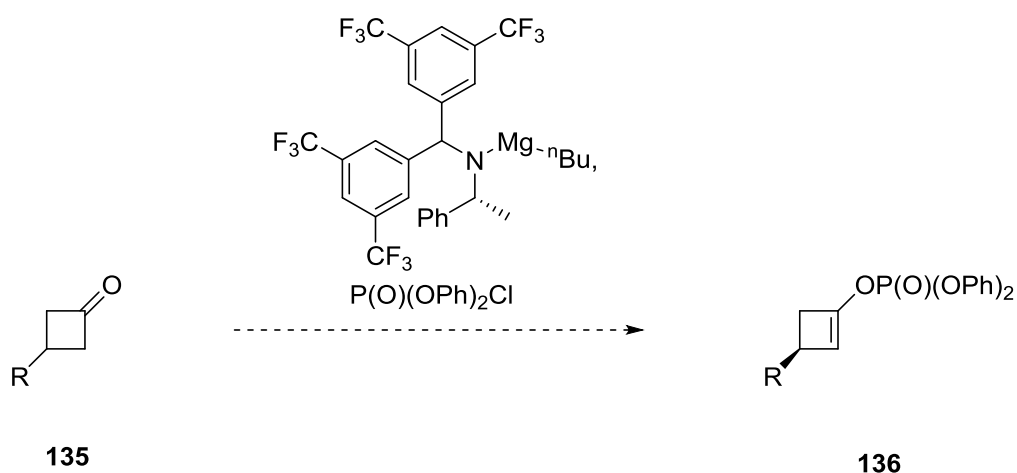
The enantioselective deprotonation of a series of cyclobutanone substrates was performed using conditions developed in the Kerr group, with the ultimate aim of elaborating the enantio-enriched products to desirable heterocyclic motifs. Employing identical deprotonation conditions to that previously reported,¹⁰³ it was realised that the corresponding phosphoryl enol ether products were obtained with a significantly lower enantiomeric ratio. In an attempt to rationalise the results, various parameters such as the reaction solvent, the use of additives, and testing various starting cyclobutanones were explored, but to no avail. In addition to this, the same batch of the magnesium base was used for the known deprotonation of 4-*tert*-butylcyclohexanone **25a** and the reaction of interest as part of this programme of work (the deprotonation of 3-phenylcyclobutanone **135a**). In the former case, the corresponding phosphoryl enol ether **115a** was isolated with a high e.r. of 96:4, which was in line with what had been reported previously. In the latter case, the product **136a** was obtained with a low enantioselectivity (e.r. = 68:42). This result eliminated the formation of the magnesium base (*R,R*)-**63** as a possible source for the observed low selectivity. In addition to this, the integrity of the starting cyclobutanone substrate **135a** was confirmed by successfully replicating literature conditions⁵² in the preparation of the corresponding silyl enol ether **184a** derivative with high enantiomeric ratio (90:10). After these significant attempts to rationalise the results, it was realised that the issues related to a previous mis-assignment of the chiral HPLC analysis. Indeed, following further manipulation of the products *via* a cross-coupling reaction, the real enantiomeric ratios were established as those obtained as part of these studies, i.e. the lower ratios reflected the true results.

Due to the observed difficulties, a rational approach to develop a new, and effective, chiral magnesium base was undertaken. Employing a series of DOSY experiments, the main component of the commonly used base (*R,R*)-**63** in solution under the standard conditions was identified as the mixed alkylmagnesium amide (*vide infra*) and the reaction energetics were calculated computationally. After establishing an *in silico* method for the enantioselective deprotonation with a known 6-membered cyclic substrate **25a**, a novel alkylmagnesium amide (*R*)-**185** was identified as a potentially effective base for the asymmetric deprotonation of cyclobutanone **135a**.

Synthesis of the requisite novel amine (*R*)-**185** was attempted with a synthetic sequence involving Grignard addition, bromination, and nucleophilic substitution steps. The corresponding secondary alcohol **187** was readily prepared by the addition of the Grignard reagent to aldehyde **189**. Unfortunately, attempts to synthesise the bromo analogue **186a** failed. However, the corresponding

chloro **186b** and mesylate **186c** analogues were prepared in a good 66% and 87% yield, respectively. Whilst the chloro derivative **186b** did not react further, mesylate **186c** was successfully transformed into the desired novel amine (*R*)-**185**, albeit in a low 16% yield. At this stage, due to the low yielding last step and the lack of time the asymmetric deprotonation reaction was not carried out.

Future work should be focused on the optimisation of the last, nucleophilic substitution, step in order to prepare the desired amine in gram quantities. Thereafter, the alkylmagnesium amide (*R*)-**195** base will be prepared using our standard conditions and tested as a chiral base in the enantioselective deprotonation of cyclobutanones **135** (Scheme 9.106).



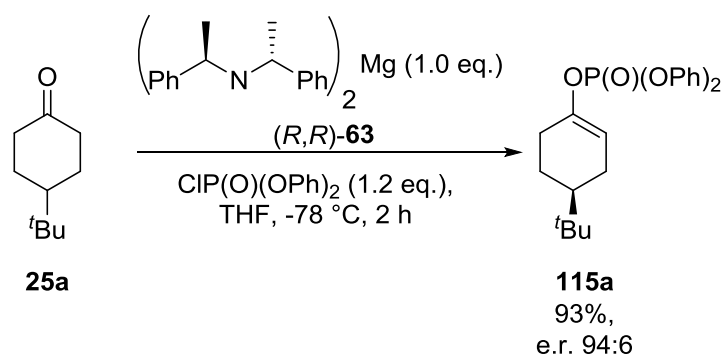
Scheme 9.106

9.3 Structural Studies of Magnesium Amides

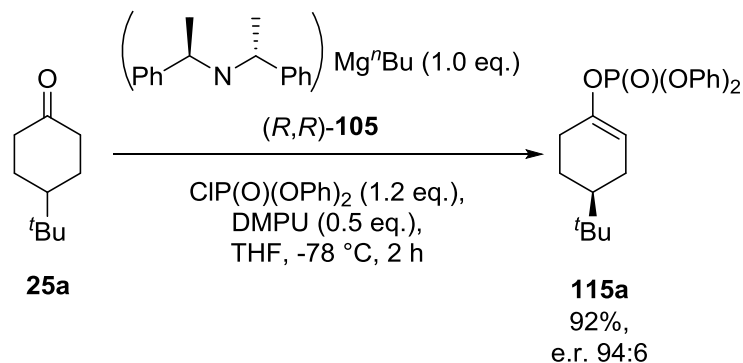
As previously mentioned during the development of magnesium-based organometallic reagents for the enantioselective deprotonation of conformationally-locked cyclic ketones, the enantiomeric induction of mixed alkylmagnesium amides was evaluated.⁸⁹ Interestingly, when only 1 equivalent of (*R*)-bis((*R*)-1-phenylethyl)amine was used in the preparation of the base, a mixed alkylmagnesium amide (*R,R*)-**105** was believed to form. When 4-substituted cyclohexanones **25** were reacted with this base (*R,R*)-**105**, the corresponding chiral silyl enol ethers **26** were isolated in high yield and in an excellent enantiomeric ratios of 94:6-98:2. More importantly, comparing these results with the analogous magnesium bisamide (*R,R*)-**63** mediated deprotonation, similar yields and enantioinductions were observed (**Table 8.1**).

In addition, more recently during the synthesis of chiral enol phosphates, the asymmetric induction of a mixed magnesium species was evaluated. When the alkylmagnesium amide (*R,R*)-**63** was used, comparable levels of enantioselectivity and yield were obtained, with the analogous bisamide (*R,R*)-**105** mediated deprotonation (**Scheme 9.107**).⁹²

Conditions A:

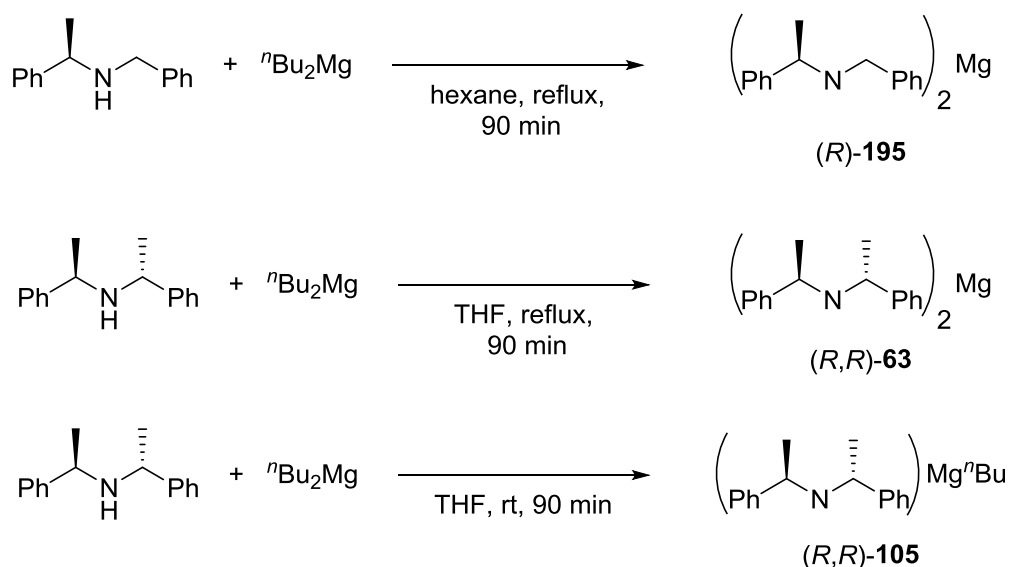


Conditions B:



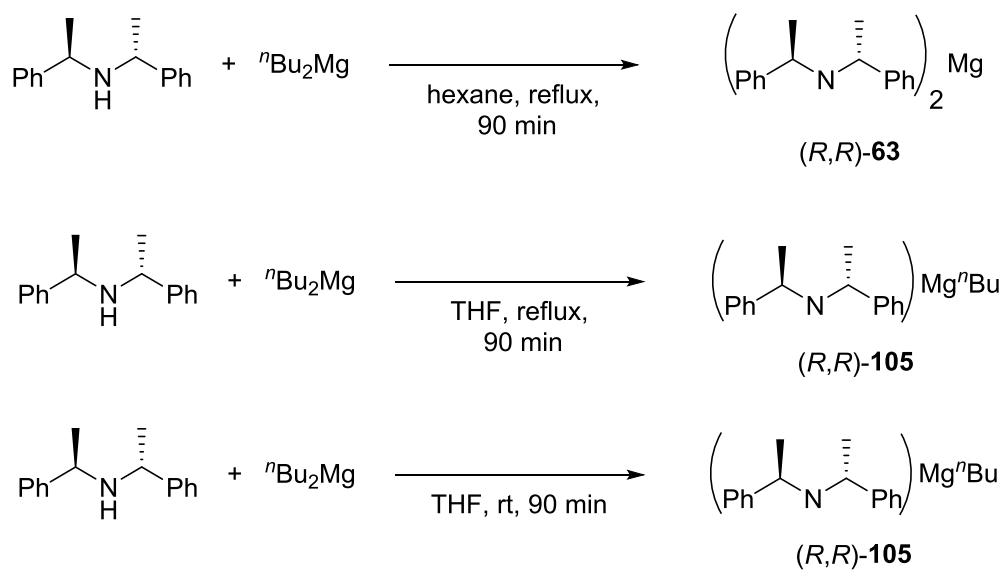
Scheme 9.107

Therefore, the question arose as to whether a different or an identical magnesium species is, responsible for the observed reactivity during the formation of chiral enol phosphates. Subsequently, a detailed ^1H NMR spectroscopic investigation of the formation of magnesium amides was performed with the previously used sets of conditions.⁸⁹ Originally, the magnesium bisamide (*R*)-**187** was formed in hexane under reflux conditions (**Scheme 9.108**).^{79,91} Later the solvent was successfully changed to THF, when C_2 -symmetric amines were used and it was believed that the bisamide (*R,R*)-**63** was formed under these conditions.⁸² Finally, the mixed alkylmagnesium amide (*R,R*)-**105** was also prepared by stirring 1 eq. of amine and 1 eq. of di-*n*-butylmagnesium in THF at room temperature for 90 min (**Scheme 9.108**).⁸⁹



Scheme 9.108

However, a series ^1H NMR spectroscopy experiments showed that different species formed in THF and hexane under these conditions. More importantly, it has recently been shown that in order to prepare the C_2 -symmetric magnesium bisamide (*R,R*)-**63**, hexane has to be used and the reaction requires heating to reflux for 90 min. If THF was used as a solvent, only the alkylmagnesium amide (*R,R*)-**105** was detected in solution (**Scheme 9.109**), even when the reaction was heated to reflux temperature for 90 min.⁹²



Scheme 9.109

Firstly, reproduction of the previously reported results in THF and hexane was attempted. Formation of the base was carried out in hexane and similar spectra was obtained as previously. A new quartet was detected at 3.65 ppm, indicating that a magnesium bisamide species (*R,R*)-**63** is formed (**Figure 9.12**).

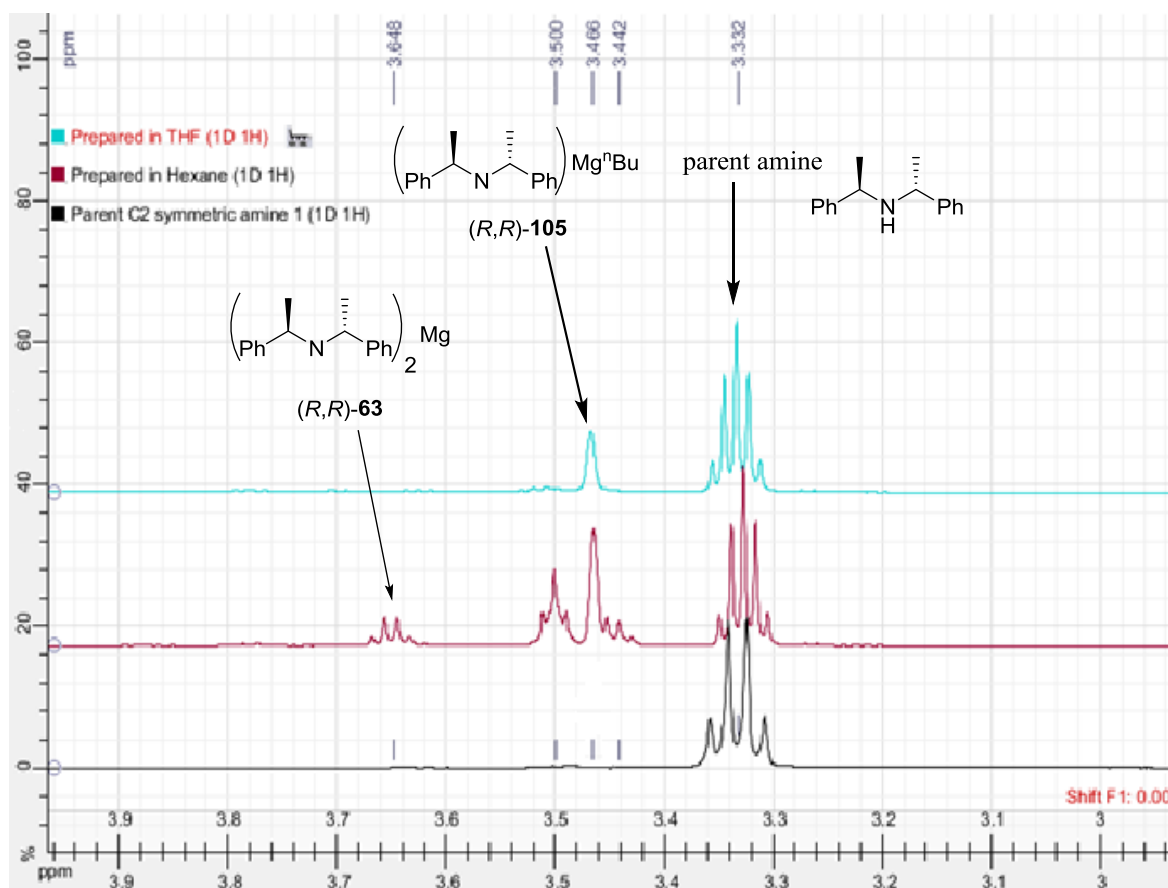
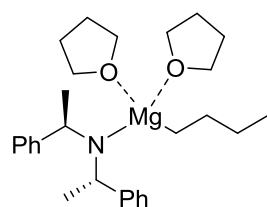
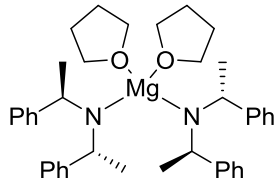


Figure 9.12

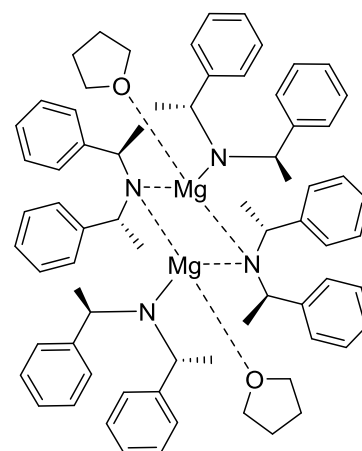
When the reaction was carried out in THF, only the alkylmagnesium amine *(R,R)*-105 was observed at 3.46 ppm. In addition, the molar mass of the species corresponding to the newly formed peaks was determined by a DOSY NMR experiment. A selection of the most probable organometallic species are summarized in **Figure 9.13**.



Molecular Weight: 450 g/mol



Molecular Weight: 617 g/mol



Molecular Weight: 1106 g/mol

Figure 9.13

The results of the DOSY experiment are summarized in **Table 9.3**. A significant difference between the diffusion coefficients for the peaks at 3.46 ppm and 3.65 ppm was observed. The former was identified as the mixed alkylmagnesium amide (*R,R*)-**105**, with a molar mass of 450 g/mol, while the latter was determined as the corresponding signal for the benzylic proton in the magnesium bisamide (*R,R*)-**63** species.

Entry	Solvent	Peak (ppm)	Diff. coeff. (m ² /s)	Molar mass (g/mol)	Difference from expected structure (% ^a)
1	THF	3.46	9.78E-10	366	-18.6
2	THF	3.46	9.65E-10	380	-15.6
3	Hexane	3.65	6.22E-10	1270	+14.8
4	Hexane	3.65	6.22E-10	1270	+14.8

Table 9.48^a: Calculated from the difference between the observed and calculated molar masses.

In an attempt, to determine the ratio between the formed alkylmagnesium amide (*R,R*)-**105** and the unreacted amine in hexane, a PureShift DOSY study was envisioned, which would simplify the spectra by collapsing the multiplets to single peaks. The experiment was carried out by Dr. John Parkinson. Unfortunately, even with this technique, an unidentified signal at 3.44 ppm and the product alkylmagnesium amide signal at 3.46 ppm, are overlapping as shown in **Figure 9.14**, and as a result the amount of alkylmagnesium amide (*R,R*)-**105** could not be determined quantitatively.

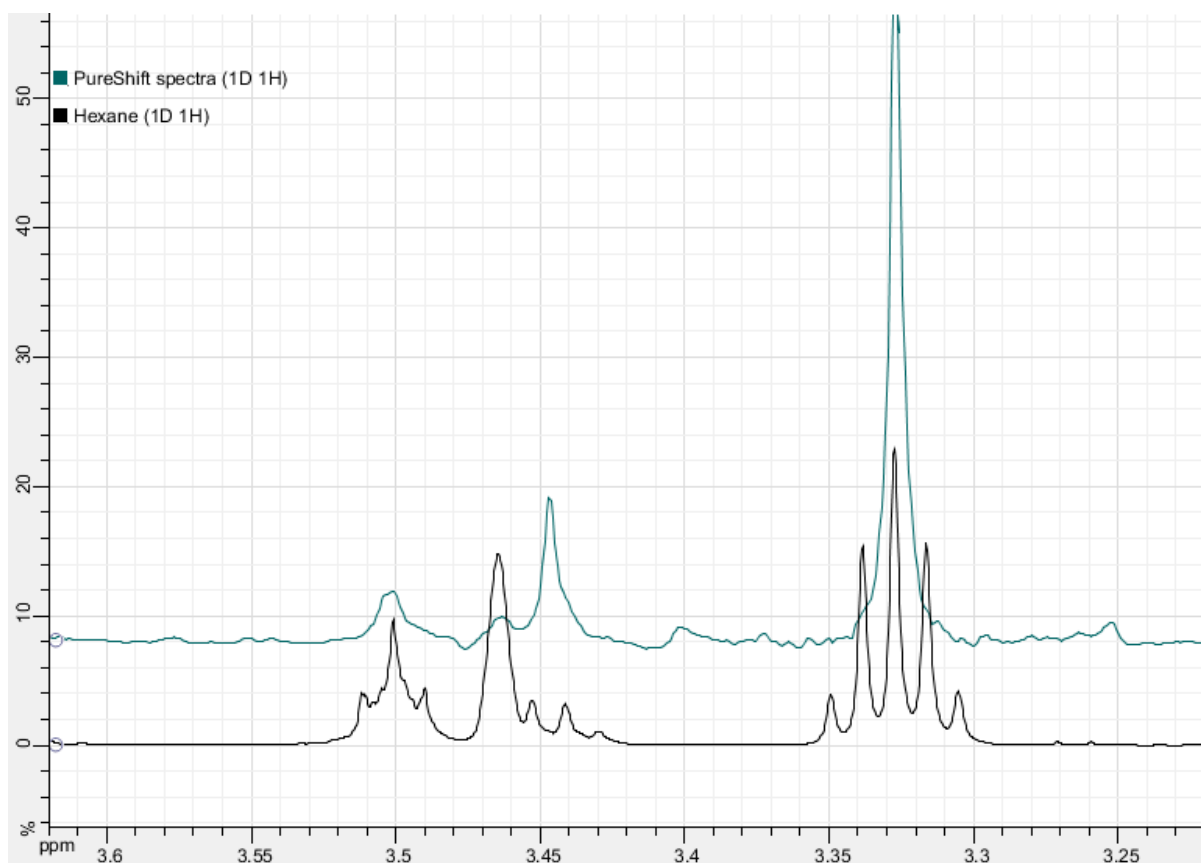
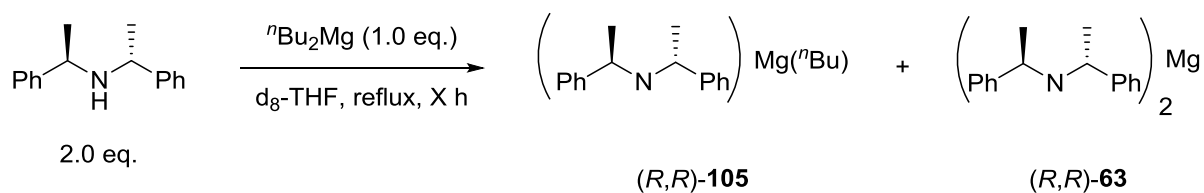


Figure 9.14

Thereafter we investigated the effect of reaction time in d_8 -THF with and attempt to synthesize the bisamide quantitatively (**Scheme 9.110**). After 90 min reflux, a good conversion of 89%, towards the desired mixed alkylmagnesium amide (*R,R*)-**105** was detected with low amount 11% of the bisamide (*R,R*)-**63** (entry 1 in **Table 9.49**). When the heating was continued, extensive decomposition of these species were detected, and the solution was slowly turned to black. After 4 h only (*R,R*)-**105** was detected with a low 10% conversion, indicating the instability of the organometallic base. By extending the reaction time further the amount of (*R,R*)-**105** decreased further to 5% (entry 3 in **Table 9.49**).

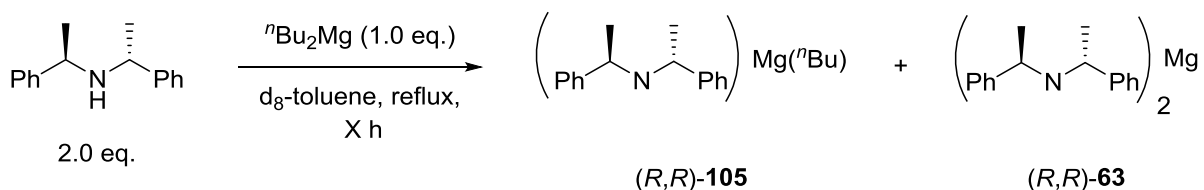


Scheme 9.110

Entry	Time (h)	(<i>R,R</i>)-105 (%)	(<i>R,R</i>)-63 (%)
1	1.5	89	11
2	4	10	-
3	24	5	-

Table 9.49

In an attempt, to drive the reaction to completion d_8 -toluene was used as a solvent, due to its higher boiling point in comparison with THF. Unfortunately, upon addition of the solvent, the reaction turned black and the desired magnesium amine signals (*R,R*-105 and (*R,R*)-63 were not detected (entries 1-3 in Table 9.41).

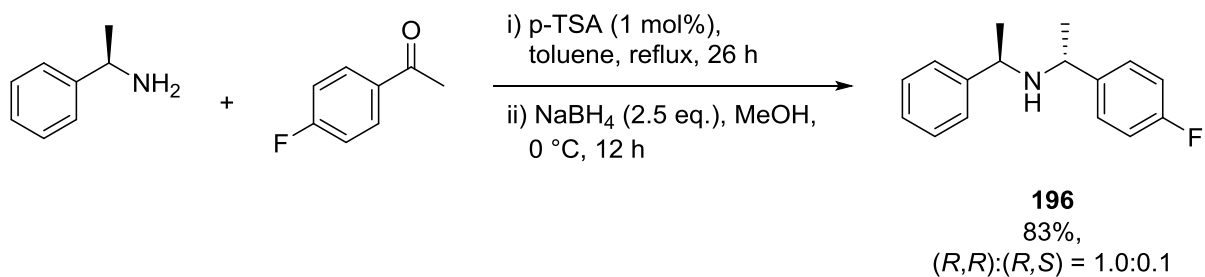


Scheme 9.111

Entry	Time (h)	Monoamine (%)	Diamine (%)
1	1.5	-	-
2	4	-	-
3	24	-	-

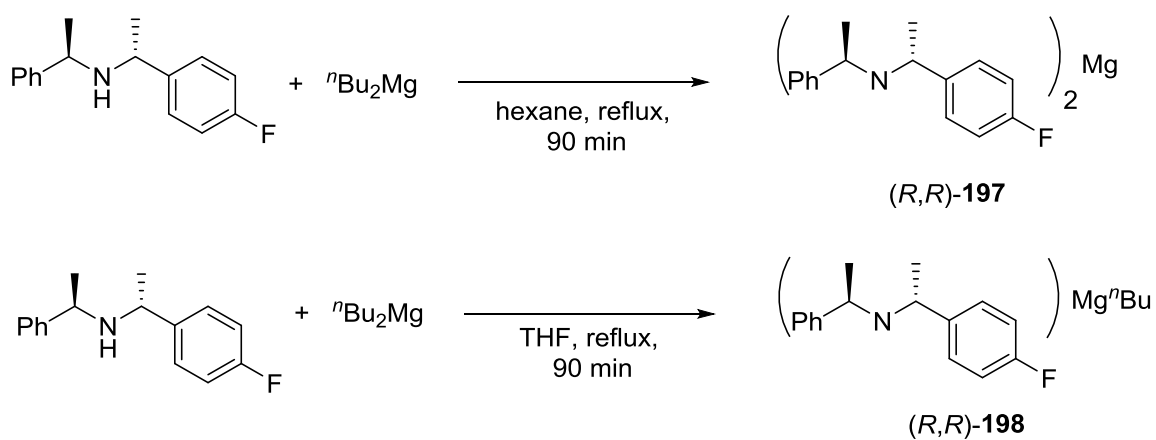
Table 9.50

In both cases isolation of the decomposition products were attempted by flash column chromatography, but proved to be challenging. At this stage, a fluorinated amine analogue (*R,R*)-196 was targeted to prepare in order to follow the formation of the two different magnesium species with a less crowded spectrum (^{19}F NMR). The synthesis of the amine was achieved through a two step sequence.¹⁴⁹ Imine formation was carried out in the presence of *p*-TSA and reduction of the intermediate was achieved under hydrogenation with Pd/C. The corresponding amine **196** was obtained in a good 83% yield and high diastereomeric ratio. of (*R,R*):(*R,S*) = 1.0:0.1 (**Scheme 9.112**). The (*R,R*) diastereomer (*R,R*)-196 was obtained after HCl salt formation and recrystallization.



Scheme 9.112

Unfortunately, when the base formation was carried out in THF and hexane, identical spectrums were obtained (**Figure 9.15**).



Scheme 9.113

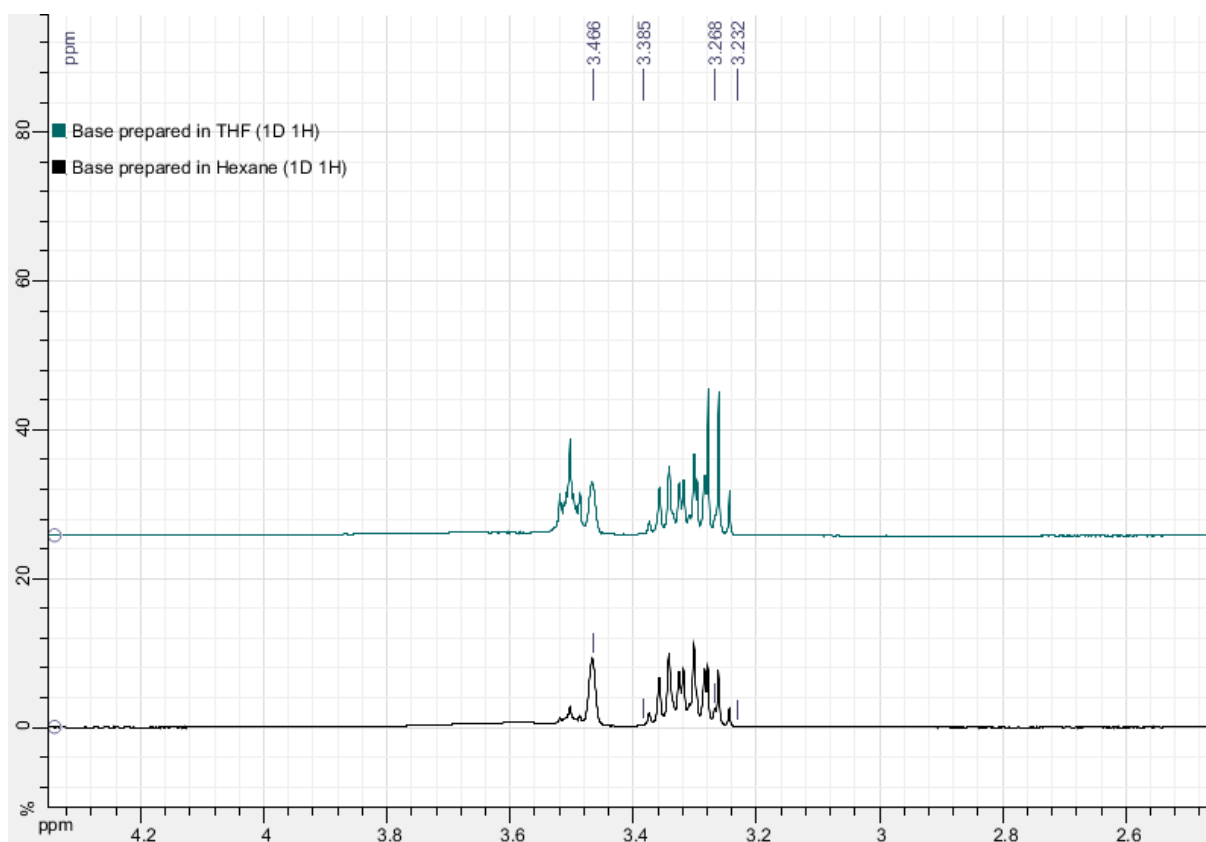
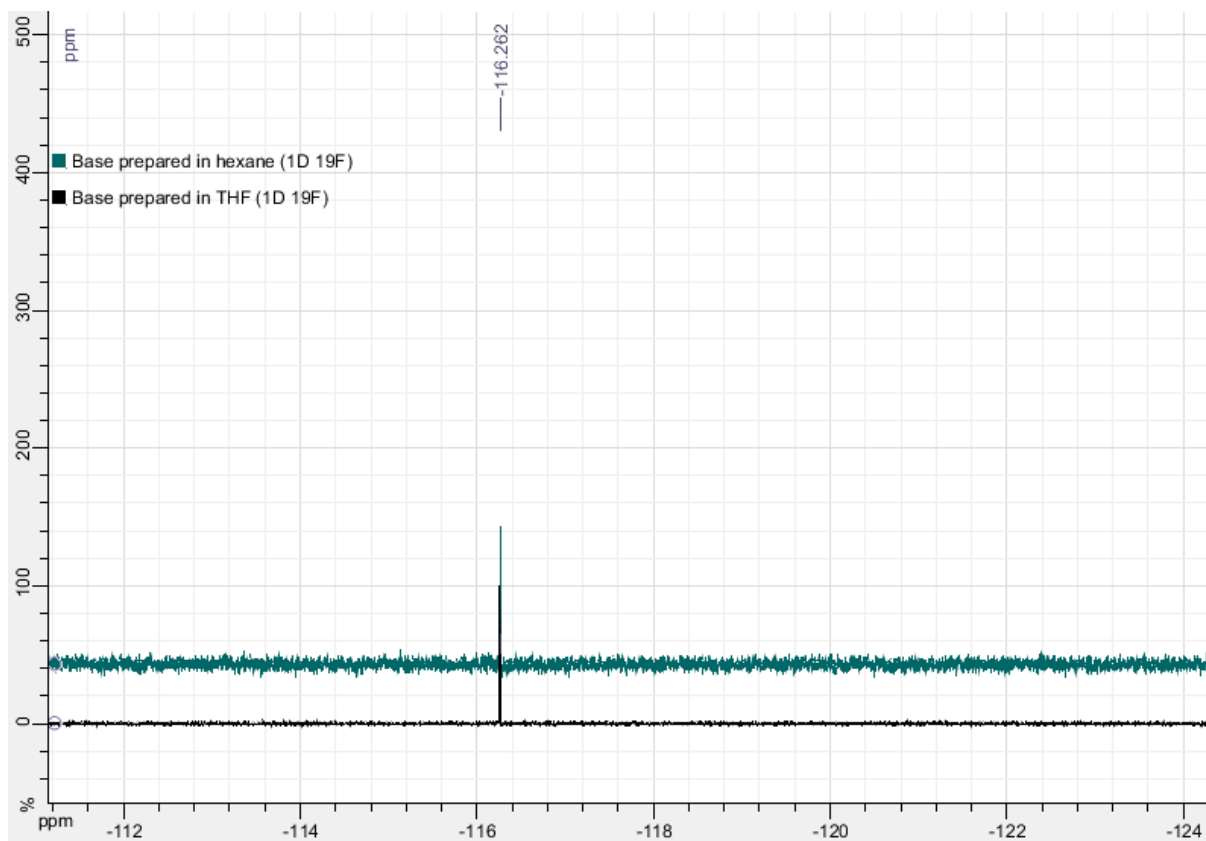
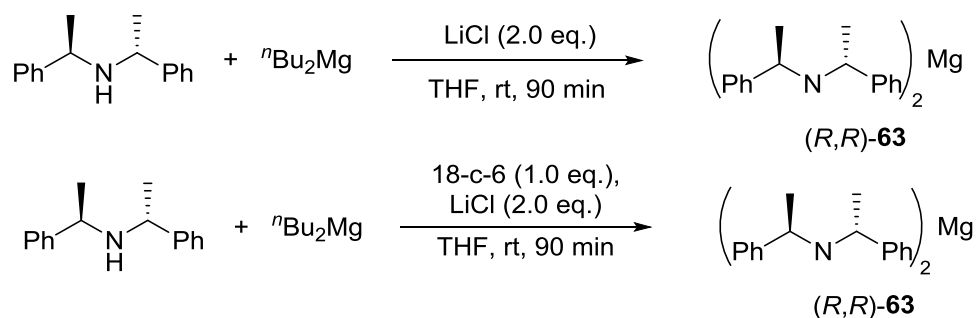


Figure 9.15

Thereafter, the effect of different additives was investigated, in an attempt to form the magnesium bisamide (*R,R*)-**63** at room temperature. Firstly, lithium chloride was used as an additive. The activation of magnesium-based organometallics in the presence of lithium chloride through a mixed-ate complex is well documented,¹⁵⁰ but the desired product bisamide (*R,R*)-**63** was not observed in this case at 3.65 ppm (**Figure 9.16**). Secondly, 18-c-6 was added as an additive. The presence of 18-c-6 as an additive has been shown to be beneficial, in the asymmetric deprotonation of 4-*tert*-butylcyclohexanone **25a**.⁸⁹ Unfortunately, even in this case the formation of magnesium bisamide (*R,R*)-**63** species was not observed (**Figure 9.16**).



Scheme 9.114

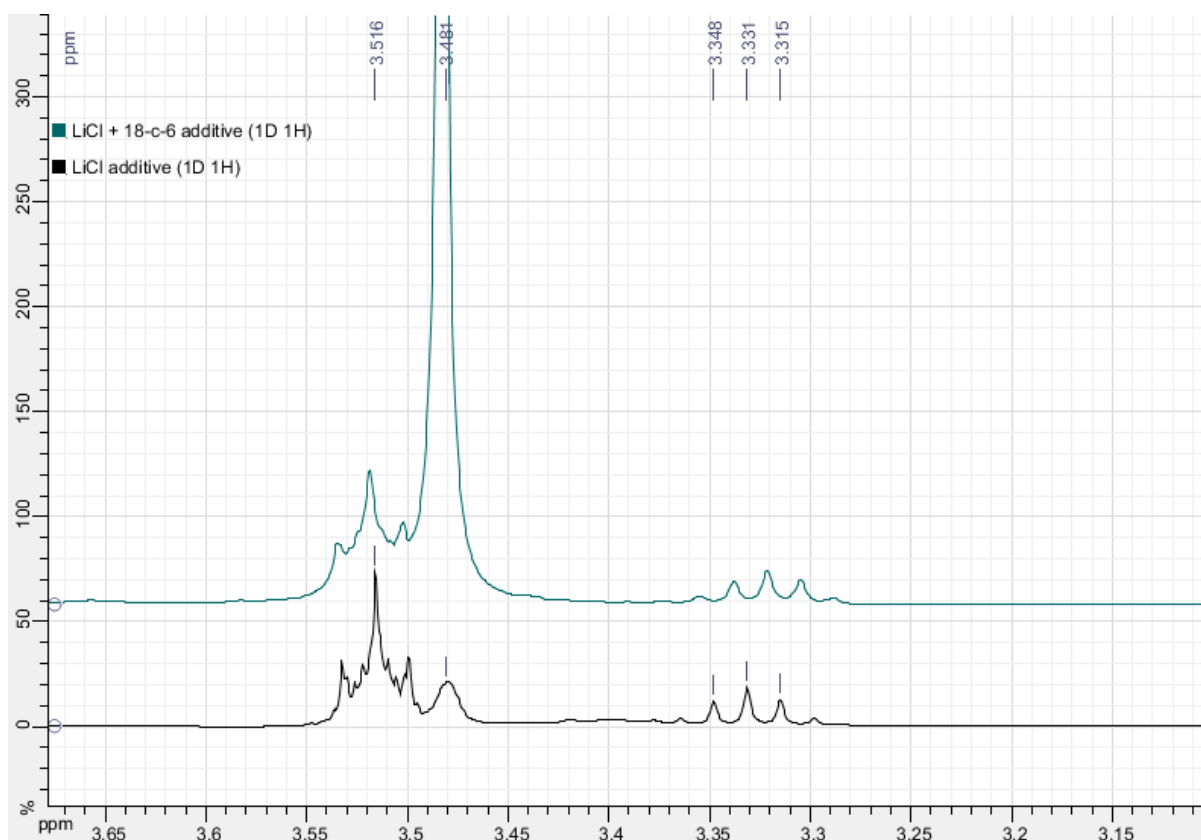
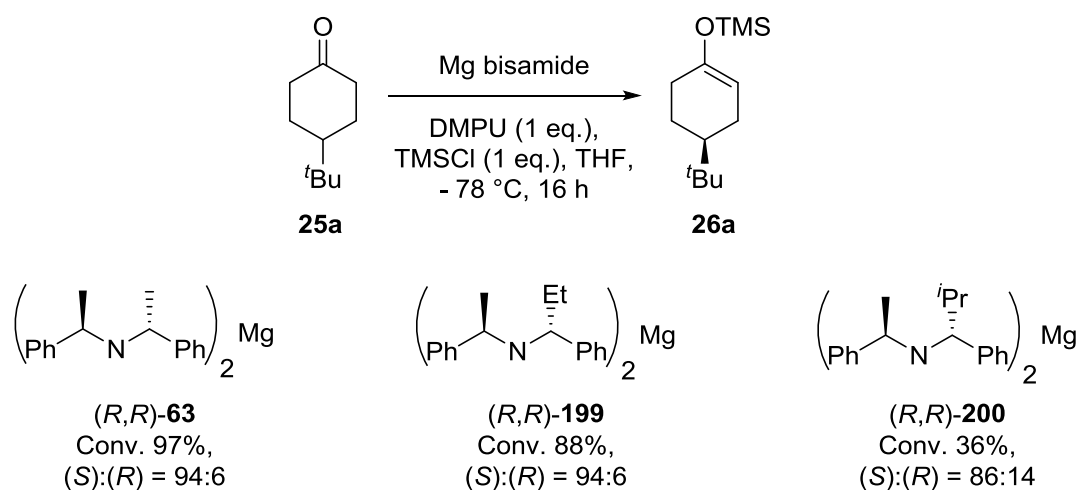


Figure 9.16

Due to the lack of time further experiments were not carried out, but in the future we intend to investigate the effect of different substituents on the α -methyl position by DOSY NMR. Previously, a series of such amides was prepared during the development of new bases for the asymmetric deprotonation of conformationally locked ketones **25** (Scheme 9.115).⁸⁰

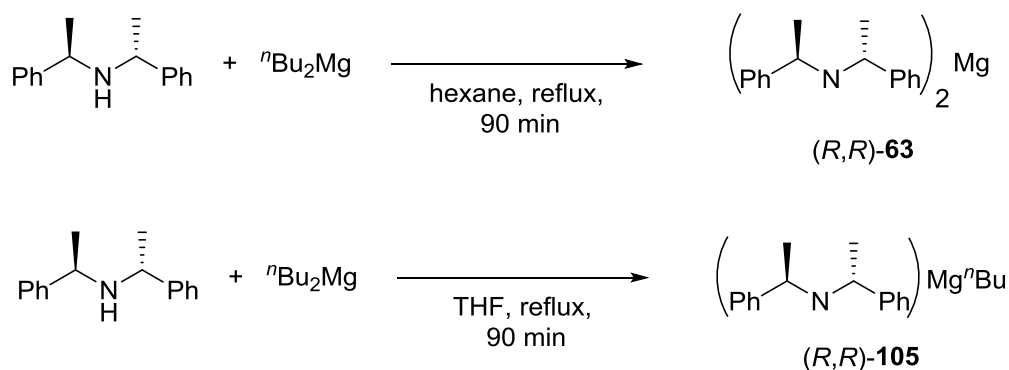


Scheme 9.115

Interestingly, with larger substituents at the α -position, the reactivity dramatically decreased. It is not clear at this point, if this effect was caused by the incomplete formation of the chiral base, or by the decreased reactivity of the *in situ* formed organometallic reactant. These reasons could be further probed using ¹H NMR techniques.

9.3.1 Summary for the Structural Studies of Magnesium Amides

Previously in the Kerr group THF and hexane were successfully used in the formation of magnesium bisamides.^{79,89,91} Interestingly when mixed alkylmagnesium amide **(R,R)-105** was prepared identical results were obtained with the corresponding bisamide **(R,R)-63**, in the deprotonation of conformationally locked cyclohexanones.⁹² Therefore, a DOSY study was performed, which formation of bisamide **(R,R)-63** only occurs in hexane, while in THF only the formation of mixed alkylmagnesium amide **(R,R)-105** was detected.



Scheme 9.116

After reproduction of the previously obtained results, PureShift DOSY technique was used in order to quantify the formation of the two different magnesium species. Unfortunately, even with this technique the quantitative determination of the alkylmagnesium amide is not possible from the obtained crowded spectra. Therefore an alternative fluorinated amine was synthesised in order to investigate the formation of magnesium bases in solution with ^{19}F NMR spectroscopy. In this case the magnesium bisamide $(R,R)\text{-197}$ and alkylmagnesium amide $(R,R)\text{-198}$ were identical by ^{19}F NMR spectroscopy. Finally, the effect of lithium chloride and 18-c-6 was also investigated, since these reagents were previously successfully reported for the activation of organometallic reagents. When the formation of the bisamide $(R,R)\text{-63}$ was attempted in the presence of these additives in THF, only the alkylmagnesium amide $(R,R)\text{-105}$ was detected. Therefore, our research efforts will focus on the quantitative determination of the different magnesium species in THF and hexane. In the future, a series of α -substituted amines $(R,R)\text{-199}$ - $(R,R)\text{-200}$ will be investigated with ^1H NMR techniques to determine the influence of substituents in the α -position.

10 Experimental

10.1 Reagents

All reagents were obtained from commercial suppliers and used without further purification, unless otherwise stated. All reactions were carried out under an inert argon atmosphere, unless otherwise stated. Purification was carried out according to standard laboratory methods.¹⁵¹

- Dichloromethane dried by heating over calcium hydride and then distilled under nitrogen, unless otherwise stated.
- 1,2-DCE was distilled from calcium hydride and stored over 4 Å molecular sieves under argon.
- THF was dried by heating to reflux over sodium wire, using benzophenone ketyl as an indicator, then distilled under nitrogen, unless otherwise stated.
- SPS grade solvents: hexane, toluene, DCM and THF were obtained from an Innovative Technology, Pure Solv., SPS-400-5 solvent purification system.
- Methyllithium was obtained as a 3.6 M solution in ether from Sigma-Aldrich. The reagent was titrated with I₂ in the presence of lithium chloride at 0 °C.¹⁵²
- Methylmagnesium chloride was obtained as a 3.0 M solution in THF from Sigma-Aldrich. The reagent was titrated with I₂ in the presence of lithium chloride at rt.¹⁵²
- *tert*-Butylmagnesium chloride was obtained as a 1.0 M solution in THF from Sigma-Aldrich. The reagent was titrated at rt using salicaldehyde phenylhydrazone as an indicator.¹⁵³
- Di-*tert*-butylmagnesium was titrated with I₂ in the presence of lithium chloride at rt prior to use.¹⁵²
- Diphenylphosphoryl chloride dried by heating over calcium chloride and then distilled under vacuum (2 mbar) and stored over 4Å molecular sieves.
- DMPU and TMEDA were distilled from calcium hydride and stored under argon.
- Di-*iso*-propylamine was distilled from CaH₂ under an argon atmosphere and stored over 4Å molecular sieves in the fridge.
- Petrol ether refers to light petroleum ether, boiling point (b.p.) range 40-60 °C.
- Low b.p. petrol ether refers to light petroleum ether, b. p. range 30-40 °C
- Liquid cyclobutanones were distilled from calcium hydride and stored over molecular sieves and under argon, unless otherwise stated.

- Solid cyclubutanones were recrystallised from hexane.
- Benzylamine was distilled from calcium hydride and stored over molecular sieves under argon.

10.2 General Instrumentation

Thin layer chromatography was carried out using Merck silica plates coated with fluorescent indicator UV₂₅₄. TLC plates were analysed using a Mineralight UVGL-25 lamp or developed using vanillin, potassium permanganate or ninhydrin stain solutions.

Flash column chromatography was carried out using Prolabo silica gel (230-400 mesh).

IR spectra were obtained on a Shimadzu IRAffinity-1 machine.

¹H and ¹³C NMR spectra were recorded on a Bruker Avance 3 (400 MHz) spectrometer at 400 MHz, and 100 MHz, respectively, or on a Bruker AV 400 spectrometer at 400 MHz and 100 MHz, respectively. ²D, ¹⁹F, and ³¹P NMR spectra were recorded on a Bruker AV 400 spectrometer at 60 MHz, 376 MHz, and 162 MHz, respectively. Chemical shifts are reported in ppm. Coupling constants are reported in Hz and refer to ³J_{H-H} interactions, unless otherwise stated.

High resolution mass spectra were recorded on a Finnigan MAT 90XLT instrument at the EPSRC Mass Spectrometry facility at the University of Wales, Swansea.

Ozone was formed using a Fischer OZ 500 ozone generator.

Microwave reactions were carried out in a CEM DISCOVER-S microwave reactor.

10.3 General Procedures

General procedure A for the synthesis of racemic enol phosphates:

A Schlenk flask was equipped with a stirrer bar, closed with a suba seal, and flame dried under an atmosphere of argon. After cool to rt, the flask was charged with the substrate (1 mmol, 1.0 eq.), DMPU (0.24 mL, 4.0 mmol, 4.0 eq.), diphenylphosphoryl chloride (0.21 mL, 1 mmol, 1.0 eq.), and THF (10 mL). To the reaction mixture di-*tert*-butylmagnesium (1 mL, c = 0.5 mmol/mL, 0.5 eq.) was added dropwise and the reaction was stirred at rt for 1 h. The mixture was quenched with sat. NaHCO₃ (10 mL), the aqueous phase was extracted with Et₂O (3 × 10 mL), and the organic phase was collected. The combined organic phase was dried over sodium sulfate, filtered, and the solvent was evaporated *in vacuo*. The crude product was purified by flash column chromatography using 0-40% diethyl ether in petrol ether as the eluent.

General procedure B for the synthesis of chiral enol phosphates:

A Schlenk flask was equipped with a stirrer bar, a suba seal, and flame dried. After cool to rt, a solution of di-n-butyl-magnesium (1 mL, c = 1 mmol/mL in heptane, 1 mmol, 1.0 eq.) was added and the solvent was removed *in vacuo*. The residue was dried under vacuum for 1 h. The flask was purged with argon and THF (10 mL) was added. Then (*R*)-bis((*R*)-1-phenylethyl)amine (0.46 mL, 2.0 mmol, 2.0 eq.) was added and the suba seal was swapped for a cold finger. The reaction was refluxed for 90 min and, subsequently, the mixture was allowed to cool to room temperature. Complete formation of the magnesium bisamide was assumed. The reaction mixture was cooled to -78 °C and diphenyl phosphoryl chloride (0.21 mL, 1 mmol, 1.0 eq.) was added at the stated temperature. The cyclic substrate (0.8 mmol, 0.8 eq) was dissolved in THF (2 mL) and added dropwise to the solution over 1 h *via* a syringe pump at -78 °C. The reaction was stirred at -78 °C for the stated time. After this time, the reaction was quenched with sat. sodium bicarbonate solution (10 mL), the aqueous phase was extracted with diethyl ether (3 × 10 mL), and the organic phase was collected. The combined organic phase was washed with 1N HCl (10 mL), dried over sodium sulfate, filtered, and the solvent was evaporated *in vacuo*. The crude product was purified by flash column chromatography using 0-40 % diethyl ether in petrol ether as the eluent.

General procedure C for the optimisation of the Kumada cross coupling reaction:

A flame-dried microwave vial was allowed to cool to room temperature under an argon atmosphere and charged with the diphenyl (1,2,3,6-tetrahydro-[1,1'-biphenyl]-4-yl) phosphate **115b** (102 mg, 0.25 mmol, 1.0 eq.) and with the appropriate catalyst. Thereafter, the stated solvent (1 mL) was added and the mixture was stirred for 5 min before the addition of phenylmagnesium bromide (0.38 mL, c = 1 M in THF, 0.38 mmol, 1.5 eq.) at rt rapidly. The reaction was stirred at rt for 1 h. Then the reaction mixture was then partitioned between water (5 mL) and diethyl ether (5 mL). The organic phase was washed with brine (2 mL), dried over sodium sulfate, filtered, and the solvent was evaporated *in vacuo*. The product was purified by flash column chromatography using petrol ether as the eluent.

General procedure D for the optimisation of the Kumada cross coupling reaction:

A flame-dried microwave vial was allowed to cool to room temperature under an argon atmosphere and charged with the diphenyl (1,2,3,6-tetrahydro-[1,1'-biphenyl]-4-yl) phosphate **115b** (102 mg, 0.25 mmol, 1.0 eq.) and PEPPSI S'Pr (2 mg, $2.5 \cdot 10^{-3}$ mmol, 1.0 mol%). Thereafter, diethyl ether (1 mL) was added and the mixture was stirred for 5 min before the addition of phenylmagnesium bromide (c = 1 M in THF). The Grignard reagent was added at the stated temperature over the stated

time. The reaction was stirred at the stated temperature for the stated time. Then the reaction mixture was then partitioned between water (5 mL) and diethyl ether (5 mL). The organic phase was washed with brine (2 mL), dried over sodium sulfate, filtered, and the solvent was evaporated *in vacuo*. The product was purified by flash column chromatography using petrol ether as the eluent.

General procedure E for the Kumada cross coupling reaction (catalyst loading screen):

A microwave vial was equipped with a stirrer bar and flame-dried. After cool to rt, diphenyl (1,2,3,6-tetrahydro-[1,1'-biphenyl]-4-yl) phosphate **115b** (102 mg, 0.25 mmol, 1.0 eq.), the appropriate amount of PEPPSI *S*'Pr catalyst, and diethyl ether (1 mL) were added, and the reaction was stirred for 5 min at room temperature. A solution of phenylmagnesium bromide (0.38 mL, c = 0.38 mmol/mL in THF, 0.38 mmol, 1.5 eq.) was added over 1 h *via* a syringe pump and then the reaction was stirred for a further 1 h. The crude product was partitioned between diethyl ether (5 mL) and water (5 mL). The aqueous phase then was washed with diethyl ether (3 × 5 mL) and the organic phase was dried over sodium sulfate, filtered, and the solvent was removed *in vacuo*. The product was purified with flash column chromatography using petrol ether as the eluent.

General procedure F for the Kumada cross coupling reaction:

A microwave vial was equipped with a stirrer bar and flame-dried. After cool to rt, the substrate (1.0 mmol, 1.0 eq.), PEPPSI *S*'Pr (35 mg, 5.0×10^{-2} mmol, 5.0 mol%) and diethyl ether (4 mL) were added, and the reaction was stirred for 5 min at room temperature. A solution of phenylmagnesium bromide (3.0 mL, c = 0.50 mmol/mL in THF, 1.5 mmol, 1.5 eq.) was added over 1 h *via* a syringe pump and then the reaction was stirred for a further hour. The unreacted Grignard reagent was quenched with methanol (5 mL) and the crude mixture was dry loaded on silica prior to purification *via* flash column chromatography using petrol ether as the eluent.

General Procedure G for the synthesis of hydrazine 145:

A 50 mL round bottom flask was equipped with a stirrer bar and charged with 4-(*tert*-butyl)cyclohexan-1-one **25a** (1.0 eq.), toluene, *N,N*-dimethylhydrazine (3.0 eq.) and *p*-TSA (5 mol%). The flask was equipped with a Dean Stark apparatus for the removal of water and the reaction mixture was refluxed for 3 hours. The solvent was removed *in vacuo* and the crude product was distilled *in vacuo* (b.p 78 °C at 2 mbar).

General Procedure H for the preparation of LDA:

A pear-shaped, two neck, 50 mL flask was equipped with a stirrer bar, closed with suba seals, and flame dried. Once cooled to rt under argon, di-*iso*-propyl-amine (0.15 mL, 1.1 mmol, 1.1 eq.) and THF

(5 mL) were added. The solution was cooled to -78 °C and *n*-BuLi (0.40 mL, *c* = 2.5 mmol/mL in hexane, 1.1 eq., 1.1 mmol) was added dropwise. The cooling bath was removed and the reaction mixture was stirred at rt for 1 hour and used in the subsequent steps.

General procedure I for the deprotonation and alkylation of hydrazine with MeI:

To the solution of LDA prepared by general procedure H, the solution of hydrazine **145** (154 mg, 1.0 mmol, 1.0 eq.) in THF (5 mL) was added at -78 °C and the reaction was stirred at -78 °C temperature for 20 h. After the stated period a small aliquot (1.0 mL, 0.1 mmol sample, 0.1 eq.) was transferred to a solution of MeI (62 µL, 1.0 eq., 1.0 mmol) in THF (1.5 mL) at -78 °C, the cooling bath was removed again and the small reaction were stirred at rt for 15 h, the crude mixture was poured into the biphasic mixture of Et₂O (5 mL) and 2 M H₂SO₄ (5 mL). The resulting biphasic mixture was stirred for 1 h vigorously and the phases were separated. The water phase was washed with Et₂O (3 × 5 mL). The combined organic phase was dried over Na₂SO₄ and filtered. The solvent was evaporated *in vacuo*. To the crude product cyclohexene (11 µL, 0.1 mmol, 0.1 eq.) was added as an internal standard, and the mixture analysed with ¹H NMR spectroscopy the conversion was determined by the relative ratio of the alkenic protons of cyclohexen at 5.69 ppm and the methyl doublet peaks in product **147** at 1.09 and 0.95 ppm.

General procedure J for the deprotonation and alkylation of hydrazine with MeI:

A Schlenk flask was equipped with a stirrer bar, closed with a suba seal and flame dried. The flask was charged with the *n*-BuLi (0.44 mL, *c* = 2.5 mmol/mL in hexane, 1.1 mmol, 1.1 eq.) and the solution of hydrazine **145** (154 mg, 1.0 mmol, 1.0 eq.) in THF (5 mL) was added at -78 °C and the reaction was stirred at the stated temperature for 8 h. After the stated period a small aliquot (1.0 mL, 0.1 mmol sample, 0.1 eq.) was transferred to a solution of MeI (62 µL, 1.0 eq., 1.0 mmol) in THF (1.5 mL) at -78 °C, the cooling bath was removed again and the small samples were stirred at rt for 15 h, the crude mixture was poured into the biphasic mixture of Et₂O (5 mL) and 2 M H₂SO₄ (5 mL). The resulting biphasic mixture was stirred for 1 h vigorously and the phases were separated. The water phase was washed with Et₂O (3 × 5 mL). The combined organic phase was dried over Na₂SO₄ and filtered. The solvent was evaporated *in vacuo*. To the crude product cyclohexene (11 µL, 0.1 mmol, 0.1 eq.) was added as an internal standard, and the mixture analysed with ¹H NMR spectroscopy the conversion was determined by the relative ratio of the alkenic protons of cyclohexen at 5.69 ppm and the methyl doublet peaks in product **147** at 1.09 and 0.95 ppm.

General procedure K for the alkylation of hydrazine 145 with bromo acyclic electrophiles:

A pear-shape flask was equipped with a stirrer bar, closed with suba seals, and flame dried under an atmosphere of argon. After cool to rt, the flask was charged with hydrazine **145** (196 mg, 1.0 mmol, 1.0 eq.) and THF (5 mL). The solution was cooled to -78 °C and n-BuLi (0.44 mL, c = 2.5 mmol/mL in hexane, 1.1 mmol, 1.1 eq.) was added dropwise over a period of 5 min. The solution was warmed to 0 °C and stirred for 2 h prior to the addition of the electrophile (1.2 mmol, 1.2 eq.). The reaction was let to warm rt and stirred O/N. The crude mixture was poured into a biphasic mixture of Et₂O (5 mL) and 2 M H₂SO₄ (5 mL). The resulting mixture was vigorously stirred for 1 h. The phases were separated and the water phase was washed with Et₂O (3 × 5 mL). The combined organic phase was dried over Na₂SO₄ and filtered. The solvent was evaporated *in vacuo* and the crude product was purified by flash column chromatography using 0-20% Et₂O in PE as the eluent.

General procedure L for the preparation D-146:

A small vial was equipped with a stirred bar, closed with a suba seal and flame dried under an atmosphere of argon. After cool to rt, the vial was then charged with ketone **146** (21 mg, 0.1 mmol, 1.0 eq.), the additive and THF (0.5 mL). The mixture was stirred for 5 min and the appropriate base was added dropwise. The solution was then stirred for 2 h at the stated temperature. Subsequently, the reaction was quenched with D₂O (18 µL, 1 mmol, 10.0 eq.). The crude mixture was diluted with THF (5 mL), dried over Na₂SO₄ and filtered. The solvent was evaporated *in vacuo*. The reaction was monitored by the disappearance of the signal at 2.38-2.29 ppm.

General Procedure M for the preparation enol phosphates with Mes₂Mg:

A Schlenk flask was equipped with a stirrer bar, closed with a suba seal and flame dried under an atmosphere of argon. After cool to rt, the flask was charged with the substrate **146** (1 mmol, 1.0 eq.), DMPU (0.24 mL, 4.0 mmol, 4.0 eq.), diphenylphosphoryl chloride (0.21 mL, 1 mmol, 1.0 eq.) and THF (10 mL). To the reaction mixture bismesitylmagnesium (1.5 mL, c = 0.5 mmol/mL, 0.75 mmol, 0.75 eq.) was added dropwise and the reaction was stirred at rt for 1 h. The mixture was quenched with sat. NaHCO₃ (10 mL), the aqueous phase was extracted with Et₂O (3 × 10 mL) and the organic phase was collected. The combined organic phase was dried over sodium sulfate, and the solvent was evaporated *in vacuo*. The crude product was purified by flash column chromatography using 0-30% diethyl ether in petrol ether.

General procedure N for the cross coupling of the mechanistic probe:

A microwave vial was equipped with a stirrer bar and flame-dried under an atmosphere of argon. The substrate (0.5 mmol, 1.0 eq.), the additive (if required), PEPPSI S'Pr (18 mg, 2.5*10⁻² mmol, 5.0 mol%) and diethyl ether (2 mL) were added, and the reaction was stirred for 5 min at rt. A solution of

phenylmagnesium bromide (1.5 mL, c = 0.5 mmol/mL in THF, 0.75 mmol, 1.5 eq.) was added over 1 h *via* a syringe pump and then the reaction was stirred for a further 1 h. The unreacted Grignard reagent was quenched with methanol (5 mL), the crude mixture was dry loaded on silica, and the solvent was removed *in vacuo*. The product was purified with flash column chromatography using petrol ether.

General procedure O for the optimisation of the cross coupling of enol phosphate 115a with *n*-butylmagnesium chloride

A 2 mL microwave vial was equipped with a stirrer bar, closed with a suba seal, and flame dried under an atmosphere of argon. Once cool, the vial was charged with 4-(*tert*-butyl)cyclohex-1-en-1-yl diphenyl phosphate **262a** (20 mg, 0.05 mmol, 1.0 eq.), PEPSSI *S*ⁱPr, and solvent (0.1 mL). The reaction was set to the stated temperature, *n*-butylmagnesium chloride (0.075 mmol, 1.5 eq.) was added rapidly, and the reaction mixture was stirred for 16 h. After this time, MeOH (4 mL) was added to the mixture to quench the unreacted Grignard reagent and the organic phase was filtered, dried over Na₂SO₄, and the solvent was evaporated *in vacuo*. To the crude mixture, internal standard, 1,2-dibromomethane (3.5 μL, 0.05 mmol, 1.0 eq.), was added and the reaction was analysed by ¹H NMR spectroscopy.

General Procedure P for the preparation of alkyl Grignard reagents

A two neck, 250 mL, round bottom flask was equipped with a stirrer bar, a condenser and closed with suba seals. The flask was charged with magnesium turnings (4.86 g, 200 mmol, 5.0 eq.) and flame dried under an atmosphere of argon. Once cool, Et₂O (40 mL) was added and the biphasic mixture was cooled to 0 °C whilst stirring vigorously. Two crystals of iodine were added and the colour of the solution turned from purple to yellow-brown. The appropriate alkyl halide (50 mmol, 1.0 eq.) was added dropwise as a solution in Et₂O (40 mL). After the addition (approx. 15 min), the cooling bath was removed and the solution was allowed to warm to rt. Thereafter, the solution was refluxed over a period of 4 h. The colour of the solution during this time slowly turned from brown-yellow to black. Subsequently, the heating was turned off and the mixture was allowed to cool to rt. The supernatant was transferred to a flame dried pear shape flask *via* cannulation and the solution was titrated with iodine to determine the concentration.¹⁵²

General procedure Q for the cross coupling of enol phosphates with alkyl Grignard reagents:

A 20 mL microwave vial was equipped with a stirrer bar, closed with a suba seal, and flame dried under an atmosphere of argon. Once cool, the vial was charged with the appropriate enol phosphate substrate **115** (1.0 mmol, 1.0 eq.), PEPSSI *S*ⁱPr (20.5 mg, 0.03 mmol, 3 mol%) and toluene (2 mL). The

reaction mixture was cooled to 0 °C and the appropriate Grignard reagent (1.5 mmol, 1.5 eq.) was added rapidly. The reaction mixture was stirred for 16 h. After this time, MeOH (20 mL) was added to the mixture to quench the unreacted Grignard reagent and the organic phase was filtered, dried over Na₂SO₄, filtered, and the solvent was evaporated *in vacuo*. The crude product was dry loaded on silica and purified by flash column chromatography using petrol ether.

General procedure R for the ozonolysis of cyclic alkenes:

A 25 mL three-neck round-bottom flask was equipped with a stirrer bar and fitted with a suba seal and two glass stoppers was flame-dried. Once cool, the alkene (1.0 eq.) was dissolved in a 4:1 = DCM:MeOH mixture (10 mL/mmol alkene). Then sodium bicarbonate (17 mg/mL methanol) was added and the reaction was stirred at room temperature for 15 min. The reaction mixture was cooled down to -78 °C and ozone was bubbled through the solution until the blue colour (unreacted O₃) appeared. Thereafter the ozone was purged with argon or oxygen, and dimethyl sulphide (20 eq.) was added and the reaction was allowed to warm room temperature and then stirred for 12 h. The solvent was removed *in vacuo* and the crude product was purified by flash column chromatography using 30% ethyl acetate in petrol ether.

General procedure S for the reductive amination of keto-aldehyde :

A small microwave vial was equipped with a stir bar. The vial was charged with the solution of 6-oxoheptanal **163** (20 mg, 0.16 mmol, 1.0 eq.) in the appropriate solvent (26 mL/mmol substrate), the appropriate amount of benzylamine (1.05 eq.) and the additive(S) (if required). Finally the appropriate amount of sodium triacetoxyborohydride was added. The reaction was stirred at rt for 2 h. The reaction was quenched with sat. potassium bicarbonate solution (8 mL) and 1N NaOH solution (2 mL) was added. The organic phase was separated and the aqueous was extracted with dichloromethane (3 × 10 mL). The organic phase was combined, dried over sodium sulfate and the solvent was removed *in vacuo*. The conversion was determined by the addition of cyclohexene or COD as internal standard. The crude product was purified with flash column chromatography using 1–2% MeOH in DCM. Triethylamine (10 droplets) was added for 100 mL eluent.

General procedure T for the telescoped ozonolys/reductive aminocyclisation:

A 50 mL three neck round bottom flask was equipped with a stirrer bar closed a suba seal, two glass stoppers and flame dried. The substrate (0.25 mmol, 1.0 eq.) was dissolved in a 4:1 = DCM:MeOH mixture (40 mL/mmol). Then sodium bicarbonate (35 mg, 1.68 eq., 0.42 mmol) was added and the reaction was stirred at room temperature for 5 min. The reaction was cooled down to -78 °C and ozone was bubbled through until the blue colour appeared. The ozone flux was turned off and the

reaction mixture was bubbled through with argon or oxygen over a period 10-15 min. Thereafter dimethyl sulphide (20 eq.) was added and the reaction was let to warm to rt and stirred O/N. The solvent was removed *in vacuo* and the crude product was dissolved in CPME (12 mL/mmol). Benzylamine (28 μ L, 0.26 mmol, 1.05 eq.) and sodium triacetoxyborohydride (148 mg, 0.70 mmol, 2.8 eq.) were added rapidly and the reaction was stirred for 4 h at rt. The reaction was quenched with the mixture of sat. potassium bicarbonate solution (8 mL) and 1N NaOH solution (2 mL). The organic phase was separated and the aqueous phase was extracted with dichloromethane (3 \times 10 mL). The organic phase was combined, dried over sodium sulfate and the solvent was removed *in vacuo*. The crude product was purified by flash column chromatography using 1–2% MeOH in DCM. Triethylamine (10 droplets) was added for every 100 mL eluent.

General procedure U for the deprotection of 168b with Pd:

A flame dried 5 mL round bottom flask was equipped with a stirrer bar, a condenser if required and closed with suba seals. The substrate **168b** (20 mg, 0.06 mmol, 1.0 eq.), the appropriate catalyst and the solvent were added. Then hydrogen was bubbled through the solution over a period of 10-15 min. Thereafter the reaction was stirred at the stated temperature for the appropriate time. The crude mixture was filtered through celite and the filtrate was washed with DCM (3 \times 10 mL). The combined organic phase was dried over Na₂SO₄, filtered and the solvent was removed *in vacuo*. The crude mixture was analysed by ¹H NMR spectroscopy and the starting material **168b** was recovered by flash column chromatography using 1-2% MeOH in DCM.

General procedure V for the reductive amination of 168b:

A flame dried 5 mL round bottom flask was equipped with a stirrer bar, a condenser if required and closed with suba seals. The substrate **168b** (20 mg, 0.06 mmol, 1.0 eq.), the appropriate solvent and the additives were added. Thereafter the reaction was stirred at the stated temperature for the required time. The crude mixture was partitioned between DCM (4 mL) and sat. K₂CO₃ (4 mL). The aqueous phase was washed with DCM (3 \times 4 mL) and the organic phase was collected. The combined organic phase was dried over Na₂SO₄, filtered and the solvent was removed *in vacuo*. The crude mixture was analysed by ¹H NMR spectroscopy and the starting material was recovered by flash column chromatography using 1-2% MeOH in DCM.

Following general procedure W for the reductive amination of 164b with sodium cyanoborohydride:

A flame dried microwave vial was equipped with a stirrer bar and charged with the appropriate amount of 4-methoxy benzylamine and MeOH (2 mL). The solution was acidified with glacial acetic

acid and pH was set to 6. To this solution the solution of the aldehyde-ketone **164b** (20 mg, 0.075mmol, 1.0 eq.) made with the stated amount of MeOH was slowly added over the reported time. Thereafter sodium cyanoborohydride (10 mg, 0.075 mmol, 2.0 eq.) was added in one portion and the reaction was stirred for 2 h at rt. The crude mixture was partitioned between DCM (5 mL) and the prepared mixture of 1N NaOH:sat. K₂CO₃ = 1:4 (5 mL). The aqueous phase was washed with DCM (3 × 5 mL) and the organic phase was collected. The combined organic phase was dried over Na₂SO₄, filtered and the solvent was removed *in vacuo*. The crude mixture was analysed by ¹H NMR spectroscopy using cyclohexene as an internal standard and the product was isolate by flash column chromatography using 1-2% MeOH in DCM.

General procedure X for the deprotection of 173 under acidic conditions:

A flame dried microwave vial was equipped with a stirrer bar and charged with the substrate **173** (20 mg, 0.05 mmol, 1.0 eq.), any additive if required and the reported solvent. The solution was stirred at the stated temperature for the reported time. The crude mixture was partitioned between DCM (5 mL) and a mixture of 1N NaOH:sat. K₂CO₃ = 1:4 (5 mL). The aqueous phase was washed with DCM (3 × 5 mL) and the organic phase was collected. The combined organic phase was dried over Na₂SO₄, filtered and the solvent was removed *in vacuo*. The crude mixture was analysed by ¹H NMR spectroscopy using the starting material **173** was recovered by flash column chromatography using 1-2% MeOH in DCM.

General procedure Y for the deprotection of 173:¹⁴⁴

A flame dried microwave vial was equipped with a stirrer bar and charged with the substrate **173** (28 mg, 0.075 mmol, 1.0 eq.), and dissolved in 5:1 mixture of MeCN (0.60 mL): H₂O (0.12 mL). Thereafter the reductant was added and the solution was stirred at rt for 1 d. The crude mixture was partitioned between DCM (5 mL) and a mixture of 1N NaOH:sat. K₂CO₃ = 1:4 (5 mL). The aqueous phase was washed with DCM (3 × 5 mL) and the organic phase was collected. The combined organic phase was dried over Na₂SO₄, filtered and the solvent was removed *in vacuo*. The crude mixture was analysed by ¹H NMR spectroscopy, the starting material **173** was recovered by flash column chromatography using 1-2% MeOH in DCM.

General procedure Z for the reductive aminocyclisation of aldehyde-ketones:

A flame dried microwave vial was equipped with a stirrer bar and charged with the appropriate amount of ammonia and stated amount of the solvent (2 mL). The solution was acidified with glacial acetic acid and pH was set to 6. To this solution the solution of the aldehyde-ketone substrate **324b** (0.075mmol, 1.0 eq.) made with the stated amount of MeOH was slowly added ovet the reported

time. Thereafter sodium cyanoborohydride (10 mg, 0.15 mmol, 2.0 eq.) was added in one portion. The reaction was stirred for O/N at rt. The crude mixture was partitioned between DCM (5 mL) and the mixture of 1N NaOH:sat. $K_2CO_3 = 1:4$ (5 mL). The aqueous phase was washed with DCM (3 × 5 mL) and the organic phase was collected. The combined organic phase was dried over Na_2SO_4 , filtered and the solvent was removed *in vacuo*. The crude mixture was analysed by 1H NMR spectroscopy using COD or cyclohexene as an internal standard and the product was isolated by flash column chromatography using 1-2% MeOH in DCM.

General procedure AA for the reductive aminocyclisation of aldehyde-ketones with different reducing agents:

A flame dried microwave vial was equipped with a stirrer bar and charged with the ammonia (55 μ L, $c = 7$ mmol/mL in MeOH, 0.375 mmol, 5 eq.) or ammonium acetate (29 mg, 0.375 mmol, 5.0 eq.) and MeOH (2 mL). The solution was acidified with glacial acetic acid and pH was set to 6. To this solution the solution of the aldehyde-ketone substrate **164b** (20 mg, 0.075 mmol, 1.0 eq.) made with MeOH (4 mL) was slowly added over the reported time. Thereafter the reducing agent (0.15 mmol, 2.0 eq.) was added in one portion. The reaction was stirred for O/N at rt. The crude mixture was partitioned between DCM (5 mL) and the mixture of 1N NaOH:sat. $K_2CO_3 = 1:4$ (5 mL). The aqueous phase was washed with DCM (3 × 5 mL) and the organic phase was collected. The combined organic phase was dried over Na_2SO_4 , filtered and the solvent was removed *in vacuo*. The crude mixture was analysed by 1H NMR spectroscopy using COD or cyclohexene as an internal standard and the product was isolated by flash column chromatography using 1-2% MeOH in DCM.

General procedure AB for the preparation of styrene derivatives via a Wittig reaction:

A flame-dried, three-neck, round-bottom flask was charged with methyltriphenylphosphonium bromide (1.5 eq.) and THF (5.4 mL/mmol of methyltriphenylphosphonium bromide) was added. The suspension was cooled to 0 °C and a solution of *n*-butyllithium ($c = 2.5$ mmol/mL in hexane, 1.3 eq.) was added dropwise. The colour of the solution changed from white to bright yellow, indicating formation of the ylide. The reaction was stirred at 0 °C for a further 20 min before the addition of the substrate (1.0 eq.). The ice bath was then removed and the reaction was allowed to warm up to rt and stirred for 16 h. The reaction was then quenched with sat. ammonium chloride solution (5.4 mL/mmol of substrate) and diluted with diethyl ether (2.7 mL/mmol of substrate). The water phase was extracted with diethyl ether (3 × 2 mL/mmol of substrate) and the combined organic phase was washed with brine and water (2 × 2 mL/mmol of substrate). The organic phase was dried over sodium sulfate, and the solvent was evaporated *in vacuo*. The crude product was purified by flash column chromatography using petrol ether.

General procedure AC for the [2+2]-cycloaddition with trichloroacetyl chloride:

A three-neck round-bottom flask was equipped with a stirrer bar and a dropping funnel, and was flame-dried under nitrogen. After cooling to room temperature, the flask was charged with diethyl ether (3.33 mL/mmol of styrene derivative), zinc-copper couple (3 eq.) and the styrene derivative (1.0 eq.), and then stirred vigorously. The dropping funnel was charged with diethyl ether (1.67 mL/mmol of styrene derivative), trichloroacetyl chloride (2.5 eq.), and phosphoryloxy(V) trichloride (2.5 eq.). The solution was added dropwise over 1 h to the stirred solution of styrene and then stirred at room temperature for 16 h. After this time, the mixture was filtered through celite and washed with hexane. The filtrate was diluted with hexane (3.33 mL/mmol of styrene derivative) and concentrated to 1/3 of its volume *in vacuo* to induce the precipitation of zinc salts. The dilution-concentration sequence was repeated twice and the final concentrate was washed with sat. sodium bicarbonate (3.33 mL/mmol of styrene derivative) solution and sat. brine solution (3.33 mL/mmol of styrene derivative). Progress of the reaction was checked with TLC analysis and ¹H NMR spectroscopy. The crude material was used in the subsequent step without further purification.

General procedure AD for the reduction of dichlorocyclobutanones:

The crude product of the previous step was dissolved in acetic acid (6.5 mL/mmol of styrene derivative) and zinc dust (6 eq.) was then added portion-wise. The suspension was then stirred for 16 h at rt. The reaction mixture was filtered and diluted with diethyl ether (50 mL). The organic layer was washed with water (2 × 50 mL), saturated sodium bicarbonate (2 × 50 mL) and brine (50 mL). The organic phase was dried over sodium sulfate, filtered, and the solvent was evaporated *in vacuo*. The crude product was purified by flash column chromatography using 0-20% diethyl ether in petrol ether as the eluent.

General procedure AE for the synthesis of racemic enol phosphates using LDA:

A Schlenk flask was equipped with a stirrer bar and flame-dried under a nitrogen atmosphere. Once cool, di-*iso*-propylamine (1.0 eq) and THF (1 mL/ mmol of di-*iso*-propylamine) were added then the solution was cooled to -78 °C and a solution of *n*-butyllithium (c = 2.5 mmol/mL in hexane, 1.0 eq.) was added dropwise. The reaction was then allowed to warm to rt over 30 min. The solution was - cooled to -78 °C again and the substrate (0.9 eq.) was added dropwise as a solution in THF (6 mL/mmol substrate). The reaction was then stirred for 30 min at -78 °C, before the addition of diphenyl phosphoryl chloride (1.0 eq.) at -78 °C. The reaction mixture was warmed to room temperature over 30 min and stirred for 2 h. The reaction was quenched with sat. sodium bicarbonate solution (10 mL) and the aqueous phase was extracted with diethyl ether (3 × 10 mL).

The organic phase was dried over sodium sulfate, filtered, and the solvent was evaporated *in vacuo*. The crude product was purified by flash column chromatography using 30% diethyl ether in petrol ether as the eluent.

General procedure AF for the synthesis of chiral enol phosphates:

A Schlenk flask was equipped with a stirrer bar and a suba seal, and flame dried. Once cool to rt, a solution of di-*n*-butyl-magnesium (1 mL, c = 1 mmol/mL in heptane, 1 mmol, 1.0 eq.) was added and the solvent was removed *in vacuo*. The residue was dried under vacuum for 1 h. The flask was purged with argon and THF (10 mL) was added. Then (*R*)-bis((*R*)-1-phenylethyl)amine (0.46 mL, 2.0 mmol, 2.0 eq.) was added and the suba seal was swapped for a cold finger. The reaction was refluxed for 90 min and, subsequently, the mixture was allowed to cool to room temperature. Complete formation of the magnesium bisamide was assumed. The reaction mixture was cooled to -78 °C and diphenyl phosphoryl chloride (0.21 mL, 1 mmol, 1.0 eq.) was added at the stated temperature. The cyclic substrate (0.8 mmol, 0.8 eq) was dissolved in THF (2 mL) and added dropwise to the solution over 1 h *via* a syringe pump at -78 °C. The reaction was stirred at -78 °C for the stated time. After this time, the reaction was quenched with sat. sodium bicarbonate solution (10 mL), the aqueous phase was extracted with diethyl ether (3 × 10 mL), and the organic phase was collected. The combined organic phase was washed with 1N HCl (10 mL), dried over sodium sulfate, filtered, and the solvent was evaporated *in vacuo*. The crude product was purified by flash column chromatography using 0-40 % diethyl ether in petrol ether as the eluent.

General procedure AG for the synthesis of chiral enol phosphates:

A Schlenk flask was equipped with a stirrer bar and a suba seal, and flame dried. Once cooled to rt, a solution of di-*n*-butyl-magnesium (1 mL, c = 1 mmol/mL in heptane, 1 mmol, 1.0 eq.) was added and the solvent was removed *in vacuo* and the residue was dried under vacuum for 1 h. The flask was purged with argon and hexane (10 mL) was added. Then (*R*)-bis((*R*)-1-phenylethyl)amine (0.46 mL, 2.0 mmol, 2.0 eq.) was added and the suba seal was swapped for a cold finger. The reaction mixture was refluxed for 90 min then allowed to cool down to room temperature. Complete formation of the magnesium bisamide was assumed. The reaction mixture was cooled to -78 °C and diphenyl phosphoryl chloride (0.21 mL, 1 mmol, 1.0 eq.) was added at the stated temperature. The cyclic substrate (0.8 mmol, 0.8 eq) was dissolved in THF (2 mL) and added dropwise to the solution over 1 h *via* a syringe pump at -78 °C. The reaction was stirred at -78 °C for the stated time. After this time, the reaction was quenched with sat. sodium bicarbonate solution (10 mL), the aqueous phase was extracted with diethyl ether (3 × 10 mL), and the organic phase was collected. The combined organic

phase was washed with 1N HCl (10 mL), dried over sodium sulfate, filtered, and the solvent was evaporated *in vacuo*. The crude product was purified by flash column chromatography using 0-40 % diethyl ether in petrol ether as the eluent.

General procedure AJ for the synthesis of racemic enol phosphates:

A Schlenk flask was equipped with a stirrer bar, closed with a suba seal, and flame dried under an atmosphere of argon. When cool, the flask was charged with the substrate (1 mmol, 1.0 eq.), DMPU (0.24 mL, 4.0 mmol, 4.0 eq.), diphenylphosphoryl chloride (0.21 mL, 1 mmol, 1.0 eq.), and THF (10 mL). To the reaction mixture di-*tert*-butylmagnesium (1 mL, c = 0.5 mmol/mL, 0.5 eq.) was added dropwise and the reaction was stirred at rt for 1 h. The mixture was quenched with sat. NaHCO₃ (10 mL), the aqueous phase was extracted with Et₂O (3 × 10 mL), and the organic phase was collected. The combined organic phase was dried over sodium sulfate, filtered, and the solvent was evaporated *in vacuo*. The crude product was purified by flash column chromatography using 0-40% diethyl ether in petrol ether as the eluent.

General procedure AK for the synthesis of chiral enol phosphates:

A Schlenk flask was equipped with a stirrer bar and a suba seal, and flame dried. Once cool, a solution of di-*n*-butyl-magnesium (1 mL, c = 1 mmol/mL in heptane, 1 mmol, 1.0 eq.) was added and the solvent was removed *in vacuo*. The residue was dried under vacuum for 1 h. The flask was purged with argon and THF (10 mL) was added. Then (*R*)-bis((*R*)-1-phenylethyl)amine (0.46 mL, 2.0 mmol, 2.0 eq.) was added and the suba seal was swapped for a cold finger. The reaction was refluxed for 90 min and, subsequently, the mixture was allowed to cool to room temperature. Complete formation of the magnesium bisamide was assumed. The reaction mixture was cooled to -78 °C and diphenyl phosphoryl chloride (0.21 mL, 1 mmol, 1.0 eq.) and the appropriate additive (0.5 mmol, 0.5 eq.) were added at the stated temperature. The cyclic substrate (0.8 mmol, 0.8 eq) was dissolved in THF (2 mL) and added dropwise to the solution over 1 h *via* a syringe pump at -78 °C. The reaction was stirred at -78 °C for the stated time. After this time, the reaction was quenched with sat. sodium bicarbonate solution (10 mL), the aqueous phase was extracted with diethyl ether (3 × 10 mL), and the organic phase was collected. The combined organic phase was washed with 1N HCl (10 mL), dried over sodium sulfate, filtered, and the solvent was evaporated *in vacuo*. The crude product was purified by flash column chromatography using 0-40 % diethyl ether in petrol ether as the eluent.

General procedure AK for 1,2-addition of Grignard to aldehydes:

A Schlenk flask was equipped with a stirrer bar and a suba seal, and flame dried. When cool, the solution of the in THF (2 mL) aldehyde (1 mmol, 1.0 eq.) was added. Thereafter the solution was cooled down to 0 °C and the Grignard reagent (3 mL, c = 0.5 mmol/mL in Et₂O, 1.5 mmol, 1.5 eq.) was added dropwise. Thereafter the reaction was let to warm up to rt and stirred for 6 h. The Grignard reagent was quenched with sat. NH₄Cl (5 mL). The phases were separated and the organic phase was washed with brine (2 mL), dried over sodium sulfate, filtered, and the solvent was evaporated *in vacuo*. The product was purified by flash column chromatography using 5-10% diethyl ether in petrol ether as the eluent.

General procedure AM for the bromination of secondary alcohols:

A 100 mL round bottom flask was equipped with a stirrer bar and a suba seal, and flame dried. After cool, the flask was charged with the secondary alcohol (1 mmol, 1.0 eq.) and DCM (19 mL). The solution was cooled to 0 °C and Phosphorous(III) bromide (1.88 mL, 20 mmol, 20.0 eq.) was added dropwise to the solution. The reaction was stirred at the stated temperature O/N. The reaction was quenched with sat. NaHCO₃ solution (10 mL) and the phases were separated. The aqueous phase was washed with DCM (3 × 20 mL). The organic phase was combined and the solvent was evaporated *in vacuo* to give the desired product which was used without further purification in the next step.

General procedure AN for the nucleophilic substitution with benzhydryl electrophiles:

A 25 mL round bottom flask was equipped with a stirrer bar, a suba seal, a condenser and flame dried. The flask was charged with the the primary amine (0.24 mL, 1.87 mmol, 3.0 eq.) and the appropriate solvent (8 mL). To this solution the electrophile (0.62 mmol, 1.0 eq.) was added and the reaction was refluxed for the stated time. The mixture was allowed to cool down to rt and the organic phase was washed with sat. NaHCO₃ solution (3 × 5 mL) and the phases were separated. The organic phase was dried over sodium sulfate, filtered, and the solvent was evaporated *in vacuo*. The product was isolated with flash column chromatography using 0-2% diethyl in petrol ether as an eluent.

10.4 Experimental Procedures

Synthesis of Chiral sp^3 -rich Azepanes

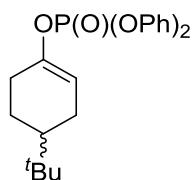
Entry 1 in Table 9.1

Following General procedure A for the synthesis enol phosphates, data is presented in the following format: (a) substrate and (b) yield of product.

(a) 4-*tert*-butylcyclohexan-1-one **25a** (154 mg, 1 mmol, 1.0 eq.) and (b) 274 mg (71%).

Characterisation of 4-((*tert*)butyl)cyclohex-1-en-1-yl diphenyl phosphate **115a**:⁹⁵

Obtained as a colourless oil.



115a

¹H NMR (CDCl₃): 7.29-7.23 (m, 4H, ArH), 7.20-7.09 (m, 6H, ArH), 5.49-5.51 (m, 1H, CH=C), 2.27-2.10 (m, 2H, CH₂), 2.06-1.97 (m, 1H, CH), 1.85-1.72 (m, 2H, CH₂), 1.29-1.14 (m, 2H, CH₂), 0.79 (s, 9H, CH₃) ppm.

¹³C NMR (CDCl₃): 150.9 (d, 1C, ²J_{C-P} = 7.3 Hz), 148.0 (d, 2C, ²J_{C-P} = 9.8 Hz), 130.0, 125.6, 120.4 (d, 1C, ³J_{C-P} = 4.7 Hz), 112.1 (d, 4C, ³J_{C-P} = 7.3 Hz), 43.4, 32.3, 28.8 (d, 1C, ³J_{C-P} = 3.2 Hz), 27.5, 25.1, 24.2 (3C) ppm.

³¹P NMR (CDCl₃): -17.4 ppm.

ν_{\max} (cm⁻¹): 2956, 1693, 1587, 1487, , 1304, 1182, 1109, , 997, 958, , 765, 752, 731.

Entry 2 in Table 9.1

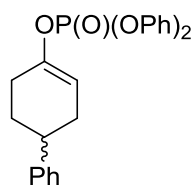
Following General procedure A for the synthesis pf racemic enol phosphates, data is presented in the following format: (a) substrate and (b) yield of product.

(a) 4-phenylcyclohexan-1-one **25b** (174 mg, 1 mmol, 1.0 eq.) and (b) 333 mg (80%).

Characterisation of 4-(phenyl)cyclohex-1-en-1-yl diphenyl phosphate **115b**:⁹⁵

Obtained as a white solid.

M.p.: 148-150 °C (lit.: not reported)



115b

^1H NMR (CDCl_3): 7.43-7.36 (m, 4H, ArH), 7.37-7.27 (m, 6H, ArH), 7.26-7.20 (m, 5H, ArH), 5.77-5.64 (m, 1H, CH=C), 2.89-2.76 (m, 1H, PhCH), 2.57-2.22 (m, 4H, CH_2), 2.12-1.87 (m, 2H, CH_2) ppm.

^{13}C NMR (CDCl_3): 150.8 (d, 1C, $^2J_{\text{C-P}} = 8.5$ Hz), 147.9 (d, 2C, $^2J_{\text{C-P}} = 10.4$ Hz), 145.8, 130.0, 128.7, 127.0, 126.5, 125.6, 120.3 (d, 1C, $^3J_{\text{C-P}} = 5.0$ Hz), 111.7 (d, 4C, $^3J_{\text{C-P}} = 5.6$ Hz), 39.4, 31.7, 29.9, 28.2 (d, 1C, $^3J_{\text{C-P}} = 4.4$ Hz) ppm.

^{31}P NMR (CDCl_3): -17.4 ppm

ν_{max} (cm^{-1}): 2922, 2885, 1690, 1589, 1489, 1284, 1191, 1106, 916, 782, 766, 691.

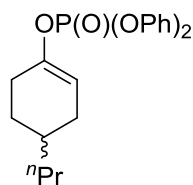
Entry 3 in Table 9.1

Following General procedure A for the synthesis enol phosphates, data is presented in the following format: (a) substrate and (b) yield of product.

(a) 4-*n*-propylcyclohexan-1-one **25g** (140 mg, 1 mmol, 1.0 eq.) and (b) 328 mg (88%).

Characterisation of 4-*n*-propylcyclohex-1-en-1-yl diphenyl phosphate **115g**:

Obtained as a colourless oil.



115g

^1H NMR (CDCl_3): 7.30-7.22 (m, 4H, ArH), 7.20-7.09 (m, 6H, ArH), 5.49-5.42 (m, 1H, CH=C), 2.31-2.02 (m, 3H, CH_2), 1.76-1.58 (m, 2H, CH_2), 1.53-1.40 (m, 1H, CH_2), 1.34-1.11 (m, 5H, CH, CH_2), 0.81 (t, 3H, $J = 7.4$ Hz, CH_3) ppm.

^{13}C NMR (CDCl_3): 150.9 (d, 1C, $^2J_{\text{C-P}} = 6.5$ Hz), 148.0 (d, 2C, $^2J_{\text{C-P}} = 9.3$ Hz), 130.0, 125.6, 120.3 (d, 1C, $^3J_{\text{C-P}} = 4.9$ Hz), 111.5 (d, 4C, $^3J_{\text{C-P}} = 5.5$ Hz), 38.1, 32.6, 30.2, 29.0, 27.2 (d, 1C, $^3J_{\text{C-P}} = 4.1$ Hz), 20.4, 14.5 ppm.

^{31}P NMR (CDCl_3): -17.4 ppm

ν_{max} (cm^{-1}): 2954, 2920, 1487, 1296, 1184, 1161, 1120, 1101, 947, 823, 725.

HR-MS (ESI): m/z calculated for $\text{M} = \text{C}_{21}\text{H}_{26}\text{O}_4\text{P}$, theoretical $[\text{M}+\text{H}]^+$: 373.1563. Found: 373.1557.

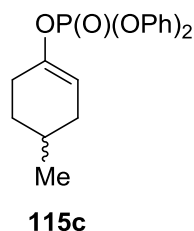
Entry 4 in Table 9.1

Following General procedure A for the synthesis enol phosphates, data is presented in the following format: (a) substrate and (b) yield of product.

(a) 4-methyl-propylcyclohexan-1-one **25c** (112 mg, 1 mmol, 1.0 eq.) and (b) 310 mg (90%).

Characterisation of 4-methyl-cyclohex-1-en-1-yl diphenyl phosphate **115c**:⁹⁵

Obtained as a colourless oil.



^1H NMR (CDCl_3): 7.31-7.22 (m, 4H, ArH), 7.20-7.08 (m, 6H, ArH), 5.49-5.42 (m, 1H, CH=C), 2.33-2.01 (m, 2H, CH₂), 1.71-1.54 (m, 4H, CH₂), 1.35-1.24 (m, 1H, CH), 0.88 (d, 3H, $J = 6.5$ Hz, CH₃) ppm.

^{13}C NMR (CDCl_3): 150.9 (d, 1C, $^2J_{\text{C-P}} = 7.4$ Hz), 147.9 (d, 2C, $^2J_{\text{C-P}} = 9.7$ Hz), 130.0, 125.6, 120.3 (d, 1C, $^3J_{\text{C-P}} = 4.4$ Hz), 111.5 (d, 4C, $^3J_{\text{C-P}} = 5.4$ Hz), 32.1, 30.9, 27.9, 27.6 (d, 1C, $^3J_{\text{C-P}} = 3.6$ Hz), 21.2 ppm.

^{31}P NMR (CDCl_3): -17.4 ppm

ν_{max} (cm^{-1}): 2951, 2924, 1589, 1487, 1296, 1184, 1161, 1114, 945, 904, 821, 767, 752.

Entry 5 in Table 9.1

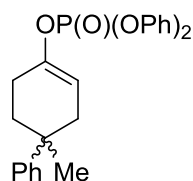
Following General procedure A for the synthesis enol phosphates, data is presented in the following format: (a) substrate and (b) yield of product.

(a) 4-methyl-4-phenylcyclohexan-1-one **25d** (188 mg, 1 mmol, 1.0 eq.) and (b) 341 mg (81%).

Characterisation of 4-methyl-4-phenylcyclohex-1-en-1-yl diphenyl phosphate **115d**:⁹⁵

Obtained as a white solid.

M. p.: 154°C (lit.: not reported).



115d

¹H NMR (CDCl₃): 7.30-7.22 (m, 8H, ArH), 7.14-7.07 (m, 7H, ArH), 5.65-5.55 (m, 1H, CH=C), 2.59-2.46 (m, 1H, CH₂), 2.21-2.11 (m, 2H, CH₂), 2.03-1.89 (m, 2H, CH₂), 1.83-1.75 (m, 1H, CH₂), 1.22 (s, 3H, CH₃) ppm.

¹³C NMR (CDCl₃): 150.9 (d, 1C, ²J_{C-P} = 6.7 Hz), 147.3, 146.7 (d, 2C, ²J_{C-P} = 8.9 Hz), 129.3, 127.8, 125.4, 125.1, 124.9, 119.6 (d, 1C, ³J_{C-P} = 5.1 Hz), 110.0 (d, 4C, ³J_{C-P} = 5.2 Hz), 35.6, 35.2, 34.4, 27.9, 25.0 ppm (d, 1C, ³J_{C-P} = 4.3 Hz).

³¹P NMR (CDCl₃): -17.7 ppm

ν_{\max} (cm⁻¹): 2956, 2926, 1589, 1489, 1188, 1117, 944, 907, 756, 689.

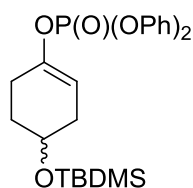
Entry 6 in Table 9.1

Following General procedure A for the synthesis enol phosphates, data is presented in the following format: (a) substrate and (b) yield of product.

(a) 4-((*tert*-butyldimethylsilyl)oxy)cyclohexan-1-one **25e** (228 mg, 1 mmol, 1.0 eq.) and (b) 286 mg (62%).

Characterisation of 4-((*tert*-butyldimethylsilyl)oxy)cyclohex-1-en-1-yl diphenyl phosphate **115e**:⁹⁵

Obtained as a colourless oil.



115e

^1H NMR (CDCl_3): 7.36-7.27 (m, 4H, ArH), 7.26-7.13 (m, 6H, ArH), 5.44-5.38 (m, 1H, CH=C), 3.93-3.85 (m, 1H, OCH), 2.36-2.18 (m, 3H, CH_2), 2.10-1.99 (m, 1H, CH_2), 1.82-1.66 (m, 2H, CH_2), 0.85 (s, 9H, CH_3), 0.02 (s, 6H, SiCH_3) ppm.

^{13}C NMR (CDCl_3): 150.8 (d, 1C, $^2J_{\text{C-P}} = 8.2$ Hz), 147.3 (d, 2C, $^2J_{\text{C-P}} = 11.5$ Hz), 130.0, 125.7, 120.3 (d, 1C, $^3J_{\text{C-P}} = 4.3$ Hz), 109.3 (d, 4C, $^3J_{\text{C-P}} = 6.5$ Hz), 66.4, 33.2, 31.4, 26.0, 25.9 (d, 1C, $^3J_{\text{C-P}} = 3.6$ Hz), 18.5 (3C), -4.50 (2C) ppm.

^{31}P NMR (CDCl_3): -17.6 ppm

ν_{max} (cm^{-1}): 2950, 2926, 2854, 1591, 1491, 1299, 1190, 1102, 944, 836, 756, 689.

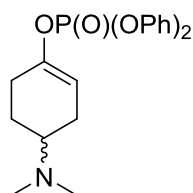
Entry 7 in Table 9.1

Following General procedure A for the synthesis enol phosphates, data is presented in the following format: (a) substrate and (b) yield of product.

(a) 4-(dimethylamino)cyclohexan-1-one **25f** (141 mg, 1 mmol, 1.0 eq.) and (b) 321 mg (86%).

Characterisation of 4-(dimethylamino)cyclohex-1-en-1-yl diphenyl phosphate **115f**.⁹⁵

Obtained as a colourless oil.



115f

^1H NMR (CDCl_3): 7.31-7.24 (m, 4H, ArH), 7.19-7.09 (m, 6H, ArH), 5.47-5.43 (m, 1H, CH=C), 2.44-2.34 (m, 1H, CH), 2.29-2.17 (m, 9H, NCH_3 , CH_2), 2.07-1.97 (m, 1H, CH_2), 1.94-1.86 (m, 1H, CH_2), 1.56-1.43 (m, 1H, CH_2) ppm.

^{13}C NMR (CDCl_3): 150.8 (d, 1C, $^2J_{\text{C-P}} = 6.6$ Hz), 147.5 (d, 2C, $^2J_{\text{C-P}} = 9.2$ Hz), 130.0, 125.6, 120.3 (d, 1C, $^3J_{\text{C-P}} = 4.7$ Hz), 110.4 (d, 4C, $^3J_{\text{C-P}} = 5.7$ Hz), 59.5, 42.0 (2C), 27.7 (d, 1C, $^3J_{\text{C-P}} = 3.9$ Hz), 26.0, 25.5 ppm.

^{31}P NMR (CDCl_3): -17.5 ppm

ν_{max} (cm^{-1}): 2930, 2772, 1589, 1489, 1290, 1188, 1113, 942, 775, 756, 689.

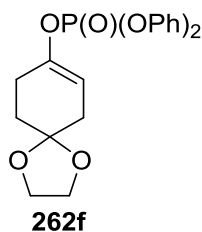
Entry 8 in Table 9.1

Following General procedure A for the synthesis enol phosphates, data is presented in the following format: (a) substrate and (b) yield of product.

(a) 1,4-dioxaspiro[4.5]decan-8-one **25h** (156 mg, 1 mmol, 1.0 eq.) and (b) 284 mg (73%).

Characterisation of diphenyl (1,4-dioxaspiro[4.5]dec-7-en-8-yl) phosphate **115h**:⁹⁵

Obtained as a colourless oil.



¹H NMR (CDCl₃): 7.31-7.23 (m, 4H, ArH), 7.20-7.09 (m, 6H, ArH), 5.45-5.38 (m, 1H, CH=C), 3.83-3.88 (m, 4H, OCH₂), 2.42-2.33 (m, 2H, CH₂), 2.29-2.23 (m, 2H, CH₂), 1.79 (t, 2H, *J* = 6.2 Hz, CH₂) ppm.

¹³C NMR (CDCl₃): 150.8 (d, 1C, ²*J*_{C-P} = 7.7 Hz), 147.7 (d, 2C, ²*J*_{C-P} = 9.7 Hz), 130.0, 125.7, 120.4 (d, 1C, ³*J*_{C-P} = 4.4 Hz), 109.3 (d, 4C, ³*J*_{C-P} = 5.2 Hz), 107.7, 64.7 (2C), 34.0, 31.1, 26.7 (d, 1C, ³*J*_{C-P} = 4.0 Hz) ppm.

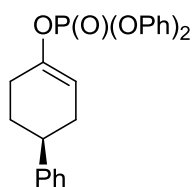
³¹P NMR (CDCl₃): -17.7 ppm

ν_{\max} (cm⁻¹): 2928, 2956, 2880, 1589, 1487, 1294, 1188, 1112, 1022, 940, 756, 689.

Entry 1 in Table 9.2

Following General procedure B for the synthesis of chiral enol phosphates, data is presented in the following format: (a) substrate, (b) yield of product, and (c) enantiomeric ratio.

(a) 4-*tert*-butylcyclohexan-1-one **25a** (123 mg, 0.8 mmol, 0.8 eq.), (b) 247 mg (80%), and (c) 93:7.

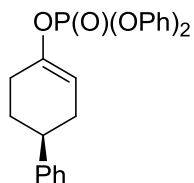


Chiral analysis: OD-H column, 1.40 mL/min, detector 254 nm, 1% IPA in hexane. *t*₁ = 25.4 min and *t*₂ = 26.2 min.

Entry 2 in Table 9.2

Following General procedure B for the synthesis of chiral enol phosphates, data is presented in the following format: (a) substrate, (b) yield of product, and (c) enantiomeric ratio.

(a) 4-phenylcyclohexan-1-one **25b** (139 mg, 0.8 mmol, 0.8 eq.), (b) 253 mg (76%), and (c) 99:1.



115b

Chiral analysis: HPLC OJ column, 1.20 mL/min, detector 254 nm, 3% IPA in hexane. $t_1 = 60.3$ min (major) and $t_2 = 66.8$ min (minor).

Entry 3 in Table 9.2

Following General procedure B for the synthesis of chiral enol phosphates, data is presented in the following format: (a) substrate, (b) yield of product, and (c) enantiomeric ratio.

(a) 4-*n*-propylcyclohexan-1-one **25g** (112 mg, 0.8 mmol, 0.8 eq.), (b) 268 mg (88%), and (c) N.D.

Entry 4 in Table 9.2

Following General procedure B for the synthesis of chiral enol phosphates, data is presented in the following format: (a) substrate, (b) yield of product, and (c) enantiomeric ratio.

(a) 4-methyl-propylcyclohexan-1-one **25d** (90 mg, 0.8 mmol, 0.8 eq.), (b) 256 mg (93%), and (c) N.D.

Entry 5 in Table 9.2

Following General procedure B for the synthesis of chiral enol phosphates, data is presented in the following format: (a) substrate, (b) yield of product and (c) enantiomeric ratio.

(a) 4-*n*-propylcyclohexan-1-one **25g** (112 mg, 0.8 mmol, 0.8 eq.), (b) 295 mg (97%), and (c) N.D.

Entry 6 in Table 9.2

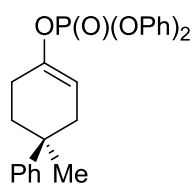
Following General procedure B for the synthesis of chiral enol phosphates, data is presented in the following format: (a) substrate, (b) yield of product and (c) enantiomeric ratio.

(a) 4-methyl-propylcyclohexan-1-one **25c** (90 mg, 0.8 mmol, 0.8 eq.), (b) 248 mg (90%), and (c) N.D.

Entry 7 in Table 9.2

Following General procedure B for the synthesis of chiral enol phosphates, data is presented in the following format: (a) substrate, (b) yield of product, and (c) enantiomeric ratio.

(a) 4-methyl-4-phenylcyclohexan-1-one **25d** (150 mg, 0.8 mmol, 0.8 eq.), (b) 248 mg (93%), and (c) 86:14.



115d

Chiral analysis: HPLC OJ column, 1.00 mL/min, detector 254 nm, 10% IPA in hexane. t_1 = 17.3 min (major) and t_2 = 18.3 min (minor).

Entry 8 in Table 9.2

Following General procedure B for the synthesis of chiral enol phosphates, data is presented in the following format: (a) substrate, (b) yield of product, and (c) enantiomeric ratio.

(a) 4-((*tert*-butyldimethylsilyl)oxy)cyclohexan-1-one **190h** (182 mg, 0.8 mmol, 0.8 eq.), (b) 273 mg (74%), and (c) N.D.

Entry 9 in Table 9.2

Following General procedure B for the synthesis of chiral enol phosphates, data is presented in the following format: (a) substrate, (b) yield of product and (c) enantiomeric ratio.

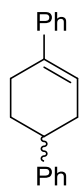
(a) 4-(dimethylamino)cyclohexan-1-one **190g** (113 mg, 0.8 mmol, 0.8 eq.), (b) 257 mg (86%), and (c) N.D.

Scheme 9.5

A flame-dried microwave vial was allowed to cool to room temperature under an argon atmosphere and charged with the diphenyl (1,2,3,6-tetrahydro-[1,1'-biphenyl]-4-yl) phosphate **115b** (102 mg, 0.25 mmol, 1.0 eq.) and PEPPSI S'Pr (2 mg, 2.5×10^{-3} mmol, 1.0 mol%). Thereafter, diethyl ether (1 mL) was added and the mixture was stirred for 5 min before the addition of phenylmagnesium

bromide (0.38 mL, $c = 1$ M in THF, 0.38 mmol, 1.5 eq.) at rt rapidly. The reaction was stirred at rt for 1 h. Then the reaction mixture was then partitioned between water (5 mL) and diethyl ether (5 mL). The organic phase was washed with brine (2 mL), dried over sodium sulfate, filtered, and the solvent was evaporated *in vacuo*. The product was purified by flash column chromatography using petrol ether as the eluent. Yield of product **140b** 39 mg (66%) and yield of by-product **141b**: 5 mg (6%).

Characterisation of 1',2',3',6'-tetrahydro-1,1':4',1''-terphenyl **140b**:¹⁵⁴



140b

Obtained as a white solid.

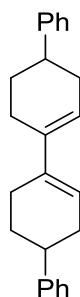
M.p.: 103 °C (lit.: 102 °C).¹⁵⁴

¹H NMR (400 MHz, CDCl₃): 7.38-7.33 (m, 2H, ArH), 7.29-7.12 (m, 8H, ArH), 6.15-6.13 (dd, ³J = 4.6 Hz, 1.9 Hz, 1H, CH=C), 2.86-2.76 (m, 1H, CH), 2.60-2.40 (m, 3H, CH₂), 2.35-2.21 (m, 1H, CH₂), 2.10-2.00 (m, 1H, CH₂), 1.93-1.78 (m, 1H, CH₂) ppm.

¹³C NMR (100 MHz, CDCl₃): 146.3, 141.5, 135.8, 127.9 (2C), 127.8 (2C), 126.4 (2C), 126.2, 125.6 (2C), 124.5, 123.7, 39.2, 33.6, 29.7, 27.5 ppm.

ν_{\max} (cm⁻¹): 2912, 1489, 1190, 1070, 1028, 968, 912, 746.

Characterisation of 4,4'-diphenyl-[1,1'-bi(cyclohexane)]-1,1'-diene **141b**:¹²³



141b

Obtained as a white solid.

M.p.: 160-165 °C (lit.: not reported)

^1H NMR (CDCl_3): 7.38-7.20 (m, 10H, ArH), 5.95-5.91 (dd, $^3J = 4.6$ Hz, 1.9 Hz, 2H, CH=C), 2.89-2.76 (m, 2H, CH), 2.56-2.25 (m, 8H, CH_2), 2.20-2.14 (m, 2H, CH_2), 1.90-1.78 (m, 2H, CH_2) ppm.

^{13}C NMR (CDCl_3): 147.3 (2C), 128.6 (4C), 127.1 (4C), 126.2 (2C), 121.8 (2C), 121.6 (2C), 40.4 (2C), 34.4 (2C), 30.4 (2C), 26.7 (2C) ppm.

$\nu_{\text{max}}(\text{cm}^{-1})$: 2922, 1597, 1259, 1103, 1022, 960, 800, 761.

Entry 1 in Table 9.3

Following General procedure C for the cross coupling of enol phosphates, data is presented in the following format: (a) catalyst, (b) amount of solvent, (c) yield of product **140b**, and (f) yield of homocoupled enol phosphate **141b**.

(a) PEPPSI *i*Pr (2 mg, 2.5×10^{-3} mmol, 1.0 mol%), (b) diethyl ether (1 mL), (e) 35 mg (60%), and (f) 7 mg (8%).

Entry 2 in Table 9.3

Following General procedure C for the cross coupling of enol phosphates, data is presented in the following format: (a) catalyst, (b) amount of solvent, (c) yield of product **140b**, and (f) yield of homocoupled enol phosphate **141b**.

(a) PEPPSI *i*Pr (2 mg, 2.5×10^{-3} mmol, 1.0 mol%), (b) diethyl ether (1 mL), (c) 37 mg (64%), and (f) 5 mg (6%).

Entry 3 in Table 9.3

A microwave vial was equipped with a stirrer bar and flame-dried. After cooling to rt, palladium(II) chloride (10 mg, 1.25×10^{-3} mmol, 5.0 mol%), diphenyl (1,2,3,6-tetrahydro-[1,1'-biphenyl]-4-yl) phosphate **115b** (102 mg, 0.25 mmol, 1.0 eq.), and THF (0.5 mL) were added. Thereafter, phenylmagnesium bromide (0.38 mL, $c = 1$ M in THF, 0.38 mmol, 1.5 eq.) was added to the stirred solution over 10 min. Then the reaction was stirred at rt for 24 h. The reaction was quenched with methanol (5 mL) and concentrated *in vacuo*. The crude product was purified by flash column chromatography using petrol ether as the eluent. The yield of product **140b** 20 mg (34%) alongside with the undesired homocoupled enol phosphate **141b** 3 mg (3%).

Entry 4 in Table 9.3

Following General procedure C for the cross coupling of enol phosphates, data is presented in the following format: (a) catalyst, (b) amount of solvent, (c) yield of product **140b**, and (f) yield of homocoupled enol phosphate **141b**.

(a) PEPPSI *i*Pr (2 mg, 2.5×10^{-3} mmol, 1.0 mol%), (b) THF (1 mL), (c) 26 mg (44%), and (f) 2 mg (2%).

Entry 1 in Table 9.4

Following General procedure D for the optimisation of the Kumada cross coupling reaction, data is presented in the following format: (a) amount of phenylmagnesium bromide, (b) addition time of phenylmagnesium bromide, (c) reaction temperature, (d) reaction time, (e) yield of product **140b**, and (f) yield of homocoupled enol phosphate **141b**.

(a) phenylmagnesium bromide (0.38 mL, c = 1 M in THF, 0.38 mmol, 1.5 eq.), (b) 1 min, (c) 0 °C, (d) 1 h, (e) 12 mg (20%), and (g) 3 mg (3%).

Entry 2 in Table 9.4

Following General procedure D for the optimisation of the Kumada cross coupling reaction, data is presented in the following format: (a) amount of phenylmagnesium bromide, (b) addition time of phenylmagnesium bromide, (c) reaction temperature, (d) reaction time, (e) yield of product **140b**, and (f) yield of homocoupled enol phosphate **141b**.

(a) phenylmagnesium bromide (0.38 mL, c = 1 M in THF, 0.38 mmol, 1.5 eq.), (b) 1 min, (c) 40 °C, (d) 1 h, (e) 38 mg (63%), and (g) 10 mg (13%).

Entry 3 in Table 9.4

A microwave vial was equipped with a stirrer bar and flame-dried. Diphenyl (1,2,3,6-tetrahydro-[1,1'-biphenyl]-4-yl) phosphate **115b** (102 mg, 0.25 mmol, 1.0 eq.), PEPPSI *S*'Pr (2 mg, 2.5×10^{-3} mmol, 1.0 mol%), diethyl ether (1 mL), and phenylmagnesium bromide (0.38 mL, c = 1 M in THF, 0.38 mmol, 1.5 eq.) were added. The reaction vessel was heated to 80 °C under microwave irradiation for 15 min. The crude product was partitioned between diethyl ether (5 mL) and water (5 mL). The aqueous phase was washed with diethyl ether (3 × 5 mL) and the organic phase was dried over sodium sulfate, filtered, and the solvent was removed *in vacuo*. The product was purified with flash column chromatography using petrol ether as the eluent. Yield of the desired product **140b**: 30 mg (50%) yield of the homocoupled enol phosphate **141b**: 4 mg (5% yield).

Entry 4 in Table 9.4

Following General procedure D for the optimisation of the Kumada cross coupling reaction, data is presented in the following format: (a) amount of phenylmagnesium bromide, (b) addition time of phenylmagnesium bromide, (c) reaction temperature, (d) reaction time, (e) yield of product **140b**, and (f) yield of homocoupled enol phosphate **141b**.

(a) phenylmagnesium bromide (0.76 mL, c = 1 M in THF, 0.76 mmol, 3.0 eq.), (b) 1 min, (c) 0 °C, (d) 1 h, (e) 38 mg (63%) and (g) 8 mg (10%).

Entry 5 in Table 9.4

A flame-dried microwave vial was allowed to cool to room temperature under an argon atmosphere and charged with PEPPSI SⁱPr (2 mg, 2.5*10⁻³ mmol, 1.0 mol%) and phenylmagnesium bromide (0.38 mL, c = 1 M in THF, 0.38 mmol, 1.50 eq.). Thereafter, the mixture was stirred for 5 min before the addition of the solution of diphenyl (1,2,3,6-tetrahydro-[1,1'-biphenyl]-4-yl) phosphate **115b** (102 mg, 0.25 mmol, 1.0 eq.) in diethyl ether (1 mL) over 1 h. The reaction was stirred for 1 hour, then the reaction mixture was partitioned between water (5 mL) and diethyl ether (5 mL). The organic phase was washed with brine (2 mL), dried over sodium sulfate, filtered, and the solvent was evaporated *in vacuo*. The product was purified by flash column chromatography using petrol ether as the eluent. Yield of product **140b**: 40 mg (66%), yield of the by-product enol phosphate **141b** : (13 mg (16%).

Entry 6 in Table 9.4

A microwave vial was equipped with a stirrer bar and flame-dried. diphenyl (1,2,3,6-tetrahydro-[1,1'-biphenyl]-4-yl) phosphate **115b** (102 mg, 0.25 mmol, 1.0 eq.), PEPPSI SⁱPr (2 mg, 2.5*10⁻³ mmol, 1.0 mol%), diethyl ether (1 mL) were added and the reaction was stirred for 5 min at room temperature. The solution of phenylmagnesium bromide (0.38 mL, c = 1 M in THF, 0.38 mmol, 1.50 eq.) was added over 1 h *via* a syringe pump and then the reaction was stirred for a further hour. The crude product was partitioned between diethyl ether (5 mL) and water (5 mL). The aqueous phase was washed with diethyl ether (3 × 5 mL) and the organic phase was dried over sodium sulfate, filtered, and the solvent was removed *in vacuo*. The product was purified with flash column chromatography using petrol ether as the eluent. Yield of the desired product **140b**: 48 mg (82%), yield of the homocoupled by-product: 2 mg (2%).

Entry 1 in Table 9.5

Following General procedure E for the Kumada cross coupling reaction (catalyst loading screen), data is presented in the following format: (a) amount of PEPPSI SⁱPr, (b) yield of cross coupled product **140b**, and (c) yield of homocoupled product **141b**.

(a) PEPPSI S'Pr (1 mg, 1.25×10^{-3} mmol, 0.5 mol%), (b) 26 mg (44%), and (c) 4 mg (4%).

Entry 2 in Table 9.5

Following General procedure E for the Kumada cross coupling reaction (catalyst loading screen), data is presented in the following format: (a) amount of PEPPSI S'Pr, (b) yield of cross coupled product **140b**, and (c) yield of homocoupled product **141b**.

(a) PEPPSI S'Pr (10 mg, 1.25×10^{-2} mmol, 5.0 mol%), (b) 51 mg (87%), and (c) 0 mg (0%).

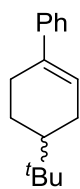
Entry 1 in Table 9.6

Following General procedure F for the Kumada cross coupling reaction, data is presented in the following format: (a) substrate and (b) yield of product **140a**.

(a) 4-(*tert*-butyl)cyclohex-1-en-1-yl diphenyl phosphate **115a** (386 mg, 1.0 mmol, 1.0 eq.) and (b) 188 mg (88%).

Characterisation of 4-(*tert*-butyl)-2,3,4,5-tetrahydro-1,1'-biphenyl **140a**:¹⁵⁵

Obtained as a white solid.



140a

M. p. 85-88 °C (lit.: not reported)

¹H NMR (CDCl₃): 7.39-7.34 (m, 2H, ArH), 7.31-7.26 (m, 2H, ArH), 7.22-7.16 (m, 1H, ArH), 6.13-6.10 (m, 1H, CH=CH₂), 2.56-2.35 (m, 2H, CH₂), 2.29-2.19 (m, 1H, CH), 2.01-1.90 (m, 2H, CH₂), 1.40-1.22 (m, 2H, CH₂), 0.90 (s, 9H, CH₃) ppm.

¹³C NMR (CDCl₃): 142.5, 136.6, 128.4 (2C), 128.2 (2C), 126.7, 125.1, 44.0, 32.4, 29.1, 27.7, 27.5, 24.6 (3C) ppm.

ν_{\max} (cm⁻¹): 2951, 2916, 2866, 2835, 1494, 1467, 1442, 1363, 912, 746.

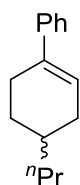
Entry 2 in Table 9.6

Following General procedure F for the Kumada cross coupling reaction, data is presented in the following format: (a) substrate and (b) yield of product **140g**.

(a) 4-(*n*-propyl)cyclohex-1-en-1-yl diphenyl phosphate **115g** (372 mg, 1.0 mmol, 1.0 eq.) and (b) 174 mg (87%).

Characterisation of 4-(*n*-propyl)-2,3,4,5-tetrahydro-1,1'-biphenyl **140g**:

Obtained as a colourless oil.



140g

^1H NMR (CDCl_3): 7.33-7.28 (m, 2H, ArH), 7.25-7.19 (m, 2H, ArH), 7.15-7.09 (m, 1H, ArH), 6.06-5.99 (m, 1H, CH=CH₂), 2.42-2.34 (m, 2H, CH₂), 2.29-2.20 (m, 1H, CH₂), 1.88-1.69 (m, 2H, CH₂), 1.58-1.48 (m, 1H, CH₂), 1.36-1.11 (m, 5H, CH₂, CH), 0.85 (t, $J = 7.0$ Hz, 3H, CH₃) ppm.

^{13}C NMR (CDCl_3): 142.6, 136.6, 128.4 (2C), 126.7 (2C), 125.2, 124.6, 38.9, 33.1, 32.9, 29.6, 27.7, 20.3, 14.6 ppm.

ν_{max} (cm^{-1}): 2953, 2910, 2868, 1492, 1452, 916, 758, 742.

HR-MS (EI): m/z calculated for $\text{M} = \text{C}_{15}\text{H}_{20}$, theoretical $[\text{M}^+]$: 200.1565. Found: 200.1571.

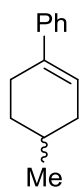
Entry 3 in Table 9.6

Following General procedure F for the Kumada cross coupling reaction, data is presented in the following format: (a) substrate and (b) yield of product **140c**.

(a) 4-methylcyclohex-1-en-1-yl diphenyl phosphate **115c** (344 mg, 1.0 mmol, 1.0 eq.) and (b) 112 mg (65%).

Characterisation of 4-methyl-2,3,4,5-tetrahydro-1,1'-biphenyl **140c**:

Obtained as a colourless oil.



140c

^1H NMR (CDCl_3): 7.34-7.29 (m, 2H, ArH), 7.25-7.20 (m, 2H, ArH), 7.16-7.11 (m, 1H, ArH), 6.04-5.99 (m, 1H, CH=CH₂), 2.43-2.34 (m, 2H, CH₂), 2.28-2.14 (m, 1H, CH), 1.83-1.60 (m, 3H, CH₂), 1.36-1.25 (m, 1H, CH₂), 0.94 (d, $J = 6.5$ Hz, 3H, CH₃) ppm.

^{13}C NMR (CDCl_3): 142.7, 136.4, 128.4 (2C), 126.8 (2C), 125.1, 124.5, 34.7, 31.5, 28.3, 27.6, 21.9 ppm.

ν_{max} (cm^{-1}): 2947, 2920, 2868, 2850, 1494, 1454, 1257, 894, 783, 740.

HR-MS (EI): m/z calculated for $\text{M} = \text{C}_{13}\text{H}_{16}$, theoretical [M^+]: 172.1252. Found: 172.1254.

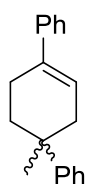
Entry 4 in Table 9.6

Following General procedure F for the Kumada cross coupling reaction, data is presented in the following format: (a) substrate and (b) yield of product **140d**.

(a) 1-methyl-1,2,3,6-tetrahydro-[1,1'-biphenyl]-4-yl diphenyl phosphate **115d** (420 mg, 1.0 mmol, 1.0 eq.) and (b) 236 mg (95%).

Characterisation of 1'-methyl-1',2',3',6'-tetrahydro-1,1':4',1''-terphenyl **140d**:

Obtained as a colourless oil.



140d

^1H NMR (CDCl_3): 7.34-7.26 (m, 4H, ArH), 7.25-7.18 (m, 4H, ArH), 7.15-7.07 (m, 2H, ArH), 6.16-6.11 (m, 1H, CH=CH₂), 2.59-2.63 (m, 1H, CH₂), 2.42-2.32 (m, 1H, CH₂), 2.62 (m, 1H, CH₂), 2.19-2.07 (m, 1H, CH₂), 2.06-1.97 (m, 1H, CH₂), 1.87-1.78 (m, 1H, CH₂), 1.26 (s, 3H, CH₃) ppm.

^{13}C NMR (CDCl_3): 149.3, 142.1, 136.0, 128.4 (2C), 128.3 (2C), 126.9 (2C), 125.9, 125.6 (2C), 125.1, 123.5, 38.5, 36.4, 35.6, 28.9, 25.5 ppm.

ν_{\max} (cm⁻¹): 2950, 2915, 2898, 1597, 1495, 1444, 1026, 905, 762, 745, 693.

HR-MS (EI): m/z calculated for M = C₁₉H₂₀, theoretical [M⁺]: 248.1565. Found: 248.1570.

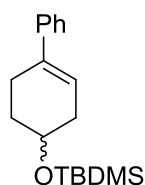
Entry 5 in Table 9.6

Following General procedure F for the Kumada cross coupling reaction, data is presented in the following format: (a) substrate and (b) yield of product **140e**.

(a) 4-((*tert*-butyldimethylsilyl)oxy)cyclohex-1-en-1-yl diphenyl phosphate **115e** (461 mg, 1.0 mmol, 1.0 eq.) and (b) 254 mg (88%).

Characterisation of *tert*-butyldimethyl((2,3,4,5-tetrahydro-[1,1'-biphenyl]-4-yl)oxy)silane **140e**:

Obtained as a yellow oil.



140e

¹H NMR (CDCl₃): 7.39-7.34 (m, 2H, ArH), 7.31-7.26 (m, 2H, ArH), 7.22-7.17 (m, 1H, ArH), 5.99-5.93 (m, 1H, CH=CH₂), 4.04-3.89 (m, 1H, OCH), 2.66-2.54 (m, 1H, CH₂), 2.53-2.38 (m, 1H, CH₂), 2.25-2.13 (m, 2H, CH₂), 1.98-1.71 (m, 2H, CH₂), 0.91 (s, 9H, CCH₃), 0.10 (s, 3H, CH₃), 0.09 (s, 3H, CH₃) ppm.

¹³C NMR (CDCl₃): 142.0, 136.4, 128.4 (2C), 126.9 (2C), 125.2, 122.4, 67.8, 35.8, 32.3, 26.6, 26.2 (3C), 17.8, -4.37 (2C) ppm.

ν_{\max} (cm⁻¹): 2950, 2926, 2885, 2854, 1463, 1253, 1100, 872, 836, 777, 756, 695.

HR-MS (CI): m/z calculated for M = C₁₈H₂₈OSi, theoretical [M⁺]: 288.1931. Found: 288.1910.

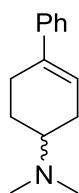
Entry 6 in Table 9.6

Following General procedure F for the Kumada cross coupling reaction, data is presented in the following format: (a) substrate and (b) yield of product **140f**.

(a) 4-(dimethylamino)cyclohex-1-en-1-yl diphenyl phosphate **115f** (373 mg, 1.0 mmol, 1.0 eq.) and (b) 164 mg (82%).

Characterisation of N,N-dimethyl-2,3,4,5-tetrahydro-[1,1'-biphenyl]-4-amine **140f**:

Obtained as a yellow oil.



140f

^1H NMR (CDCl_3): 7.30-7.12 (m, 5H, ArH), 5.94-5.87 (m, 1H, CH=CH₂), 2.85-2.72 (m, 1H, NCH), 2.62-2.44 (m, 3H, CH₂), 2.43 (s, 6H, NCH₃), 2.30-2.12 (m, 2H, CH₂), 1.68-1.55 (m, 1H, CH₂) ppm.

^{13}C NMR (CDCl_3): 140.8, 136.9, 128.5 (2C), 127.4 (2C), 125.2, 121.6, 61.5, 40.3 (2C), 27.5, 26.6, 24.5 ppm.

ν_{max} (cm^{-1}): 2964, 2924, 2560, 2467, 1489, 1251, 1210, 1091, 762, 745, 693.

HR-MS (APCI): m/z calculated for M = C₁₄H₂₀N, theoretical [M+H]⁺: 202.1589. Found: 202.1590.

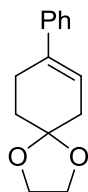
Entry 7 in Table 9.6

Following General procedure F for the Kumada cross coupling reaction, data is presented in the following format: (a) substrate and (b) yield of product **140h**.

(a) diphenyl (1,4-dioxaspiro[4.5]dec-7-en-8-yl) phosphate **115h** (388 mg, 1.0 mmol, 1.0 eq.) and (b) 162 mg (75%).

Characterisation of 8-phenyl-1,4-dioxaspiro[4.5]dec-7-ene **140h**:¹⁵⁶

Obtained as a colourless oil.



140h

^1H NMR (CDCl_3): 7.39-7.29 (m, 2H, ArH), 7.26-7.20 (m, 2H, ArH), 7.18-7.12 (m, 1H, ArH), 5.94-5.88 (m, 1H, CH=CH₂), 3.97-3.93 (m, 4H, OCH₂), 2.63-2.55 (m, 2H, CH₂), 2.42-2.38 (m, 2H, CH₂), 1.86 ppm (m, 2H, CH₂).

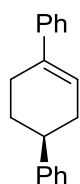
^{13}C NMR (CDCl_3): 141.7, 136.6, 128.4 (2C), 127.2 (2C), 125.4, 121.8, 108.1, 64.7 (2C), 36.4, 31.6, 30.0 ppm.

ν_{max} (cm^{-1}): 2947, 2924, 2877, 1242, 1112, 1056, 1022, 864, 761, 738, 692.

Entry 1 in Table 9.7

Following General procedure F for the Kumada cross coupling reaction, data is presented in the following format: (a) substrate, (b) yield of product **140b** and (c) enantiomeric ratio of product **140b**.

(a) 4-phenylcyclohex-1-en-1-yl diphenyl phosphate **115b** (406 mg, 1.0 mmol, 1.0 eq.), (b) 225 mg (87%) and (c) 99:1.



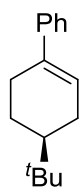
291b

Chiral analysis: HPLC OJ column, 0.40 mL/min, detector 254 nm, hexane. t_1 = 77.4 min (major) and t_2 = 82.3 min (minor).

Entry 2 in Table 9.7

Following General procedure F for the Kumada cross coupling reaction, data is presented in the following format: (a) substrate, (b) yield of product **140a** and (c) enantiomeric ratio of product **140a**.

(a) 4-(*tert*-butyl)cyclohex-1-en-1-yl diphenyl phosphate **115a** (386 mg, 1.0 mmol, 1.0 eq.), (b) 171 mg (80%) and (c) 93:7.



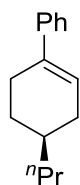
140a

Chiral analysis: HPLC OD-H column, 0.40 mL/min, detector 254 nm, hexane. t_1 = 34.8 min (major) and t_2 = 38.2 min (minor).

Entry 3 in Table 9.7

Following General procedure F for the Kumada cross coupling reaction, data is presented in the following format: (a) substrate, (b) yield of product **140g** and (c) enantiomeric ratio of product **140g**.

(a) 4-(*n*-propyl)cyclohex-1-en-1-yl diphenyl phosphate **115g** (372 mg, 1.0 mmol, 1.0 eq.), (b) 180 mg (90%) and (c) 91:9.



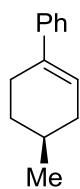
291c

Chiral analysis: HPLC OD-H column, 0.20 mL/min, detector 254 nm, hexane. t_1 = 62.3 min (major) and t_2 = 66.1 min (minor).

Entry 4 in Table 9.7

Following General procedure F for the Kumada cross coupling reaction, data is presented in the following format: (a) substrate, (b) yield of product **140c** and (c) enantiomeric ratio of product **140c**.

(a) 4-methylcyclohex-1-en-1-yl diphenyl phosphate **115c** (344 mg, 1.0 mmol, 1.0 eq.), (b) 158 mg (92%) and (c) 52:48.



115c

Chiral analysis: HPLC OD-H column, 0.30 mL/min, detector 254 nm, hexane. t_1 = 37.7 min (major) and t_2 = 39.8 min (minor).

Entry 5 in Table 9.7

Following General procedure F for the Kumada cross coupling reaction, data is presented in the following format: (a) substrate, (b) yield of product **140g** and (c) enantiomeric ratio of product **140g**.

(a) 4-(*n*-propyl)cyclohex-1-en-1-yl diphenyl phosphate **115g** (372 mg, 1.0 mmol, 1.0 eq.), (b) 182 mg (91%) and (c) 91:9.

Entry 6 in Table 9.7

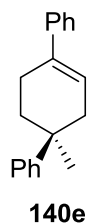
Following General procedure F for the Kumada cross coupling reaction, data is presented in the following format: (a) substrate, (b) yield of product **140c** and (c) enantiomeric ratio of product **140c**.

(a) 4-methylcyclohex-1-en-1-yl diphenyl phosphate **115c** (344 mg, 1.0 mmol, 1.0 eq.), (b) 160 mg (93%) and (c) 84:16.

Entry 7 in Table 9.7

Following General procedure F for the Kumada cross coupling reaction, data is presented in the following format: (a) substrate, (b) yield of product **140e** and (c) enantiomeric ratio of product **140e**

(a) 1-methyl-1,2,3,6-tetrahydro-[1,1'-biphenyl]-4-yl diphenyl phosphate **115e** (420 mg, 1.0 mmol, 1.0 eq.), (b) 234 mg (94%) and (c) 86:14.

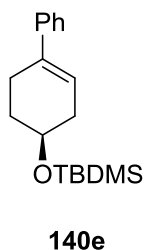


Chiral analysis: HPLC OD-H column, 0.40 mL/min, detector 254 nm, hexane. t_1 = 85.6 min (major) and t_2 = 89.0 min (minor).

Entry 8 in Table 9.7

Following General procedure F for the Kumada cross coupling reaction, data is presented in the following format: (a) substrate, (b) yield of product **140e** and (c) enantiomeric ratio of product **140e**

(a) 4-((*tert*-butyldimethylsilyl)oxy)cyclohex-1-en-1-yl diphenyl phosphate **115e** (461 mg, 1.0 mmol, 1.0 eq.), (b) 260 mg (90%) and (c) 95:5.

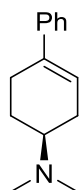


Chiral analysis: HPLC OD-H column, 0.30 mL/min, detector 254 nm, hexane. t_1 = 32.4 min (major) and t_2 = 44.1 min (minor).

Entry 9 in Table 9.7

Following General procedure F for the Kumada cross coupling reaction, data is presented in the following format: (a) substrate, (b) yield of product **140f** and (c) enantiomeric ratio of product **140f**

(a) 4-(dimethylamino)cyclohex-1-en-1-yl diphenyl phosphate **115f** (373 mg, 1.0 mmol, 1.0 eq.), (b) 160 mg (80%) and (c) -:-.



291g

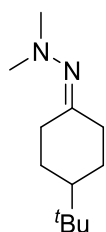
Chiral analysis: -.

Entry 1 in Table 9.8

Following general procedure G, data is presented in the following format: (a) amount of ketone **25a**, (b) amount of toluene, (c) amount of *p*-TSA and (d) yield of product **145**.

(a) 4-(*tert*-butyl)cyclohexan-1-one **25a** (154 mg, 1.0 mmol, 1.0 eq., (b) 10 mL, (c) *N,N*-dimethylhydrazine, 0.23 mL, 3.0 mmol, 3.0 eq., (d) *p*-TSA, 10 mg, 0.05 mmol, 5 mol%, and (e) 122 mg (62%).

Characterisation of 2-(4-(*tert*-butyl)cyclohexylidene)-1,1-dimethylhydrazine **145**.¹⁵⁷



145

Obtained as a yellow oil.

¹H NMR (CDCl₃): 3.31-3.24 (m, 1H, CH₂), 2.46-2.38 (m, 7H, NCH₃, CH₂), 2.14-2.04 (m, 1H, CH₂), 1.98-1.86 (m, 2H, CH₂), 1.79-1.65 (m, 1H, CH₂), 1.31-1.07 (m, 3H, CH₂, CH), 0.85 (s, 9H, CH₃) ppm.

¹³C NMR (CDCl₃): 170.4, 47.9, 47.8 (2C), 35.9, 32.7, 28.5, 28.3, 27.8, 27.5 (3C) ppm.

ν_{\max} (cm⁻¹): 2945, 1465, 1365, 993, 964, 557, 534, 526, 509, 499, 484, 478, 468, 454, 432, 406.

Entry 2 in Table 9.8

Following general procedure G, data is presented in the following format: (a) amount of ketone **25a**, (b) amount of toluene, (c) amount of *p*-TSA and (d) yield of product **145**.

(a) 4-(*tert*-butyl)cyclohexan-1-one **25a** (462 mg, 3.0 mmol, 1.0 eq.), (b) 30 mL, (c) *N,N*-dimethylhydrazine (0.69 mL, 9.0 mmol, 3.0 eq.), (d) *p*-TSA (30 mg, 0.15 mmol, 5 mol%) and (e) 389 mg (66%).

Scheme 9.13^{158,159}

A solution of LDA in THF was prepared as described in General Procedure H. The solution was cooled to -78 °C and hydrazine **145** (154 mg, 1.0 mmol, 1.0 eq.) in THF (5 mL) was added. The resulting reaction mixture was stirred for 15 h. After this period, the reaction mixture was cooled to -78 °C and 4-bromo-1-butene (0.12 mL, 1.2 mmol, 1.2 eq.) was added. The cooling bath was removed and the reaction was stirred at rt for 15 h. The crude mixture was poured into a biphasic mixture of Et₂O (20 mL) and 2 M H₂SO₄ (20 mL). The resulting mixture was stirred for 1 h vigorously and then the phases were separated. The aqueous phase was washed with Et₂O (3 × 20 mL) and the combined organic phase was dried over Na₂SO₄ and filtered. The solvent was evaporated *in vacuo* and the crude product was analysed by ¹H NMR spectroscopy. Unfortunately, no product formation was detected and, 4-(*tert*-butyl)cyclohexan-1-one **25a** was recovered 171 mg (87%, resulting from hydrolysis of the starting hydrazine).

Entry 1 in Table 9.9

Following General Procedure H for the deprotonation and alkylation of hydrazine **145** with MeI, data is presented in the following format: (a), deprotonation reaction time, (b) conversion towards product **147**, and (c) conversion towards 4-(*tert*-butyl)cyclohexan-1-one **25a**.

(a) 1 h, (b) –, and (c) 99%.

Entry 2 in Table 9.9

Following General Procedure H for the deprotonation and alkylation of hydrazine **145** with MeI, data is presented in the following format: (a), deprotonation reaction time, (b) conversion towards product **147**, and (c) conversion towards 4-(*tert*-butyl)cyclohexan-1-one **25a**.

(a) 2 h, (b) –, and (c) 98%.

Entry 3 in Table 9.9

Following General Procedure H for the deprotonation and alkylation of hydrazine **145** with MeI, data is presented in the following format: (a), deprotonation reaction time, (b) conversion towards product **147**, and (c) conversion towards 4-(*tert*-butyl)cyclohexan-1-one **25a**.

(a) 4 h, (b) –, and (c) 99%.

Entry 4 in Table 9.9

Following General Procedure H for the deprotonation and alkylation of hydrazine **145** with MeI, data is presented in the following format: (a), deprotonation reaction time, (b) conversion towards product **147**, and (c) conversion towards 4-(*tert*-butyl)cyclohexan-1-one **25a**.

(a) 4 h, (b) –, and (c) 97%.

Entry 1 in Table 9.10

Following General procedure J for the deprotonation and alkylation of hydrazine **145** with MeI, data is presented in the following format: (a) deprotonation temperature, (b) deprotonation reaction time, (c) conversion towards product **147** and (d) conversion towards unreacted starting material 4-(*tert*-butyl)cyclohexan-1-one **25a**.

(a) -78 °C, (b) 1 h, (c) – and (d) 99%.

Entry 2 in Table 9.10

Following General procedure J for the deprotonation and alkylation of hydrazine **145** with MeI, data is presented in the following format: (a) deprotonation temperature, (b) deprotonation reaction time, (c) conversion towards product **147** and (d) conversion towards unreacted starting material 4-(*tert*-butyl)cyclohexan-1-one **25a**.

(a) -78 °C, (b) 2 h, (c) – and (d) 99%.

Entry 3 in Table 9.10

Following General procedure J for the deprotonation and alkylation of hydrazine **145** with MeI, data is presented in the following format: (a) deprotonation temperature, (b) deprotonation reaction time, (c) conversion towards product **147** and (d) conversion towards unreacted starting material 4-(*tert*-butyl)cyclohexan-1-one **25a**.

(a) -78 °C, (b) 4 h, (c) – and (d) 99%.

Entry 4 in Table 9.10

Following General procedure J for the deprotonation and alkylation of hydrazine **145** with MeI, data is presented in the following format: (a) deprotonation temperature, (b) deprotonation reaction time, (c) conversion towards product **147** and (d) conversion towards unreacted starting material 4-(*tert*-butyl)cyclohexan-1-one **25a**.

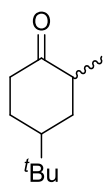
(a) -78 °C, (b) 8 h, (c) – and (d) 99%.

Entry 1 in Table 9.11

Following General procedure J for the deprotonation and alkylation of hydrazine **145** with MeI, data is presented in the following format: (a) deprotonation temperature, (b) deprotonation reaction time and (c) conversion towards product **147**.

(a) 0 °C, (b) 1 h, (c) 60%

Characterisation of 4-(*tert*-butyl)-2-methylcyclohexan-1-one **147**:¹⁶⁰



147

Obtained as a yellow oil

Mixture of diastereomers is reported d.r. = 1.0 : 0.7.

¹H NMR (CDCl₃): 2.38-2.18 (m, 3.4H, CH₂), 2.06-1.97 (m, 1.7H, CH₂), 1.98-1.85 (m, 0.7H, CH₂), 1.70-1.57 (m, 1.7H, CH₂), 1.57-1.48 (m, 1.7H, CH₂), 1.45-1.16 (m, 4.1H, CH₂), 1.09 (d, *J* = 6.9 Hz, 2.1H, CH₃), 0.95 (d, *J* = 7.3 Hz, 3H, CH₃), 0.83 (s, 9H, C(CH₃)₃), 0.84 (s, 6.3H, C(CH₃)₃) ppm.

¹³C NMR (CDCl₃): 216.7, 214.0, 47.3, 44.8, 41.5, 38.8, 37.5, 30.5, 29.2, 28.9, 27.9 (3C), 27.6 (3C), 23.8, 23.2, 17.0, 15.0, 14.2, 11.2 ppm.

ν_{max} (cm⁻¹): 2954, 2933, 1712, 1271, 1120, 1070, 742.

Entry 2 in Table 9.11

Following General procedure J for the deprotonation and alkylation of hydrazine **145** with MeI, data is presented in the following format: (a) deprotonation temperature, (b) deprotonation reaction time and (c) conversion towards product **147**.

(a) 0 °C, (b) 1 h, (c) 73%

Entry 3 in Table 9.11

Following General procedure J for the deprotonation and alkylation of hydrazine **145** with MeI, data is presented in the following format: (a) deprotonation temperature, (b) deprotonation reaction time and (c) conversion towards product **147**.

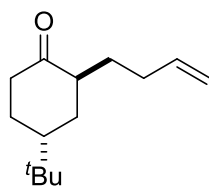
(a) 0 °C, (b) 1 h, (c) 62%

Scheme 9.17

Following General procedure W for the alkylation of hydrazine **297** with bromo acyclic electrophiles, data is presented in the following format: (a) electrophile and (b) yield of product.

(a) 4-bromo-1-butene, 0.12 mL, 1.2 mmol, 1.2 eq. and (b) 142 mg (68%).

Characterisation of 2-(but-3-en-1-yl)-4-(*tert*-butyl)cyclohexan-1-one **146**:¹⁶¹



146

Obtained as a colourless oil.

¹H NMR (CDCl₃): 5.79-5.72 (m, 1H, CH), 4.98-4.96 (dq, ³J = 17.4 Hz, 1.6 Hz, 1H, CH), 4.93-4.88 (m, 1H, CH), 2.38-2.29 (m, 2H, CH₂), 2.27-2.18 (m, 1H, CH), 2.07-1.87 (m, 3H, CH₂), 1.81-1.70 (m, 2H, CH₂), 1.64-1.33 (m, 4H, CH₂), 0.84 (s, 9H, C(CH₃)₃) ppm.

¹³C NMR (CDCl₃): 215.9, 138.0, 115.4, 48.7, 41.6, 38.7, 32.6, 31.59, 31.56, 30.9, 27.6 (3C), 27.1 ppm.

ν_{\max} (cm⁻¹): 2943, 2908, 2866, 1708, 1365, 908.

Scheme 9.18

Following General Procedure C for the synthesis of racemic enol phosphates, data is presented in the following format: (a) substrate **146** and (b) yield of product **142**.

(a) 2-(but-3-en-1-yl)-4-(*tert*-butyl)cyclohexan-1-one **146** (208 mg, 1 mmol, 1.0 eq., and (b) 0%; starting ketone **146** was recovered quantitatively 208 mg (100%) yield.

Entry 1 in Table 9.12

Following General Procedure L for the preparation **D-298**, data is presented in the following format: (a) additive, (b) base, (c) reaction temperature, and (d) deuterium incorporation.

(a) DMPU, 0.05 mL, 0.40 mmol, 4 eq., (b) di-*tert*-butylmagnesium, 0.1 mL, c = 0.5 mmol/mL, 0.05 mmol, 0.5 eq., (c) rt, and (d) 0% D.

Entry 2 in Table 9.12

Following General Procedure L for the preparation **D-298**, data is presented in the following format: (a) additive, (b) base, (c) reaction temperature, and (d) deuterium incorporation.

(a) LiCl, 42 mg, 1.0 mmol, 10 eq., (b) di-*tert*-butylmagnesium, 0.1 mL, c = 0.5 mmol/mL, 0.05 mmol, 0.5 eq., (c) rt, and (d) 0% D.

Entry 3 in Table 9.12

Following General Procedure L for the preparation **D-298**, data is presented in the following format: (a) additive, (b) base, (c) reaction temperature, and (d) deuterium incorporation.

(a) LiCl, 42 mg, 1.0 mmol, 10 eq., (b) di-*tert*-butylmagnesium, 0.1 mL, c = 0.5 mmol/mL, 0.05 mmol, 0.5 eq., (c) reflux, and (d) 0% D.

Entry 4 in Table 9.12

Following General Procedure L for the preparation **D-298**, data is presented in the following format: (a) additive, (b) base, (c) reaction temperature, and (d) deuterium incorporation.

(a) LiCl, 42 mg, 1.0 mmol, 10 eq., (b) *tert*-butylmagnesium chloride, 0.05 mL, c = 2.0 mmol/mL, 0.1 mmol, 1.0 eq., (c) 0 °C, and (d) 0% D.

Entry 5 in Table 9.12

Following General Procedure L for the preparation **D-298**, data is presented in the following format: (a) additive, (b) base, (c) reaction temperature, and (d) deuterium incorporation.

(a) LiCl, 42 mg, 1.0 mmol, 10 eq.), (b) *tert*-butylmagnesium chloride, 0.05 mL, c = 2.0 mmol/mL, 0.1 mmol, 1.0 eq., (c) rt, and (d) 0% D.

Entry 6 in Table 9.12

Following General Procedure L for the preparation **D-298**, data is presented in the following format:

(a) additive, (b) base, (c) reaction temperature, and (d) deuterium incorporation.

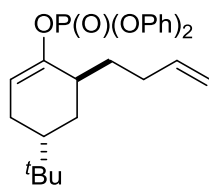
(a) DMPU, 0.05 mL, 0.40 mmol, 4 eq., (b) bismesitylmagnesium, 0.15 mL, c = 0.5 mmol/mL, 0.75 mmol, 0.75 eq., (c) rt, and (d) >99% D.

Scheme 9.20

Following General Procedure M for the preparation enol phosphates with Mes₂Mg, data is presented in the following format: (a) substrate and (b) yield of product.

(a) 2-(but-3-en-1-yl)-4-(*tert*-butyl)cyclohexan-1-one, 208 mg, 1.0 mmol, 1.0 eq. and (b) 374 mg, 85% yield.

Characterisation of 6-(but-3-en-1-yl)-4-(*tert*-butyl)cyclohex-1-en-1-yl diphenyl phosphate **142**:



142

Obtained as colourless oil.

¹H NMR (CDCl₃): 7.41-7.33 (m, 4H, ArH), 7.29-7.18 (m, 5H, ArH), 6.92-6.80 (m, 1H, ArH), 5.76-5.65 (m, 1H, CH), 5.63-5.58 (m, 1H, CH), 5.02-4.92 (m, 2H, CH₂), 2.34-2.26 (m, 2H, CH₂), 2.16-2.04 (m, 2H, CH₂), 2.00-1.82 (m, 2H, CH₂), 1.81-1.66 (m, 2H, CH), 1.40-1.34 (m, 2H, CH₂), 0.89 (s, 9H, CH₃) ppm.

¹³C NMR (CDCl₃): 151.2 (d, ²J_{C-P} = 10.6 Hz), 150.8 (d, ²J_{C-P} = 8.2 Hz), 138.5, 130.0 (4C), 126.6 (4C), 120.4 (d, 4C, ³J_{C-P} = 4.4 Hz), 114.9, 111.7 (d, 2C, ³J_{C-P} = 4.8 Hz), 38.3, 37.3 (d, 1C, ³J_{C-P} = 4.7 Hz), 32.1, 31.9, 31.0, 27.5 (3C), 27.4, 25.5 ppm.

³¹P NMR (CDCl₃): -17.5 ppm

ν_{\max} (cm⁻¹): 2951, 2935, 1487, 1296, 1186, 1101, 945, 906, 769, 752, 686.

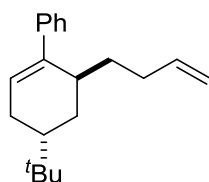
HR-MS (APCI): *m/z* calculated for M = C₂₆H₃₄O₄P, theoretical [M+H]⁺ : 441.2195. Found: 441.2190.

Scheme 9.21

Following General Procedure N, data is presented in the following format: (a) substrate, (b) additive, and (c) yield of product.

(a) 6-(but-3-en-1-yl)-4-(*tert*-butyl)cyclohex-1-en-1-yl diphenyl phosphate **142** (220 mg, 0.5 mmol, 0.5 eq.), (b) none, and (c) 26 mg (19%).

Characterisation of 2-(but-3-en-1-yl)-4-(*tert*-butyl)-2,3,4,5-tetrahydro-1,1'-biphenyl **143**:



143

Obtained as a colourless oil.

^1H NMR (CDCl_3): 7.35-7.29 (m, 2H, ArH), 7.24-7.18 (m, 3H, ArH), 5.96-5.83 (m, 1H, CH), 5.80-5.63 (m, 1H, CH), 5.60-5.32 (dd, $^3J = 18.6$ Hz, 1.7 Hz, 1H, CH), 5.02-4.85 (m, 1H, CH), 2.85-2.68 (m, 2H, CH_2), 2.44-2.16 (m, 3H, CH_2), 2.15-2.08 (m, 2H, CH_2), 2.07-1.95 (m, 1H, CH_2), 1.46-1.40 (m, 1H, CH), 1.39-1.35 (m, 1H, CH), 0.90 (s, 9H, CH_3) ppm.

^{13}C NMR (CDCl_3): 143.1, 142.6, 142.1, 139.2, 129.4, 128.2, 126.7, 125.8, 37.6, 36.4, 33.8, 33.3, 32.3, 28.2, 27.5, 27.4 ppm.

ν_{max} (cm^{-1}): 2937, 2912, 2860, 1492, 1467, 1452, 1363, 906, 758, 696.

HR-MS (APCI): m/z calculated for $\text{M} = \text{C}_{20}\text{H}_{29}$, theoretical $[\text{M}+\text{H}]^+$: 269.2269. Found: 269.2262.

Scheme 9.22

Following General Procedure N, data is presented in the following format: (a) substrate, (b) additive, and (c) yield of product.

(a) 6-(but-3-en-1-yl)-4-(*tert*-butyl)cyclohex-1-en-1-yl diphenyl phosphate **142** (220 mg, 0.5 mmol, 0.5 eq.), (b) *iso*-propyl iodide (0.055 mL, 0.55 mmol, 1.1 eq.) and (c) 30 mg (22%).

Scheme 9.22

Following General Procedure N, data is presented in the following format: (a) substrate, (b) additive, and (c) yield of product.

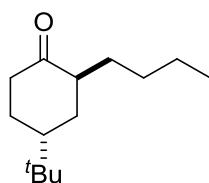
(a) 6-(but-3-en-1-yl)-4-(*tert*-butyl)cyclohex-1-en-1-yl diphenyl phosphate **142**(220 mg, 0.5 mmol, 1.0 eq.), (b) *iso*-propyl iodide(0.055 mL, 0.55 mmol, 1.1 eq.) and (c) 30 mg (22%).

Scheme 9.23

Following General Procedure K for the alkylation of hydrazine **145** with bromo acyclic electrophiles, data is presented in the following format: (a) electrophile and (b) yield of product.

(a) 1-bromo-butane (0.13 mL, 1.2 mmol, 1.2 eq.) and (b) 143 mg (62%).

Characterisation of 4-(*tert*-butyl)-2-butylcyclohexan-1-one **149**:



149

Obtained as a colourless oil.

^1H NMR (CDCl_3): 2.43-2.24 (m, 2H, CH_2), 2.23-2.14 (m, 1H, CH), 1.98-1.88 (m, 1H, CH_2), 1.80-1.71 (m, 1H, CH_2), 1.68-1.49 (m, 3H, CH_2), 1.44-1.36 (m, 2H, CH_2), 1.29-1.17 (m, 4H, CH_2), 0.83 (s, 9H, $\text{C}(\text{CH}_3)_3$), 0.82 (t, $J = 7.2$ Hz, 3H, CH_3) ppm.

^{13}C NMR (CDCl_3): 216.2, 49.6, 41.5, 38.6, 32.5, 31.7, 31.0, 29.6, 27.7 (3C), 27.4, 22.7, 14.1 ppm.

ν_{max} (cm^{-1}): 2951, 2931, 2866, 1708, 1365.

HR-MS (APCI): m/z calculated for $\text{M} = \text{C}_{14}\text{H}_{27}\text{O}$, theoretical $[\text{M}+\text{H}]^+$: 211.2056. Found: 211.2058.

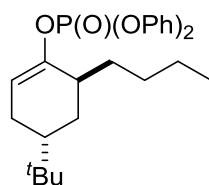
Scheme 9.24

Following General Procedure M for the preparation enol phosphates with Mes_2Mg , data is presented in the following format: (a) substrate and (b) yield of product.

(a) 4-(*tert*-butyl)-2-butylcyclohexan-1-one **149**:(210 mg, 1.0 mmol, 1.0 eq.) and (b) 372 mg (84%).

Characterisation of 4-(*tert*-butyl)-6-butylcyclohex-1-en-1-yl diphenyl phosphate **148**:

Obtained as a colourless oil.



148

^1H NMR (CDCl_3): 7.31-7.23 (m, 3H, ArH), 7.19-7.08 (m, 6H, ArH), 6.58-6.71 (m, 1H, ArH), 5.67-5.60 (m, 1H, C=CH), 2.18-2.09 (m, 1H, CH), 2.03-1.92 (m, 1H, CH_2), 1.83-1.71 (m, 1H, CH), 1.70-1.64 (m, 1H, CH_2), 1.52-1.43 (m, 1H, CH_2), 1.30-1.00 (m, 7H, CH_2), 0.79 (s, 9H, CH_3), 0.77 (t, $J = 7.1$ Hz, 3H, CH_3) ppm.

^{13}C NMR (CDCl_3): 151.6 (d, $^2J_{\text{C-P}} = 10.3$ Hz), 150.9 (d, $^2J_{\text{C-P}} = 8.0$ Hz), 129.9 (4C), 125.6 (4C), 120.4 (4C, $^3J_{\text{C-P}} = 4.4$ Hz), 111.3 (d, 2C, $^3J_{\text{C-P}} = 4.8$ Hz), 43.6, 38.3, 37.9 (d, $^3J_{\text{C-P}} = 4.8$ Hz), 32.1, 31.4, 30.0, 27.5 (3C), 25.6, 22.9, 14.3 ppm.

^{31}P NMR (CDCl_3): -17.5 ppm

ν_{max} (cm^{-1}): 2954, 2929, 2862, 1487, 1184, 948, 752, 686.

HR-MS (APCI): m/z calculated for $\text{M} = \text{C}_{26}\text{H}_{35}\text{O}_4\text{P}$, theoretical $[\text{M}+\text{H}]^+$: 443.2351. Found: 443.2349.

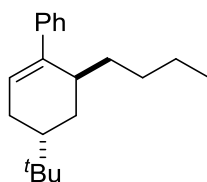
Scheme 9.25

Following General Procedure N, data is presented in the following format: (a) substrate, (b) additive and (c) yield of product **150**.

(a) 4-(*tert*-butyl)-6-butylcyclohex-1-en-1-yl diphenyl phosphate **148** (221 mg, 0.5 mmol, 1.0 eq.), (b)- and (c) 31 mg (23%).

Characterisation of 4-(*tert*-butyl)-2-butyl-2,3,4,5-tetrahydro-1,1'-biphenyl **150**:

Obtained as a colourless oil.



150

^1H NMR (CDCl_3): 7.30-7.24 (m, 1H, ArH), 7.23-7.18 (m, 2H, ArH), 7.15-7.11 (m, 2H, ArH), 5.76-5.73 (m, 1H, C=CH), 2.71-2.60 (m, 1H, CH), 2.16-2.08 (m, 1H, CH), 2.01-1.95 (m, 1H, CH_2), 1.91-1.74 (m, 2H, CH_2), 1.40-1.28 (m, 2H, CH_2), 1.16-1.07 (m, 2H, CH_2), 1.03-0.93 (m, 3H, CH_2) 0.84 (s, 9H, CH_3), 0.70 (t, $J = 7.2$ Hz, 3H, CH_3) ppm.

^{13}C NMR (CDCl_3): 142.6, 142.2, 127.5 (2C), 126.9 (2C), 125.9, 125.5, 43.3, 37.5, 33.6, 30.3, 29.3, 29.1, 27.2, 26.7 (3C), 22.3, 13.6 ppm.

ν_{max} (cm^{-1}): 2953, 2924, 2854, 1465, 1363, 1259, 1018, 798, 759.

HR-MS (APCI): m/z calculated for $\text{M} = \text{C}_{20}\text{H}_{30}$, theoretical $[\text{M}-\text{H}]^+$: 269.2269. Found: 269.2271.

Scheme 9.82

A 2 mL microwave vial was equipped with a stirrer bar, closed with a suba seal, and flame dried under an atmosphere of argon. Once cool, the vial was charged with 4-(*tert*-butyl)cyclohex-1-en-1-yl diphenyl phosphate **262a** (20 mg, 0.05 mmol, 1.0 eq.), PEPSSI *S*'Pr, and solvent (0.1 mL). The reaction was set to -40 °C, *n*-butylmagnesium chloride (0.075 mmol, 1.5 eq.) was added rapidly, and the reaction mixture was stirred for 16 h. After this time, MeOH (4 mL) was added to the mixture to quench the unreacted Grignard reagent and the organic phase was filtered, dried over Na_2SO_4 , and the solvent was evaporated *in vacuo*. To the crude mixture, internal standard, 1,2-dibromomethane (3.5 μL , 0.05 mmol, 1.0 eq.), was added and the reaction was analysed by ^1H NMR spectroscopy.

Entry 1 in Table 9.13

Following General Procedure O for the optimisation of the cross coupling of enol phosphate **115a** with *n*-butylmagnesium chloride, data is presented in the following format: (a) amount of catalyst, (b) solvent, (c) amount of *n*-butylmagnesium chloride, (d) temperature, (e) amount of unreacted **115a**, (f) conversion to product **122a**, and (g) conversion to homocoupled **141a**.

(a) PEPSSI *S*'Pr (2.55 mg, 3.75×10^{-2} mmol, 7.5 mol%), (b) toluene (1 mL), (c) commercial Grignard solution (38 μ L, $c = 2.0$ mmol/mL in Et₂O, 0.075 mmol, 1.5 eq.), (d) -40 °C, (e) 95%, (f) <5% and (g) N/A.

Entry 2 in Table 9.13

Following General Procedure O for the optimisation of the cross coupling of enol phosphate **115a** with *n*-butylmagnesium chloride, data is presented in the following format: (a) amount of catalyst, (b) solvent, (c) amount of *n*-butylmagnesium chloride, (d) temperature, (e) amount of unreacted **115a**, (f) conversion to product **122a**, and (g) conversion to homocoupled **141a**.

(a) PEPSSI *S*'Pr (0.34 mg, 5×10^{-4} mmol, 1.0 mol%), (b) toluene (1 mL), (c) commercial Grignard solution (38 μ L, $c = 2.0$ mmol/mL in Et₂O, 0.075 mmol, 1.5 eq.), (d) 0 °C, (e) 68%, (f) 25% and (g) 6%.

Entry 3 in Table 9.13

Following General Procedure O for the optimisation of the cross coupling of enol phosphate **115a** with *n*-butylmagnesium chloride, data is presented in the following format: (a) amount of catalyst, (b) solvent, (c) amount of *n*-butylmagnesium chloride, (d) temperature, (e) amount of unreacted **115a**, (f) conversion to product **122a**, and (g) conversion to homocoupled **141a**.

(a) PEPSSI *S*'Pr (0.34 mg, 5×10^{-4} mmol, 1.0 mol%), (b) toluene (1 mL), (c) commercial Grignard solution (38 μ L, $c = 2.0$ mmol/mL in Et₂O, 0.075 mmol, 1.5 eq.), (d) rt, (e) 51%, (f) 38% and (g) 11%.

Entry 4 in Table 9.13

Following General Procedure O for the optimisation of the cross coupling of enol phosphate **115a** with *n*-butylmagnesium chloride, data is presented in the following format: (a) amount of catalyst, (b) solvent, (c) amount of *n*-butylmagnesium chloride, (d) temperature, (e) amount of unreacted **115a**, (f) conversion to product **122a**, and (g) conversion to homocoupled **141a**.

(a) PEPSSI *S*'Pr (0.68 mg, 1×10^{-3} mmol, 2.0 mol%), (b) toluene (1 mL), (c) commercial Grignard solution (38 μ L, $c = 2.0$ mmol/mL in Et₂O, 0.075 mmol, 1.5 eq.), (d) 0 °C, (e) 44%, (f) 44% and (g) 8%.

Entry 5 in Table 9.13

Following General Procedure O for the optimisation of the cross coupling of enol phosphate **115a** with *n*-butylmagnesium chloride, data is presented in the following format: (a) amount of catalyst, (b) solvent, (c) amount of *n*-butylmagnesium chloride, (d) temperature, (e) amount of unreacted **115a**, (f) conversion to product **122a**, and (g) conversion to homocoupled **141a**.

(a) PEPSSI *S*ⁱPr (0.68 mg, $1 \cdot 10^{-3}$ mmol, 2.0 mol%), (b) toluene (1 mL), (c) commercial Grignard solution (38 μ L, $c = 2.0$ mmol/mL in Et₂O, 0.075 mmol, 1.5 eq.), (d) 0 °C, (e) 74%, (f) 21% and (g) 4%.

Entry 6 in Table 9.13 (*note: glassware was washed with aqua regia prior to use*)

Following General Procedure O for the optimisation of the cross coupling of enol phosphate **115a** with *n*-butylmagnesium chloride, data is presented in the following format: (a) amount of catalyst, (b) solvent, (c) amount of *n*-butylmagnesium chloride, (d) temperature, (e) amount of unreacted **115a**, (f) conversion to product **122a**, and (g) conversion to homocoupled **141a**.

(a) PEPSSI *S*ⁱPr (0.68 mg, $1 \cdot 10^{-3}$ mmol, 2.0 mol%), (b) toluene (1 mL), (c) commercial Grignard solution (38 μ L, $c = 2.0$ mmol/mL in Et₂O, 0.075 mmol, 1.5 eq.), (d) 0 °C, (e) 56%, (f) 40% and (g) 4%.

Entry 7 in Table 9.13 (*note: glassware was washed with aqua regia prior to use*)

Following General Procedure O for the optimisation of the cross coupling of enol phosphate **115a** with *n*-butylmagnesium chloride, data is presented in the following format: (a) amount of catalyst, (b) solvent, (c) amount of *n*-butylmagnesium chloride, (d) temperature, (e) amount of unreacted **115a**, (f) conversion to product **122a**, and (g) conversion to homocoupled **141a**.

(a) PEPSSI *S*ⁱPr (0.68 mg, $1 \cdot 10^{-3}$ mmol, 2.0 mol%), (b) dist. toluene (1 mL), (c) commercial Grignard solution (38 μ L, $c = 2.0$ mmol/mL in Et₂O, 0.075 mmol, 1.5 eq.), (d) 0 °C, (e) 58%, (f) 38% and (g) 4%.

Entry 8 in Table 9.13 (*note: glassware was washed with aqua regia prior to use*)

(a) PEPSSI *S*ⁱPr (0.68 mg, $1 \cdot 10^{-3}$ mmol, 2.0 mol%), (b) Et₂O (1 mL), (c) commercial Grignard solution (38 μ L, $c = 2.0$ mmol/mL in Et₂O, 0.075 mmol, 1.5 eq.), (d) 0 °C, (e) 90%, (f) 10% and (g) N/A.

Entry 9 in Table 9.13 (*note: glassware was washed with aqua regia prior to use*)

Following General Procedure O for the optimisation of the cross coupling of enol phosphate **115a** with *n*-butylmagnesium chloride, data is presented in the following format: (a) amount of catalyst, (b) solvent, (c) amount of *n*-butylmagnesium chloride, (d) temperature, (e) amount of unreacted **115a**, (f) conversion to product **122a**, and (g) conversion to homocoupled **141a**.

(a) PEPSSI *S*ⁱPr (0.68 mg, $1 \cdot 10^{-3}$ mmol, 2.0 mol%), (b) THF (1 mL), (c) commercial Grignard solution (38 μ L, $c = 2.0$ mmol/mL in Et₂O, 0.075 mmol, 1.5 eq.), (d) 0 °C, (e) N/A, (f) N/A, and (g) N/A.

Entry 10 in Table 9.13 (*note: glassware was washed with aqua regia prior to use*)

Following General Procedure O for the optimisation of the cross coupling of enol phosphate **115a** with *n*-butylmagnesium chloride, data is presented in the following format: (a) amount of catalyst, (b) solvent, (c) amount of *n*-butylmagnesium chloride, (d) temperature, (e) amount of unreacted **115a**, (f) conversion to product **122a**, and (g) conversion to homocoupled **141a**.

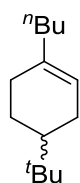
(a) PEPSSI *S*ⁱPr (0.68 mg, $1 \cdot 10^{-3}$ mmol, 2.0 mol%), (b) THF (1 mL), (c) the Grignard solution (0.15 mL, $c = 0.50$ mmol/mL in Et₂O, 0.075 mmol, 1.5 eq.) was prepared by General procedure P, (d) 0 °C, (e) 29%, (f) 71% and (g) N/A.

Entry 11 in Table 9.13 (note: glassware was washed with aqua regia prior to use)

Following General Procedure O for the optimisation of the cross coupling of enol phosphate **115a** with *n*-butylmagnesium chloride, data is presented in the following format: (a) amount of catalyst, (b) solvent, (c) amount of *n*-butylmagnesium chloride, (d) temperature, (e) amount of unreacted **115a**, (f) conversion to product **122a**, and (g) conversion to homocoupled **141a**.

(a) PEPSSI *S*ⁱPr (1.12 mg, $1.5 \cdot 10^{-3}$ mmol, 3.0 mol%), (b) THF (1 mL), (c) *n*-butylmagnesium chloride (3 (0.15 mL, $c = 0.50$ mmol/mL in Et₂O, 0.075 mmol, 1.5 eq.) was prepared by General procedure P, (d) 0 °C, (e) N/A, (f) 87%, and (g) N/A.

Characterisation of 4-(*tert*-butyl)-1-butylcyclohex-1-ene **122a**.¹⁶²



122a

Obtained as colourless oil.

¹H NMR (CDCl₃): 5.35-5.28 (m, 1H, C=CH), 1.99-1.82 (m, 6H, CH₂), 1.77-1.62 (m, 2H, CH₂), 1.34-1.02 (m, 3H, CH, CH₂), 1.16-1.02 (m, 2H, CH₂) 0.82 (t, $J = 6.8$ Hz, 3H, CH₃), 0.79 (s, 9H, C(CH₃)₃) ppm.

¹³C NMR (CDCl₃): 138.1, 120.9, 44.5, 37.5, 32.4, 30.3, 30.0, 27.5 (3C), 27.0, 24.6, 22.7, 14.2 ppm.

ν_{\max} (cm⁻¹): 2953, 2922, 2870, 1465, 1363, 912, 808.

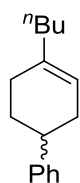
Entry 1 in Table 9.14 (note: glassware was washed with aqua regia prior to use)

Following General Procedure Q for the cross coupling of enol phosphates with alkyl Grignard reagents, data is presented in the following format: (a) substrate, (b) Grignard reagent and (c) yield of product.

(a) 4-phenylcyclohex-1-en-1-yl diphenyl phosphate **122b** (406 mg, 1.0 mmol, 1.0 eq.), (b) *n*-butylmagnesium chloride (3 mL, *c* = 0.5 mmol/mL in Et₂O, 1.5 eq. 1.5 mmol) was prepared by General procedure P and (c) 171 mg (80%).

Characterisation of 4-butyl-1,2,3,6-tetrahydro-1,1'-biphenyl **122b**:

Obtained as a colourless oil.



122b

¹H NMR (CDCl₃): 7.31-7.20 (m, 2H, ArH), 7.17-7.08 (m, 3H, ArH), 5.45-5.37 (m, 1H, C=CH), 2.73-2.63 (m, 1H, CH), 2.27-2.16 (m, 1H, CH₂), 2.14-2.01 (m, 2H, CH₂), 1.99-1.81 (m, 4H, CH₂), 1.75-1.58 (m, 1H, CH₂), 1.37-1.13 (m, 4H, CH₂), 0.84 (t, *J* = 7.1 Hz, 3H, CH₃) ppm.

¹³C NMR (CDCl₃): 147.6, 138.1, 128.5 (2C), 127.1 (2C), 126.1, 120.4, 40.5, 37.5, 33.2, 30.4, 30.2, 29.2, 22.7, 14.3 ppm.

ν_{\max} (cm⁻¹): 2954, 2920, 2852, 1730, 1454, 1257, 1070, 1008, 786, 698.

HR-MS (EI): *m/z* calculated for M = C₁₆H₂₂, theoretical [M⁺]: 214.1721. Found: 214.1724.

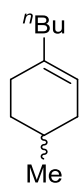
Entry 2 in Table 9.14 (note: glassware was washed with aqua regia prior to use)

Following General procedure Q for the cross coupling of enol phosphates with alkyl Grignard reagents, data is presented in the following format: (a) substrate, (b) Grignard reagent and (c) yield of product.

(a) 4-methylcyclohex-1-en-1-yl diphenyl phosphate **115b** (344 mg, 1.0 mmol, 1.0 eq.) .), (b) *n*-butylmagnesium chloride (3 mL, *c* = 0.5 mmol/mL in Et₂O, 1.5 eq. 1.5 mmol) was prepared by General procedure P and (c) 61 mg (40%).

Characterisation of 1-butyl-4-methylcyclohex-1-ene **122b**.¹⁶²

Obtained as a colourless oil.



122b

^1H NMR (CDCl_3): 5.36-5.30 (m, 1H, C=CH), 2.09-2.00 (m, 1H, CH), 1.95-1.85 (m, 3H, CH_2), 1.71-1.63 (m, 1H, CH_2), 1.62-1.54 (m, 2H, CH_2), 1.38-1.16 (m, 6H, CH_2), 0.92 (d, $J = 5.8$ Hz, 3H, CHCH_3), 0.87 (t, $J = 7.2$ Hz, 3H, CH_2CH_3) ppm.

^{13}C NMR (CDCl_3): 138.0, 120.3, 37.6, 34.2, 31.6, 30.2, 28.8, 28.6, 22.7, 22.0, 14.2 ppm.

$\nu_{\text{max}}(\text{cm}^{-1})$: 2951, 2906, 2870, 2854, 1456, 1435, 1375, 894.

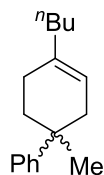
Entry 3 in Table 9.14 (note: glassware was washed with aqua regia prior to use)

Following General procedure Q for the cross coupling of enol phosphates with alkyl Grignard reagents, data is presented in the following format: (a) substrate, (b) Grignard reagent and (c) yield of product.

(a) 1-methyl-1,2,3,6-tetrahydro-[1,1'-biphenyl]-4-yl diphenyl phosphate **115c** (420 mg, 1.0 mmol, 1.0 eq.), (b) *n*-butylmagnesium chloride (3 mL, $c = 0.5$ mmol/mL in Et_2O , 1.5 eq. 1.5 mmol) was prepared by General procedure P and (c) 144 mg (63%).

Characterisation of 4-butyl-1-methyl-1,2,3,6-tetrahydro-1,1'-biphenyl **122c**:

Obtained as a colourless oil.



122c

^1H NMR (CDCl_3): 7.32-7.25 (m, 2H, ArH), 7.23-7.18 (m, 2H, ArH), 7.11-7.05 (m, 1H, ArH), 5.41-5.35 (m, 1H, C=CH), 2.40-2.36 (m, 1H, CH_2), 2.09-1.99 (m, 1H, CH_2), 1.91-1.80 (m, 4H, CH_2), 1.73-1.64 (m, 2H, CH_2), 1.29-1.08 (m, 7H, CH_3 , CH_2), 0.78 (t, $J = 7.2$ Hz, 3H, CH_2CH_3) ppm.

^{13}C NMR (CDCl_3): 149.8, 137.5, 128.1, 126.0 (2C), 125.6 (2C), 119.7, 37.9, 37.3, 36.4, 35.5, 30.0, 28.7, 26.4, 22.5, 14.2 ppm.

$\nu_{\text{max}}(\text{cm}^{-1})$: 2953, 2922, 2858, 1494, 1444, 1079, 761, 696.

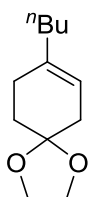
HR-MS (APCI): m/z calculated for $\text{M} = \text{C}_{17}\text{H}_{24}$ [M^+]: 229.1951. Found: 229.1954.

Entry 4 in Table 9.14 (note: glassware was washed with aqua regia prior to use)

Following General procedure Q for the cross coupling of enol phosphates with alkyl Grignard reagents, data is presented in the following format: (a) substrate, (b) Grignard reagent and (c) yield of product.

(a) diphenyl (1,4-dioxaspiro[4.5]dec-7-en-8-yl) phosphate **115d** (388 mg, 1.0 mmol, 1.0 eq.) ., (b) *n*-butylmagnesium chloride (3 mL, $c = 0.5$ mmol/mL in Et_2O , 1.5 eq. 1.5 mmol) was prepared by General procedure P and (c) 137 mg (70%).

Characterisation of 8-butyl-1,4-dioxaspiro[4.5]dec-7-ene **122d**:



122d

Obtained as a colourless oil.

^1H NMR (CDCl_3): 5.30-5.26 (m, 1H, $\text{C}=\text{CH}$), 3.96 (t, $J = 2.8$ Hz, 4H), 2.29-2.20 (m, 2H, CH_2), 2.19-2.09 (m, 2H, CH_2), 2.00-1.92 (m, 2H, CH_2), 1.78-1.70 (m, 2H, CH_2), 1.43-1.22 (m, 4H, CH_2), 0.86 (t, $J = 7.2$ Hz, 3H, CH_3) ppm.

^{13}C NMR (CDCl_3): 138.0, 117.8, 108.5, 64.6 (2C), 37.0, 35.8, 31.5, 30.2, 27.8, 22.7, 14.2 ppm.

$\nu_{\text{max}}(\text{cm}^{-1})$: 2953, 2924, 2870, 1431, 1375, 1251, 1116, 1056, 1039, 1012, 945, 856.

HR-MS (APCI): m/z calculated for $\text{M} = \text{C}_{17}\text{H}_{24}$, theoretical [M^+]: 229.1951. Found: 229.1954.

Entry 1 in Table 9.15 (note: glassware was washed with aqua regia prior to use)

Following General procedure Q for the cross coupling of enol phosphates with alkyl Grignard reagents, data is presented in the following format: (a) substrate, (b) Grignard reagent, and (c) yield of product **122a**.

(a) 4-(*tert*-butyl)cyclohex-1-en-1-yl diphenyl phosphate **115a** (95:5 e.r.), 386 mg, 1.0 mmol, 1.0 eq., (b) *n*-butylmagnesium chloride (3 mL, c = 0.5 mmol/mL in Et₂O, 1.5 eq. 1.5 mmol) was prepared by General procedure P, (c) 171 mg (88%) and (d) 95:5.

Entry 2 in Table 9.15 (*note: glassware was washed with aqua regia prior to use*)

Following General procedure Q for the cross coupling of enol phosphates with alkyl Grignard reagents, data is presented in the following format: (a) substrate, (b) Grignard reagent, (c) yield of product **122b** and (d) e.r. (determined as enol phosphate).

(a) 4-phenylcyclohex-1-en-1-yl diphenyl phosphate **115b** (406 mg, 1.0 mmol, 1.0 eq.), (b) *n*-butylmagnesium chloride (3 mL, c = 0.5 mmol/mL in Et₂O, 1.5 eq. 1.5 mmol) was prepared by General procedure P, (c) 162 mg (76%) and (d) 99:1.

Entry 3 in Table 9.15 (*note: glassware was washed with aqua regia prior to use*)

Following General procedure Q for the cross coupling of enol phosphates with alkyl Grignard reagents, data is presented in the following format: (a) substrate, (b) Grignard reagent, (c) yield of product and (c) e.r. (determined as enol phosphate).

(a) 4-methylcyclohex-1-en-1-yl diphenyl phosphate **115c** (344 mg, 1.0 mmol, 1.0 eq.), (b) *n*-butylmagnesium chloride (3 mL, c = 0.5 mmol/mL in Et₂O, 1.5 eq. 1.5 mmol) was prepared by General procedure P, (c) 66 mg (43%) and (d) 84:16.

Entry 4 in Table 9.14 (*note: glassware was washed with aqua regia prior to use*)

Following General procedure Q for the cross coupling of enol phosphates with alkyl Grignard reagents, data is presented in the following format: (a) substrate, (b) Grignard reagent, (c) yield of product and (c) e.r. (determined as enol phosphate).

(a) 1-methyl-1,2,3,6-tetrahydro-[1,1'-biphenyl]-4-yl diphenyl phosphate **115d** (420 mg, 1.0 mmol, 1.0 eq.), (b) *n*-butylmagnesium chloride (3 mL, c = 0.5 mmol/mL in Et₂O, 1.5 eq. 1.5 mmol) was prepared by General procedure P, (c) 142 mg (62%) and (d) 86:14.

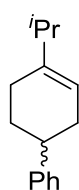
Entry 1 in Table 9.16 (*note: glassware was washed with aqua regia prior to use*)

Following General procedure Q for the cross coupling of enol phosphates with alkyl Grignard reagents, data is presented in the following format: (a) substrate, (b) Grignard reagent and (c) yield of product **121b**.

(a) 4-phenylcyclohex-1-en-1-yl diphenyl phosphate **115b** (406 mg, 1.0 mmol, 1.0 eq.), (b) *iso*-propylmagnesium chloride (3.0 mL, c = 0.5 mmol/mL, 1.5 eq. 1.5 mmol) was prepared by General procedure P and (c) 158 mg (79%).

Characterisation of 4-*iso*-propyl-1,2,3,6-tetrahydro-1,1'-biphenyl **121b**:

Obtained as a colourless oil.



121b

^1H NMR (CDCl_3): 7.26-7.19 (m, 2H, ArH), 7.17-7.09 (m, 3H, ArH), 5.45-5.39 (m, 1H, C=CH), 2.73-2.58 (m, 1H, CH), 2.30-1.96 (m, 5H, CH, CH_2), 1.93-1.86 (m, 1H, CH), 1.74-1.60 (m, 1H, CH_2), 0.95 (d, $J = 6.8$ Hz, 6H, CH_3) ppm.

^{13}C NMR (CDCl_3): 147.7, 143.7, 128.6 (2C), 127.1 (2C), 126.1, 118.3, 40.7, 35.2, 33.9, 30.4, 26.8, 21.9, 21.5 ppm.

ν_{max} (cm^{-1}): 2956, 2916, 2887, 1429, 1452, 815, 756, 696.

HR-MS (EI): m/z calculated for $\text{M} = \text{C}_{15}\text{H}_{20}$, theoretical $[\text{M}^+]$:200.1565. Found: 200.1565.

Entry 2 in Table 9.16 (note: glassware was washed with aqua regia prior to use)

Following General procedure Q for the cross coupling of enol phosphates with alkyl Grignard reagents, data is presented in the following format: (a) substrate, (b) Grignard reagent and (c) yield of product.

(a) 4-phenylcyclohex-1-en-1-yl diphenyl phosphate **115b** (406 mg, 1.0 mmol, 1.0 eq.), (b) *iso*-propylmagnesium bromide (3.0 mL, c = 0.5 mmol/mL, 1.5 eq. 1.5 mmol) was prepared by General procedure P and (c) 160 mg (80%).

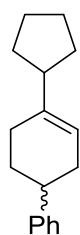
Entry 3 in Table 9.16 (note: glassware was washed with aqua regia prior to use)

Following General procedure Q for the cross coupling of enol phosphates with alkyl Grignard reagents, data is presented in the following format: (a) substrate, (b) Grignard reagent and (c) yield of product.

(a) 4-phenylcyclohex-1-en-1-yl diphenyl phosphate **115b** (406 mg, 1.0 mmol, 1.0 eq.), (b) cyclopentylmagnesium bromide (3.0 mL, c = 0.5 mmol/mL, 1.5 eq. 1.5 mmol) was prepared by General procedure P and (c) 190 mg (84%).

Characterisation of 4-cyclopentyl-1,2,3,6-tetrahydro-1,1'-biphenyl **118b**:

Obtained as a colourless oil.



118b

^1H NMR (CDCl_3): 7.25-7.19 (m, 2H, ArH), 7.17-7.08 (m, 3H, ArH), 5.47-5.42 (m, 1H, C=CH), 2.73-2.60 (m, 1H, CH), 2.35-2.15 (m, 2H, CH_2), 2.14-1.97 (m, 3H, CH, CH_2), 1.93-1.85 (m, 1H, CH), 1.80-1.39 (m, 7H, CH_2) 1.39-1.25 (m, 2H, CH_2) ppm.

^{13}C NMR (CDCl_3): 147.7, 141.0, 128.5 (2C), 127.1 (2C), 126.1, 118.7, 47.4, 40.7, 33.9, 31.4, 31.0, 30.5, 27.9, 25.43, 25.40 ppm.

$\nu_{\text{max}}(\text{cm}^{-1})$: 2945, 2910, 2864, 1490, 1450, 754, 693.

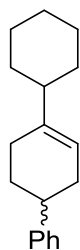
Entry 4 in Table 9.16 (note: glassware was washed with aqua regia prior to use)

Following General procedure Q for the cross coupling of enol phosphates with alkyl Grignard reagents, data is presented in the following format: (a) substrate, (b) Grignard reagent and (c) yield of product.

(a) 4-phenylcyclohex-1-en-1-yl diphenyl phosphate **115b** (406 mg, 1.0 mmol, 1.0 eq.), (b) cyclohexylmagnesium bromide (3.0 mL, c = 0.5 mmol/mL, 1.5 eq. 1.5 mmol) was prepared by General procedure P and (c) 216 mg (90%).

Characterisation of 4-cyclohexyl-1,2,3,6-tetrahydro-1,1'-biphenyl **119b**:

Obtained as a colourless oil.



119b

^1H NMR (CDCl_3): 7.24-7.19 (m, 2H, ArH), 7.17-7.13 (m, 2H, ArH), 7.12-7.07 (m, 1H, ArH), 5.42-5.36 (m, 1H, C=CH), 2.74-2.59 (m, 1H, CH), 2.28-2.16 (m, 1H, CH), 2.13-1.94 (m, 3H, CH_2), 1.93-1.83 (m, 1H, CH_2), 1.79-1.55 (m, 7H, CH_2), 1.29-1.00 (m, 5H, CH_2) ppm.

^{13}C NMR (CDCl_3): 147.7, 143.2, 128.5 (2C), 127.1 (2C), 126.1, 118.7, 45.8, 40.7, 33.9, 32.4, 32.1, 30.5, 27.6, 27.1 (2C), 26.7 ppm.

ν_{max} (cm^{-1}): 2945, 2910, 2864, 1490, 1450, 754, 693.

HR-MS (EI): m/z calculated for $\text{M} = \text{C}_{18}\text{H}_{24}$, theoretical $[\text{M}^+]$: 240.1878. Found: 240.1875.

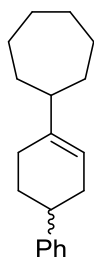
Entry 5 in Table 9.16 (note: glassware was washed with aqua regia prior to use)

Following General procedure Q for the cross coupling of enol phosphates with alkyl Grignard reagents, data is presented in the following format: (a) substrate, (b) Grignard reagent and (c) yield of product.

(a) 4-phenylcyclohex-1-en-1-yl diphenyl phosphate **115b** (406 mg, 1.0 mmol, 1.0 eq.), (b) cycloheptylmagnesium bromide (3.0 mL, $c = 0.5$ mmol/mL, 1.5 eq. 1.5 mmol) and (c) 198 mg (78%).

Characterisation of 4-cycloheptyl-1,2,3,6-tetrahydro-1,1'-biphenyl **120b**:

Obtained as a colourless oil.



120b

^1H NMR (CDCl_3): 7.25-7.18 (m, 2H, ArH), 7.17-7.07 (m, 3H, ArH), 5.43-5.35 (m, 1H, C=CH), 2.72-2.62 (m, 1H, CH), 2.25-2.15 (m, 1H, CH), 2.13-1.81 (m, 5H, CH_2), 1.93-1.83 (m, 1H, CH_2), 1.69-1.29 (m, 12H, CH_2) ppm.

^{13}C NMR (CDCl_3): 147.7, 144.6, 128.5 (2C), 127.1 (2C), 126.1, 118.2, 48.0, 40.6, 34.4, 34.0, 33.8, 30.5, 28.4 (2C), 27.49, 27.45, 27.0 ppm.

$\nu_{\text{max}}(\text{cm}^{-1})$: 2916, 2848, 1490, 1450, 968, 754, 732, 696.

HR-MS (EI): m/z calculated for $\text{M} = \text{C}_{19}\text{H}_{26}$, theoretical $[\text{M}^+]$: 254.2034. Found: 254.2033.

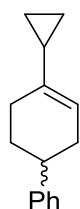
Entry 6 in Table 9.16 (note: glassware was washed with aqua regia prior to use)

Following General procedure Q for the cross coupling of enol phosphates with alkyl Grignard reagents, data is presented in the following format: (a) substrate, (b) Grignard reagent and (c) yield of product.

(a) 4-phenylcyclohex-1-en-1-yl diphenyl phosphate **115b** (406 mg, 1.0 mmol, 1.0 eq.), (b) cyclopropylmagnesium bromide (3.0 mL, $c = 0.5$ mmol/mL, 1.5 eq. 1.5 mmol) was prepared by General procedure P, and (c) 85 mg (43%).

Characterisation of 4-cyclopropyl-1,2,3,6-tetrahydro-1,1'-biphenyl **151b**:

Obtained as a colourless oil.



151b

^1H NMR (CDCl_3): 7.25-7.18 (m, 2H, ArH), 7.16-7.08 (m, 3H, ArH), 5.48-5.43 (m, 1H, C=CH), 2.75-2.63 (m, 1H, CH), 2.28-2.15 (m, 1H, CH), 2.14-1.95 (m, 2H, CH_2), 1.94-1.84 (m, 2H, CH_2), 1.75-1.61 (m, 1H, CH_2), 1.34-1.21 (m, 1H, CH_2), 0.56-0.32 (m, 4H, CH_2) ppm.

^{13}C NMR (CDCl_3): 147.5, 138.4, 128.5 (2C), 127.1 (2C), 126.2, 119.4, 40.6, 33.7, 30.2, 27.3, 17.3, 4.9, 4.1 ppm.

$\nu_{\text{max}}(\text{cm}^{-1})$: 2910, 2887, 2833, 1490, 1452, 1016, 754, 696.

HR-MS (EI): m/z calculated for $\text{M} = \text{C}_{15}\text{H}_{18}$, theoretical $[\text{M}^+]$: 198.1409. Found: 198.1409.

Ozonolysis/Reductive Amination Sequence

Attempted synthesis of 1-benzylazepane **154**¹²⁰

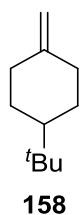
Scheme 9.34

A 25 mL three-neck round-bottom flask was equipped with a stirrer bar, fitted with suba seals, and flame dried under an atmosphere of argon. Thereafter, cyclohexene **153** (0.10 mL, 1 mmol, 1.0 eq.), methanol (0.3 mL), and distilled DCM (10 mL) were added. The reaction was cooled to -78 °C and ozone was bubbled through for 30 min. The ozone was then purged with argon. Sodium triacetoxyborohydride (211 mg, 1 mmol, 1.0 eq.) was added and the cooling bath was removed. The reaction was stirred at rt for 45 min, after which, benzylamine (0.11 mL, 1.0 mmol, 1.0 eq.) and further quantity of sodium triacetoxyborohydride (422 mg, 2 mmol, 2.0 eq.) were added. The reaction was stirred for a further 2 h before being filtered through celite. The celite pad was washed with DCM (2 × 20 mL) and the organic phase was washed with saturated sodium bicarbonate solution (20 mL) and brine (20 mL). The organic phase was dried over sodium sulfate, filtered, and the solvent was removed *in vacuo* (mass of the crude material, 340 mg). Upon analysis of the ¹H NMR spectrum, none of the desired product was observed.

Scheme 9.35

Two 100 mL round-bottom flasks were equipped with a stirrer bar and flame dried under an atmosphere of argon. In the first flask, triphenylmethylphosphonium bromide (4.00 g, 11.25 mmol, 5.0 eq.) was added and dissolved in diethyl ether (10 mL). The resulting solution was cooled to 0 °C, n-butyllithium (4.72 mL, c = 2.5 M in hexane, 11.8 mmol, 5.25 eq.) was added dropwise, and the solution was stirred for 1 h. In the second flask, 4-*tert*-butylcyclohexanone (347 mg, 2.25 mmol, 1.0 eq.) was dissolved in diethyl ether (60 mL). To the solution of the ketone, 1/5 of the Wittig solution (3 mL, 2.25 mmol, 2.25 eq.) was added and the resulting reaction mixture was stirred for 15 min at room temperature. Water (0.04 mL, 2.25 mmol, 1.0 eq.) was added to quench the unreacted Wittig reagent and the cycle was repeated 5 times to add the Wittig reagent. Once all of the Wittig reagent had been added, the reaction was quenched with water (10 mL) and the aqueous phase was extracted with diethyl ether (3 × 40 mL). The organic phase was dried over sodium sulfate, filtered, and the solvent was removed *in vacuo*. The product was purified *via* flash column chromatography using petrol ether as the eluent (232 mg, 68% yield)

Characterisation of 1-(*tert*-butyl)-4-methylenecyclohexane **158**¹²¹



Obtained as a colourless oil.

^1H NMR (CDCl_3): 4.57 (t, $J = 1.7$ Hz, 2H, $\text{CH}_2=\text{C}$), 2.37-2.26 (m, 2H, CH_2), 2.03-1.91 (m, 2H, CH_2), 1.89-1.79 (m, 2H, CH_2), 1.17-0.94 (m, 3H, CH_2+CH), 0.83 ppm (s, 9H, $\text{C}(\text{CH}_3)_3$).

^{13}C NMR (CDCl_3): 150.3, 106.2, 48.1, 35.5, 32.6 (2C), 29.2 (2C), 27.9 (3C) ppm.

ν_{max} (cm^{-1}): 2943, 2920, 2866, 2835, 1606, 1510, 1363, 1242, 1228, 1178, 1037, 981, 968, 798.

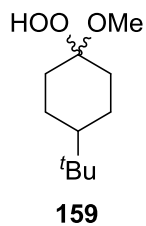
Scheme 9.36

A 25 mL three-neck round-bottom flask was equipped with a stirrer bar, fitted with suba seals, and flame dried under an atmosphere of argon. Thereafter, 1-(*tert*-butyl)-4-methylenecyclohexane **158** (76 mg, 0.5 mmol, 1.0 eq.), methanol (0.15 mL), and distilled DCM (5 mL) were added. The reaction was cooled to -78 °C and ozone was bubbled through for 30 min. The ozone was purged with argon. The reaction was partitioned between DCM (10 mL) and saturated sodium bicarbonate (10 mL). The aqueous phase was extracted with DCM (3×10 mL). The organic phase was then dried over sodium sulfate, filtered, and the solvent was removed *in vacuo*. Upon analysis of the ^1H NMR spectrum, none of the desired product was detected.

Scheme 9.37

A 25 mL three-neck round-bottom flask was equipped with a stirrer bar, fitted with suba seals, and flame-dried under an atmosphere of argon. Thereafter, 1-(*tert*-butyl)-4-methylenecyclohexane (76 mg, 0.5 mmol, 1.0 eq.), methanol (0.15 mL), and distilled DCM (5 mL) were added. The reaction was cooled to -78 °C and ozone was bubbled through until the blue colour appeared (*ca.* 30 min.). The ozone flow was then immediately stopped and the solution was purged with oxygen under high flux over 10-15 min. The reaction was partitioned between DCM (10 mL) and saturated sodium bicarbonate (10 mL). The aqueous phase was extracted with DCM (3×10 mL). The organic phase was then dried over sodium sulfate, filtered, and the solvent was removed *in vacuo*. The product was purified by flash column chromatography using 20% EtOAc in PE as the eluent (76 mg, 75% yield, 1:0.4 d.r.)

Characterisation of 4-(*tert*-butyl)-1-hydroperoxy-1-methoxycyclohexane **159**¹²⁰



Obtained as a white solid, as a mixture of diastereomers d.r. = 1.0:0.4

Melting Point: 54-56 °C (lit.:53-56°C)¹²⁰

¹H NMR (CDCl₃): 7.82-7.67 (s, 1.4H, OOH), 3.29 (s, 1.2H, CH₃), 3.26 (s, 3.0H, CH₃), 2.24-2.13 (m, 0.8H, CH), 2.13-2.03 (m, 2H, CH₂), 1.75-1.64 (m, 2.8H, CH), 1.44-1.32 (m, 2.8H, CH₂), 1.29-1.11 (m, 2.8H, CH₂), 1.10-0.99 (m, 1.4H, CH), 0.88 (s, 12.6H, C(CH₃)₃) ppm.

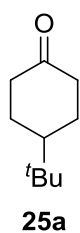
¹³C NMR (CDCl₃): 105.8, 105.6, 48.7, 48.4, 47.8, 47.7, 32.5 (2C), 31.7 (2C), 31.2 (3C), 27.8 (3C), 23.8 (2C), 23.6 (2C) ppm.

ν_{\max} (cm⁻¹): 3392, 3348, 2947, 2864, 1363, 1082, 1029, 958, 904, 817, 738.

Scheme 9.38

A microwave vial was equipped with a stirrer bar, fitted with a suba seal, and flame dried under an atmosphere of argon. Thereafter, 4-(*tert*-butyl)-1-hydroperoxy-1-methoxycyclohexane **318** (36 mg, 0.18 mmol, 1.0 eq.), sodium triacetoxyborohydride (40 mg, 0.18 mmol, 1.0 eq.), and DCM (4 mL) were added. The reaction was stirred at room temperature for 5 h. The reaction was partitioned between DCM (10 mL) and saturated sodium bicarbonate (10 mL). The aqueous phase was extracted with DCM (3 × 10 mL). The organic phase was dried over sodium sulfate, filtered, and the solvent was removed *in vacuo*. The product was purified by flash column chromatography using 20% diethyl ether in petrol ether as the eluent (18 mg, 66% yield).

Characterisation of 4-(*tert*-butyl)cyclohexan-1-one **25a**.¹²⁰



Obtained as a white solid.

Melting Point: 47-49 °C (lit.: 48-50 °C)¹²⁰

^1H NMR (CDCl_3): 2.42-2.20 (m, 4H, CH_2), 2.11-1.98 (m, 2H, CH_2), 1.53-1.34 (m, 3H, $\text{CH}+\text{CH}_2$), 0.89 ppm (s, 9H, $\text{C}(\text{CH}_3)_3$).

^{13}C NMR (CDCl_3): 212.8, 46.9 (2C), 41.5 (2C), 32.7, 27.8, 25.8 (3C) ppm.

ν_{max} (cm^{-1}): 2945, 2900, 2866, 1718, 1363, 1220, 1161, 943, 775.

Scheme 9.39

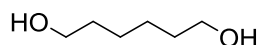
A 25 mL three neck round-bottom flask was equipped with a stirrer bar, fitted with suba seals and flame-dried. Thereafter cyclohexene **153** (0.10 mL, 1 mmol, 1.0 eq.), methanol (0.30 mL) and distilled DCM (10 mL) were added. The reaction was cooled to $-78\text{ }^\circ\text{C}$ and ozone was bubbled through until the blue colour appeared. The ozone was then purged with argon. Sodium triacetoxyborohydride (211 mg, 1 mmol, 1.0 eq.) was added and the cooling bath was removed. The reaction was stirred at rt for a further 45 min, after which benzylamine (0.11 mL, 1.0 mmol, 1.0 eq.) and sodium triacetoxyborohydride (422 mg, 2 mmol, 2.0 eq.) were added. The reaction was then stirred for 2 h and filtered through celite. The celite pad was washed with DCM (2×20 mL). The organic phase was washed with saturated sodium bicarbonate solution (20 mL) and brine (20 mL). The organic phase was dried over sodium sulfate, filtered and the solvent was removed *in vacuo*. Mass of the crude product: 138 mg, yield of the product: 0%.

Scheme 9.40

A 25 mL three-neck round-bottom flask was equipped with a stirrer bar, fitted with suba seals and flame dried. Thereafter, cyclohexene **153** (0.10 mL, 1 mmol, 1.0 eq.), methanol (0.30 mL) and distilled DCM (10 mL) were added. The reaction was cooled to $-78\text{ }^\circ\text{C}$ and ozone was bubbled through until the blue colour appeared. The ozone was then purged with argon or oxygen over a period of 10-15 min and dimethyl sulphide (1.47 mL, 20 mmol, 20 eq.) was added, the reaction was allowed to warm room temperature and stirred for 4 h. The solvent was then removed *in vacuo*. The crude product was dissolved in methanol (10 mL) and cooled to $0\text{ }^\circ\text{C}$. Sodium borohydride (190 mg, 5 mmol, 5.0 eq) was added to the solution and the reaction allowed to warm to room temperature and stirred for a further 4 h. The reaction mixture was filtered through celite and concentrated *in vacuo*. The crude product was purified by flash column chromatography using 10% methanol in DCM. Yield of the product: 18 mg (15%).

Characterisation of hexane-1,6-diol **160**.¹⁶³

Obtained as a colourless oil.



160

^1H NMR (CDCl_3): 3.68-3.59 (m, 4H, CH_2) and 1.74-1.32 (m, 8H, CH_2) ppm.

^{13}C NMR (CDCl_3): 62.7 (2C), 32.7 (2C), 25.8 (2C) ppm.

$\nu_{\text{max}}(\text{cm}^{-1})$: 2927, 2865, 2068, 1480, 1466, 1375, 1251, 1082, 1020, 1006.

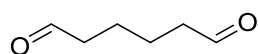
Scheme 9.41

Following general procedure R for the ozonolysis of cyclic alkenes, data is presented in the following format (a) substrate, (b) amount of solvent, (c) amount of dimethyl sulfide and (d) yield of product.

(a) cyclohexene **312** (0.10 mL, 1 mmol, 1.0 eq.), (b) DCM (8 mL) and MeOH (2 mL), (c) dimethyl sulphide (1.47 mL, 20 mmol, 20 eq.) and (d) 58 mg (51%).

Characterisation of adipaldehyde **161**.¹⁶⁴

Obtained as a colourless liquid.



161

^1H NMR (CDCl_3): 9.75 (t, $J = 1.5$ Hz, 2H, CHO), 2.50-2.41 (m, 4H, CH_2CHO) and 1.68-1.59 (m, 4H, CH_2) ppm.

^{13}C NMR (CDCl_3): 202.1 (2C), 47.8 (2C), 21.7 (2C) ppm.

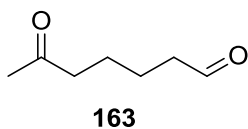
$\nu_{\text{max}}(\text{cm}^{-1})$: 2937, 2868, 1712, 1409, 1390, 1166, 1093, 995.

Entry 1 in Table 9.17

Following general procedure R for the ozonolysis of cyclic alkenes, data is presented in the following format (a) substrate, (b) amount of solvent, (c) amount of dimethyl sulfide and (d) yield of product **163**.

(a) 1-methyl-cyclohexene **162** (0.12 mL, 1 mmol, 1.0 eq.), (b) DCM (8 mL) and MeOH (2 mL), (c) dimethyl sulfide (1.47 mL, 20 mmol, 20 eq.) and (d) 96 mg (75%).

Characterisation of 6-oxoheptanal **163**.¹⁶⁵



^1H NMR (CDCl_3): 9.74 (t, $J = 1.4$ Hz, 1H, CHO), 2.47-2.40 (m, 4H, CH_2), 2.12 (s, 3H, CH_3) and 1.65-1.55 (m, 4H, CH_2) ppm.

^{13}C NMR (CDCl_3): 208.3, 202.1, 43.6, 43.2, 29.9, 23.1, 21.5 ppm.

ν_{max} (cm^{-1}): 2937, 1708, 1409, 1359, 1159.

Entry 2 in Table 9.17

Following general procedure R for the ozonolysis of cyclic alkenes, data is presented in the following format (a) substrate, (b) amount of solvent, (c) amount of dimethyl sulfide and (d) yield of product **163**.

(a) 1-methyl-cyclohexene **162** (0.36 mL, 3 mmol, 1.0 eq.), (b) DCM (24 mL) + MeOH (6 mL), (c) dimethyl sulfide (1.47 mL, 20 mmol, 20 eq.) and (d) 320 mg (83%).

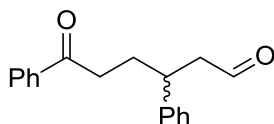
Scheme 9.43

Following general procedure R for the ozonolysis of cyclic alkenes, data is presented in the following format (a) substrate, (b) amount of solvent, (c) amount of dimethyl sulfide and (d) yield of product **164b**.

(a) 1',2',3',6'-tetrahydro-1,1':4',1''-terphenyl **140b** (58 mg, 0.25 mmol, 1.0 eq.), (b) DCM (8 mL) and MeOH (2 mL), (c) dimethyl sulfide (0.37 mL, 5 mmol, 20 eq.) and (d) 56 mg (84%).

Characterisation of 6-oxo-3,6-diphenylhexanal **164b**:

Obtained as a colourless oil.



^1H NMR (CDCl_3): 9.60 (t, $J = 1.8$ Hz, 1H, CHO), 7.79-7.71 (m, 2H), 7.50-7.41 (m, 1H), 7.40-7.37 (m, 2H), 7.37-7.30 (m, 2H), 7.27-7.21 (m, 3H), 3.29-3.19 (m, 1H, PhCH), 2.92-2.59 (m, 4H, CH_2), 2.18-2.06 (m, 1H, CH_2), and 2.01-1.87 (m, 1H, CH_2) ppm.

^{13}C NMR (CDCl_3): 201.6, 199.8, 143.0, 137.0, 133.2 (2C), 129.1 (2C), 128.8 (2C), 128.2 (2C), 127.8, 127.2, 50.9, 39.6, 36.4, 30.7 ppm.

ν_{max} (cm^{-1}): 2949, 2927, 2883, 2846, 2742, 1707, 1676, 1446, 1396, 1255, 1211, 914, 758.

HR-MS: m/z calculated for $\text{C}_{18}\text{H}_{19}\text{O}_2$, theoretical $[\text{M}+\text{H}]^+$: 267.1381. Found: 267.1380.

Scheme 9.44

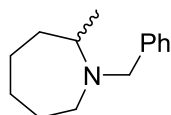
6-oxoheptanal **163** (20 mg, 0.16 mmol, 1.0 eq.) was dissolved in DCM (4 mL). Benzylamine (0.02 mL, 0.16 mmol, 1.0 eq.) and sodium triacetoxyborohydride (68 mg, 0.32 mmol, 2.0 eq.) was added. The reaction was stirred at rt for 2 h and filtered through celite. The celite pad was washed with DCM (2 \times 20 mL). The organic phase was washed with saturated sodium bicarbonate solution (20 mL) and brine (20 mL). The organic phase was dried over sodium sulfate, filtered and the solvent was removed *in vacuo*. Mass of the crude product: 60 mg, yield of product: 0%.

Entry 1 in Table 9.18

Following general procedure S for the reductive amination of aldehyde-ketone **163**, data is presented in the following format: (a) solvent, (b) amount of benzylamine, (c) amount sodium triacetoxyborohydride, (d) amount of additive(s) and (e) conversion towards product **165**.

(a) DCE (4 mL), (b) Benzylamine (0.02 mL, 0.18 mmol, 1.05 eq.), (c) sodium triacetoxyborohydride (48 mg, 0.22 mmol, 1.4 eq.), (d) - and (e) 22%.

Characterisation of 1-benzyl-2-methylazepane **165**:



165

^1H NMR (CDCl_3): 7.34-7.27 (m, 2H), 7.26-7.20 (m, 2H), 7.20-7.19 (m, 1H), 3.64 (s, 2H, CH_2Ph), 2.96-2.79 (m, 1H, CH), 2.75-2.64 (m, 1H, CH), 2.55-2.40 (m, 1H, CH), 1.83-1.67 (m, 1H, CH), 1.63-1.1.32 (m, 7H, CH+ CH_2) and 1.01 (d, $J = 6.5$ Hz, 3H) ppm.

^{13}C NMR (CDCl_3): 129.0, 128.9 (2C), 128.3 (2C), 126.8, 57.5, 57.0, 49.3, 36.1, 29.1, 28.5, 25.5, 19.3 ppm.

$\nu_{\text{max}}(\text{cm}^{-1})$: 2920, 2846, 1492, 1450, 1365, 1354, 1157, 956, 740, 715.

HR-MS (ESI): m/z calculated for $\text{M} = \text{C}_{14}\text{H}_{21}\text{N}$, theoretical $[\text{M}+\text{H}]^+$: 204.1756. Found: 204.1752.

Entry 2 in Table 9.18

Following general procedure S for the reductive amination of aldehyde-ketone **163**, data is presented in the following format: (a) solvent, (b) amount of benzylamine, (c) amount sodium triacetoxyborohydride, (d) amount of additive(s) and (e) conversion towards product **165**.

(a) DCE (4 mL), (b) Benzylamine (0.02 mL, 0.18 mmol, 1.05 eq.), (c) sodium triacetoxyborohydride (48 mg, 0.22 mmol, 1.4 eq.), (d) acetic acid (9 μL , 0.16 mmol, 1.0 eq.) and sodium acetate (13 mg, 0.16 mmol, 1.0 eq.) and (e) 18%.

Entry 3 in Table 9.18

Following general procedure S for the reductive amination of aldehyde-ketone **163**, data is presented in the following format: (a) solvent, (b) amount of benzylamine, (c) amount sodium triacetoxyborohydride, (d) amount of additive(s) and (e) conversion towards product **165**.

(a) DCE (4 mL), (b) Benzylamine (0.02 mL, 0.18 mmol, 1.05 eq.), (c) sodium triacetoxyborohydride (48 mg, 0.22 mmol, 1.4 eq.), (d) acetic acid (9 μL , 0.16 mmol, 1.0 eq.) and (e) -.

Entry 4 in Table 9.18

Following general procedure S for the reductive amination of aldehyde-ketone **163**, data is presented in the following format: (a) solvent, (b) amount of benzylamine, (c) amount sodium triacetoxyborohydride, (d) amount of additive(s) and (e) conversion towards product **165**.

(a) DCE (4 mL), (b) Benzylamine (0.02 mL, 0.18 mmol, 1.05 eq.), (c) sodium triacetoxyborohydride (48 mg, 0.22 mmol, 1.4 eq.), (d) sodium acetate (13 mg, 0.16 mmol, 1.0 eq.) and (e) -.

Entry 5 in Table 9.18

Following general procedure S for the reductive amination of aldehyde-ketone **163**, data is presented in the following format: (a) solvent, (b) amount of benzylamine, (c) amount sodium triacetoxyborohydride, (d) amount of additive(s) and (e) conversion towards product **165**.

(a) DCE (4 mL), (b) Benzylamine (0.02 mL, 0.18 mmol, 1.05 eq.), (c) sodium triacetoxyborohydride (95 mg, 0.44 mmol, 2.8 eq.), (d) - and (e) 44%.

Entry 6 in Table 9.18

Following general procedure S for the reductive amination of aldehyde-ketone **163**, data is presented in the following format: (a) solvent, (b) amount of benzylamine, (c) amount sodium triacetoxyborohydride, (d) amount of additive(s) and (e) conversion towards product **165** .

(a) DCE (4 mL), (b) Benzylamine (0.02 mL, 0.18 mmol, 1.05 eq.), (c) sodium triacetoxyborohydride (143 mg, 0.66 mmol, 4.2 eq.), (d) - and (e) 43%.

Entry 7 in Table 9.18

Following general procedure S for the reductive amination of aldehyde-ketone **163**, data is presented in the following format: (a) solvent, (b) amount of benzylamine, (c) amount sodium triacetoxyborohydride, (d) amount of additive(s) and (e) conversion towards product **165** .

(a) DCE (4 mL), (b) Benzylamine (0.04 mL, 0.36 mmol, 2.10 eq.), (c) sodium triacetoxyborohydride (95 mg, 0.44 mmol, 2.8 eq.), (d) - and (e) 46%.

Entry 1 in Table 9.19

Following general procedure S for the reductive amination of aldehyde-ketone **163**, data is presented in the following format: (a) solvent, (b) amount of benzylamine, (c) amount sodium triacetoxyborohydride, (d) amount of additive(s) and (e) conversion towards product **165** .

(a) THF (4 mL), (b) Benzylamine (0.04 mL, 0.36 mmol, 2.10 eq.), (c) sodium triacetoxyborohydride (95 mg, 0.44 mmol, 2.8 eq.), (d) - and (e) 28%.

Entry 2 in Table 9.19

Following general procedure S for the reductive amination of aldehyde-ketone **163**, data is presented in the following format: (a) solvent, (b) amount of benzylamine, (c) amount sodium triacetoxyborohydride, (d) amount of additive(s) and (e) conversion towards product **165** .

(a) EtOAc (4 mL), (b) Benzylamine (0.04 mL, 0.36 mmol, 2.10 eq.), (c) sodium triacetoxyborohydride (95 mg, 0.44 mmol, 2.8 eq.), (d) - and (e) 10%.

Entry 3 in Table 9.19

Following general procedure S for the reductive amination of aldehyde-ketone **163**, data is presented in the following format: (a) solvent, (b) amount of benzylamine, (c) amount sodium triacetoxyborohydride, (d) amount of additive(s) and (e) conversion towards product **165**.

(a) DMC (4 mL), (b) Benzylamine (0.04 mL, 0.36 mmol, 2.10 eq.), (c) sodium triacetoxyborohydride (95 mg, 0.44 mmol, 2.8 eq.), (d) - and (e) <5%.

Entry 4 in Table 9.19

Following general procedure S for the reductive amination of aldehyde-ketone **163**, data is presented in the following format: (a) solvent, (b) amount of benzylamine, (c) amount sodium triacetoxyborohydride, (d) amount of additive(s) and (e) conversion towards product **165**.

(a) IPA (4 mL), (b) Benzylamine (0.04 mL, 0.36 mmol, 2.10 eq.), (c) sodium triacetoxyborohydride (95 mg, 0.44 mmol, 2.8 eq.), (d) - and (e) <5%.

Entry 5 in Table 9.19

Following general procedure S for the reductive amination of aldehyde-ketone **163**, data is presented in the following format: (a) solvent, (b) amount of benzylamine, (c) amount sodium triacetoxyborohydride, (d) amount of additive(s) and (e) conversion towards product **165**.

(a) CPME (4 mL), (b) Benzylamine (0.04 mL, 0.36 mmol, 2.10 eq.), (c) sodium triacetoxyborohydride (95 mg, 0.44 mmol, 2.8 eq.), (d) - and (e) 70%.

Scheme 9.47

Following general procedure T for the telescoped ozonolysis-reductive amination, data is presented in the following format: (a) amount of substrate and (b) yield of product.

(a) 1-methylcyclohex-1-ene **162** (0.03 mL, 0.25 mmol, 1.0 eq.) and yield of **165a**: 29 mg (56%).

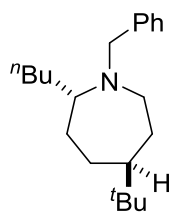
Entry 1 in Table 9.20

Following general procedure T for the telescoped ozonolysis-reductive amination, data is presented in the following format: (a) amount of substrate and (b) yield of product.

(a) 4-(*tert*-butyl)-1-butylcyclohex-1-ene **122a** (49 mg, 0.25 mmol, 1.0 eq.) and yield of **166a**: 38 mg (50%).

Characterisation of 1-benzyl-5-(*tert*-butyl)-2-butylazepane **166a**:

Obtained as a yellow oil.



166a

^1H NMR (CDCl_3): 7.30-7.25 (m, 2H, ArH), 7.24-7.18 (m, 2H, ArH), 7.16-7.10 (m, 1H, ArH), 3.63 (d, $^2J = 14.3$ Hz, 1H, CH_2Ph), 3.57 (d, $^2J = 14.3$ Hz, 1H, CH_2Ph), 2.81-2.72 (m, 1H, CH), 2.69-2.61 (m, 1H, CH_2), 2.49-2.39 (m, 1H, CH), 1.67-1.42 (m, 5H, $\text{CH}+\text{CH}_2$), 1.34-1.20 (m, 8H, CH_2), 0.82 (t, $J = 7.2$ Hz, 3H, CH_3) and 0.78 (s, 9H, $\text{C}(\text{CH}_3)_3$) ppm.

^{13}C NMR (CDCl_3): 141.6, 128.7 (2C), 128.3 (2C), 126.6, 61.5, 54.9, 50.7, 49.0, 34.1, 33.7, 30.9, 29.8, 29.7, 27.8 (3C), 25.7, 23.2, 14.5 ppm.

$\nu_{\text{max}}(\text{cm}^{-1})$: 2951, 2927, 2858, 1732, 1456, 1452, 1363, 729, 696.

HR-MS (EI): m/z calculated for $\text{M} = \text{C}_{21}\text{H}_{35}\text{N}$, theoretical $[\text{M}]^+$: 301.2769. Found: 301.2763.

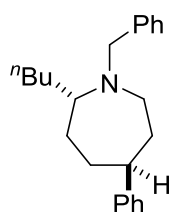
Entry 2 in Table 9.20

Following general procedure T for the telescoped ozonolysis-reductive amination of aldehyde-ketones, data is presented in the following format: (a) amount of substrate and (b) yield of product.

(a) 4-butyl-1,2,3,6-tetrahydro-1,1'-biphenyl **122b** (54 mg, 0.25 mmol, 1.0 eq.) and yield of **166b**: 43 mg (54%).

Characterisation of 1-benzyl-2-butyl-5-phenylazepane **166b**:

Obtained as a yellow oil.



166b

^1H NMR (CDCl_3): 7.34-7.29 (m, 1H, ArH), 7.26-7.03 (m, 9H, ArH), 3.74 (d, $^2J = 14.6$ Hz, 1H, CH_2Ph), 3.63 (d, $^2J = 14.6$ Hz, 1H, CH_2Ph), 2.85-2.75 (m, 2H, CH_2), 2.72-2.55 (m, 2H, PhCH, NCH), 1.93-1.62 (m, 6H, CH_2), 1.56-1.33 (m, 2H, CH_2), 1.32-1.18 (m, 4H, CH_2), and 0.84 (t, $J = 7.0$ Hz, 3H, CH_3) ppm.

^{13}C NMR (CDCl_3): 149.3, 141.4, 128.7 (2C), 128.6 (2C), 128.4 (2C), 126.79 (2C), 126.75, 125.9, 62.0, 55.1, 50.9, 45.7, 37.8, 34.3, 32.7, 30.7, 29.8, 23.2, 14.5 ppm.

ν_{max} (cm^{-1}): 2924, 2854, 1654, 1450, 752, 731, 696.

HR-MS (NSI): m/z calculated for $\text{M} = \text{C}_{23}\text{H}_{31}\text{N}$, theoretical $[\text{M}+\text{H}]^+$: 322.2529. Found: 322.2529.

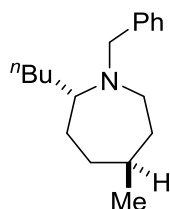
Entry 3 in Table 9.20

Following general procedure T for the telescoped ozonolysis-reductive amination, data is presented in the following format: (a) amount of substrate and (b) yield of product.

(a) 4-methyl-1-butylcyclohex-1-ene **122c** (38 mg, 0.25 mmol, 1.0 eq.) and yield of **166c**: 29 mg (45%).

Characterisation of 1-benzyl-5-methyl-2-butylazepane **166c**:

Obtained as a yellow oil.



166d

^1H NMR (CDCl_3): 7.30-7.25 (m, 2H, ArH), 7.24-7.19 (m, 2H, ArH), 7.16-7.10 (m, 1H, ArH), 3.65 (d, $^2J = 13.8$ Hz, 1H, CH_2Ph), 3.57 (d, $^2J = 13.8$ Hz, 1H, CH_2Ph), 2.74-2.22 (m, 2H, CH_2), 2.52-2.43 (m, 1H, CH), 1.66-1.41 (m, 7H, CH+ CH_2), 1.36-1.14 (m, 6H, CH_2), 0.91 (t, $J = 7.4$ Hz, 3H, CH_3) and 0.84 (d, $J = 6.1$ Hz, 3H, CHCH_3) ppm.

^{13}C NMR (CDCl_3): 141.6, 128.7 (2C), 128.3 (2C), 126.7, 62.1, 54.8, 50.2, 37.5, 34.5, 33.7, 33.4, 30.2, 29.7, 24.1, 23.2, 14.4 ppm.

ν_{max} (cm^{-1}): 2953, 2922, 1726, 1454, 1267, 1118, 1070, 736, 693.

HR-MS (EI): m/z calculated for $\text{M} = \text{C}_{18}\text{H}_{29}\text{N}$, theoretical $[\text{M}]^+$: 259.2300. Found: 259.2296.

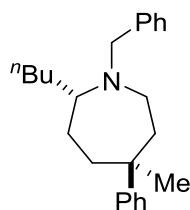
Entry 4 in Table 9.20

Following general procedure T for the telescoped ozonolysis-reductive amination of aldehyde-ketones, data is presented in the following format: (a) amount of substrate and (b) yield of product.

(a) 4-butyl-1-methyl-1,2,3,6-tetrahydro-1,1'-biphenyl **122d** (57 mg, 0.25 mmol, 1.0 eq.) and yield of **166d**: 45 mg (54%).

Characterisation of 1-benzyl-2-butyl-5-methyl-5-phenylazepane **166d**:

Obtained as a yellow oil.



166d

$^1\text{H NMR}$ (CDCl_3): 7.32-7.18 (m, 8H, ArH), 7.16-7.07 (m, 2H, ArH), 3.72 (d, $^2J = 13.8$ Hz, 1H, CH_2Ph), 3.60 (d, $^2J = 13.8$ Hz, 1H, CH_2Ph), 2.74-2.73 (m, 1H, NCH), 2.59-2.51 (m, 1H, NCH), 2.59-2.51 (m, 1H, NCH), 2.49-2.41 (m, 1H, CH), 2.12-2.02 (m, 2H, CH_2), 1.93-1.62 (m, 1H, CH), 1.61-1.39 (m, 2H, CH_2), 1.28 (t, $J = 6.2$ Hz, 3H, CH_3), 1.25 (s, 3H, CHCH_3), and 0.96-0.83 (m, 6H, CH_2) ppm.

$^{13}\text{C NMR}$ (CDCl_3): 150.2, 140.6, 129.0 (2C), 128.4 (2C), 128.3 (2C), 127.0, 126.2 (2C), 125.6, 62.7, 57.3, 46.5, 40.7, 39.0, 37.0, 33.8, 31.9, 29.2, 27.9, 23.1, 14.4 ppm.

$\nu_{\text{max}}(\text{cm}^{-1})$: 2951, 2924, 1726, 1492, 1444, 1028, 761, 731, 696.

HR-MS (EI): m/z calculated for $\text{M} = \text{C}_{24}\text{H}_{33}\text{N}$, theoretical $[\text{M}]^+$: 335.2613. Found: 335.2608.

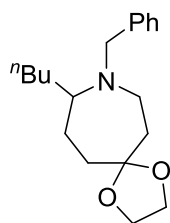
Entry 5 in Table 9.20

Following general procedure T for the telescoped ozonolysis-reductive amination, data is presented in the following format: (a) amount of substrate and (b) yield of product.

(a) 8-butyl-1,4-dioxaspiro[4.5]dec-7-ene **122h** (49 mg, 0.25 mmol, 1.0 eq.) and yield of **166h**: 39 mg (52%).

Characterisation of 8-benzyl-9-butyl-1,4-dioxaspiro[4.6]undecane **166f**:

Obtained as a yellow oil.



166f

^1H NMR (CDCl_3): 7.30-7.24 (m, 1H, ArH), 7.23-7.19 (m, 2H, ArH), 7.17-7.11 (m, 2H, ArH), 3.87- 3.79 (t, $J = 3.1$ Hz, 4H, OCH_2), 3.68 (s, 2H, CH_2Ph), 2.85-2.74 (m, 1H, NCH), 2.68-2.60 (m, 1H, NCH), 2.50-2.42 (m, 1H, NCH), 1.84-1.42 (m, 6H, CH_2), 1.33-1.15 (m, 6H, CH_2) and 0.81 (t, $J = 6.8$ Hz, 3H, CH_3) ppm.

^{13}C NMR (CDCl_3): 141.1, 128.8 (2C), 128.3 (2C), 126.8, 111.8, 64.2 (2C), 62.3, 57.6, 43.2, 37.1, 34.8, 33.7, 28.9, 26.5, 23.2, 14.4 ppm.

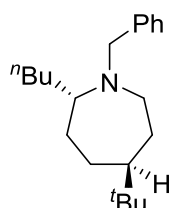
$\nu_{\text{max}}(\text{cm}^{-1})$: 2949, 2926, 2868, 1639, 1490, 1365, 1138, 1095, 1070, 1058, 1026, 945, 732, 696.

HR-MS (NSI): m/z calculated for $\text{M} = \text{C}_{19}\text{H}_{29}\text{NO}_2$, theoretical $[\text{M}+\text{H}]^+$: 304.2271. Found: 304.2270.

Entry 1 in Table 9.21

Following general procedure T for the telescoped ozonolysis-reductive amination, data is presented in the following format: (a) amount of substrate, (b) yield of product and (c) e.r.

(a) 4-(*tert*-butyl)-1-butylcyclohex-1-ene **122a** (49 mg, 0.25 mmol, 1.0 eq.), (b) yield of **166a**: 39 mg (51%) and (c) e.r. = 93:7.



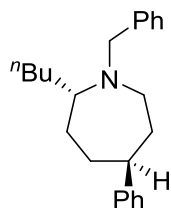
166a

Chiral analysis: HPLC OD-H column, 0.40 mL/min, detector 254 nm, 0.5% IPA in hexane. $t_1 = 23.9$ min (minor) and $t_2 = 24.6$ min (major).

Entry 2 in Table 9.21

Following general procedure T for the telescoped ozonolysis-reductive amination, data is presented in the following format: (a) amount of substrate, (b) yield of product and (c) e.r.

(a) 4-butyl-1,2,3,6-tetrahydro-1,1'-biphenyl **122b** (54 mg, 0.25 mmol, 1.0 eq.), (b) yield of **166b**: 42 mg (53%) and (c) e.r. = 99:1.



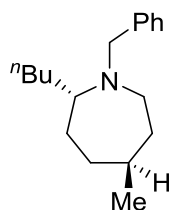
166b

Chiral analysis: HPLC OD-H column, 0.40 mL/min, detector 254 nm, 0.5% IPA in hexane. t_1 = 17.1 min (minor) and t_2 = 20.2 min (major).

Entry 3 in Table 9.21

Following general procedure T for the telescoped ozonolysis-reductive amination, data is presented in the following format: (a) amount of substrate, (b) yield of product and (c) e.r.

(a) 4-methyl-1-butylcyclohex-1-ene **122c** (38 mg, 0.25 mmol, 1.0 eq.), (b) yield of **166c**: 31 mg (48%) and (c) e.r. = 82:18.



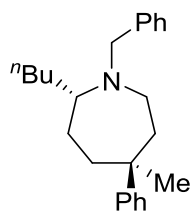
166c

Chiral analysis: HPLC OD-H column, 0.40 mL/min, detector 254 nm, 0.5% IPA in hexane. t_1 = 17.4 min (minor) and t_2 = 21.4 min (major).

Entry 4 in Table 9.21

Following general procedure T for the telescoped ozonolysis-reductive amination, data is presented in the following format: (a) amount of substrate, (b) yield of product and (c) e.r.

(a) 4-butyl-1-methyl-1,2,3,6-tetrahydro-1,1'-biphenyl **122d** (57 mg, 0.25 mmol, 1.0 eq.), (b) yield of **166d**: 45 mg (54%).and (c) e.r. = 87:13.



166d

Chiral analysis: HPLC OD-H column, 0.40 mL/min, detector 254 nm, 0.1% IPA in hexane. t_1 = 23.7 min (minor) and t_2 = 27.0 min (major).

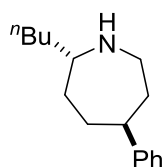
Preparation of 5-(*tert*-butyl)-2-phenylazepane

Scheme 9.50

A microwave vial was equipped with a stirrer bar, closed with a suba seal and flame dried. Then it was charged with the substrate azepane (26 mg, 0.08 mmol, 1.0 eq.), DCM (1 mL), MeOH (0.5 mL) and Pd/C (8 mg, 0.008 mmol, 10 mol%) and the atmosphere was changed to hydrogen with a balloon. The reaction was stirred at rt for 24 h. The crude mixture was filtered through celite and the filtrate was washed with Et₂O (3 × 5 mL). To this solution 5 dropletts of concentrated HCl was added and the solvent was evaporated *in vacuo*. The azepane salt was dissolved in DCM (3 mL) and 1N NaOH (3 mL) mixture and stirred for an 1 h. The organic phase was separated and the aqueous was washed with DCM (3 × 3 mL). The combined organic phase was dried over Na₂SO₄, filtered and the solvent was removed *in vacuo*. The crude product was columned by flash column chromatography 10% MeOH in DCM. Mass of the product: 15 mg (81%).

Characterisation of 5-(*tert*-butyl)-2-phenylazepane **167**:

Obtained as a yellow oil.



167

¹H NMR (CDCl₃): 7.22-7.16 (m, 2H, ArH), 7.15-7.10 (m, 2H, ArH), 7.09-7.05 (m, 1H, ArH), 4.39 (br s, 1H, NH), 3.20 (dt, ²J = 13.4 Hz, J = 3.9 Hz, 1H, NCH₂), 2.95-2.85 (m, 1H, NCH₂), 2.75-2.69 (m, 1H, NCH),

2.59 (m, 1H, PhCH), 1.97-1.82 (m, 4H, CH₂), 1.80-1.65 (m, 2H, CH₂), 1.57-1.49 (m, 2H, CH₂), 1.34-1.21 (m, 4H, CH₂) and 0.83 (t, *J* = 7.2 Hz, 3H, CH₃). ppm.

¹³C NMR (CDCl₃): 148.4, 128.5 (2C), 126.8 (2C), 126.0, 58.4, 47.6, 46.3, 39.2, 36.4, 32.1, 31.5, 28.7, 22.8, 14.2 ppm.

ν_{\max} (cm⁻¹): 2951, 2924, 2854, 1450, 754, 698.

HR-MS (NSI): *m/z* calculated for M = C₁₆H₂₅N, theoretical [M+H]⁺: 232.2060. Found: 232.2060.

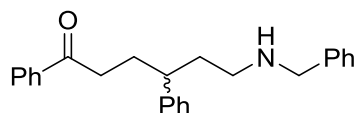
Entry 1 in Table 9.22

Following general procedure T for the telescoped ozonolysis-reductive amination, data is presented in the following format: (a) amount of substrate and (b) yield of product.

(a) 1',2',3',6'-tetrahydro-1,1':4',1''-terphenyl **140b** (59 mg, 0.25 mmol, 1.0 eq.) and (b) yield of **168b**: 46 mg (52%).

Characterisation of 6-(benzylamino)-1,4-diphenylhexan-1-one **168b**:

Obtained as a yellow solid.



168b

¹H NMR (CDCl₃): 7.77-7.69 (m, 2H, ArH), 7.48-7.40 (m, 1H, ArH), 7.34-7.29 (m, 2H, ArH), 7.25-7.11 (m, 8H, ArH), 7.09-7.05 (m, 2H, ArH), 3.66 (d, ²*J* = 13.1 Hz, 1H, CH₂Ph), 3.60 (d, ²*J* = 13.1 Hz, 1H, CH₂Ph), 2.79-2.59 (m, 3H, CH₂, PhCH), 2.55-2.42 (m, 2H, CH₂), 2.11-2.02 (m, 1H, CH₂), 1.96-1.70 (m, 3H, CH₂), and 1.35 (m, 1H, NH) ppm.

¹³C NMR (CDCl₃): 200.5, 144.5, 140.2, 137.0, 133.0 (2C), 128.8 (2C), 128.7 (2C), 128.6 (2C), 128.4 (2C), 128.2 (2C), 127.9 (2C), 127.2, 126.7, 54.0, 47.6, 43.6, 37.3, 36.7, 16.8 ppm.

ν_{\max} (cm⁻¹): 2926, 1676, 1446, 744, 731.

HR-MS (NSI): *m/z* calculated for M = C₂₅H₂₇NO, theoretical [M+H]⁺: 358.2165. Found: 358.2165.

M.p.: 74-78 °C

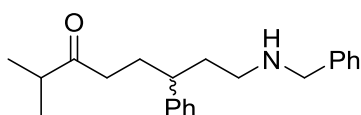
Entry 2 in Table 9.22

Following general procedure T for the telescoped ozonolysis-reductive amination, data is presented in the following format: (a) amount of substrate and (b) yield of product.

(a) 4-isopropyl-1,2,3,6-tetrahydro-1,1'-biphenyl **121b** (50 mg, 0.25 mmol, 1.0 eq.) and (b) yield of **169**: 48 mg (59%).

Characterisation of 8-(benzylamino)-2-methyl-6-phenyloctan-3-one **169**:

Obtained as a yellow oil.



169

^1H NMR (CDCl_3): 7.25-7.09 (m, 8H, ArH), 7.08-6.97 (m, 2H, ArH), 3.64 (d, $^2J = 13.4$ Hz, 1H, CH_2Ph), 3.58 (d, $^2J = 13.4$ Hz, 1H, CH_2Ph), 2.59-2.48 (m, 1H, CH), 2.47-2.23 (m, 3H, CH, CH_2), 2.27-2.06 (m, 2H, CH_2), 1.97-1.85 (m, 1H, CH), 1.82-1.64 (m, 2H, CH_2), 1.52-1.43 (m, 1H, NH), 0.92 (d, $J = 6.5$ Hz, 3H, CH_3) and 0.90 (d, $J = 6.5$ Hz, 3H, CH_3) ppm.

^{13}C NMR (CDCl_3): 214.9, 144.6, 140.5, 128.7 (2C), 128.5 (2C), 128.3 (2C), 127.8 (2C), 127.1, 126.5, 54.1, 47.7, 43.4, 41.0, 38.4, 37.5, 30.6, 18.5, 18.3 ppm.

ν_{max} (cm^{-1}): 2924, 2854, 1654, 1450, 752, 731, 671.

HR-MS (NSI): m/z calculated for $\text{M} = \text{C}_{22}\text{H}_{29}\text{NO}$, theoretical $[\text{M}+\text{H}]^+$: 324.2323. Found: 324.2323.

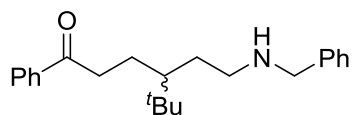
Entry 1 in Table 9.23

Following general procedure T for the telescoped ozonolysis-reductive amination, data is presented in the following format: (a) amount of substrate and (b) yield of product.

(a) 4-(*tert*-butyl)-2,3,4,5-tetrahydro-1,1'-biphenyl **140a** (54 mg, 0.25 mmol, 1.0 eq.) and (b) yield of **168a**: 46 mg (54%).

Characterisation of 4-(2-(benzylamino)ethyl)-5,5-dimethyl-1-phenylhexan-1-one **168a**:

Obtained as a yellow oil.



168a

^1H NMR (CDCl_3): 7.90-7.84 (m, 1H, ArH), 7.54-7.43 (m, 1H, ArH), 7.42-7.37 (m, 3H, ArH), 7.27-7.09 (m, 5H, ArH), 3.86 (s, 2H, NCH_2Ph), 3.11-2.96 (m, 1H, CH), 2.91-2.79 (m, 1H, CH), 2.77-2.70 (m, 2H, CH_2), 2.08 (m, 1H, CH), 1.91-1.78 (m, 2H, CH_2), 1.44-1.34 (m, 2H, CH_2), 1.04 (m, 1H, NH) and 0.80 (s, 9H, CH_3) ppm.

^{13}C NMR (CDCl_3): 200.8, 133.2, 128.8 (2C), 128.7 (2C), 128.6 (2C), 128.4, 128.3 (2C), 127.23, 127.20, 52.8, 47.7, 46.0, 37.7, 33.6, 29.2, 27.3, 27.1 (3C) ppm.

ν_{max} (cm^{-1}): 2958, 2865, 1682, 1448, 1366, 745, 701.

HR-MS (NSI): m/z calculated for $\text{M} = \text{C}_{23}\text{H}_{31}\text{NO}$, theoretical $[\text{M}+\text{H}]^+$: 338.2480. Found: 338.2478.

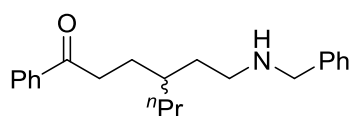
Entry 2 in Table 9.23

Following general procedure T for the telescoped ozonolysis-reductive amination, data is presented in the following format: (a) amount of substrate and (b) yield of product.

(a) 4-propyl-2,3,4,5-tetrahydro-1,1'-biphenyl **140g** (50 mg, 0.25 mmol, 1.0 eq.) and (b) yield of **168g**: 43 mg (53%).

Characterisation of 4-(2-(benzylamino)ethyl)-1-phenylheptan-1-one **168g**:

Obtained as a yellow oil.



168g

^1H NMR (CDCl_3): 7.89-7.82 (m, 2H, ArH), 7.52-7.44 (m, 1H, ArH), 7.40-7.33 (m, 2H, ArH), 7.32-7.18 (m, 5H, ArH), 3.77 (s, 2H, NCH_2Ph), 2.91-2.86 (m, 2H, CH_2), 2.67-2.60 (m, 2H, CH_2), 1.61 (q, $J = 6.7$ Hz, 2H, CH_2), 1.56-1.47 (m, 2H, CH_2), 1.46-1.38 (m, 1H, CH), 1.32-1.16 (m, 4H, CH_2), 0.90-0.80 (m, 1H, NH) and 0.81 (t, $J = 6.7$ Hz, 3H, CH_3) ppm.

^{13}C NMR (CDCl_3): 200.1, 138.2, 136.2, 132.5, 128.1 (2C), 128.0 (2C), 127.6 (2C), 126.9 (2C), 125.3, 53.1, 53.0, 46.2, 35.5, 35.3, 34.7, 27.4, 19.7, 13.9 ppm.

$\nu_{\text{max}}(\text{cm}^{-1})$: 2921, 2861, 1679, 1448, 1268, 738, 691.

HR-MS (NSI): m/z calculated for $\text{M} = \text{C}_{22}\text{H}_{29}\text{NO}$, theoretical $[\text{M}+\text{H}]^+$: 324.2323. Found: 324.2323.

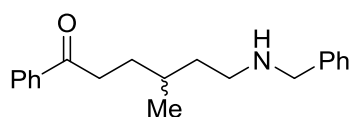
Entry 3 in Table 9.23

Following general procedure T for the telescoped ozonolysis-reductive amination, data is presented in the following format: (a) amount of substrate and (b) yield of product.

(a) 4-methyl-2,3,4,5-tetrahydro-1,1'-biphenyl **140c** (43 mg, 0.25 mmol, 1.0 eq.) and (b) yield of **168c**: 43 mg (58%).

Characterisation of 6-(benzylamino)-4-methyl-1-phenylhexan-1-one **168c**:

Obtained as a yellow oil.



168c

^1H NMR (CDCl_3): 7.89-7.85 (m, 2H, ArH), 7.51-7.43 (m, 1H, ArH), 7.39-7.32 (m, 2H, ArH), 7.26-7.14 (m, 5H, ArH), 3.71 (s, 2H, NCH_2Ph), 2.96-2.84 (m, 2H, CH_2), 2.69-2.51 (m, 2H, CH_2), 1.76-1.65 (m, 1H, CH), 1.59-1.43 (m, 4H, CH_2) 1.35-1.26 (m, 1H, NH) and 0.86 (d, $J = 6.3$ Hz, 3H, CH_3) ppm.

^{13}C NMR (CDCl_3): 200.8, 140.6, 137.2, 133.1, 128.8 (2C), 128.6 (2C), 128.3 (2C), 128.2 (2C), 127.1, 54.4, 47.4, 37.3, 36.3, 31.4, 30.9, 19.8 ppm.

$\nu_{\text{max}}(\text{cm}^{-1})$: 2951, 2920, 1681, 1448, 1205, 732, 690.

HR-MS (NSI): m/z calculated for $\text{M} = \text{C}_{20}\text{H}_{25}\text{NO}$, theoretical $[\text{M}+\text{H}]^+$: 296.2009. Found: 296.2011.

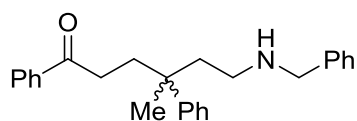
Entry 4 in Table 9.23

Following general procedure T for the telescoped ozonolysis-reductive amination, data is presented in the following format: (a) amount of substrate and (b) yield of product.

(a) 1'-methyl-1',2',3',6'-tetrahydro-1,1':4',1''-terphenyl **140d** (62 mg, 0.25 mmol, 1.0 eq.) and (b) yield of **168d**: 55 mg (59%).

Characterisation of 6-(benzylamino)-4-methyl-1,4-diphenylhexan-1-one **168d**:

Obtained as a yellow oil.



168d

^1H NMR (CDCl_3): 7.73-7.68 (m, 2H, ArH), 7.46-7.40 (m, 1H, ArH), 7.33-7.28 (m, 2H, ArH), 7.27-7.08 (m, 10H, ArH), 3.61 (s, 2H, NCH_2Ph), 2.77-2.66 (m, 1H, CH), 2.59-2.48 (m, 2H, CH_2), 2.38-2.29 (m, 1H, CH_2), 2.19-2.11 (m, 1H, CH_2), 2.04-1.86 (m, 2H, CH_2), 1.85-1.76 (m, 1H, CH), 1.29 (s, 3H, CH_3) and 1.18 (m, 1H, NH) ppm.

^{13}C NMR (CDCl_3): 200.7, 146.4, 139.7, 137.1, 133.1 (2C), 128.7 (2C), 128.63 (2C), 128.61, 128.4 (2C), 128.2 (2C), 127.3, 126.5 (2C), 126.2, 54.0, 45.2, 43.4, 40.1, 37.7, 34.0, 24.0 ppm.

$\nu_{\text{max}}(\text{cm}^{-1})$: 2927, 2853, 1680, 1633, 1446, 1317, 1211, 740, 696.

HR-MS (APCI): m/z calculated for $\text{M} = \text{C}_{26}\text{H}_{29}\text{NO}$, theoretical $[\text{M}+\text{H}]^+$: 372.2322. Found: 372.2319.

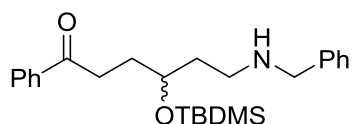
Entry 5 in Table 9.23

Following general procedure T for the telescoped ozonolysis-reductive amination, data is presented in the following format: (a) amount of substrate and (b) yield of product.

(a) *tert*-butyldimethyl((2,3,4,5-tetrahydro-[1,1'-biphenyl]-4-yl)oxy)silane **140e** (72 mg, 0.25 mmol, 1.0 eq.) and (b) yield of **168e**: 45 mg (44%).

Characterisation of 6-(benzylamino)-4-((*tert*-butyldimethylsilyl)oxy)-1-phenylhexan-1-one **168e**:

Obtained as a yellow oil.



168e

^1H NMR (CDCl_3): 7.93-7.88 (m, 1H, ArH), 7.54-7.49 (m, 1H, ArH), 7.44-7.38 (m, 2H, ArH), 7.30-7.26 (m, 4H, ArH), 7.23-7.18 (m, 2H, ArH), 3.91-3.83 (m, 1H, OCH), 3.75 (s, 2H, NCH_2Ph), 3.02-2.96 (m, 2H,

CH₂), 2.72-2.62 (m, 2H, CH₂), 1.94-1.74 (m, 2H, CH₂), 1.73-1.64 (m, 2H, CH₂), 1.21(m, 1H, NH), 0.83 (s, 9H, C(CH₃)₃) and 0.01 (s, 6H, SiCH₃) ppm.

¹³C NMR (CDCl₃): 200.4, 140.3, 137.2, 133.2, 128.8 (2C), 128.6 (2C), 128.5 (2C), 128.2 (2C), 127.2, 70.0, 54.3, 45.9, 37.4, 34.2, 31.4, 26.0(3C), 18.2, -4.25 (2C) ppm.

ν_{\max} (cm⁻¹): 2951, 2926, 2852, 1683, 1448, 1251, 1096, 833, 688, 667, 657.

HR-MS (APCI): m/z calculated for M = C₂₅H₃₇NO₂Si, theoretical [M+H]⁺: 412.2672. Found: 412.2669.

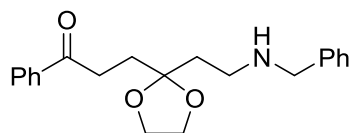
Entry 6 in Table 9.23

Following general procedure T for the telescoped ozonolysis-reductive amination, data is presented in the following format: (a) amount of substrate and (b) yield of product.

(a 8-phenyl-1,4-dioxaspiro[4.5]dec-7-ene **140h** (54 mg, 0.25 mmol, 1.0 eq.) and (b) yield of **168h**: 51 mg (60%).

Characterisation of 3-(2-(2-(benzylamino)ethyl)-1,3-dioxolan-2-yl)-1-phenylpropan-1-one **168h**:

Obtained as a yellow oil.



168h

¹H NMR (CDCl₃): 7.89-7.84 (m, 2H, ArH), 7.51-7.44 (m, 1H, ArH), 7.40-7.32 (m, 2H, ArH), 7.28-7.16 (m, 5H, ArH), 3.84-3.80 (m, 4H, OCH₂), 3.54 (s, 2H, NCH₂Ph), 2.56-2.47 (m, 2H, CH₂), 2.40-2.32 (m, 1H, CH), 1.83-1.75 (m, 2H, CH₂), 1.74-1.64 (m, 2H, CH₂), 1.58-1.40 (m, 1H, CH) and 0.87 (m, 1H, NH) ppm.

¹³C NMR (CDCl₃): 200.0, 137.2, 133.0 (2C), 129.0, 128.7 (2C), 128.4 (2C), 128.2 (2C), 128.2 (2C), 127.5, 110.7, 65.1 (2C), 58.8, 47.4, 37.3, 34.6, 31.5 ppm.

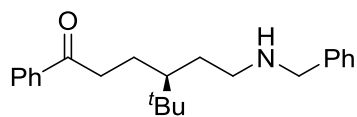
ν_{\max} (cm⁻¹): 2954, 2874, 1734, 1682, 1635, 1448, 1177, 1130, 1030, 742, 693.

HR-MS (APCI): m/z calculated for M = C₂₁H₂₅NO₃, theoretical [M+H]⁺: 324.1964. Found: 324.1965.

Entry 1 in Table 9.24

Following general procedure T for the telescoped ozonolysis-reductive amination, data is presented in the following format: (a) amount of substrate, (b) yield of product and (c) e.r.

(a) 4-(*tert*-butyl)-2,3,4,5-tetrahydro-1,1'-biphenyl **140a** (54 mg, 0.25 mmol, 1.0 eq.), (b) yield of **168a**: 44 mg (52%) and (c) 94:6.



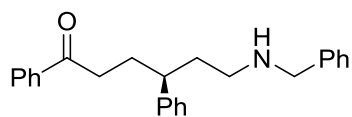
168a

Chiral analysis: HPLC OJ column, 0.40 mL/min, detector 254 nm, 10% IPA in hexane. t_1 = 15.6 min (major) and t_2 = 16.6 min (minor).

Entry 2 in Table 9.24

Following general procedure T for the telescoped ozonolysis-reductive amination, data is presented in the following format: (a) amount of substrate, (b) yield of product and (c) e.r.

(a) 1',2',3',6'-tetrahydro-1,1':4',1''-terphenyl **140b** (59 mg, 0.25 mmol, 1.0 eq.), (b) yield of **168b**: 48 mg (54%) and (c) 99:1



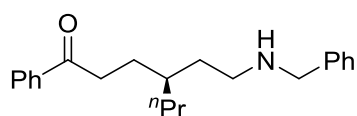
168b

Chiral analysis: HPLC OJ column, 0.40 mL/min, detector 254 nm, 0.5% IPA in hexane. t_1 = 70.8 min (major) and t_2 = 76.9 min (minor).

Entry 3 in Table 9.24

Following general procedure T for the telescoped ozonolysis-reductive amination, data is presented in the following format: (a) amount of substrate, (b) yield of product and (c) e.r.

(a) 4-propyl-2,3,4,5-tetrahydro-1,1'-biphenyl **140g** (50 mg, 0.25 mmol, 1.0 eq.), (b) yield of **168g**: 44 mg (54%) and (c) 90:10.



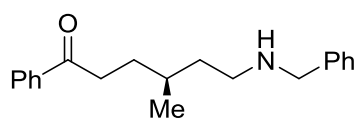
168g

Chiral analysis: HPLC OD-H column, 1.00 mL/min, detector 254 nm, 10% IPA in hexane. t_1 = 42.0 min (minor) and t_2 = 51.9 min (major).

Entry 4 in Table 9.24

Following general procedure T for the telescoped ozonolysis-reductive amination, data is presented in the following format: (a) amount of substrate, (b) yield of product and (c) e.r.

(a) 4-methyl-2,3,4,5-tetrahydro-1,1'-biphenyl **140c** (43 mg, 0.25 mmol, 1.0 eq.), (b) yield of **168c**: 45 mg (61%) and (c) 86:14.



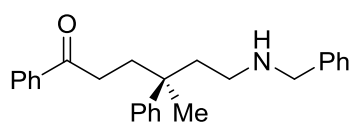
168c

Chiral analysis: HPLC OD-H column, 1.00 mL/min, detector 254 nm, 10% IPA in hexane. t_1 = 42.0 min (minor) and t_2 = 51.9 min (major).

Entry 5 in Table 9.24

Following general procedure T for the telescoped ozonolysis-reductive amination, data is presented in the following format: (a) amount of substrate, (b) yield of product and (c) e.r.

(a) 1'-methyl-1',2',3',6'-tetrahydro-1,1':4',1''-terphenyl **140d** (62 mg, 0.25 mmol, 1.0 eq.), (b) yield of **168d**: 56 mg (60%) and (c) 88:12.



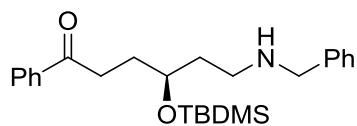
168d

Chiral analysis: HPLC OD-H column, 0.40 mL/min, detector 254 nm, 0.5% IPA in hexane. t_1 = 24.9 min (minor) and t_2 = 25.7 min (major).

Entry 6 in Table 9.24

Following general procedure T for the telescoped ozonolysis-reductive amination, data is presented in the following format: (a) amount of substrate, (b) yield of product and (c) e.r.

(a) *tert*-butyldimethyl((2,3,4,5-tetrahydro-[1,1'-biphenyl]-4-yl)oxy)silane **140e** (72 mg, 0.25 mmol, 1.0 eq.), (b) yield of **168e**: 43 mg (42%) and (c) 97:3.



168e

Chiral analysis: HPLC OD-H column, 0.40 mL/min, detector 254 nm, 10% IPA in hexane. t_1 = 39.6 min (minor) and t_2 = 70.4 min (major).

Entry 1 in Table 9.25¹⁶⁶

Following general procedure U for the deprotection of **168b** with Pd, data is presented in the following format: (a) amount of catalyst used, (b) hydrogen source, (c) conditions and (d) recovered SM **168b**.

(a) Pd/C (6.4 mg, 10 wt%, 0.006 mmol, 10 mol%), (b) H₂ balloon, (c) MeOH (4 mL), DCM (2 mL), rt, 1d and (d) 19 mg (95%).

Entry 2 in Table 9.25¹²⁹

Following general procedure U for the deprotection of **168b** with Pd, data is presented in the following format: (a) amount of catalyst used, (b) hydrogen source, (c) conditions and (d) recovered SM **168b**.

(a) Pd(OH)₂ (26 mg, 30 wt% on C, 50% wet, 0.018 mmol, 30 mol%), (b) H₂ balloon, (c) THF (3 mL), ⁱPrOH (1 mL), rt, 1d and (d) -.

Entry 3 in Table 9.25¹³⁰

Following general procedure U for the deprotection of **168b** with Pd, data is presented in the following format: (a) amount of catalyst used, (b) hydrogen source, (c) conditions and (d) recovered SM **168b**.

(a) Pd/C (20 mg, 10 wt% on C, 0.0096 mmol, 16 mol%), (b) NH₄HCO₂ (19 mg, 0.30 mmol, 5.0 eq.), (c) MeOH (0.4 mL), reflux, 90 min and (d) 9 mg 46%.

Entry 1 in Table 9.26

Following general procedure V for the reductive amination of **168b**, data is presented in the following format: (a) amount of solvent, (b) amount of additive(s), (c) reaction temperature, (d) reaction time and (e) recovered SM **168b**.

(a) toluene (1.3 mL), (b)-, (c) reflux, (d)O/N and (e) 19 mg (95%).

Entry 2 in Table 9.26

Following general procedure V for the reductive amination of **168b**, data is presented in the following format: (a) amount of solvent, (b) amount of additive(s), (c) reaction temperature, (d) reaction time and (e) recovered SM **168b**.

(a) CPME (1.3 mL), (b)-, (c) reflux, (d)O/N and (e) 16 mg (80%).

Entry 3 in Table 9.26

Following general procedure V for the reductive amination of **168b**, data is presented in the following format: (a) amount of solvent, (b) amount of additive(s), (c) reaction temperature, (d) reaction time and (e) recovered SM **168b**.

(a) CPME (1.3 mL), (b) acetic acid (12 μ L, 0.06 mmol, 1.0 eq.), (c) reflux, (d)O/N and (e) 16 mg (80%).

Entry 4 in Table 9.26

Following general procedure V for the reductive amination of **168b**, data is presented in the following format: (a) amount of solvent, (b) amount of additive(s), (c) reaction temperature, (d) reaction time and (e) recovered SM **168b**.

(a) CPME (1.3 mL), (b) acetic acid (12 μ L, 0.06 mmol, 1.0 eq.), 4 Å mol. sieves (50 mg), (c) reflux, (d) O/N and (e) 19 mg (95%).

Entry 5 in Table 9.26

Following general procedure V for the reductive amination of **168b**, data is presented in the following format: (a) amount of solvent, (b) amount of additive(s), (c) reaction temperature, (d) reaction time and (e) recovered SM **168b**.

(a) CPME (1.3 mL), (b)-, (c) 120 °C (μ w), (d) 2 h and (e) 8 mg (40%).

Entry 6 in Table 9.26

Following general procedure V for the reductive amination of **168b**, data is presented in the following format: (a) amount of solvent, (b) amount of additive(s), (c) reaction temperature, (d) reaction time and (e) recovered SM **168b**.

(a) CPME (1.3 mL), (b) Ti(OⁱPr)₄ (0.06 mL, 0.18 mmol, 3.03 eq.), (c) reflux, (d) O/N and (e) 19 mg (95%).

Entry 7 in Table 9.26

Following general procedure V for the reductive amination of **168b**, data is presented in the following format: (a) amount of solvent, (b) amount of additive(s), (c) reaction temperature, (d) reaction time and (e) recovered SM **168b**.

(a) -, (b) Ti(OⁱPr)₄ (0.06 mL, 0.18 mmol, 3.03 eq.), (c) 110 °C, (d) O/N and (e) 18 mg (90%).

Entry 8 in Table 9.26

Following general procedure T for the reductive amination of **168b**, data is presented in the following format: (a) amount of solvent, (b) amount of additive(s), (c) reaction temperature, (d) reaction time and (e) recovered SM **168b**.

(a) CPME (1.3 mL), (b) ZnCl₂ (25 mg, 0.18 mmol, 3.03 eq.), (c) reflux, (d) O/N and (e) -.

Entry 9 in Table 9.26

Following general procedure AH for the reductive amination of **168b**, data is presented in the following format: (a) amount of solvent, (b) amount of additive(s), (c) reaction temperature, (d) reaction time and (e) recovered SM **168b**.

(a) CPME (1.3 mL), (b) NiCl₂*6 H₂O (43 mg, 0.18 mmol, 3.03 eq.), (c) reflux, (d) O/N and (e) 19 mg (95%).

Entry 10 in Table 9.26¹³⁷

A flame dried 5 mL round bottom flask was equipped with a stirrer bar, and closed with a suba seal. The substrate **168b** (20 mg, 0.06 mmol, 1.0 eq.) was dissolved in DCM (3 mL) and TMSCl (0.04 mL, 0.30 mmol, 5.0 eq.) was added. The solution was stirred at rt for O/N. The solvent and by-products were removed *in vacuo*. The crude product was dissolved in DCM (1.3 mL) and the solution was cooled to 0 °C under an argon atmosphere. To this solution NaBH(OAc)₃ (36 mg, 0.168 mmol, 2.80 eq.) was added and the reaction was stirred at rt for 36 h. The crude mixture was partitioned between DCM (4 mL) and sat. K₂CO₃ (4 mL). The aqueous phase was washed with DCM (3 × 4 mL)

and the organic phase was collected. The combined organic phase was dried over Na_2SO_4 , filtered and the solvent was removed *in vacuo*. The crude mixture was analysed by ^1H NMR spectroscopy and the starting material was recovered by flash column chromatography using 1-2% MeOH in DCM. Recovered SM **168b**: 12 mg (60%)

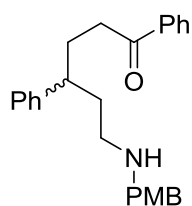
Entry 1 in Table 9.27

Following general procedure S for the reductive amination of aldehyde-ketone **164b**, data is presented in the following format: (a) solvent, (b) amount of benzylamine, (c) amount sodium triacetoxyborohydride, (d) amount of additive(s), (e) yield of product **173** and (f) yield of product **174**.

(a) CPME (4 mL), (b) Benzylamine (47 μL , 0.36 mmol, 2.10 eq.), (c) sodium triacetoxyborohydride (95 mg, 0.44 mmol, 2.8 eq.), (d) - , (e) 20 mg (31%) and (f) 21 mg (19%) .

Characterisation of 6-((4-methoxybenzyl)amino)-1,4-diphenylhexan-1-one **173**:

Obtained as a yellow oil.



173

^1H NMR (CDCl_3): 7.75-7.70 (m, 2H, ArH), 7.45-7.39 (m, 1H, ArH), 7.35-7.28 (m, 2H, ArH), 7.24-7.16 (m, 2H, ArH), 7.15-7.04 (m, 5H, ArH), 6.78-6.72 (m, 2H, ArH), 3.69 (s, 3H, OCH_3), 3.59 (d, $^2J = 12.5$ Hz, 1H, CH_2Ph), 3.53 (d, $^2J = 12.5$ Hz, 1H, CH_2Ph), 2.81-2.55 (m, 3H, CH_2 , PhCH), 2.52-2.36 (m, 2H, CH_2), 2.25 (m, 1H, NH), 2.10-1.98 (m, 1H, CH_2) and 1.92-1.69 (m, 3H, CH_2), ppm.

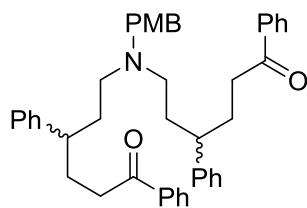
^{13}C NMR (CDCl_3): 200.4, 158.8, 144.3, 137.1, 133.1, 131.8, 129.6 (2C), 128.8 (2C), 128.6 (2C), 128.2 (2C), 127.8 (2C), 126.6, 114.0 (2C), 55.4, 53.3, 47.3, 43.6, 37.0, 36.7, 31.2 ppm.

$\nu_{\text{max}}(\text{cm}^{-1})$: 2935, 2358, 1672, 1508, 1446, 1234, 1029, 758, 744, 729, 700, 688.

HR-MS (APCI): m/z calculated for $\text{M} = \text{C}_{26}\text{H}_{29}\text{NO}_2$, theoretical $[\text{M}+\text{H}]^+$: 388.2277. Found: 388.2266.

Characterisation of 6,6'-((4-methoxybenzyl)azanediyl)bis(1,4-diphenylhexan-1-one) **174**:

Obtained as a yellow oil. Mixture of diastereomers is reported d.r. = 1:1.



174

^1H NMR (CDCl_3): 7.74-7.69 (m, 8H, ArH), 7.45-7.39 (m, 4H, ArH), 7.33-7.24 (m, 8H, ArH), 7.19-7.11 (m, 10H, ArH), 7.10-7.05 (m, 4H, ArH), 7.03-6.95 (m, 12H, ArH), 6.71-6.65 (m, 2H, ArH), 3.67 (s, 3H, OCH_3), 3.66 (s, 3H, OCH_3), 3.37 (d, $^2J = 12.6$ Hz, 1H, CH_2Ph), 3.29 (s, 2H, CH_2Ph), 3.20 (d, $^2J = 12.6$ Hz, 1H, CH_2Ph), 2.73-2.47 (m, 12H, PhCH, CH_2), 2.27-2.00 (m, 8H, CH_2), 1.96-1.89 (m, 4H, CH_2), 1.83-1.73 (m, 4H, CH_2) and 1.70-1.51 (m, 8H, CH_2), ppm.

^{13}C NMR (CDCl_3): 200.5, 158.6, 144.9, 144.3, 137.2, 132.9 (4C), 132.0, 130.2 (2C), 128.6 (4C), 128.2 (4C), 127.9 (4C), 126.4 (4C), 113.6 (2C), 58.1, 55.4, 51.8, 51.7, 43.4, 36.8, 34.4, 34.3, 31.4, 29.8 ppm.

$\nu_{\text{max}}(\text{cm}^{-1})$: 2924, 2354, 1680, 1508, 1448, 1242, 1031, 756, 747.

HR-MS (NSI): m/z calculated for $\text{M} = \text{C}_{44}\text{H}_{47}\text{NO}_3$, theoretical $[\text{M}+\text{H}]^+$: 638.3629. Found: 638.3613.

Entry 2 in Table 9.27

A flame dried microwave vial was equipped with a stirrer bar and charged with sodium cyanoborohydride (5 mg, 0.075 mmol, 1.0 eq.), zinc(II) chloride (5 mg, 0.038 mmol, 0.5 eq.) and dissolve in MeOH (1 mL). The substrate **164b** (20 mg, 0.075mmol, 1.0 eq.) and 4-methoxy benzylamine (0.02 mL, 0.15 mmol, 2.0 eq.) were dissolved in MeOH (0.3 mL) and this solution was added dropwise to the solution of the reducing agent. The reaction was stirred at rt for 15 h. The crude mixture was partitioned between DCM (4 mL) and sat. K_2CO_3 (4 mL). The aqueous phase was washed with DCM (3 \times 4 mL) and the organic phase was collected. The combined organic phase was dried over Na_2SO_4 , filtered and the solvent was removed *in vacuo*. The crude mixture was analysed by ^1H NMR spectroscopy and the product was isolate by flash column chromatography using 1-2% MeOH in DCM. Mass of product **173**: 12 mg (40%)

Entry 3 in Table 9.27

Following general procedure W for the reductive amination of **164b** with sodium cyanoborohydride, data is presented in the following format: : (a) addition time of substrate **164b**, (b) amount of MeOH use to prepare the solution of **164b**, (c) amount of 4-methoxybenzylamine and (d) yield of product **173**.

(a) 0.5 h, (b) MeOH (2 mL), (c) 4-methoxybenzylamine (10 μ L, 0.075 mmol, 1.0 eq.) and (d) 16 mg (54%)

Entry 1 in Table 9.28

Following general procedure W for the reductive amination of **164b** with sodium cyanoborohydride, data is presented in the following format: : (a) addition time of substrate **164b**, (b) amount of MeOH use to prepare the solution of **164b**, (c) amount of 4-methoxybenzylamine and (d) yield of product **173**.

(a) 1.25 h, (b) MeOH (2 mL), (c) 4-methoxybenzylamine (50 μ L, 0.375 mmol, 5.0 eq.) and (d) 50%.

Entry 2 in Table 9.28

Following general procedure W for the reductive amination of **164b** with sodium cyanoborohydride, data is presented in the following format: : (a) addition time of substrate **164b**, (b) amount of MeOH use to prepare the solution of **164b**, (c) amount of 4-methoxybenzylamine and (d) yield of product **173**.

(a) 1.25 h, (b) MeOH (2 mL), (c) 4-methoxybenzylamine (50 μ L, 0.375 mmol, 5.0 eq.) and (d) 54%.

Entry 3 in Table 9.28

Following general procedure W for the reductive amination of **164b** with sodium cyanoborohydride, data is presented in the following format: : (a) addition time of substrate **164b**, (b) amount of MeOH use to prepare the solution of **164b**, (c) amount of 4-methoxybenzylamine and (d) yield of product **173**.

(a) 2 h, (b) MeOH (1 mL), (c) 4-methoxybenzylamine (70 μ L, 0.525 mmol, 7.0 eq.) and (d) 48%.

Entry 4 in Table 9.28

Following general procedure W for the reductive amination of **164b** with sodium cyanoborohydride, data is presented in the following format: : (a) addition time of substrate **164b**, (b) amount of MeOH use to prepare the solution of **164b**, (c) amount of 4-methoxybenzylamine and (d) yield of product **173**.

(a) 2 h, (b) MeOH (4 mL), (c) 4-methoxybenzylamine (70 μ L, 0.525 mmol, 7.0 eq.) and (d) 39%.

Entry 5 in Table 9.28

Following general procedure W for the reductive amination of **164b** with sodium cyanoborohydride, data is presented in the following format: : (a) addition time of substrate **164b**, (b) amount of MeOH

use to prepare the solution of **164b**, (c) amount of 4-methoxybenzylamine and (d) yield of product **173**.

(a) 1.25 h, (b) MeOH (2 mL), (c) 4-methoxybenzylamine (50 μ L, 0.375 mmol, 5.0 eq.) and (d) 50%.

Entry 6 in Table 9.28

Following general procedure W for the reductive amination of **164b** with sodium cyanoborohydride, data is presented in the following format: : (a) addition time of substrate **164b**, (b) amount of MeOH use to prepare the solution of **164b**, (c) amount of 4-methoxybenzylamine and (d) yield of product **173**.

(a) 0.5 h, (b) MeOH (4 mL), (c) 4-methoxybenzylamine (70 μ L, 0.525 mmol, 7.0 eq.) and (d) 71%.

Entry 7 in Table 9.28

Following general procedure W for the reductive amination of **164b** with sodium cyanoborohydride, data is presented in the following format: : (a) addition time of substrate **164b**, (b) amount of MeOH use to prepare the solution of **164b**, (c) amount of 4-methoxybenzylamine and (d) yield of product **173**.

(a) 2 h, (b) MeOH (4 mL), (c) 4-methoxybenzylamine (30 μ L, 0.225 mmol, 3.0 eq.) and (d) 59%.

Entry 8 in Table 9.28

Following general procedure W for the reductive amination of **164b** with sodium cyanoborohydride, data is presented in the following format: : (a) addition time of substrate **164b**, (b) amount of MeOH use to prepare the solution of **164b**, (c) amount of 4-methoxybenzylamine and (d) yield of product **173**.

(a) 0.5 h, (b) MeOH (1 mL), (c) 4-methoxybenzylamine (30 μ L, 0.225 mmol, 3.0 eq.) and (d) 54%.

Entry 9 in Table 9.28

Following general procedure W for the reductive amination of **164b** with sodium cyanoborohydride, data is presented in the following format: : (a) addition time of substrate **164b**, (b) amount of MeOH use to prepare the solution of **164b**, (c) amount of 4-methoxybenzylamine and (d) yield of product **173**.

(a) 2 h, (b) MeOH (1mL), (c) 4-methoxybenzylamine (30 μ L, 0.225 mmol, 3.0 eq.) and (d) 40%.

Entry 10 in Table 9.28

Following general procedure W for the reductive amination of **164b** with sodium cyanoborohydride, data is presented in the following format: : (a) addition time of substrate **164b**, (b) amount of MeOH use to prepare the solution of **164b**, (c) amount of 4-methoxybenzylamine and (d) yield of product **173**.

(a) 0.5 h, (b) MeOH (1 mL), (c) 4-methoxybenzylamine (70 μ L, 0.525 mmol, 7.0 eq.) and (d) 65%.

Entry 11 in Table 9.28

Following general procedure W for the reductive amination of **164b** with sodium cyanoborohydride, data is presented in the following format: : (a) addition time of substrate **164b**, (b) amount of MeOH use to prepare the solution of **164b**, (c) amount of 4-methoxybenzylamine and (d) yield of product **173**.

(a) 0.5 h, (b) MeOH (4 mL), (c) 4-methoxybenzylamine (30 μ L, 0.225 mmol, 3.0 eq.) and (d) 68%.

Entry 1 in Table 9.29¹⁴³

Following general procedure X for the deprotection of **173** under acidic conditions, data is presented in the following format: : (a) amount of additive, (b) amount of solvent, (c) reaction temperature, (d) reaction time, (e) conversion towards desired product and (f) recovered **173**.

(a) TFA (0.02 mL, 0.25 mmol, 5.0 eq.), (b) DCM (0.5 mL), (c) rt, (d) 24 h, (e) - and (f) 100%.

Entry 2 in Table 9.29¹⁴¹

Following general procedure X for the deprotection of **173** under acidic conditions, data is presented in the following format: : (a) amount of additive, (b) amount of solvent, (c) reaction temperature, (d) reaction time, (e) conversion towards desired product and (f) recovered **173**.

(a) Triflic acid (14 μ L, 0.15 mmol, 3.0 eq.), (b) TFA (0.5 mL), (c) rt, (d) 4 h, (e) - and (f) 100%.

Entry 3 in Table 9.29¹⁴⁰

Following general procedure X for the deprotection of **173** under acidic conditions, data is presented in the following format: : (a) amount of additive, (b) amount of solvent, (c) reaction temperature, (d) reaction time, (e) conversion towards desired product and (f) recovered **173**.

(a) TFA (0.02 mL, 0.25 mmol, 5.0 eq.), (b) -, (c) reflux, (d) 4 h, (e) - and (f) 100%.

Entry 4 in Table 9.29¹⁴²

Following general procedure X for the deprotection of **173** under acidic conditions, data is presented in the following format: : (a) amount of additive, (b) amount of solvent, (c) reaction temperature, (d) reaction time, (e) conversion towards desired product and (f) recovered **173**.

(a) TFA (0.02 mL, 0.25 mmol, 5.0 eq.), (b) -, (c) 120 °C, (d) 10 min, (e) - and (f) 100%.

Entry 1 in Table 9.30

Following general procedure Y for the deprotection of **173**, data is presented in the following format: (a) amount of reductant, (b) conversion towards desired product and (f) recovered **173**.

(a) CAN (86 mg, 0.158 mmol, 2.1 eq.), (b) - and (c) 100%.

Entry 2 in Table 9.30

Following general procedure Y for the deprotection of **173**, data is presented in the following format: (a) amount of reductant, (b) conversion towards desired product and (f) recovered **173**.

(a) DDQ (21 mg, 0.09 mmol, 1.2 eq.), (b) - and (c) -.

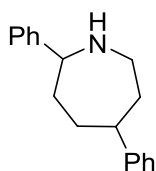
Scheme 9.62

Following general procedure Z for the reductive aminocyclisation of aldehyde-ketones, data is presented in the following format: : (a) amount of ammonia, (b) substrate, (c) solvent for reducing agent, (d) solvent for substrate solution, (e) addition time of substrate solution and (f) yield of product **172b**.

(a) NH₃ (0.11 mL, c = 7 mmol/mL in MeOH, 0.75 mmol, 10 eq.), (b) aldehyde-ketone **164b** (20 mg, 0.075 mmol, 1.0 eq.), (c) MeOH (2 mL), (d) MeOH (4 mL), (e) 0.5 h and (f) 4 mg (21%).

Characterisation of 2,5-diphenylazepane **172b**:

Obtained as a yellow oil.



172b

^1H NMR (CDCl_3): 7.37-7.32 (m, 2H, ArH), 7.28-7.15 (m, 8H, ArH), 3.96 (t, $J = 6.3$ Hz, 1H, NCHPh), 3.16 (dt, $^2J = 13.2$ Hz, $J = 3.2$ Hz, 1H, NCHPh), 2.85-2.73 (m, 2H, NCH_2Ph) and 2.11-1.74 (m, 7H, NH, CH_2). ppm.

^{13}C NMR (CDCl_3): 149.1, 147.1, 128.7 (2C), 128.6 (2C), 127.1, 126.9 (2C), 126.8 (2C), 126.0, 63.7, 49.1, 46.1, 41.2, 36.1, 32.4 ppm.

ν_{max} (cm^{-1}): 2928, 2850, 1683, 1598, 1490, 1448, 1138, 1072, 1028, 800.

HR-MS (NSI): m/z calculated for $\text{M} = \text{C}_{18}\text{H}_{21}\text{N}$, theoretical $[\text{M}+\text{H}]^+$: 252.1747. Found: 252.1740.

Entry 1 in Table 9.31

Following general procedure Z for the reductive aminocyclisation of aldehyde-ketones, data is presented in the following format: : (a) amount of ammonia, (b) substrate, (c) solvent for reducing agent, (d) solvent for substrate solution, (e) addition time of substrate solution and (f) yield of product **172b**.

(a) NH_3 (0.11 mL, $c = 7$ mmol/mL in MeOH, 0.75 mmol, 10 eq.), (b) aldehyde-ketone **164b** (20 mg, 0.075 mmol, 1.0 eq.), (c) CPME (2 mL), (d) MeOH (4 mL), (e) 0.5 h and (f) 24%.

Entry 2 in Table 9.31

Following general procedure Z for the reductive aminocyclisation of aldehyde-ketones, data is presented in the following format: : (a) amount of ammonia, (b) substrate, (c) solvent for reducing agent, (d) solvent for substrate solution, (e) addition time of substrate solution and (f) yield of product **172b**.

(a) NH_3 (0.11 mL, $c = 7$ mmol/mL in MeOH, 0.75 mmol, 10 eq.), (b) aldehyde-ketone **164b** (20 mg, 0.075 mmol, 1.0 eq.), (c) DCE (2 mL), (d) MeOH (4 mL), (e) 0.5 h and (f) 25%.

Entry 3 in Table 9.31

Following general procedure Z for the reductive aminocyclisation of aldehyde-ketones, data is presented in the following format: : (a) amount of ammonia, (b) substrate, (c) solvent for reducing agent, (d) solvent for substrate solution, (e) addition time of substrate solution and (f) yield of product **172b**.

(a) NH_3 (0.11 mL, $c = 7$ mmol/mL in MeOH, 0.75 mmol, 10 eq.), (b) aldehyde-ketone **172b** (20 mg, 0.075 mmol, 1.0 eq.), (c) THF (2 mL), (d) MeOH (4 mL), (e) 0.5 h and (f) 13%.

Entry 4 in Table 9.31

Following general procedure Z for the reductive aminocyclisation of aldehyde-ketones, data is presented in the following format: : (a) amount of ammonia, (b) substrate, (c) solvent for reducing agent, (d) solvent for substrate solution, (e) addition time of substrate solution and (f) yield of product **172b**.

(a) NH₃ (0.11 mL, c = 7 mmol/mL in MeOH, 0.75 mmol, 10 eq.), (b) aldehyde-ketone **164b** (20 mg, 0.075 mmol, 1.0 eq.), (c) DCM (2 mL), (d) MeOH (4 mL), (e) 0.5 h and (f) 35%.

Entry 5 in Table 9.31

Following general procedure Z for the reductive aminocyclisation of aldehyde-ketones, data is presented in the following format: : (a) amount of ammonia, (b) substrate, (c) solvent for reducing agent, (d) solvent for substrate solution, (e) addition time of substrate solution and (f) yield of product **172b**.

(a) NH₃ (0.11 mL, c = 7 mmol/mL in MeOH, 0.75 mmol, 10 eq.), (b) aldehyde-ketone **164b** (20 mg, 0.075 mmol, 1.0 eq.), (c) DCM (2 mL), (d) DCM (4 mL), (e) 0.5 h and (f) 14%.

Entry 6 in Table 9.31

Following general procedure Z for the reductive aminocyclisation of aldehyde-ketones, data is presented in the following format: : (a) amount of ammonia, (b) substrate, (c) solvent for reducing agent, (d) solvent for substrate solution, (e) addition time of substrate solution and (f) yield of product **172b**.

(a) NH₃ (55 μ L, c = 7 mmol/mL in MeOH, 0.375 mmol, 5 eq.), (b) aldehyde-ketone **164b** (20 mg, 0.075 mmol, 1.0 eq.), (c) DCM (2 mL), (d) MeOH (4 mL), (e) 0.5 h and (f) 34%.

Entry 7 in Table 9.31

Following general procedure Z for the reductive aminocyclisation of aldehyde-ketones, data is presented in the following format: : (a) amount of ammonia, (b) substrate, (c) solvent for reducing agent, (d) solvent for substrate solution, (e) addition time of substrate solution and (f) yield of product **172b**.

(a) NH₃ (55 μ L, c = 7 mmol/mL in MeOH, 0.375 mmol, 5 eq.), (b) aldehyde-ketone **164b** (20 mg, 0.075 mmol, 1.0 eq.), (c) DCM (2 mL), (d) MeOH (4 mL), (e) 15 min and (f) 20%.

Entry 8 in Table 9.31

Following general procedure Z for the reductive aminocyclisation of aldehyde-ketones, data is presented in the following format: : (a) amount of ammonia, (b) substrate, (c) solvent for reducing agent, (d) solvent for substrate solution, (e) addition time of substrate solution and (f) yield of product **172b**.

(a) NH₃ (55 µL, c = 7 mmol/mL in MeOH, 0.375 mmol, 5 eq.), (b) aldehyde-ketone **164b** (20 mg, 0.075 mmol, 1.0 eq.), (c) DCM (2 mL), (d) MeOH (4 mL), (e) 1 h and (f) 15%.

Entry 1 in Table 9.32

Following general procedure AA for the reductive aminocyclisation of aldehyde-ketones with different reducing agents, data is presented in the following format: : (a) ammonia source, (b) reducing agent and (c) conversion of product **172b**.

(a) NH₃ (55 µL, c = 7 mmol/mL in MeOH, 0.375 mmol, 5 eq.), (b) sodium triacetoxyborohydride (32 mg, 0.15 mmol, 2.0 eq.) and (c) 9%.

Entry 2 in Table 9.32

Following general procedure AA for the reductive aminocyclisation of aldehyde-ketones with different reducing agents, data is presented in the following format: : (a) ammonia source, (b) reducing agent and (c) conversion of product **172b**.

(a) NH₃ (55 µL, c = 7 mmol/mL in MeOH, 0.375 mmol, 5 eq.), (b) tetrabutylammonium borohydride (39 mg, 0.15 mmol, 2.0 eq.) and (c) -.

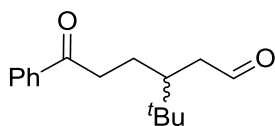
Entry 1 in Table 9.33

Following general procedure R for the ozonolysis of cyclic alkenes, data is presented in the following format (a) substrate, (b) amount of solvent, (c) amount of dimethyl sulfide and (d) yield of product.

(a) 4-(*tert*-butyl)-2,3,4,5-tetrahydro-1,1'-biphenyl **140a** (54 mg, 0.25 mmol, 1.0 eq.), (b) DCM (8 mL) and MeOH (2 mL), (c) dimethyl sulfide (0.37 mL, 5 mmol, 20 eq.) and (d) 46 mg (75%).

Characterisation of 3-(*tert*-butyl)-6-oxo-6-phenylhexanal **164a**:

Obtained as a colorless oil.



164a

^1H NMR (CDCl_3): 9.81 (t, $J = 1.6$ Hz, 1H, CHO), 7.9-7.89 (m, 2H, ArH), 7.56-7.51 (m, 1H, ArH), 7.47-7.40 (m, 2H, ArH), 2.96-2.90 (m, 2H, $\text{CH}_2, \text{PhC(O)CH}_2$), 2.63 (ddd, $^2J = 17.6$ Hz, $J = 5.1$ Hz, $J = 1.6$ Hz, 1H, CHOCHH), 2.25 (ddd, $^2J = 17.6$ Hz, $J = 5.1$ Hz, $J = 1.6$ Hz, 1H, CHOCHH), 2.11-2.00 (m, 2H, CH_2), 1.92-1.82 (m, 1H, CH), and 0.90 (s, 9H, $(\text{CH}_3)_3$) ppm.

^{13}C NMR (CDCl_3): 203.1, 200.2, 133.3, 128.8 (2C), 128.2 (2C), 125.0, 46.4, 42.3, 38.0, 33.9, 27.8 (3C), 25.9 ppm.

$\nu_{\text{max}}(\text{cm}^{-1})$: 2966, 2918, 1694, 1365, 1235, 1040, 700.

HR-MS (APCI): m/z calculated for $\text{M} = \text{C}_{16}\text{H}_{22}\text{O}_2$, theoretical $[\text{M}-\text{H}]^+$: 245.1542. Found: 245.1545.

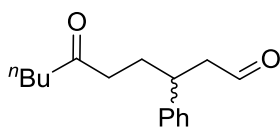
Entry 2 in Table 9.33

Following general procedure R for the ozonolysis of cyclic alkenes, data is presented in the following format (a) substrate, (b) amount of solvent, (c) amount of dimethyl sulfide and (d) yield of product.

(a) 4-butyl-2,3,4,5-tetrahydro-1,1'-biphenyl **122b** (54 mg, 0.25 mmol, 1.0 eq.), (b) DCM (8 mL) and MeOH (2 mL), (c) dimethyl sulfide (0.37 mL, 5 mmol, 20 eq.) and (d) 50 mg (81%).

Characterisation of 6-oxo-3-phenyldecanal **176b**:

Obtained as a colorless oil.



176b

^1H NMR (CDCl_3): 9.59 (t, $J = 1.9$ Hz, 1H, CHO), 7.27-7.21 (m, 2H, ArH), 7.18-7.12 (m, 1H, ArH), 7.12-7.06 (m, 2H, ArH), 3.10 (m, 1H, PhCH), 2.68 (t, $J = 7.1$ Hz, 1H, $^n\text{BuC(O)CHH}$), 2.64 (t, $J = 7.1$ Hz, 1H, $^n\text{BuC(O)CHH}$), 2.24-2.16 (m, 2H, CHOCH₂), 1.97-1.88 (m, 1H, CH), 1.81-1.72 (m, 1H, CH), 1.44-1.32 (m, 2H, CH₂), 1.22-1.16 (m, 4H, CH₂), and 0.79 (t, $J = 7.2$ Hz, 3H, CH₃) ppm.

^{13}C NMR (CDCl_3): 210.8, 201.6, 143.0, 129.0 (2C), 127.7 (2C), 127.1, 51.0, 42.8, 40.4, 39.5, 30.2, 26.1, 22.5, 15.9 ppm.

$\nu_{\text{max}}(\text{cm}^{-1})$: 2954, 2927, 1710, 700.

HR-MS (NSI): m/z calculated for $M = \text{C}_{16}\text{H}_{22}\text{O}_2$, theoretical $[\text{M}+\text{H}]^+$: 247.1695. Found: 247.1693.

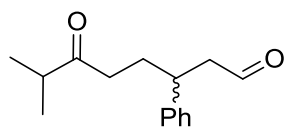
Entry 3 in Table 9.33

Following general procedure R for the ozonolysis of cyclic alkenes, data is presented in the following format (a) substrate, (b) amount of solvent, (c) amount of dimethyl sulfide and (d) yield of product.

(a) 4-*iso*-propyl-2,3,4,5-tetrahydro-1,1'-biphenyl **121b** (50 mg, 0.25 mmol, 1.0 eq.), (b) DCM (8 mL) and MeOH (2 mL), (c) dimethyl sulfide (0.37 mL, 5 mmol, 20 eq.) and (d) 58 mg (99%).

Characterisation of 7-methyl-6-oxo-3-phenyloctanal **177b**:

Obtained as a colourless oil.



177b

^1H NMR (CDCl_3): 9.59 (t, $J = 1.9$ Hz, 1H, CHO), 7.27-7.21 (m, 2H, ArH), 7.18-7.12 (m, 1H, ArH), 7.11-7.07 (m, 2H, ArH), 3.21 (m, 1H, $(\text{CH}_3)_2\text{CH}$), 3.16-3.07 (m, 1H, PhCH), 2.66 (m, 2H, CH_2), 2.43-2.37 (m, 1H, CH), 2.33-2.13 (m, 2H, CH_2), 1.96-1.89 (m, 1H, CH_2), 0.94 (d, $J = 6.9$ Hz, 3H, CH_3) and 0.92 (d, $J = 6.9$ Hz, 3H, CH_3) ppm.

^{13}C NMR (CDCl_3): 214.4, 201.7, 143.1, 129.0 (2C), 127.8 (2C), 127.1, 51.0, 41.1, 39.4, 38.0, 30.2, 18.5, 18.3 ppm.

$\nu_{\text{max}}(\text{cm}^{-1})$: 2966, 2922, 1708, 1240, 1045, 761, 700.

HR-MS (APCI): m/z calculated for $M = \text{C}_{15}\text{H}_{20}\text{O}_2$, theoretical $[\text{M}+\text{H}]^+$: 233.1542. Found: 233.1544.

Entry 1 in Table 9.34

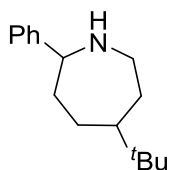
Following general procedure Z for the reductive aminocyclisation of aldehyde-ketones, data is presented in the following format: : (a) amount of ammonia, (b) substrate, (c) solvent for reducing

agent, (d) solvent for substrate solution, (e) addition time of substrate solution and (f) yield of product **178**.

(a) NH₃ (0.11 mL, c = 7 mmol/mL in MeOH, 0.75 mmol, 5 eq.), (b) aldehyde-ketone **164a** (32 mg, 0.15 mmol, 1.0 eq.), (c) DCM (2 mL), (d) MeOH (4 mL), (e) 0.5 h and (f) 9 mg (27%).

Characterisation of 5-(*tert*-butyl)-2-phenylazepane **178**:

Obtained as a yellow oil.



178

¹H NMR (CDCl₃): 7.32-7.26 (m, 2H, ArH), 7.25-7.20 (m, 2H, ArH), 7.17-7.12 (m, 1H, ArH), 3.79 (dd, *J* = 8.9 Hz, *J* = 4.6 Hz, 1H, NCHPh), 3.16 (dq, ²*J* = 13.4 Hz, *J* = 2.8 Hz, 1H, NCHH), 2.63 (m, 1H, NCHH), 3.03 (br s, 1H, NH), 2.00-1.71 (m, 4H, CH₂), 1.60-1.48 (m, 1H, CH), 1.45-1.33 (m, 1H, CH), 1.31-1.24 (m, 1H, CH) and 0.82 (s, 9H, CH₃). ppm.

¹³C NMR (CDCl₃): 146.3, 128.7 (2C), 127.2, 126.8 (2C), 63.7, 49.8, 48.8, 36.0, 33.9, 32.3, 27.3 (3C), 26.3 ppm.

ν_{\max} (cm⁻¹): 2937, 1438, 1363, 752, 698.

HR-MS (NSI): *m/z* calculated for M = C₁₆H₂₅N, theoretical [M+H]⁺: 232.2060. Found: 232.2062.

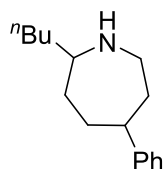
Entry 2 in Table 9.34

Following general procedure Z for the reductive aminocyclisation of aldehyde-ketones, data is presented in the following format: : (a) amount of ammonia, (b) substrate, (c) solvent for reducing agent, (d) solvent for substrate solution, (e) addition time of substrate solution and (f) yield of product **179**.

(a) NH₃ (0.11 mL, c = 7 mmol/mL in MeOH, 0.75 mmol, 5 eq.), (b) aldehyde-ketone **176b** (32 mg, 0.15 mmol, 1.0 eq.), (c) DCM (2 mL), (d) MeOH (4 mL), (e) 0.5 h and (f) 11 mg (32%).

Characterisation of 5-(*tert*-butyl)-2-phenylazepane **176b**:

Obtained as a yellow oil.



176b

^1H NMR (CDCl_3): 7.22-7.16 (m, 2H, ArH), 7.15-7.10 (m, 2H, ArH), 7.09-7.05 (m, 1H, ArH), 4.39 (br s, 1H, NH), 3.20 (dt, $J = 13.4$ Hz, 3.9 Hz, 1H, NCHPh), 2.95-2.85 (m, 1H, NCHH), 2.75-2.59 (m, 2H, NCHH, CH_2), 1.97-1.82 (m, 3H, CH, CH_2), 1.80-1.65 (m, 2H, CH_2), 1.57-1.49 (m, 2H, CH_2), 1.34-1.21 (m, 5H, CH_2) and 0.83 (t, $J = 7.2$ Hz, 3H, CH_3). ppm.

^{13}C NMR (CDCl_3): 148.4, 128.5 (2C), 126.8 (2C), 126.0, 58.4, 47.6, 46.3, 39.2, 36.4, 32.1, 31.5, 28.7, 22.8, 14.2 ppm.

$\nu_{\text{max}}(\text{cm}^{-1})$: 2951, 2924, 2854, 1450, 754, 698.

HR-MS (NSI): m/z calculated for $\text{M} = \text{C}_{16}\text{H}_{25}\text{N}$, theoretical $[\text{M}+\text{H}]^+$: 232.2060. Found: 232.2060.

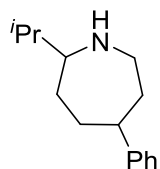
Entry 3 in Table 9.34

Following general procedure Z for the reductive aminocyclisation of aldehyde-ketones, data is presented in the following format: : (a) amount of ammonia, (b) substrate, (c) solvent for reducing agent, (d) solvent for substrate solution, (e) addition time of substrate solution and (f) yield of product **180**.

(a) NH_3 (0.11 mL, $c = 7$ mmol/mL in MeOH, 0.75 mmol, 5 eq.), (b) aldehyde-ketone **177b** (32 mg, 0.15 mmol, 1.0 eq.), (c) DCM (2 mL), (d) MeOH (4 mL), (e) 0.5 h and (f) 11 mg (32%).

Characterisation of 2-*iso*-propyl-5-phenylazepane **180**:

Obtained as a yellow oil.



180

^1H NMR (CDCl_3): 7.22-7.16 (m, 2H, ArH), 7.14-7.09 (m, 2H, ArH), 7.09-7.05 (m, 1H, ArH), 3.71 (br s, 1H, NH), 3.25 (dt, $J = 13.4$ Hz, 3.7 Hz, 1H, NCHPh), 2.75-2.61 (m, 1H, CH, CH_2), 1.99-1.62 (m, 8H, CH_2), 0.96-0.88 (m, 1H, CH), 0.90 (d, $J = 1.3$ Hz, 3H, CH_3). and 0.89 (d, $J = 1.3$ Hz, 3H, CH_3). ppm.

^{13}C NMR (CDCl_3): 148.9, 128.6 (2C), 126.8 (2C), 126.0, 64.4, 49.4, 45.7, 39.8, 33.7, 32.8, 29.3, 19.3, 18.7 ppm.

ν_{max} (cm^{-1}): 2953, 2924, 1450, 754, 698.

HR-MS (NSI): m/z calculated for $\text{M} = \text{C}_{15}\text{H}_{23}\text{N}$, theoretical $[\text{M}+\text{H}]^+$: 218.1904. Found: 218.1903.

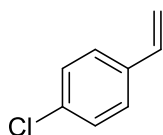
Asymmetric deprotonation of cyclobutanones

Entry 1 in Table 9.35

Following General Procedure AB, data is presented in the following format: (a) amount of methyltriphenylphosphonium bromide, (b) amount of THF, (c) amount of n-butyllithium, (d) amount of substrate, and (e) yield.

(a) 10.72 g, 1.5 eq., 30 mmol, (b) 162 mL, (c) 10.4 mL, $c = 2.50$ mmol/mL in hexane, 1.3 eq., 26 mmol, (d) 4-chlorobenzaldehyde (2.81 g, 1.0 eq., 20 mmol) and (e) 1.21 g (44%).

Synthesis of 1-chloro-4-vinylbenzene **181c**¹⁴⁵



181c

Obtained as a colourless oil.

^1H NMR (CDCl_3): 7.28-7.17 (m, 4H, ArH), 6.59 (dd, $J = 17.3$ Hz, $J = 10.9$ Hz, 1H, $\text{H}_2\text{C}=\text{CH}$), 5.65 (d, $J = 17.3$ Hz, 1H, $\text{H}_2\text{C}=\text{CH}$), 5.15 ppm (d, $J = 10.9$ Hz, 1H, $\text{H}_2\text{C}=\text{CH}$).

^{13}C NMR (CDCl_3): 136.3, 135.9, 133.6 (2C), 128.9 (2C), 127.6, 114.7 ppm.

ν_{max} (cm^{-1}): 3088, 2956, 1629, 1490, 1395, 1090, 1012, 911, 823.

Entry 2 in Table 9.35

Following General Procedure AB, data is presented in the following format: (a) amount of methyltriphenylphosphonium bromide, (b) amount of THF, (c) amount of n-butyllithium, (d) amount of substrate, and (e) yield.

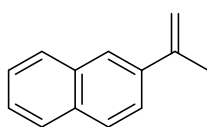
(a) 21.43 g, 1.5 eq., 60 mmol, (b) 324 mL, (c) 20.8 mL, $c = 2.50$ mmol/mL in hexane, 1.3 eq., 52 mmol, (d) 4-chlorobenzaldehyde, 5.62 g, 1.0 eq., 40 mmol, and (e) 3.45 g (63%).

Entry 3 in Table 9.35

Following General Procedure AB, data is presented in the following format: (a) amount of methyltriphenylphosphonium bromide, (b) amount of THF, (c) amount of n-butyllithium, (d) amount of substrate, and (e) yield.

(a) 15.43 g, 1.5 eq., 43 mmol, (b) 232 mL, (c) 14.8 mL, $c = 2.50$ mmol/mL in hexane, 1.3 eq., 37 mmol, (d) 1-(naphthalen-2-yl)ethan-1-one, 4.77 g, 1.0 eq., 28 mmol, and (e) 4.05 g (86%).

Synthesis of 2-(prop-1-en-2-yl)naphthalene 181e¹⁰³



181e

Obtained as a white solid.

Melting Point: 52-54 °C. Lit. 54-55 °C.¹⁰³

¹H NMR (CDCl₃): 7.85-7.75 (m, 4H, ArH), 7.64 (m, 1H, ArH), 7.48-7.40 (m, 2H, ArH) 5.51 (s, 1H, H₂C=C), 5.18 (m, 1H, H₂C=C), 2.22 (s, 3H, CH₃) ppm.

¹³C NMR (CDCl₃): 136.9, 134.9, 133.5, 133.1, 128.1, 128.0, 127.6, 126.4, 126.2, 125.8, 123.0, 114.1, 21.9 ppm.

ν_{\max} (cm⁻¹): 3051, 2920, 1456, 1435, 1375, 1274, 1134, 952, 881, 821.

Scheme 9.68

A solution of copper(II) sulfate pentahydrate (0.76 g, 3 mol%, 3 mmol) in water (5 mL) was added in two portions, with a 1 min interval, to a stirred suspension of zinc dust (6.50 g, 100 mmol, 1.0 eq.) in water (10 mL). The resulting mixture was stirred for 5 minutes before being filtered, and the solid

phase was washed with water (2 × 5 mL), acetone (2 × 5 mL) and diethyl ether (5 mL). The solid was then dried at 100 °C *in vacuo* for 16 h and then stored under an argon atmosphere until ready to use.

Entry 1 in Table 9.36

Following General Procedure AC, data is presented in the following format: (a) amount of diethyl ether, (b) amount of zinc-copper couple, (c) amount of substrate, (d) amount of trichloroacetyl chloride, (e) amount of phosphoryloxy(V) trichloride, and (f) mass of crude product (conversion).

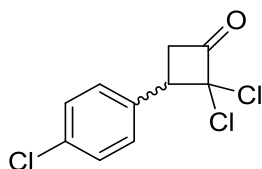
(a) 16 mL, (b) 0.71 g, 10.8 mmol, 3 eq., (c) 1-chloro-4-vinylbenzene, 0.86 mL, 3.6 mmol, 1.0 eq., (d) 1.00 mL, 9 mmol, 2.5 eq., (e) 0.83 mL, 9 mmol, 2.5 eq., and (f) 385 mg (conv. 43%).

Entry 2 in Table 9.36

Following General Procedure AC, data is presented in the following format: (a) amount of diethyl ether, (b) amount of zinc-copper couple, (c) amount of substrate, (d) amount of trichloroacetyl chloride, (e) amount of phosphoryloxy(V) trichloride, and (f) mass of crude product (conversion).

(a) 100 mL, (b) 4.89 g, 69.0 mmol, 3 eq., (c) 1-chloro-4-vinylbenzene, 2.75 mL, 23 mmol, 1.0 eq., (d) 6.50 mL, 58 mmol, 2.5 eq., (e) 5.41 mL, 58 mmol, 2.5 eq., and (f) 3.59 g (conv. 63%).

Characterisation of 2,2-dichloro-3-(4-chlorophenyl)cyclobutan-1-one **181c**¹⁶⁹



181c

Obtained as a colourless oil.

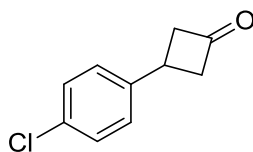
¹H NMR (CDCl₃): 7.34-7.30 (m, 2H, ArH), 7.18-7.10 (m, 2H, ArH), 4.12 (dd, *J* = 10.4 Hz, *J* = 10.2 Hz, 1H, PhCH), 3.59 (t, ²*J* = 10.2, *J* = 10.2 Hz, 1H, CH₂), 3.47 ppm (dd, ²*J* = 10.4, *J* = 10.2 Hz, 1H, CH₂).

Entry 1 in Table 9.37

Following General Procedure AD, data is presented in the following format: (a) amount of acetic acid, (b) amount of zinc dust, (c) amount of substrate, and (d) yield of product.

(a) 10 mL, (b) 0.61 g, 9.24 mmol, 6 eq., (c) crude 2,2-dichloro-3-(4-chlorophenyl)cyclobutan-1-one, 385 mg, 1.54 mmol, 1.0 eq., and (d) 104 mg, 37% yield.

Synthesis of 3-(4-chlorophenyl)cyclobutan-1-one **135c**¹⁷⁰



135c

Appearance: colourless oil.

¹H NMR (CDCl₃): 7.38-7.28 (m, 2H, ArH), 7.25-7.19 (m, 2H, ArH), 3.69-3.59 (m, 1H, PhCH), 3.54-3.43 (m, 2H, CH₂), 3.54-3.43 ppm (m, 2H, CH₂).

¹³C NMR (CDCl₃): 205.7, 142.5, 132.3, 129.1, 128.1, 55.0, 28.2 ppm.

ν_{\max} (cm⁻¹): 2920, 1780, 1710, 1491, 1377, 1197, 1069, 1012, 817.

Entry 2 in Table 9.37

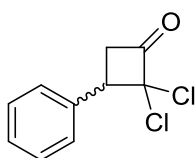
Following General Procedure AD, data is presented in the following format: (a) amount of acetic acid, (b) amount of zinc dust, (c) amount of substrate, and (d) yield of product.

(a) 90 mL, (b) 5.62 g, 86 mmol, 6 eq., (c) crude 2,2-dichloro-3-(4-chlorophenyl)cyclobutan-1-one, 3.59 g, 14.4 mmol, 1.0 eq., and (d) 2.04 g, 78% yield.

Scheme 9.71

Following General Procedure AC, data is presented in the following format: (a) amount of diethyl ether, (b) amount of zinc-copper couple, (c) amount of substrate, (d) amount of trichloroacetyl chloride, (e) amount of phosphoryloxy(V) trichloride and (f) mass of crude product (conversion).

(a) 150 mL, (b) 10.63 g, 150 mmol, 3 eq., (c) styrene, 5.73 mL, 50 mmol, 1.0 eq., (d) 13.95 mL, 125 mmol, 2.5 eq., (e) 11.65 mL, 125 mmol, 2.5 eq., and (f) 7.42 g (conv. 69%).



182a

Characterisation of 2,2-dichloro-3-phenylcyclobutan-1-one **182a**¹⁰³

Obtained as a colourless oil.

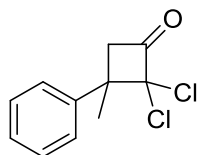
^1H NMR (CDCl_3): 7.46-7.34 (m, 3H, ArH), 7.32-7.28 (m, 2H, ArH), 4.23 (d, $J = 10.6$ Hz, $J = 10.2$ Hz, 1H, PhCH), 3.71 (dd, $^2J = 10.6$, $J = 10.0$ Hz, 1H, CH_2), 3.53 (dd, $^2J = 10.2$, $J = 10.0$ Hz, 1H, CH_2) ppm.

Scheme 9.71

Following General Procedure AC, data is presented in the following format: (a) amount of diethyl ether, (b) amount of zinc-copper couple, (c) amount of substrate, (d) amount of trichloroacetyl chloride, (e) amount of phosphoryloxy(V) trichloride, and (f) mass of crude product (conversion).

(a) 150 mL, (b) 10.63 g, 150 mmol, 3 eq., (c) α -methylstyrene 6.50 mL, 50 mmol, 1.0 eq., (d) 13.95 mL, 125 mmol, 2.5 eq., (e) 11.65 mL, 125 mmol, 2.5 eq., and (f) 10.34 g, (conv. 90%).

Characterisation of 2,2-dichloro-3-methyl-3-phenylcyclobutan-1-one **182b**¹⁰³



182b

Obtained as colourless oil.

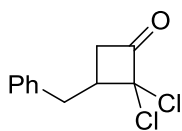
^1H NMR (CDCl_3): 7.43-7.37 (m, 2H, ArH), 7.37-7.32 (m, 1H, ArH), 7.28-7.23 (m, 2H, ArH), 3.97 (d, $^2J = 16.5$ Hz, 1H, CH_2), 3.06 ppm (d, $^2J = 16.5$ Hz, 1H, CH_2), 1.45 (s, 3H, CH_3) ppm.

Scheme 9.71

Following General Procedure AC, data is presented in the following format: (a) amount of diethyl ether, (b) amount of zinc-copper couple, (c) amount of substrate, (d) amount of trichloroacetyl chloride, (e) amount of phosphoryloxy(V) trichloride, and (f) mass of crude product (conversion).

(a) 150 mL, (b) 10.63 g, 150 mmol, 3 eq., (c) benzylstyrene, 6.50 mL, 50 mmol, 1.0 eq., (d) 13.95 mL, 125 mmol, 2.5 eq., (e) 11.65 mL, 125 mmol, 2.5 eq., and (f) 6.93 g (conv. 60%).

Characterisation of 2,2-dichloro-3-methyl-3-(naphthalen-2-yl)cyclobutan-1-one **182d**¹⁰³



182d

Obtained as a colourless oil.

^1H NMR (CDCl_3): 7.34-7.15 (m, 5H, ArH), 3.39-3.29 (m, 2H, PhCH_2), 3.24-3.16 (m, 1H, PhCH_2CH), 3.06 (dd, $^2J = 9.2$ Hz, $J = 8.0$ Hz, 1H, CH_2), 2.81 (dd, $^2J = 9.2$ Hz, $J = 8.0$ Hz, 1H, CH_2) ppm.

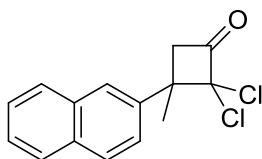
Scheme 9.71

Following General Procedure AC, data is presented in the following format: (a) amount of diethyl ether, (b) amount of zinc-copper couple, (c) amount of substrate, (d) amount of trichloroacetyl chloride, (e) amount of phosphoryloxy(V) trichloride, and (f) mass of crude product (conversion).

(a) 100 mL, (b) 6.38 g, 90 mmol, 3 eq., (c) 2-(prop-1-en-2-yl)naphthalene, 5.04 g, 30 mmol, 1.0 eq., (d) 8.37 mL, 75 mmol, 2.5 eq., (e) 7.00 mL, 75 mmol, 2.5 eq., and (f) 6.43 g (conv. 81%).

Characterisation of 2,2-dichloro-3-methyl-3-(naphthalen-2-yl)cyclobutan-1-one **182e**¹⁰³

Obtained as colourless oil.



182e

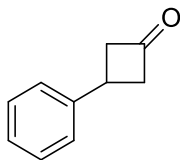
^1H NMR (CDCl_3): 7.92-7.73 (m, 3H, ArH), 7.63 (s, 1H, ArH), 7.50-7.34 (m, 3H, ArH), 4.13 (d, $^2J = 16.4$ Hz, 1H, CH_2), 3.17 (d, $^2J = 16.4$ Hz, 1H, CH_2), 1.75 (s, 3H, CH_3) ppm.

Scheme 9.72

Following General Procedure AD, data is presented in the following format: (a) amount of acetic acid, (b) amount of zinc dust, (c) amount of substrate, and (d) yield of product.

(a) 215 mL, (b) 13.53 g, 207 mmol, 6 eq., (c) crude 2,2-dichloro-3-phenylcyclobutan-1-one, 7.42 g, 34.5 mmol, 1.0 eq., and (d) 3.34 g, 66% yield.

Characterisation of 3-phenylcyclobutan-1-one **135a**¹⁷⁰



135a

Obtained as a colourless oil.

¹H NMR (CDCl₃): 7.31-7.15 (m, 5H, ArH), 3.65-3.55 (m, 1H, PhCH), 3.47-3.36 (m, 2H, CH₂), 3.23-3.12 (m, 2H, CH₂) ppm.

¹³C NMR (CDCl₃): 207.0, 143.7, 128.3, 126.9, 126.7, 54.9, 28.7 ppm.

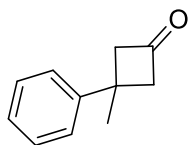
ν_{\max} (cm⁻¹): 3026, 2091, 1774, 1496, 1452, 1379, 1097, 910, 731.

Scheme 9.72

Following General Procedure AD, data is presented in the following format: (a) amount of acetic acid, (b) amount of zinc dust, (c) amount of substrate, and (d) yield of product.

(a) 215 mL, (b) 14 g, 214 mmol, 6 eq., (c) crude 2,2-dichloro-3-methyl-3-phenylcyclobutan-1-one, 8.16 g, 35.6 mmol, 1.0 eq., and (d) 2.48 g, 46% yield.

Characterisation of 3-methyl-3-phenylcyclobutan-1-one **135b**¹⁷⁰



135b

Obtained as a colourless oil.

¹H NMR (CDCl₃): 7.34-7.20 (m, 4H, ArH), 7.20-7.14 (m, 1H, ArH), 3.43-3.34 (m, 2H, CH₂), 3.07-2.98 (m, 2H, CH₂), 1.52 (s, 3H, CH₃) ppm.

^{13}C NMR (CDCl_3): 206.8, 148.3, 128.7, 126.4, 125.8, 59.4, 34.1, 31.3 ppm.

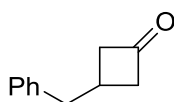
ν_{max} (cm^{-1}): 2954, 1778, 1444, 1379, 1300, 1139, 1078, 1028, 869.

Scheme 9.72

Following General Procedure AD, data is presented in the following format: (a) amount of acetic acid, (b) amount of zinc dust, (c) amount of substrate, and (d) yield of product.

(a) 100 mL, (b) 6.62 g, 101 mmol, 6 eq., (c) crude 2,2-dichloro-3-benzylcyclobutan-1-one, 3.86 g, 17 mmol, 1.0 eq., and (d) 1.25 g, 46% yield.

Synthesis of 3-benzylcyclobutan-1-one **135d**¹⁷¹



135d

Obtained as a colourless oil.

^1H NMR (CDCl_3): 7.27-7.20 (m, 3H, ArH), 7.19-7.09 (m, 2H, ArH), 3.11-3.01 (m, 2H, CH_2), 2.83-2.76 (d, $J = 7.2$ Hz, 2H, PhCH_2), 2.76-2.59 (m, 3H, $\text{CH}+\text{CH}_2$) ppm.

^{13}C NMR (CDCl_3): 207.9, 140.2, 128.8, 128.7, 126.6, 52.5, 42.1, 25.2 ppm.

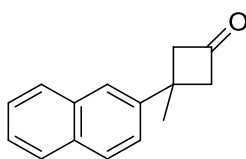
ν_{max} (cm^{-1}): 2910, 1774, 1600, 1496, 1452, 1379, 1097, 910, 731.

Scheme 9.72

Following General Procedure AD, data is presented in the following format: (a) amount of acetic acid, (b) amount of zinc dust, (c) amount of substrate, and (d) yield of product.

(a) 150 mL, (b) 9.55 g, 146 mmol, 6 eq., (c) crude 2,2-dichloro-3-methyl-3-(naphthalen-2-yl)cyclobutan-1-one, 6.44 g, 24 mmol, 1.0 eq., and (d) 1.11 g, 22% yield.

Characterisation of 3-methyl-3-(naphthalen-2-yl)cyclobutan-1-one **135e**¹⁷²



135e

Obtained as a colourless oil.

^1H NMR (CDCl_3): 7.87-7.79 (m, 3H, ArH), 7.71 (d, $J = 1.6$ Hz, 1H, ArH), 7.52-7.41 (m, 3H, ArH), 3.60-3.53 (m, 2H, CH_2), 3.22-3.15 (m, 2H, CH_2), 1.68 (s, 3H, CH_3) ppm.

^{13}C NMR (CDCl_3): 206.8, 145.1, 133.4, 132.1, 128.8, 127.9, 127.8, 126.7, 126.1, 124.7, 123.9, 59.5, 34.4, 31.1 ppm.

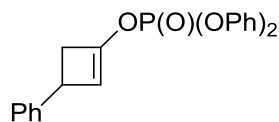
ν_{max} (cm^{-1}): 3054, 2957, 2921, 1782, 1600, 1505, 1378, 1297, 1200, 1131, 1077, 906.

Entry 1 in Table 9.38

Following General Procedure AE for the synthesis of racemic enol phosphates, data is presented in the following format: (a) amount of THF, (b) amount of di-*iso*-propylamine, (c) amount of *n*-butyllithium, (d) substrate, (e) amount of THF, (f) amount of diphenyl phosphoryl chloride, and (h) yield of product.

(a) 5 mL, (b) 0.14 mL, 1 mmol, 1.0 eq., (c) 0.40 mL, $c = 2.50$ mmol/mL in hexane, 1.0 mmol, 1.0 eq., (d) 3-phenylcyclobutan-1-one, 134 mg, 0.9 mmol, 0.9 eq., (e) 6 mL, (f) 0.21 mL, 1.0 mmol, 1.0 eq., and (h) 242 mg (80%).

Characterisation of rac-diphenyl (3-phenylcyclobut-1-en-1-yl) phosphate **136a**¹⁰³



136a

Obtained as colourless oil.

^1H NMR (CDCl_3): 7.39-7.31 (m, 4H, ArH), 7.28-7.16 (m, 11H, ArH), 5.57-5.53 (m, 1H, $\text{CH}=\text{C}$), 3.69-3.64 (m, 1H, CHPh), 3.28 (dd, $^2J = 4.5$ Hz, $J = 1.5$ Hz, 1H, CH_2), 2.58 (t, $^2J = 1.5$ Hz, $J = 1.5$ Hz, 1H, CH_2) ppm.

^{13}C NMR (CDCl_3): 150.5 (d, 1C, $^2J_{\text{C-P}} = 7.7$ Hz), 142.3, 141.7 (d, 2C, $^2J_{\text{C-P}} = 8.9$ Hz), 130.1, 128.6, 126.84, 126.80, 125.9, 120.3 (d, 4C, $^3J_{\text{C-P}} = 5.0$ Hz), 114.0 (d, 1C, $^2J_{\text{C-P}} = 7.2$ Hz), 43.1 (d, 1C, $^3J_{\text{C-P}} = 6.5$ Hz), 38.0 ppm.

^{31}P NMR (CDCl_3): -18.2 ppm

ν_{max} (cm^{-1}): 2927, 1629, 1589, 1487, 1300, 1282, 1269, 1219, 1180, 1161, 1024, 1008, 937, 904, 875, 823, 754.

Chiral HPLC: OD-J column, 1.40 mL/min, detector 254 nm, 10% IPA in hexane. $t_1 = 25.4$ min and $t_2 = 28.8$ min.

Entry 2 in Table 9.38

Following General Procedure AE for the synthesis of racemic enol phosphates, data is presented in the following format: (a) amount of THF, (b) amount of di-*iso*-propylamine, (c) amount of *n*-butyllithium, (d) substrate, (e) amount of THF, (f) amount of diphenyl phosphoryl chloride, and (h) yield of product.

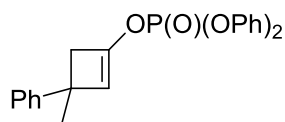
(a) 10 mL, (b) 0.28 mL, 2 mmol, 1.0 eq., (c) 0.80 mL, $c = 2.50$ mmol/mL in hexane, 2.0 mmol, 1.0 eq., (d) 3-methyl-3-phenylcyclobutan-1-one, 288 mg, 1.8 mmol, 0.9 eq., (e) 12 mL, (f) 0.42 mL, 2.0 mmol, 1.0 eq., and (g) 387 mg (64%).

Entry 3 in Table 9.38

Following General Procedure AE for the synthesis of racemic enol phosphates, data is presented in the following format: (a) amount of THF, (b) amount of di-*iso*-propylamine, (c) amount of *n*-butyllithium, (d) substrate, (e) amount of THF, (f) amount of diphenyl phosphoryl chloride, and (h) yield of product.

(a) 10 mL, (b) 0.28 mL, 2 mmol, 1.0 eq., (c) 0.80 mL, $c = 2.50$ mmol/mL in hexane, 2.0 mmol, 1.0 eq., (d) 3-methyl-3-phenylcyclobutan-1-one, 288 mg, 1.8 mmol, 0.9 eq., (e) 12 mL, (f) 0.42 mL, 2.0 mmol, 1.0 eq., and (g) 520 mg (67%).

Characterisation of diphenyl (3-phenylcyclobut-1-en-1-yl) phosphate **136b**¹⁰³



136b

Obtained as a colourless oil.

¹H NMR (CDCl₃): 7.60-7.36 (m, 1H, ArH), 7.46-7.15 (m, 14H, ArH), 6.71 (s, 1H, CH=C), 2.96 (d, ²J = 12.6 Hz, 1H, CH₂), 2.89 (d, ²J = 12.6 Hz, 1H, CH₂), 1.61 (s, 3H, CH₃) ppm.

^{13}C NMR (CDCl_3): 151.5 (d, 1C, $^2J_{\text{C-P}} = 7.5$ Hz), 146.4, 141.9 (d, 2C, $^2J_{\text{C-P}} = 12.2$ Hz), 130.1, 128.4, 126.3, 126.1, 125.9, 120.3 (d, 4C, $^3J_{\text{C-P}} = 6.0$ Hz), 118.0 (d, 1C, $^3J_{\text{C-P}} = 7.4$ Hz), 48.8 (d, 1C, $^3J_{\text{C-P}} = 5.6$ Hz), 42.3, 27.4 ppm.

^{31}P NMR (CDCl_3): -18.1 ppm

ν_{max} (cm^{-1}): 2958, 1645, 1631, 1589, 1487, 1300, 1276, 1265, 1205, 1182, 1161, 1078, 1066, 1024, 1008, 941, 904, 887, 873, 802, 754.

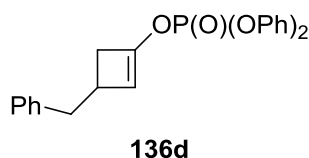
Chiral HPLC: OD-J column, 1.00 mL/min, detector 254 nm, 20% IPA in hexane. $t_1 = 24.3$ min and $t_2 = 25.5$ min.

Entry 4 in Table 9.38

Following General Procedure AE for the synthesis of racemic enol phosphates, data is presented in the following format: (a) amount of THF, (b) amount of di-*iso*-propylamine, (c) amount of *n*-butyllithium, (d) substrate, (e) amount of THF, (f) amount of diphenyl phosphoryl chloride, and (h) yield of product.

(a) 10 mL, (b) 0.28 mL, 2 mmol, 1.0 eq., (c) 0.80 mL, $c = 2.50$ mmol/mL in hexane, 2.0 mmol, 1.0 eq.), (d) 3-benzylcyclobutan-1-one, 288 mg, 1.8 mmol, 0.9 eq., (e) 12 mL, (f) 0.42 mL, 2.0 mmol, 1.0 eq., and (g) 536 mg (69%).

Characterisation of diphenyl (3-phenylcyclobut-1-en-1-yl) phosphate **136d**¹⁰³



Obtained as colourless oil.

^1H NMR (400 MHz, CDCl_3): 7.40-7.34 (m, 4H, ArH), 7.31-7.12 (m, 11H, ArH), 5.27 (m, 1H, CH=C), 2.91 (d, $J = 13.6$ Hz, 1H, CH_2), 2.78-2.71 (m, 3H, $\text{CH}+\text{CH}_2$), 2.43 (d, $^2J = 13.6$ Hz, 1H, CH_2) ppm.

^{13}C NMR (100 MHz, CDCl_3): 150.2 (d, 1C, $^2J_{\text{C-P}} = 7.3$ Hz), 141.1 (d, 2C, $^2J_{\text{C-P}} = 9.9$ Hz), 140.6, 130.1, 128.8, 128.6, 126.3, 125.9, 120.3 (4C, $^3J_{\text{C-P}} = 4.6$ Hz), 114.8 (1C, $^3J_{\text{C-P}} = 6.1$ Hz), 40.7, 38.9 (1C, $^3J_{\text{C-P}} = 6.0$ Hz), 35.3 ppm.

^{31}P NMR (162 MHz, CDCl_3): -18.1 ppm

$\nu_{\max}(\text{cm}^{-1})$: 2924, 1641, 1625, 1589, 1487, 1298, 1263, 1220, 1182, 1159, 1024, 1008, 995, 939, 904, 881, 819, 763, 754, 738, 700.

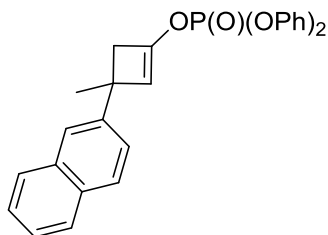
Chiral HPLC: OD-J column, 1.50 mL/min, detector 254 nm, 10% IPA in hexane. $t_1 = 14.1$ min and $t_2 = 18.7$ min.

Entry 5 in Table 9.38

Following General Procedure AE for the synthesis of racemic enol phosphates, data is presented in the following format: (a) amount of THF, (b) amount of di-*iso*-propylamine, (c) amount of *n*-butyllithium, (d) substrate, (e) amount of THF, (f) amount of diphenyl phosphoryl chloride, and (h) yield of product.

(a) 10 mL, (b) 0.28 mL, 2 mmol, 1.0 eq., (c) 0.80 mL, $c = 2.50$ mmol/mL in hexane, 2.0 mmol, 1.0 eq., (d) 3-methyl-3-(naphthalen-2-yl)cyclobutan-1-one (420 mg, 1.8 mmol, 0.9 eq.), (e) 12 mL, (f) 0.42 mL, 2.0 mmol, 1.0 eq. and (g) 547 mg (62%).

Characterisation of diphenyl (3-phenylcyclobut-1-en-1-yl) phosphate **136e**¹⁰³



136e

Obtained as colourless oil.

^1H NMR (400 MHz, CDCl_3): 7.81-7.74 (m, 3H, ArH), 7.67-7.65 (m, 1H, ArH), 7.50-7.45 (m, 3H, ArH), 7.34-7.28 (m, 5H, ArH), 7.25-7.16 (m, 5H, ArH), 5.69 (s, 1H, CH=C), 2.96-2.94 (m, 2H, CH_2), 1.63 (s, 3H, CH_3) ppm.

^{13}C NMR (100 MHz, CDCl_3): 150.5 (d, 1C, $^2J_{\text{C-P}} = 7.3$ Hz), 143.8, 142.0 (d, 2C, $^2J_{\text{C-P}} = 10.0$ Hz), 133.4, 132.1, 130.1, 128.0, 127.9, 127.7, 126.3, 125.9, 125.7, 124.9, 124.2, 120.3 (1C, $^3J_{\text{C-P}} = 5.5$ Hz), 117.9 (4C, $^3J_{\text{C-P}} = 8.1$ Hz), 48.6 (1C, $^3J_{\text{C-P}} = 5.4$ Hz), 42.4, 27.1 ppm.

^{31}P NMR (162 MHz, CDCl_3): -18.1 ppm

$\nu_{\max}(\text{cm}^{-1})$: 2958, 1647, 1629, 1589, 1487, 1300, 1278, 1265, 1205, 1182, 1159, 1089, 1068, 1024, 1008, 941, 900, 885, 869, 854, 815, 765, 746.

Chiral HPLC: OD-J column, 1.40 mL/min, detector 254 nm, 40% IPA in hexane. t_1 = 20.0 min and t_2 = 38.4 min.

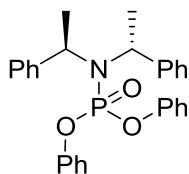
Asymmetric deprotonation of cyclobutanones

Scheme 9.74

Following General Procedure AF for the synthesis of chiral enol phosphates, data is presented in the following format: (a) substrate, (b) addition temperature of electrophile, (c) conversion, (d) yield of product, and (e) e.r.

(a) 3-phenylcyclobutan-1-one (117 mg, 0.8 mmol, 0.8 eq.), (b) rt, (c) 12%, (d) by-product **288** was coeluted with the desired product **136a**, and (e) -.

Characterisation of **288**:



288

^1H NMR (400 MHz, CDCl_3): 7.38-7.05 (m, 20H, ArH), 3.79 (q, J = 7.0 Hz, 2H, CH_3CH), 1.85 (d, 6H, J = 7.0 Hz, 6H, CH_3CH) ppm.

Scheme 9.75

Following General Procedure AF for the synthesis of chiral enol phosphates, data is presented in the following format: (a) substrate, (b) addition temperature of electrophile, (c) conversion, (d) yield of product, and (e) e.r.

(a) 3-phenylcyclobutan-1-one (117 mg, 0.8 mmol, 0.8 eq.), (c) rt, (d) 10%, (e) by-product **288** was coeluted with the desired product **136a**, and (f) -.

Entry 1 in Table 9.39

Following General Procedure AF for the synthesis of chiral enol phosphates, data is presented in the following format: (a) substrate, (b) addition temperature of electrophile, (c) conversion, (d) yield of product, and (e) e.r.

(a) 3-phenylcyclobutan-1-one (117 mg, 0.8 mmol, 0.8 eq.), (c) -78 °C, (d) 75%, (e) 173 mg, 57% yield, and (f) 59:41.

Entry 2 in Table 9.39

Following General Procedure AF for the synthesis of chiral enol phosphates, data is presented in the following format: (a) substrate, (b) addition temperature of electrophile, (c) conversion, (d) yield of product, and (e) e.r.

(a) 3-phenylcyclobutan-1-one, 117 mg, 0.8 mmol, 0.8 eq., (c) -78 °C, (d) 166 mg, 55% yield, and (e) 55:45.

Scheme 9.77

Following General Procedure AF for the synthesis of chiral enol phosphates, with the exception of, quenching the reaction with methanol (10 mL) instead of saturated sodium bicarbonate solution, data is presented in the following format: (a) substrate, (c) addition temperature of electrophile, (d) conversion, (e) yield of product, and (f) enantiomeric ratio.

(a) 3-phenylcyclobutan-1-one, 117 mg, 0.8 mmol, 0.8 eq., (c) -78°C, (d) >99%, (e) 179 mg, 55% yield, and (e) 62:38.

Entry 1 in Table 9.40

Following General Procedure AG for the synthesis of chiral enol phosphates, data is presented in the following format: (a) substrate, (b) addition temperature of electrophile, (c) conversion, (d) yield of product, and (e) e.r.

(a) 3-phenylcyclobutan-1-one, 117 mg, 0.8 mmol, 0.8 eq., (c) -78°C, (d) >99%, (e) 142 mg, 47% yield, and (e) 66:34.

Entry 2 in Table 9.40

Following General Procedure AG for the synthesis of chiral enol phosphates, data is presented in the following format: (a) substrate, (b) addition temperature of electrophile, (c) conversion, (d) yield of product, and (e) e.r.

(a) 3-phenylcyclobutan-1-one, 117 mg, 0.8 mmol, 0.8 eq., (c) -78°C, (d) >99%, (e) 157 mg, 52% yield, and (e) 62:38.

Scheme 9.79 (*re-distilling the starting cyclobutanone over calcium hydride*)

Following General Procedure AF for the synthesis of chiral enol phosphates, data is presented in the following format: (a) substrate, (b) addition temperature of electrophile, (c) conversion, (d) yield of product, and (e) e.r.

(a) 3-phenylcyclobutan-1-one (117 mg, 0.8 mmol, 0.8 eq.), (c) -78°C, (d) >99%, (e) 142 mg (47%), and (e) 58:42.

Entry 1 in Table 9.41

Following General Procedure AF for the synthesis of chiral enol phosphates, data is presented in the following format: (a) substrate, (b) addition temperature of electrophile, (c) yield of product, and (d) e.r.

(a) 3-methyl-3-phenylcyclobutan-1-one (128 mg, 0.8 mmol, 0.8 eq.), (b) -78 °C, (c) 138 mg (44%), and (e) 57:43.

Chiral analysis: HPLC OD-J column, 1.00 mL/min, detector 254 nm, 20% IPA in hexane. t_1 = 24.3 min (major) and t_2 = 25.5 min (minor).

Entry 2 in Table 9.41

Following General Procedure AF for the synthesis of chiral enol phosphates, data is presented in the following format: (a) substrate, (b) addition temperature of electrophile, (c) yield of product, and (d) e.r.

(a) 3-benzylcyclobutan-1-one (128 mg, 0.8 mmol, 0.8 eq.), (b) -78 °C, (c) 138 mg (44%), and (d) 59:41.

Chiral HPLC: OD-J column, 1.50 mL/min, detector 254 nm, 10% IPA in hexane. t_1 = 14.1 min (minor) and t_2 = 18.7 min (major).

Entry 3 in Table 9.41

Following General Procedure AF for the synthesis of chiral enol phosphates, data is presented in the following format: (a) substrate, (b) addition temperature of electrophile, (c) yield of product, and (d) e.r.

(a) 2-naphthyl-3-methyl-cyclobutan-1-one (128 mg, 0.8 mmol, 0.8 eq.), (b) -78 °C, (c) 119 mg (38%), and (d) 59:41.

Chiral analysis: HPLC OD-J column, 1.40 mL/min, detector 254 nm, 40% IPA in hexane. t_1 = 20.0 min (major) and t_2 = 38.4 min (minor).

Scheme 9.81

Following General Procedure AE for the synthesis of racemic enol phosphates, data is presented in the following format: (a) amount of THF, (b) amount of di-*iso*-propylamine, (c) amount of *n*-butyllithium, (d) substrate, (e) amount of THF, (f) amount of diphenyl phosphoryl chloride, and (h) yield of product.

(a) 10 mL, (b) 0.28 mL, 2 mmol, 1.0 eq., (c) 0.80 mL, c = 2.50 mmol/mL in hexane, 2.0 mmol, 1.0 eq., (d) 4-*tert*-butyl-cyclohexanone (308 mg, 1.8 mmol, 0.9 eq.), (e) 12 mL, (f) 0.42 mL, 2.0 mmol, 1.0 eq., and (h) 472 mg (64%).

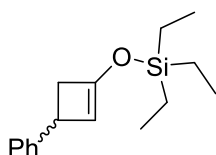
Scheme 9.82

A Schlenk flask was equipped with a stirrer bar and a suba seal, and flame dried. A solution of di-*n*-butyl-magnesium (1 mL, c = 1 mmol/mL in heptane, 1 mmol, 1.0 eq.) was added and the solvent was removed *in vacuo*. The residue was dried under vacuum for 1 h. The flask was purged with argon and THF (10 mL) was added. Then (*R*)-bis((*R*)-1-phenylethyl)amine (0.46 mL, 2.0 mmol, 2.0 eq.) was added and the suba seal was swapped for a cold finger. The reaction was refluxed for 90 min and, subsequently, the mixture was allowed to cool to room temperature. Complete formation of the magnesium bisamide was assumed. Half of this solution (5 mL) was transferred to a flame-dried Schlenk flask and the other half (5 mL) was used in the deprotonation of 3-phenyl-cyclobutanone (see **Scheme 10.36** below). The solution was cooled to -78 °C and diphenyl phosphoryl chloride (0.42 mL, 2 mmol, 2.0 eq.) was added. The substrate **135a** or **115a** (0.8 mmol, 0.8 eq) was dissolved in THF (2 mL) and added dropwise to the solution of magnesium amide (1.0 mmol, 1.0 eq.) in THF over 1 h *via* a syringe pump. The reactions were stirred at -78 °C for a further 16 h. After this time, the reaction were quenched with sat. sodium bicarbonate solution (10 mL), the aqueous phase was extracted with diethyl ether (3 × 10 mL), and the organic phase were collected. The organic phase were washed with 1N HCl (10 mL) then dried over sodium sulfate, filtered, and the solvent was evaporated *in vacuo*. The crude product was purified by flash column chromatography using 0-20% diethyl ether in petrol ether as the eluent, to give **115a** as a colourless oil (194 mg, 66%, 96:4 e.r.) and **136a** as a colourless oil (133 mg, 44%, 68:42 e.r.)

Scheme 9.84

A round-bottom flask was equipped with a stirrer bar, charged with sodium iodide (90 mg, 0.6 mmol, 1.2 eq.) before being flame-dried carefully and allowed to cool under an argon atmosphere. Acetonitrile (1.4 mL) was added and the reaction mixture was cooled to 0 °C with an ice bath. Triethylsilyl chloride (0.082 mL, 0.65 mmol, 1.3 eq.) and 3-phenylcyclobutanone (73 mg, 0.5 mmol, 1.0 eq.) in acetonitrile (0.2 mL) were added and the colour of the solution turned from colourless to yellow. Thereafter, triethylamine (0.081 mL, 0.58 mmol, 1.17 eq.) was added dropwise. The colour of the solution changed to brown and the reaction was allowed to warm to room temperature before stirring for a further 6 h. To the crude mixture, diethyl ether (10 mL) was added and the organic phase was washed with water (10 mL). The organic phase was dried over sodium sulfate, filtered, and the solvent was evaporated *in vacuo*. The crude product was purified by flash column chromatography using 1% diethyl ether in petrol ether as the eluent and the desired final product was obtained as a colourless oil (10 mg, 8% yield).

Characterisation of racemic triethyl((3-phenylcyclobut-1-en-1-yl)oxy)silane **184a**⁵¹



184a

¹H NMR (CDCl₃): 7.23-7.20 (m, 4H, ArH), 7.14-7.08 (m, 1H, ArH), 4.79 (d, *J* = 0.8 Hz, 1H, CH=C), 3.60-3.55 (m, 1H, PhCH), 3.03 (dd, ²*J* = 12.9 Hz, *J* = 4.7 Hz, 1H, CH₂), 2.31 (dd, ²*J* = 12.9 Hz, *J* = 1.4 Hz, 1H, CH₂), 0.96 (t, *J* = 7.8 Hz, 9H, CH₂CH₃), 0.67 (q, *J* = 7.8 Hz, 6H, CH₂CH₃) ppm.

¹³C NMR (CDCl₃): 156.2, 128.4, 126.8 (2C), 126.3 (2C), 126.0, 106.2, 44.4, 29.9, 6.8 (3C), 5.0 (3C) ppm.

ν_{\max} (cm⁻¹): 2953, 2918, 2875, 1639, 1622, 1456, 1286, 1271, 1238, 1215, 1093, 1066, 1016, 997, 983, 946, 835, 794, 731.

Scheme 9.85 (using chiral lithium base (*R,R*)-**4**)

A Schlenk flask was equipped with a stirrer bar and fitted with a suba seal. The flask was flame-dried allowed to cool to room temperature before the addition of (*R,R*)-bis(1-phenylethyl)amine (0.08 mL, 0.31 mmol, 1.25 eq.) and THF (5 mL). The mixture was cooled to -78 °C, then *n*-butyllithium (0.12 mL, *c* = 2.5 M in hexane, 0.3 mmol, 1.2 eq.) was added dropwise and the mixture was cooled further to -85 °C with a cryo-cooler unit. Triethylsilyl chloride (0.07 mL, 0.5 mmol, 2.0 eq.) was added and the reaction mixture stirred for 30 min. Finally, 4-phenylcyclobutanone (37 mg, 0.25 mmol, 1.0 eq.) was added as a solution in THF (0.5 mL) over 1 h and the reaction was stirred for a further 16 h at -85 °C.

The reaction was quenched with water (5 mL) and extracted with diethyl ether (3 × 5 mL). The organic phases were combined, dried over sodium sulfate, filtered, and the solvent was evaporated *in vacuo*. The crude product was purified by flash column chromatography using 1% diethyl ether in petrol ether as the eluent. To obtain the desired product **184a** (57 mg, 87% yield, 90:10 e.r.).

Chiral HPLC: OD-J column, 0.40 mL/min, hexane. t_1 = 32.5 min (minor) and t_2 = 33.9 min (major)

Scheme 9.86 (using chiral magnesium base (*R,R*)-**63**)

A Schlenk flask was equipped with a stirrer bar and a suba seal, and flame dried. A solution of di-*n*-butyl-magnesium (1 mL, $c = 1$ mmol/mL in heptane, 1 mmol, 1.0 eq.) was added and the solvent was removed *in vacuo*. The residue was dried under vacuum for 1 h. The flask was purged with argon and THF (10 mL) was added. Then (*R*)-bis((*R*)-1-phenylethyl)amine (0.46 mL, 2.0 mmol, 2.0 eq.) was added and the suba seal was swapped for a cold finger. The reaction was refluxed for 90 min and, subsequently, the mixture was allowed to cool to room temperature. Complete formation of the magnesium bisamide was assumed. The solution was cooled to -85 °C with a cryo-cooler unit triethylsilyl chloride (0.26 mL, 2.0 mmol, 2.0 eq.) was added and 3-phenylcyclobutanone (118 mg, 0.80 mmol, 1.0 eq.) was added as a solution in THF (2 mL) over 1 h. The reaction was stirred for a further 16 h at -85°C. After this time, the reaction was quenched with water (5 mL) and extracted with diethyl ether (3 × 5 mL). The organic phase was then dried over sodium sulfate, filtered and the solvent was evaporated *in vacuo*. The desired product was not observed *via* analysis of the crude ¹H NMR spectrum.

Entry 1 in Table 9.42

Following General Procedure AJ for the cross coupling of enol phosphates, data is presented in the following format: (a) substrate, (b) catalyst, (c) amount of diethyl ether, (d) volume of Grignard reagent, and (e) yield of product.

(a) Diphenyl (3-phenylcyclobut-1-en-1-yl) phosphate **136a** (107 mg, 0.28 mmol, 1.0 eq.), (b) PEPPSI ^{*i*}Pr (2 mg, 0.0025 mmol, 1.0 mol%), (c) 1.5 mL, (d) phenylmagnesium bromide (0.42 mL, $c = 1$ M in THF, 0.42 mmol, 1.5 eq.), and (e) 47 mg (82%).

Characterisation of cyclobut-1-ene-1,3-diyldibenzene **137a** :¹⁰³



137a

Obtained as a colourless oil.

^1H NMR (400 MHz, CDCl_3): 7.40-7.33 (m, 2H, ArH), 7.32-7.19 (m, 7H, ArH), 7.19-7.14 (m, 1H, ArH), 6.47 (d, $J = 1.6$ Hz, 1H, CH=C), 4.04 (m, 1H, PhCH), 3.25 (dd, $^2J = 12.6$ Hz, $J = 5.0$ Hz, 1H, CH), 2.59 (dd, $^2J = 12.6$ Hz, $J = 1.6$ Hz, 1H, CH) ppm.

^{13}C NMR (100 MHz, CDCl_3): 133.1, 130.1, 129.9, 128.6, 128.5, 128.1, 127.6, 127.0, 126.5, 124.8, 43.2, 38.7 ppm.

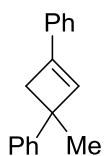
ν_{max} (cm^{-1}): 3024, 2916, 2852, 1589, 1489, 1186, 962, 948, 732.

Entry 2 in Table 10.12

Following General Procedure AJ for the cross coupling of enol phosphates, data is presented in the following format: (a) substrate, (b) catalyst, (c) amount of diethyl ether, (d) volume of Grignard reagent, and (e) yield of product.

(a) 3-methyl-3-phenylcyclobut-1-en-1-yl diphenyl phosphate **136b** (95 mg, 0.25 mmol, 1.0 eq.), (b) PEPPSI ^iPr (2 mg, 2.5×10^{-3} mmol, 1.0 mol%), (c) 1 mL, (d) phenylmagnesium bromide (0.38 mL, $c = 1$ M in THF, 0.38 mmol, 1.5 eq.) and (e) 36 mg (66%).

Characterisation of (3-methylcyclobut-1-ene-1,3-diyl)dibenzene **137b**:¹⁷³



137b

Obtained as colourless oil.

^1H NMR (400 MHz, CDCl_3): 7.55-7.49 (m, 1H, ArH), 7.39-7.21 (m, 8H, ArH), 7.14-7.08 (m, 1H, ArH), 6.65 (s, 1H, CH=C), 2.90 (d, $^2J = 12.6$ Hz, 1H, CH), 2.84 (d, $^2J = 12.6$ Hz, 1H, CH), 1.56 (s, 3H, CH_3) ppm.

^{13}C NMR (100 MHz, CDCl_3): 133.2, 128.3, 127.8, 127.6, 127.3, 126.8, 126.7, 125.3, 125.2, 124.1, 43.8, 37.6, 27.1 ppm.

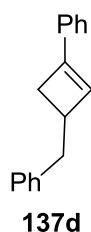
ν_{\max} (cm⁻¹): 2953, 1672, 1442, 1203, 1138, 856, 840, 813, 800, 748.

Entry 3 in Scheme 9.88

Following General Procedure AJ for the cross coupling of enol phosphates, data is presented in the following format: (a) substrate, (b) catalyst, (c) amount of diethyl ether, (d) volume of Grignard reagent, and (e) yield of product.

(a) 3-benzylcyclobut-1-en-1-yl diphenyl phosphate **136d** (98 mg, 0.25 mmol, 1.0 eq.), (b) PEPPSI ⁱPr (2 mg, 2.5*10⁻³ mmol, 1.0 mol%), (c) 1 mL, (d) phenylmagnesium bromide (0.38 mL, c = 1 M in THF, 0.38 mmol, 1.5 eq.) and (e) 54 mg (99%).

Characterisation of (3-benzylcyclobut-1-en-1-yl)benzene **137d**:



Obtained as colourless oil.

¹H NMR (400 MHz, CDCl₃): 7.42-7.32 (m, 6H, ArH), 7.30-7.22 (m, 4H, ArH), 6.43 (m, 1H, CH=C), 3.14-3.05 (m, 1H, CH), 2.96 (d, ²J = 12.9 Hz, J = 4.4 Hz, 1H, CH), 2.87 (d, J = 7.9 Hz, 2H, CH₂), 2.48 (dd, ²J = 12.9 Hz, J = 1.7 Hz, 1H, CH) ppm.

¹³C NMR (100 MHz, CDCl₃): 131.1, 129.0, 128.8, 128.5, 128.4, 127.8, 127.4, 126.1, 124.6, 124.4, 41.3, 40.3, 34.6 ppm.

ν_{\max} (cm⁻¹): 3024, 2910, 1487, 1446, 1429, 1311, 1298, 1074, 1022, 956, 906, 823, 750, 732.

HRMS (EI): m/z calculated for M = C₁₇H₁₆, theoretical [M]⁺: 220.1252. Found: 220.1257.

Chiral HPLC: OD-J column, 0.40 mL/min, detector 254 nm, hexane. t₁= 83.3 min and t₂= 96.8 min.

Entry 1 in Table 9.43

Following General procedure AJ for the cross coupling of enol phosphates, data is presented in the following format: (a) substrate, (b) catalyst, (c) amount of solvent, (d) Grignard reagent, (e) yield of product and (f) enantiomeric ratio.

(a) Diphenyl (3-phenylcyclobut-1-en-1-yl) phosphate **136a** (107 mg, 0.28 mmol, 1.0 eq.), (b) PEPPSI *i*Pr (2 mg, 2.5×10^{-3} mmol, 1.0 mol%), (c) 1.5 mL, (d) phenylmagnesium bromide (0.42 mL, $c = 1$ M in THF, 0.42 mmol, 1.5 eq.), (e) 44 mg (76%) and (f) 59:41.

Chiral analysis of cyclobut-1-ene-1,3-diylidibenzene **136a**:



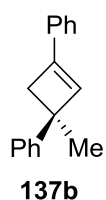
Chiral HPLC: OD-J column, 0.40 mL/min, detector 254 nm, hexane. $t_1 = 32.5$ min (minor) and $t_2 = 33.9$ min (major).

Entry 2 in Table 9.43

Following General procedure AJ for the cross coupling of enol phosphates, data is presented in the following format: (a) substrate, (b) catalyst, (c) amount of solvent, (d) Grignard reagent, (e) yield of product and (f) enantiomeric ratio.

(a) 3-methyl-3-phenylcyclobut-1-en-1-yl diphenyl phosphate **136b** (95 mg, 0.25 mmol, 1.0 eq.), (b) PEPPSI *i*Pr (2 mg, 2.5×10^{-3} mmol, 1.0 mol%), (c) 1 mL, (d) phenylmagnesium bromide (0.38 mL, $c = 1$ M in THF, 0.38 mmol, 1.5 eq.), (e) 32 mg (58%) and (f) 58:42.

Chiral analysis of (3-methylcyclobut-1-ene-1,3-diyl)dibenzene **137b**:



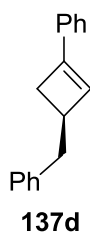
Chiral HPLC: OD-J column, 0.40 mL/min, detector 254 nm, hexane. $t_1 = 59.4$ min (minor) and $t_2 = 65.3$ min (major).

Entry 3 in Table 9.43

Following General procedure AJ for the cross coupling of enol phosphates, data is presented in the following format: (a) substrate, (b) catalyst, (c) amount of solvent, (d) Grignard reagent, (e) yield of product and (f) enantiomeric ratio.

(a) 3-benzylcyclobut-1-en-1-yl diphenyl phosphate **136d** (98 mg, 0.25 mmol, 1.0 eq.), (b) PEPPSI *i*Pr (2 mg, 2.5×10^{-3} mmol, 1.0 mol%), (c) 1 mL, (d) phenylmagnesium bromide (0.38 mL, $c = 1$ M in THF, 0.38 mmol, 1.5 eq.), (e) 53 mg (96%) and (f) 58:42.

Chiral analysis of (3-benzylcyclobut-1-en-1-yl)benzene **137d**:



Chiral HPLC: OD-J column, 0.40 mL/min, detector 254 nm, hexane. $t_1 = 83.3$ min (major) and $t_2 = 96.8$ min (minor).

Scheme 9.91

Following General procedure AG for the synthesis of chiral enol phosphates, data is presented in the following format: (a) substrate, (b) addition temperature of electrophile, (c) conversion, (d) yield of product, and (e) enantiomeric ratio.

(a) 3-phenylcyclobutan-1-one **135a** (117 mg, 0.8 mmol, 0.8 eq.), (b) -78 °C, (c) >99%, (d) 142 mg (47%), and (e) 66:34.

Scheme 9.92

Following General procedure AF for the synthesis of chiral enol phosphates, data is presented in the following format: (a) substrate, (b) addition temperature of electrophile, (c) conversion, (d) yield of product, and (e) enantiomeric ratio.

(a) 3-phenylcyclobutan-1-one **135a** (117 mg, 0.8 mmol, 0.8 eq.), (b) -78 °C, (c) >99%, (d) 166 mg (55%), and (e) 55:45.

Entry 1 in Table 9.44

Following General procedure AK for the synthesis of chiral enol phosphates, data is presented in the following format: (a) substrate, (b) additive, (c) addition temperature of electrophile and additive, (d) conversion, (e) yield of product and (f) enantiomeric ratio.

(a) 3-phenylcyclobutan-1-one **135a** (117 mg, 0.8 mmol, 0.8 eq.), (b) DMPU (0.06 mL, 0.5 mmol, 0.5 eq.) (c) -78 °C, (d) 75%, (e) 187 mg (62%), and (f) 55:45.

Entry 2 in Table 9.44

Following General procedure AK for the synthesis of chiral enol phosphates, data is presented in the following format: (a) substrate, (b) additive, (c) addition temperature of electrophile and additive, (d) conversion, (e) yield of product and (f) enantiomeric ratio.

(a) 3-phenylcyclobutan-1-one **135a** (117 mg, 0.8 mmol, 0.8 eq.), (b) TMEDA (0.08 mL, 0.5 mmol, 0.5 eq.), (c) -78°C, (d) -, (e) 106 mg (35%), and (f) 62:38.

Computational experiments

Calculations were performed with the Gaussian09 quantum chemistry package¹⁷⁵ employing the meta-GGA functional of Truhlar and Zhao¹⁷⁶ – M06L – with associated 6-31G(d) basis set for all atoms. Stationary points were confirmed to be energy minima through vibrational frequency calculations and depicted no imaginary frequencies. Transition states were located employing the Synchronous Transit-Guided Quasi-Newton method¹⁷⁷ with inclusion of relevant guesses for transition state geometry and confirmed by vibrational frequency calculation, which featured a unique imaginary frequency. Graphical elements presented in this document were generated employing the OriginPro 2017 SR2 software package.

Enantiomeric excess values were calculated according to equation [Eq. 1].¹⁷⁸

$$ee = 100 \cdot \frac{\exp\left(\frac{\Delta\Delta G_{TS}}{RT}\right) - 1}{\exp\left(\frac{\Delta\Delta G_{TS}}{RT}\right) + 1} \quad [Eq. 1]$$

Where:

ee is the enantiomeric excess in %;

$\Delta\Delta G_{TS}$ is the difference in Gibbs free energy between the two diastereomeric transition states in kcal mol⁻¹;

R is the gas constant, in kcal mol⁻¹ K⁻¹;

T is the temperature in K.

Relative energies for structures in **Figure 9.8**

Entry	Label	ΔH_{rel} (kcal mol ⁻¹)	ΔG_{rel} (kcal mol ⁻¹)
-------	-------	--	--

1	1 + 2_h	0.0	0.0
2	3_h^S	21.16214724	7.93360893
3	4_h^S	23.5630005	12.66189678
4	5_h^S	6.24686205	-4.20306198
5	3_h^R	17.42783523	5.21084304
6	4_h^R	19.26079194	7.74284589
7	5_h^R	4.37248968	-6.25188213

Relative energies employed starting magnesium adduct **1** and substrate **2_h** as reference.

Relative energies for structures in **Figure 9.9**

Entry	Label	ΔH_{rel} (kcal mol ⁻¹)	ΔG_{rel} (kcal mol ⁻¹)
1	1 + 2_b	0.0	0.0
2	3_b^S	19.00037529	6.03601869
3	4_b^S	22.06387911	11.70682656
4	5_b^S	7.31237403	-5.49322254
5	3_b^R	18.3107418	7.1787144
6	4_b^R	21.43134903	11.08057158
7	5_b^R	4.08697263	-6.57755982

Relative energies employed starting magnesium adduct **1** and substrate **2_b** as reference.

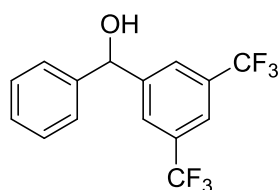
Synthesis of novel amine

Scheme 9.96

Following General Procedure AL for the 1,2-addition to aldehydes data are presented in the following format: (a) substrate and (b) yield.

(a) benzaldehyde (0.10 mL, 1.0 mmol, 1.0 eq.) and (b) 231 mg (72%).

Characterisation of (3,5-bis(trifluoromethyl)phenyl)(phenyl)methanol **191**:



191

Obtained as a white solid.

¹H NMR (CDCl₃): 7.79 (s, 2H, ArH), 7.70 (s, 1H, ArH), 7.34-7.22 (m, 5H, ArH), 5.58 (d, *J* = 3.6 Hz, 1H, CH), 2.30 (d, *J* = 3.6 Hz, 1H, OH) ppm.

¹³C NMR (CDCl₃): 146.3, 142.6, 131.9 (q, 2C, ²*J*_{C-F} = 36 Hz), 129.4, 128.9, 126.8, 126.7, 123.5 (d, 2C, ¹*J*_{C-F} = 260 Hz), 121.6, 75.6 ppm.

$\nu_{\max}(\text{cm}^{-1})$: 1377, 1336, 1280, 1168, 1139, 1046, 900, 846.

MP: 115-120 °C.

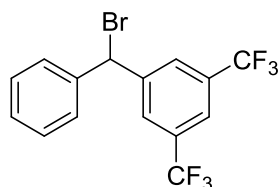
HRMS (APCI) m/z calculated for $\text{C}_{15}\text{H}_{10}\text{F}_6\text{O}$, theoretical $[\text{M}]^+$: 320.0631. Found: 320.0636.

Scheme 9.97

Following General Procedure AM for the bromination of secondary alcohols data are presented in the following format: (a) substrate, (b) temperature for O/N stirring and (c) yield.

(a) (3,5-bis(trifluoromethyl)phenyl)(phenyl)methanol **191** (320 mg, 1.0 mmol, 1.0 eq.) and (b) 331 mg (73%).

Characterisation of 1-(bromo(phenyl)methyl)-3,5-bis(trifluoromethyl)benzene **192**:



192

Obtained as a yellow oil.

^1H NMR (CDCl_3): 7.79 (s, 2H, ArH), 7.82 (s, 1H, ArH), 7.50-7.32 (m, 5H, ArH), 6.33 (s, 1H, CH) ppm.

^{13}C NMR (CDCl_3): 143.2, 139.5, 132.3 (q, 2C, $^2J_{\text{C-F}} = 36$ Hz), 129.4, 129.2, 128.9, 128.5, 123.2 (d, 2C, $^1J_{\text{C-F}} = 267$ Hz), 122.4, 52.7 ppm.

$\nu_{\max}(\text{cm}^{-1})$: 1373, 1273, 1166, 1127, 898.

HRMS (APCI) m/z calculated for $\text{C}_{15}\text{H}_9^{79}\text{BrF}_6$ $[\text{M-H}]^+$: 380.9713. Found: 380.9720.

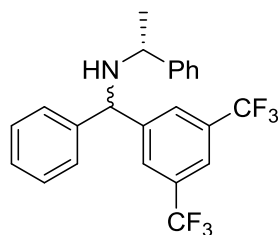
Scheme 9.98

Following General Procedure AN for the nucleophilic substitution with benzhydryl electrophiles data are presented in the following format: (a) solvent, (b) substrate, (c) reaction time and (d) yield.

(a) 1-(bromo(phenyl)methyl)-3,5-bis(trifluoromethyl)benzene **192** (239 mg, 0.62 mmol, 1.0 eq.) and (b) toluene, (c) O/N and (d) 95 mg (36%), d.r. = 1:0.7.

Characterisation of (1S)-N-((3,5-bis(trifluoromethyl)phenyl)(phenyl)methyl)-1-phenylethan-1-amine

194:



194

Obtained as a yellow oil. Mixture of diastereoisomers is reported d. r. = 1.0: 1.0 determined by the benzylic protons ratio at 4.78 and 4.75 ppm.

^1H NMR (CDCl_3): 7.97 (s, 6H, ArH), 7.92 (s, 4H, ArH), 7.81 (s, 2H, ArH), 7.75-7.68 (m, 8H, ArH), 7.65-7.62 (m, 6H, ArH), 4.78 (s, 1H, CH), 4.75 (s, 1H, CH), 3.65 (q, $J = 6.5$ Hz, 1H, CHCH₃), 3.64 (q, $J = 6.5$ Hz, 1H, CHCH₃), 1.45 (d, $J = 6.5$ Hz, 1H, CHCH₃), 1.44 (d, $J = 6.5$ Hz, 1H, CHCH₃), 1.16 (br s, 2H NH) ppm.

^{13}C NMR (CDCl_3): 146.8, 146.2, 144.2, 141.7, 138.9, 135.5, 133.12, 133.11, 131.6 (q, 2C, $^2J_{\text{C-F}} = 36$ Hz), 130.8 (q, 2C, $^2J_{\text{C-F}} = 34$ Hz), 129.5, 129.3, 128.49, 128.41, 128.3, 128.2, 128.1, 127.7, 127.1 (d, 2C, $^1J_{\text{C-F}} = 230$ Hz), 127.2, 127.0, 125.1, 125.0, 122.4 (d, 2C, $^1J_{\text{C-F}} = 272$ Hz), 63.2, 63.1, 55.4, 55.1, 23.9, 23.6 ppm.

$\nu_{\text{max}}(\text{cm}^{-1})$: 2961, 2926, 1373, 1276, 1160, 1024, 910.

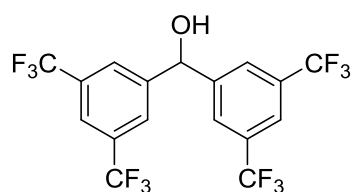
HRMS (APCI) m/z calculated for $\text{C}_{23}\text{H}_{19}\text{F}_6\text{N}$, theoretical $[\text{M}+\text{H}]^+$: 424.1489. Found: 424.1494.

Scheme 9.99

Following General Procedure AL for the 1,2-addition to aldehydes data are presented in the following format: (a) substrate and (b) yield.

(a) 3,5-bis(trifluoromethyl)benzaldehyde **189** (0.17 mL, 1.0 mmol, 1.0 eq.) and (b) 331 mg (73%).

Characterisation of bis(3,5-bis(trifluoromethyl)phenyl)methanol **187**:



187

Obtained as a yellow solid.

^1H NMR (CDCl_3): 7.86-7.80 (m, 6H, ArH), 6.05 (d, $J = 3.2$ Hz, 1H, CH), 2.62 (d, $J = 3.2$ Hz, 1H, OH) ppm.

^{13}C NMR (CDCl_3): 144.1, 131.9 (q, 4C, $^2J_{\text{C-F}} = 33$ Hz), 126.2, 122.6 (d, 2C, $^1J_{\text{C-F}} = 278$ Hz), 121.9, 73.6 ppm.

ν_{max} (cm^{-1}): 1361, 1288, 1114, 910, 889, 842.

MP: 136-140 °C.

HRMS (APCI) m/z calculated for $\text{C}_{17}\text{H}_8\text{F}_{12}\text{O}$, theoretical $[\text{M}]^+$: 456.0384. Found: 456.0385.

Entry 1 in Table 9.46

Following General Procedure AM for the bromination of secondary alcohols data are presented in the following format: (a) substrate, (b) temperature for O/N stirring and (c) yield.

(a) (3,5-bis(trifluoromethyl)phenyl)(phenyl)methanol **187** (456 mg, 1.0 mmol, 1.0 eq.), (b) rt and (b) 0 mg (0%).

Entry 1 in Table 9.46

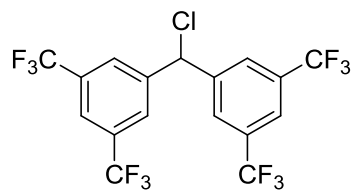
Following General Procedure AM for the bromination of secondary alcohols the solution was refluxed for O/N, data are presented in the following format: (a) substrate, (b) temperature for O/N stirring and (c) yield.

(a) (3,5-bis(trifluoromethyl)phenyl)(phenyl)methanol **187** (456 mg, 1.0 mmol, 1.0 eq.) and (b) 0 mg (0%).

Scheme 9.101

A 10 mL round bottom flask was equipped with a stirrer bar and a condenser, flame dried and purged with argon. (3,5-bis(trifluoromethyl)phenyl)(phenyl)methanol **187** (456 mg, 1 mmol, 1.0 eq.) was dissolved in dist. DCM (8 mL) and transferred to the round bottom flask. The reaction mixture was cooled to 0 °C and thionyl chloride (0.88 mL, 12 mmol, 12 eq.) was added dropwise. The reaction was refluxed for 72 hours. The solvent was removed *in vacuo* and the crude product was distilled (bp. 80 °C at 2 mbar). Yield of the product **186b**: 315 mg (66%).

Characterisation of 5,5'-(chloromethylene)bis(1,3-bis(trifluoromethyl)benzene) **186b**:



186b

Obtained as a white solid.

^1H NMR (CDCl_3): 7.79 (s, 2H, ArH), 7.76 (s, 4H, ArH), 6.15 (s, 1H, CH) ppm.

^{13}C NMR (CDCl_3): 142.1, 133.1(q, 4C, $^2J_{\text{C-F}} = 34$ Hz), 128.1, 123.3, 123.2 (d, 4C, $^1J_{\text{C-F}} = 271$ Hz), 61.0 ppm.

$\nu_{\text{max}}(\text{cm}^{-1})$: 1371, 1273, 1238, 1168, 1111, 908, 891, 858.

MP: 46-48 °C.

HRMS (CI) m/z calculated for $\text{C}_{17}\text{H}_7\text{ClF}_{12}$, theoretical $[\text{M}]^+$: 474.0045. Found: 474.0041.

Scheme 9.102

Following General Procedure AN for the nucleophilic substitution with benzhydryl electrophiles data are presented in the following format: (a) solvent, (b) substrate, (c) reaction time and (d) yield.

(a) toluene, (b) 5,5'-(chloromethylene)bis(1,3-bis(trifluoromethyl)benzene) **186b** (294 mg, 0.62 mmol, 1.0 eq.), (c) 24h and (d) 0 (0%).

Scheme 9.103

Following General Procedure AN for the nucleophilic substitution with benzhydryl electrophiles data are presented in the following format: (a) solvent, (b) substrate, (c) reaction time and (d) yield.

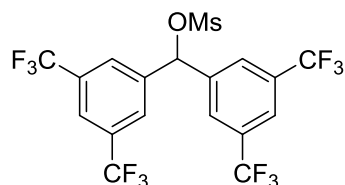
(a) xylene, (b) 5,5'-(chloromethylene)bis(1,3-bis(trifluoromethyl)benzene) **186b** (294 mg, 0.62 mmol, 1.0 eq.), (c) 24 h and (d) 0 (0%).

Scheme 9.104

To the solution of the secondary alcohol **187** (456 mg, 1.0 mmol, 1.0 eq.) in dist. DCM (5 mL) TEA (0.21 mL, 1.5 mmol, 1.5 eq.) and mesyl chloride (0.10 mL, 1.2 mmol, 1.2 eq.) were added dropwise at 0 °C and the solution was stirred for 90 min. The reaction was quenched with water (5 mL) and dist. DCM (10 mL) was added. The organic phase was washed with sat. NaHCO_3 (3 \times 5 mL). The organic

phase was separated and dried over sodium sulphate and the solvent was removed *in vacuo*. The unreacted electrophile was removed removed by fractional distillation (61 °C at 2 mbar). Mass of the product **186c** 470 mg (87%).

Characterisation of bis(3,5-bis(trifluoromethyl)phenyl)methyl methanesulfonate **186c**:



Obtained as a colourless oil.

$^1\text{H NMR}$ (CDCl_3): 7.90 (s, 2H, ArH), 7.82 (s, 4H, ArH), 6.89 (s, 1H, CH), 3.01 (s, 3H, CH_3) ppm.

$^{13}\text{C NMR}$ (CDCl_3): 139.3, 132.4 (q, 4C, $^2J_{\text{C-F}} = 37$ Hz), 126.7, 123.1, 122.2 (d, 4C, $^1J_{\text{C-F}} = 280$ Hz), 78.9, 45.2 ppm.

ν_{max} (cm^{-1}): 2914, 1338, 1273, 1163, 1122, 1112, 929, 910, 896, 862, 831.

HRMS (APCI) m/z calculated for $\text{C}_{18}\text{H}_{10}\text{F}_{12}\text{O}_3\text{S}$, theoretical $[\text{M}-\text{SO}_2\text{CH}_3]^+$: 439.0356. Found: 439.0362.

Entry 1 in Table 9.47

Following General Procedure AN for the nucleophilic substitution with benzhydryl electrophiles data are presented in the following format: (a) solvent, (b) substrate, (c) reaction time and (d) yield.

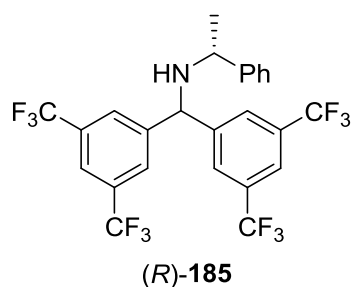
(a) toluene, (b) bis(3,5-bis(trifluoromethyl)phenyl)methyl methanesulfonate **186c** (331 mg, 0.62 mmol, 1.0 eq.), (c) 24 h and (d) 0 (0%).

Entry 2 in Table 9.47

Following General Procedure AN for the nucleophilic substitution with benzhydryl electrophiles data are presented in the following format: (a) solvent, (b) substrate, (c) reaction time and (d) yield.

(a) xylene, (b) bis(3,5-bis(trifluoromethyl)phenyl)methyl methanesulfonate **186c** (331 mg, 0.62 mmol, 1.0 eq.), (c) 72 h and (d) 55 mg (16%).

Characterisation of (R)-N-(bis(3,5-bis(trifluoromethyl)phenyl)methyl)-1-phenylethan-1-amine (R)-**185**:



Obtained as a yellow oil.

^1H NMR (CDCl_3): 7.75 (s, 1H, ArH), 7.70 (s, 2H, ArH), 7.67 (s, 1H, ArH), 7.64 (s, 2H, ArH), 7.31-7.25 (m, 2H, ArH), 7.24-7.19 (m, 2H, ArH), 7.10-7.04 (m, 1H, ArH), 3.49 (q, $J = 6.6$ Hz, 1H, CH), 1.84 (s, 1H, NH), 1.36 (d, $J = 6.6$ Hz, 1H, CHCH₃) ppm.

^{13}C NMR (CDCl_3): 145.4, 145.0, 144.0, 132.6 (q, 1C, $^2J_{\text{C-F}} = 34$ Hz), 132.4 (q, 1C, $^2J_{\text{C-F}} = 33$ Hz), 129.5, 127.9, 127.6, 126.6, 126.1 (d, 2C, $^1J_{\text{C-F}} = 271$ Hz), 123.3 (d, 2C, $^1J_{\text{C-F}} = 275$ Hz), 122.3, 122.1, 122.0, 62.6, 55.1, 23.6 ppm.

$\nu_{\text{max}}(\text{cm}^{-1})$: 2960, 2926, 1371, 1274, 1168, 1124, 904, 896, 844.

HRMS (APCI) m/z calculated for $\text{C}_{25}\text{H}_{17}\text{F}_{12}\text{N}$, theoretical $[\text{M}+\text{H}]^+$: 560.1242. Found: 560.1231.

Structural studies of magnesium amides

DOSY study

Table 9.48

A Schlenk flask was equipped with a stirrer bar and a suba seal, and flame dried. A solution of di-*n*-butyl-magnesium (0.3 mL, $c = 1$ mmol/mL in heptane, 0.3 mmol, 1.0 eq.) was added and heptane was removed *in vacuo*. The residue was dried under vacuum for 1 h. The flask was purged with argon and the appropriate solvent (3 mL) was added. Then (*R*)-bis((*R*)-1-phenylethyl)amine (0.14 mL, 0.6 mmol, 2.0 eq.) was added and the suba seal was swapped for a cold finger. The reaction was refluxed for 90 min and the mixture was allowed to cool down to room temperature. Thereafter the solvent was removed *in vacuo* and d_8 -THF (3 mL) was added and the solution was transferred to an NMR tube under argon.

^1H NMR spectroscopic data was acquired on a Bruker Avance 400 MHz spectrometer. The operating magnetic field strength was 9.4 T, and the spectrometer is equipped with a 5mm BBFO-z-atom probehead equilibrated at 298K by virtue of a BCU-05 unit. The spectrometer operates under Topspin (version 3.5, Bruker, Karlsruhe, Germany) on a HP-XW3300 workstation with a Windows XP

operation system. One-dimensional (1D) ^1H NMR spectroscopic data was acquired with 4 transients over a frequency width of 10 ppm, and centred at 5 ppm using a single pulse-acquire pulse program. Diffusion ordered NMR data were acquired with 8 transients over the same observation frequency window using a double stimulated echo pulse sequence with bipolar gradients for diffusion encoding (dstebpgp3s) according to the method of Jerschow and Muller¹⁶⁷ to compensate the effects of laminar flow caused by thermal convection. Diffusion encoding gradients (16 values) were distributed between the values of 5% and 95% of maximum according to the square gradient value. Diffusion coefficients were calculated directly by fitting the experimental data to the Stejskal-Tanner expression relating diffusion coefficient to signal intensity and diffusion encoding gradient strength. The diffusion coefficients were determined for all reference compounds identically. Alignment of data sets was carried out by a virtue of THF as both solvent and internal reference point for chemical shift and diffusion coefficients. For the calibration curve of the DOSY experiments cyclosporin A, DPPF, squalene and BHT were used as external standards in order to determine molar mass of the related compounds. The typical calibration curve is shown in **Figure 10.1**.

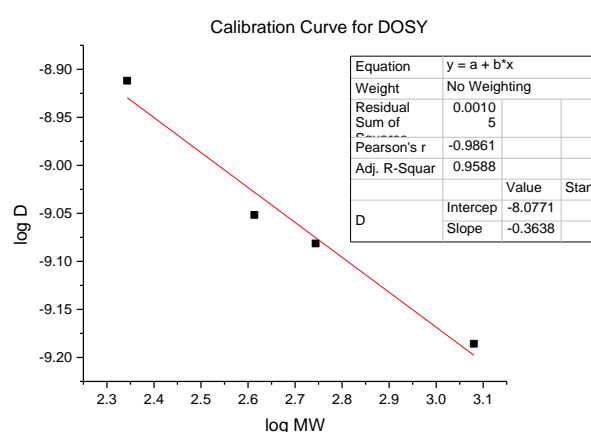


Figure 10.1

PureShift DOSY data

The spectra were acquired on a Bruker 600 MHz spectrometer equipped with a 5 mm TBI $^1\text{H}/^{13}\text{C}/\text{D}$ -BB Z-GRD Z8618/0020 probe at 298 K. The spectrometer is operating under Topspin (version 3.5, Bruker, Karlsruhe, Germany) on a HP-XW3300 workstation with a Windows XP operation system. . One-dimensional (1D) ^1H NMR spectroscopic data was acquired with 4 transients over a frequency width of 10 ppm, and centred at 5 ppm using a single pulse-acquire pulse program. Diffusion ordered NMR data were acquired with 8 transients over the same observation frequency window using a double stimulated echo pulse sequence with bipolar gradients for diffusion encoding

(dstebpgp3s) according to the method of Jerschow and Muller¹⁶⁷ to compensate the effects of laminar flow caused by thermal convection. Diffusion encoding gradients (16 values) were distributed between the values of 5% and 95% of maximum according to the square gradient value. Diffusion coefficients were calculated directly by fitting the experimental data to the Stejskal-Tanner expression relating diffusion coefficient to signal intensity and diffusion encoding gradient strength. The diffusion coefficients were determined for all reference compounds identically. Alignment of data sets was carried out by a virtue of THF as both solvent and internal reference point for chemical shift and diffusion coefficients.

Table 9.49

A Schlenk flask was equipped with a stirrer bar and a suba seal, and flame dried. A solution of di-*n*-butyl-magnesium (0.3 mL, $c = 1$ mmol/mL in heptane, 0.3 mmol, 1.0 eq.) was added and the solvent was removed *in vacuo*. The residue was dried under vacuum for 1 h. The flask was purged with argon and d_8 -THF (3 mL) was added. Then (*R*)-bis((*R*)-1-phenylethyl)amine (0.14 mL, 0.6 mmol, 2.0 eq.) was added and the suba seal was swapped for a cold finger. The reaction was refluxed for the stated time and the mixture allowed to cool down to room temperature. 0.5 mL of solution was transferred to a flame dried NMR tube, which was previously charged with toluene (23 μ L, 0.3 mmol, 1.0 eq.).

Data is represented in the following format: (a) Observed conversion towards mixed alkylmagnesium amide (*R,R*)-**105** and (b) observed conversion towards bisamide species (*R,R*)-**63**.

Entry 1 in Table 9.49

(a) 89% and (b) 11%.

Entry 2 in Table 9.49

(a) 10% and (b) -.

Entry 3 in Table 9.49

(a) 5% and (b) -.

Table 9.50

A Schlenk flask was equipped with a stirrer bar and a suba seal, and flame dried. A solution of di-*n*-butyl-magnesium (0.3 mL, $c = 1$ mmol/mL in heptane, 0.3 mmol, 1.0 eq.) was added and the solvent was removed *in vacuo*. The residue was dried under vacuum for 1 h. The flask was purged with

argon and d_8 -toluene (3 mL) was added. Then (*R*)-bis((*R*)-1-phenylethyl)amine (0.14 mL, 0.6 mmol, 2.0 eq.) was added and the suba seal was swapped for a cold finger. The reaction was refluxed for the stated time and the mixture allowed to cool down to room temperature. 0.5 mL of solution was transferred to a flame dried NMR tube. The mixed alkylmagnesium amide (*R,R*)-**105** and bisamide species (*R,R*)-**63** signals were not observed.

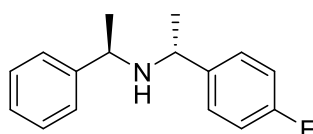
Scheme 9.112

(*R*)-1-phenylethan-1-amine (5.61 mL, 44 mmol, 1.1 eq.), 4-fluoro-acetophenone (4.85 mL, 40 mmol, 1.0 eq.) and p-TSA (152 mg, 2 mol%, 0.8 mmol) were heated in toluene (40 mL) at reflux for 26 h using a Dean Stark apparatus. The solution was filtered and the solvent was evaporated. The crude mixture was dissolved in methanol (48 mL) and cooled down to 0 °C. Finally sodium borohydride (3.78 g, 100 mmol, 2.5 eq) was added and the reaction was stirred for 12 h. The reaction was quenched with sat. ammonium chloride solution (40 mL) and the aqueous phase was extracted with DCM (3 × 40 mL). The organic phase was dried over sodium sulfate, filtered and the solvent was removed *in vacuo*. The crude product was purified by flash column chromatography using 1-10% MeOH in DCM. Yield of the product: 8.08 g (83%). (*R,R*) : (*R,S*) = 1.0:0.1.

(*R*)-1-(4-fluorophenyl)-*N*-((*R*)-1-phenylethyl)ethan-1-amine was obtained after salt formation with HCl and recrystallization with dist. ¹PrOH and hexane. Mass of (*R*)-1-(4-fluorophenyl)-*N*-((*R*)-1-phenylethyl)ethan-1-amine **196**: 2.74 g (30%).

Characterisation of (*R*)-1-(4-fluorophenyl)-*N*-((*R*)-1-phenylethyl)ethan-1-amine (*R,R*)-**196**:¹⁶⁸

Obtained as a colourless oil.



(*R,R*)-**196**

¹H NMR (CDCl₃): δ (*R,R*)-diastereomer: 7.30-7.07 (m, 7H, ArH), 6.98-6.88 (m, 2H, ArH), 3.43-3.35 (m, 2H, NHCH), 1.48 (br s, 1H, NH), 1.20 (d, 3H, *J* = 6.7 Hz, NHCHCH₃(Ar(F)) and 1.17 (d, 3H, *J* = 6.6 Hz, NHCHCH₃Ar) ppm.

¹⁹F NMR (CDCl₃): δ (*R,R*): -116.5 ppm.

¹³C NMR (CDCl₃): δ 150.3 (²*J*_{C-F} = 240 Hz), 127.9 (*J*_{C-F} = 18 Hz), 127.7, 127.6, 126.0, 114.7, 114.5, 114.4, 54.0, 53.9, 24.5 and 24.4 ppm.

ν (neat): 2960, 1602, 1506, 1492, 1469, 1450, 1369, 1220, 1201, 1153, 1124, 1095, 1024, 833, 821, 761, 732, 700 and 682 cm^{-1} .

HR-MS (ESI): m/z calculated for $M = \text{C}_{16}\text{H}_{18}\text{FN}$, theoretical $[\text{M}+\text{H}]^+$: 247.1515. Found: 247.1513.

Scheme 9.113

Synthesis of (*R,R*)-**197**:

A Schlenk flask was equipped with a stirrer bar and a suba seal, and flame dried. A solution of di-*n*-butyl-magnesium (0.3 mL, $c = 1$ mmol/mL in heptane, 0.3 mmol, 1.0 eq.) was added and the solvent was removed *in vacuo*. The residue was dried under vacuum for 1 h. The flask was purged with argon and hexane (3 mL) was added. Then (*R*)-1-(4-fluorophenyl)-*N*-((*R*)-1-phenylethyl)ethan-1-amine (*R,R*)-**196** (0.14 mL, 0.6 mmol, 2.0 eq.) was added and the suba seal was swapped for a cold finger. The reaction was refluxed for the stated time and the mixture allowed to cool down to room temperature. The solvent was removed *in vacuo* and d_8 -toluene (3 mL) was added, 0.5 mL of the solution was then transferred to a flame dried NMR tube and analysed by ^1H and ^{19}F NMR spectroscopy..

Synthesis of (*R,R*)-**198**:

A Schlenk flask was equipped with a stirrer bar and a suba seal, and flame dried. A solution of di-*n*-butyl-magnesium (0.3 mL, $c = 1$ mmol/mL in heptane, 0.3 mmol, 1.0 eq.) was added and the solvent was removed *in vacuo*. The residue was dried under vacuum for 1 h. The flask was purged with argon and THF (3 mL) was added. Then ((*R*)-1-(4-fluorophenyl)-*N*-((*R*)-1-phenylethyl)ethan-1-amine (*R,R*)-**196** (73 mg, 0.3 mmol, 1.0 eq.) was added and the suba seal was swapped for a cold finger. The reaction was refluxed for 90 min and the mixture allowed to cool down to room temperature. 0.5 mL of solution was transferred to a flame dried NMR tube and analysed by ^1H and ^{19}F NMR spectroscopy.

Scheme 9.114

A Schlenk flask was equipped with a stirrer bar and a suba seal, and flame dried. A solution of di-*n*-butyl-magnesium (0.3 mL, $c = 1$ mmol/mL in heptane, 0.3 mmol, 1.0 eq.) was added and the heptane was removed *in vacuo*. The residue was dried under vacuum for 1 h. The flask was purged with argon and THF (3 mL) was added. Then lithium chloride (25.4 mg, 0.6 mmol, 2.0 eq.) and (*R*)-bis((*R*)-1-phenylethyl)amine (0.14 mL, 0.6 mmol, 2.0 eq.) were added. The reaction was stirred for 90 min at rt. The solvent was replaced by d_8 -THF (3 mL) and 0.5 mL of solution was transferred to a flame dried NMR tube and analysed by ^1H NMR spectroscopy.

A Schlenk flask was equipped with a stirrer bar and a suba seal, and flame dried. A solution of di-n-butyl-magnesium (0.3 mL, c = 1 mmol/mL in heptane, 0.3 mmol, 1.0 eq.) was added and the heptane was removed *in vacuo*. The residue was dried under vacuum for 1 h. The flask was purged with argon and THF (3 mL) was added. Then lithium chloride (25.4 mg, 0.6 mmol, 2.0 eq.), 18-c-6 (79 mg, 0.3 mmol, 1.0 eq.) and (*R*)-bis((*R*)-1-phenylethyl)amine (0.14 mL, 0.6 mmol, 2.0 eq.) were added. The reaction was stirred for 90 min at rt . The solvent was replaced by d₈-THF (3 mL) and 0.5 mL of solution was transferred to a flame dried NMR tube and analysed by ¹H NMR spectroscopy.

13 References

- 1 E. L. Eliel and S. H. Wilen, *Stereochemistry of Organic Compounds*, Wiley, 1994.
- 2 P. O'Brien, *Tetrahedron*, 2002, **58**, 4020.
- 3 L. A. Nguyen, H. He and C. Pham-Huy, *Int. J. Biomed. Sci.*, 2006, **2**, 85.
- 4 E. M. Carreira and L. Kvaerno, *Classics in Stereoselective Synthesis*, Wiley-VCH, 2009.
- 5 S. Hanessian, *Total Synthesis of Natural Products the Chiron Approach*, Pergamon Press, 1984.
- 6 G. Roos (Ed.), *Key Chiral Auxiliary Applications*, Academic Press, Boston, Second ed., 2014.
- 7 P. O'Brien, *J. Chem. Soc., Perkin Trans. 1*, 2001, 95.
- 8 A. C. Regan, *J. Chem. Soc., Perkin Trans. 1*, 1999, 357.
- 9 P. O'Brien, *J. Chem. Soc., Perkin Trans. 1*, 2002, 1.
- 10 O. Iwao, Ed., *Catalytic Asymmetric Synthesis*, Wiley-VCH, Third ed., 2010.
- 11 A. Harrison-Marchand and J. Maddaluno (Ed.), *Advances in the Chemistry of Chiral Lithium Amides*, Wiley-VCH, 2014.
- 12 A. C. Regan, *Contemp. Org. Synth.*, 1997, **4**, 1.
- 13 P. J. Cox and N. S. Simpkins, *Tetrahedron: Asymmetry*, 1991, **2**, 1.
- 14 K. Koga, *Pure Appl. Chem.*, 1994, **66**, 1487.

- 15 P. O'Brien, *J. Chem. Soc., Perkin Trans. 1*, 1998, 1439.
- 16 R. Luisi and V. Capriati, Eds., *Lithium Compounds in Organic Synthesis*, Wiley-VCH, 2014.
- 17 P. O'Brien, *J. Chem. Soc., Perkin Trans. 1*, 2001, 95.
- 18 J. K. Crandall and M. Apparau, *Org. React.*, 1983, **29**, 345.
- 19 B. Thummel and R. P. Rickborn, *J. Am. Chem. Soc.*, 1970, **92**, 2064.
- 20 K. M. Morgan and J. J. Gajewski, *J. Org. Chem.*, 1996, **61**, 820.
- 21 J. K. Whitesell and S. W. Felman, *J. Org. Chem.*, 1980, **45**, 755.
- 22 M. Asami, *Chem. Lett.*, 1984, 829.
- 23 M. Asami, *Bull. Chem. Soc. Jpn.*, 1990, **63**, 721.
- 24 A. Mordini, E. B. Rayana, C. Margot and M. Schlosser, *Tetrahedron*, 1990, **46**, 2401.
- 25 D. Milne and P. J. Murphy, *J. Chem. Soc. Chem. Commun.*, 1993, 884.
- 26 A.H. Ingall, P.R. Moore, S. M. Roberts, K.-L. Lu, C.-M. Wang, H.-H. Lee, L.-C. Chen, Y. S. Wen, D. Mikre, P. J. Murphy, S.-C. Hung, C. C. Liao, H. C. Birrell, P. Camilleri, G. N. Okato, G. Prakash, E. T. Kool, P. D. Boyle, S. Parsons, J. Passmore, D.J. Wood, H. Suemune, Y. Takashi and K. Sakashi, *J. Chem. Soc. Chem. Commun.*, 1994, 675.
- 27 D. A. Price, N. S. Simpkins, A. M. Macleod and A. P. Watt, *J. Org. Chem.*, 1994, **59**, 1961.
- 28 R. A. Ewin, A. M. MacLeod, D. A. Price, N. S. Simpkins and A. P. Watt, *J. Chem. Soc., Perkin Trans. 1*, 1997, 401.
- 29 D. A. Price, N. S. Simpkins, A. M. MacLeod, A. P. Watt, *Tetrahedron Lett.*, 1994, **35**, 6159.
- 30 E. P. Kündig and A. Quattropiani, *Tetrahedron Lett.*, 1994, **35**, 3497.
- 31 S. Richard A. Ewin, N. Simpkins, *Synlett*, 1996, 317.
- 32 E. L. M. Cowton, S. E. Gibson (née Thomas), M. J. Schneider and M. H. Smith, *Chem. Commun.*, 1996, 839.
- 33 C. M. Cain, R. P. C. Cousins, G. Coumbarides and N. S. Simpkins, *Tetrahedron*, 1990, **46**, 523.

- 34 R. Shirai, M. Tanaka and K. Koga, *J. Am. Chem. Soc.*, 1986, **108**, 543.
- 35 P. Deslongchamps, *Stereoelectronic Effects in Organic Chemistry*, Pergamon Press, 1985.
- 36 R. Shirai, D. Sato, K. Aoki, M. Tanaka, H. Kawasaki and K. Koga, *Tetrahedron*, 1997, **53**, 5963.
- 37 E. J. Corey and A. W. Gross, *Tetrahedron Lett.*, 1984, **25**, 495.
- 38 B. J. Bunn and N. S. Simpkins, *J. Org. Chem.*, 1993, **58**, 533.
- 39 B. J. Bunn, N. S. Simpkins, Z. Z. Spavold and M. J. Crimmin, *J. Chem. Soc., Perkin Trans. 1*, 1993, 3113.
- 40 M. Majewski, R. Lazny and P. Nowak, *Tetrahedron Lett.*, 1995, **36**, 5465.
- 41 M. Majewski, D. M. Gleave and P. Nowak, *Can. J. Chem.*, 1995, **73**, 1616.
- 42 K. Sugasawa, M. Shindo, H. Noguchi and K. Koga, *Tetrahedron Lett.*, 1996, **37**, 7377.
- 43 A. J. Edwards, S. Hockey, F. S. Mair, P. R. Raithby, R. Snaith and N. S. Simpkins, *J. Org. Chem.*, 1993, **58**, 6942.
- 44 F. S. Mair, W. Clegg and P. A. O'Neil, *J. Am. Chem. Soc.*, 1993, **115**, 3388.
- 45 D. Sato, H. Kawasaki, I. Shimada, Y. Arata, K. Okamura, T. Date and K. Koga, *J. Am. Chem. Soc.*, 1992, **114**, 761.
- 46 M. Toriyama, K. Sugasawa, M. Shindo, N. Tokutake and K. Koga, *Tetrahedron Lett.*, 1997, **38**, 567.
- 47 K. Aoki, H. Noguchi, K. Tomioka and K. Koga, *Tetrahedron Lett.*, 1993, **34**, 5105.
- 48 K. Aoki, K. Tomioka, H. Noguchi and K. Koga, *Tetrahedron*, 1997, **53**, 13641.
- 49 M. Majewski and J. Mackinnon, *Can. J. Chem.*, 1994, **72**, 1699.
- 50 M. Majewski, N. M. Irvine and J. MacKinnon, *Tetrahedron: Asymmetry*, 1995, **6**, 1837.
- 51 T. Honda, N. Kimura and M. Tsubuki, *Tetrahedron: Asymmetry*, 1993, **4**, 21.
- 52 T. Honda, N. Kimura and M. Tsubuki, *Tetrahedron: Asymmetry*, 1993, **4**, 1475.

- 53 T. Honda and N. Kimura, *J. Chem. Soc., Chem. Comm.*, 1994, 77.
- 54 T. Momose, N. Toyooka and Y. Hirai, *Chem. Lett.*, 1990, 1319.
- 55 T. Momose, N. Toyooka, S. Seki and Y. Hirai, *Chem. Pharm. Bull.*, 1990, **38**, 2072.
- 56 T. Momose, M. Toshima, N. Toyooka, Y. Hirai and C. H. Eugster, *J. Chem. Soc. Chem. Commun.*, 1997, 1307.
- 57 T. Momose, M. Toshima, S. Seki, Y. Koike, N. Toyooka and Y. Hirai, *J. Chem. Soc., Perkin Trans. 1*, 1997, 1315.
- 58 J. Eames, *European J. Org. Chem.*, 2002, 393.
- 59 M. Asami, T. Ishizaki and S. Inoue, *Tetrahedron Asymmetry*, 1994, **5**, 793.
- 60 M. Asami, T. Suga, K. Honda and S. Inoue, *Tetrahedron Lett.*, 1997, **38**, 6425.
- 61 J. P. Tierney, A. Alexakis and P. Mangeney, *Tetrahedron: Asymmetry*, 1997, **8**, 1019.
- 62 T. Yamashita, D. Sato, T. Kiyoto, A. Kumar and K. Koga, *Tetrahedron Lett.*, 1996, **37**, 8195.
- 63 B. J. Wakefield, *Comprehensive Organic Chemistry Vol. 3*, Pergamon, 1979.
- 64 B. J. Wakefield, *Organolithium Methods*, Academic Press, 1988.
- 65 E. Bunce and T. Durst (ed.), *Comprehensive Carbanion Chemistry*, Elsevier, 1980.
- 66 K. W. Henderson and W. J. Kerr, *Chem. Eur. J.*, 2001, **7**, 3430.
- 67 J. L. Wardell, in *Comprehensive Organometallic Chemistry*, Elsevier, 1982, pp. 43.
- 68 J. D. Anderson, P. García García, D. Hayes, K. W. Henderson, W. J. Kerr, J. H. Moir and K. P. Fondekar, *Tetrahedron Lett.* 2001, **42**, 7111.
- 69 M. Lappert, A. Protchenko, P. Power and A. Seeber (Ed.), Wiley, 2008, pp. 39.
- 70 Y. Tang, L. N. Zakharov, A. L. Rheingold and R. A. Kemp, *Organometallics*, 2005, **24**, 836.
- 71 D. B. Collum, A. J. McNeil and A. Ramirez, *Angew. Chem. Int. Ed.*, 2007, **46**, 3002.
- 72 M. M. Olmstead, D. R. Grigsby, D. R. Chacon, T. Hascall and P. P. Power, *Inorg. Chim. Acta*,

- 1996, **251**, 273.
- 73 B. G. E. Coates and S. Road, *J.Chem.Soc.(A)*, 1967, 56–59.
- 74 W. Clegg, F. J. Craig, K. W. Henderson, A. R. Kennedy, R. E. Mulvey, P. A. O’Neil, D. Reed, P. A. O. Neil and D. Reed, *Inorg. Chem.*, 1997, **36**, 6238.
- 75 M. Westerhausen, *Inorg. Chem.*, 1991, **30**, 96.
- 76 J. L. Sebestl, T. T. Nadasdi, M. J. Heeg and C. H. Winter, *Inorg. Chem.*, 1998, **37**, 1289.
- 77 D. a. Evans and S. G. Nelson, *J. Am. Chem. Soc.*, 1997, **119**, 6452.
- 78 K. W. Henderson, W. J. Kerr and J. H. Moir, *Chem. Commun.*, 2000, 479.
- 79 K. W. Henderson, W. J. Kerr and J. H. Moir, *Synlett*, 2001 , 1253.
- 80 L. S. Bennie, *PhD Thesis*, University of Strathclyde, 2012.
- 81 J. D. Anderson, P. García García, D. Hayes, K. W. Henderson, W. J. Kerr, J. H. Moir and K. P. Fondekar, *Tetrahedron Lett.*, 2001, **42**, 7111.
- 82 L. S. Bennie, W. J. Kerr, M. Middleditch and A. J. B. Watson, *Chem. Commun.*, 2011, **47**, 2264.
- 83 W. J. Kerr, M. Middleditch and A. J. B. Watson, *Synlett*, 2011, 177.
- 84 M. J. Bassindale, J. J. Crawford, K. W. Henderson and W. J. Kerr, *Tetrahedron Lett.*, 2004, **45**, 4175.
- 85 K. W. Henderson, W. J. Kerr and J. H. Moir, *Chem. Commun.*, 2001, 1722.
- 86 M. Narita, *Bull. Chem. Soc. Jpn.*, 1978, **51**, 1477–1480.
- 87 E. L. Carswell, D. Hayes, K. W. Henderson, W. J. Kerr and C. J. Russell, *Synlett*, 2003, 1017.
- 88 E. L. Carswell, W. J. Kerr, D. McArthur, M. Pažický and A. J. B. Watson, *Tetrahedron*, 2014, **70**, 7344.
- 89 A. J. B. Watson, *PhD Thesis*, University of Strathclyde, 2007.
- 90 D. Hayes, K. W. Henderson, W. J. Kerr and C. J. Russell, *Synlett*, 2003, 1017.

- 91 K. W. Henderson, W. J. Kerr and J. H. Moir, *Tetrahedron*, 2002, **58**, 4573.
- 92 M. Rajamanickam, *PhD Thesis*, University of Strathclyde, 2015.
- 93 A. Krasovskiy and P. Knochel, *Angew. Chem. Int. Ed.*, 2004, **43**, 3333.
- 94 W. J. Kerr, A. J. B. Watson and D. Hayes, *Chem. Commun.*, 2007, 5049.
- 95 W. J. Kerr, D. M. Lindsay, V. K. Patel and M. Rajamanickam, *Org. Biomol. Chem.*, 2015, **13**, 10131.
- 96 W. J. Kerr, A. J. B. Watson and D. Hayes, *Org. Biomol. Chem.*, 2008, **6**, 1238.
- 97 W. J. Kerr, A. J. Morrison, M. Pazicky and T. Weber, *Org. Lett.*, 2012, **14**, 2250.
- 98 T. A. Reekie, M. E. Kavanagh, M. Longworth and M. Kassiou, *Synthesis*, 2013, **45**, 3211.
- 99 A. Deiters and S. F. Martin, *Chem. Rev.*, 2004, **104**, 2199.
- 100 M. Hatano, K. Yamashita and K. Ishihara, *Org. Lett.*, 2015, **17**, 2412.
- 101 S. J. Lee and P. Beak, *J. Am. Chem. Soc.*, 2006, **128**, 2178.
- 102 G. I. Georg, X. Guan and J. Kant, *Bioorg. Med. Chem. Lett.*, 1991, **1**, 125.
- 103 N. R. Monks, *PhD Thesis*, University of Strathclyde, 2013.
- 104 F. Lovering, J. Bikker and C. Humblet, *J. Med. Chem.*, 2009, **52**, 6752.
- 105 F. Lovering, *Med. Chem. Commun.*, 2013, **4**, 515.
- 106 J. B. Wright and R. E. Willette, *J. Med. Pharm. Chem.*, 1962, **5**, 815.
- 107 P. H. Ratner, S. R. Findlay, F. Hampel, J. van Bavel, M. D. Widlitz and J. J. Freitag, *J. Allergy Clin. Immunol.*, 1994, **94**, 818.
- 108 F. Horak and U. P. Ziegelmayer, *Expert Rev. Clin. Immunol.*, 2009, **5**, 659.
- 109 A. M. Geddes and P. D. Clarke, *J. Antimicrob. Chemother.*, 1977, **3**, 101.
- 110 P. D. Clarke, A. M. Geddes, D. McGhie and J. C. Wall, *Br. Med. J.*, 1976, **2**, 14.
- 111 I. Colomer, C. J. Empson, P. Craven, Z. Owen, R. G. Doveston, I. Churcher, S. P. Marsden and A.

- Nelson, *Chem. Commun.*, 2016, **52**, 7209.
- 112 W. J. Kerr, D. M. Lindsay, V. K. Patel and M. Rajamanickam, *Org. Biomol. Chem.*, 2015, **13**, 10131.
- 113 D. Gauthier, S. Beckendorf, T. M. Gøgsig, A. T. Lindhardt and T. Skrydstrup, *J. Org. Chem.*, 2009, **74**, 3536.
- 114 M. G. Organ, M. Abdel-Hadi, S. Avola, N. Hadei, J. Nasielski, C. J. O'Brien and C. Valente, *Chem. Eur. J.*, 2007, **13**, 150.
- 115 G. Manolikakes and P. Knochel, *Angew. Chem. Int. Ed.*, 2009, **48**, 205.
- 116 E. J. Corey and D. Enders, *Chem. Ber.*, 1978, **111**, 1337.
- 117 R. Neufeld, T. L. Teuteberg, R. Herbst-Irmer, R. A. Mata and D. Stalke, *J. Am. Chem. Soc.*, 2016, **138**, 4796.
- 118 A. L. Krasovskiy, S. Haley, K. Voigtritter and B. H. Lipshutz, *Org. Lett.*, 2014, **16**, 4066.
- 119 Michael E. Limmert, and Amy H. Roy and J. F. Hartwig, *J. Org. Chem.*, 2005, **70**, 9364.
- 120 S. Kyasa, T. Fisher and P. Dussault, *Synthesis*, 2011, **2011**, 3475.
- 121 F. Romanov-Michailidis, K. F. Sedillo, J. M. Neely and T. Rovis, *J. Am. Chem. Soc.*, 2015, **137**, 8892.
- 122 M. P. Rissanen, T. Kurtén, M. Sipilä, J. A. Thornton, J. Kangasluoma, N. Sarnela, H. Junninen, S. Jørgensen, S. Schallhart, M. K. Kajos, R. Taipale, M. Springer, T. F. Mentel, T. Ruuskanen, T. Petäjä, D. R. Worsnop, H. G. Kjaergaard and M. Ehn, *J. Am. Chem. Soc.*, 2014, **136**, 15596.
- 123 S. L. Schreiber, R. E. Claus and J. Reagan, *Tetrahedron Lett.*, 1982, **23**, 3867.
- 124 A. F. Abdel-Magid and S. J. Mehrman, *Org. Process Res. Dev.*, 2006, **10**, 971.
- 125 J. E. Mills, C. A. Maryanoff, D. F. McComsey, R. C. Stanzione and L. Scott, *J. Org. Chem.*, 1987, **52**, 1857.
- 126 Xinyan Wang, Yanmei Dong, Jianwei Sun, Xuenong Xu, and Rui Li and Y. Hu, *J. Org. Chem.*, 2005, **70**, 1897.

- 127 T. A. Gourdie, K. K. Valu, G. L. Gravatt, T. J. Boritzki, B. C. Baguley, L. P. G. Wakelin, W. R. Wilson, P. D. Woodgate and W. A. Denny, *J. Med. Chem.*, 1990, **33**, 1177.
- 128 T. H. Walls, S. C. Grindrod, D. Beraud, L. Zhang, A. R. Baheti, S. Dakshanamurthy, M. K. Patel, M. L. Brown and L. H. MacArthur, *Bioorg. Med. Chem.*, 2012, **20**, 5269.
- 129 R. C. Bernotas and R. V. Cube, *Synth. Commun.*, 1990, **20**, 1209.
- 130 S. Ram and L. D. Spicer, *Synth. Commun.*, 1987, **17**, 415.
- 131 M. Kawaguchi, O. Hayashi, N. Sakai, M. Hamada, Y. Yamamoto and J. Oda, *Agric. Biol. Chem.*, 1986, **50**, 3107.
- 132 G. F. Painter and A. Falshaw, *J. Chem. Soc. Perkin Trans. 1*, 2000, 1157.
- 133 T.-L. Shih, R.-Y. Yang, S.-T. Li, C.-F. Chiang and C.-H. Lin, *J. Org. Chem.*, 2007, **72**, 4258.
- 134 A. Alexakis, S. Gille, F. Prian, S. Rosset and K. Ditrach, *Tetrahedron Lett.*, 2004, **45**, 1449.
- 135 S. Bhattacharyya, A. Chatterjeeb and S. Kantha Duttachowdhuryc, *J. Chem. Soc., Perkin Trans. 1*, 1994, 1.
- 136 I. Saxena, R. Borah and J. C. Sarma, *J. Chem. Soc., Perkin Trans. 1*, 2000, 503.
- 137 L. V. Adriaenssens, C. A. Austin, M. Gibson, D. Smith and R. C. Hartley, *Eur. J. Org. Chem.*, 2006, **2006**, 4998.
- 138 P. B. Alper, M. Hendrix, P. Sears and C.-H. Wong, *J. Am. Chem. Soc.*, 1998, **120**, 1965.
- 139 K. C. Nicolaou, S. A. Snyder, D. A. Longbottom, A. Z. Nalbandian and X. Huang, *Chem. - A Eur. J.*, 2004, **10**, 5581.
- 140 T. Chan, K. Guckian, T. Jenkins, J. Thomsa, J. Vessels, G. Kumaravel, R. Meissner, J. Lyssikales, B. Lucus, J. Duffield, WO 2016011390, 2016.
- 141 L. Hu, S. D. Denim, S. M. H. Vendeville, A. Tahri, P. J.-M. B. Raboisson, WO 2015158653, 2015.
- 142 T. A. Barf, A. Oubril, F. C. Schultz, E. A. Zwart, N. Hoogenboom, W.S. de Martijn, A. Kaptein WO 201173119, 2011.
- 143 M. Weiss, E. F. Dimauro, T. Dineen, R. Graceffa, A. Guzman-Perez, H. Huang, C. Kreisman, I. E.

- Marx, H. N. Nguyen, E. Peterson, H. L. Deak, WO 2014201173, 2014.
- 144 S. D. Bull, S. G. Davies, G. Fenton, A. W. Mulvaney, R. S. Prasad and A. D. Smith, *J. Chem. Soc. Perkin Trans. 1*, 2000, 3765.
- 145 C. A. Faler and M. M. Joullie, *Org. Lett.*, 2007, **9**, 1987.
- 146 A. Nodzewska, K. Sidorowicz and M. Sienkiewicz, *Synthesis*, 2014, **46**, 1475.
- 147 R. Lazny, K. Wolosewicz, P. Zielinska, Z. Urbanczyk-Lipkowska and P. Kalicki, *Tetrahedron*, 2011, **67**, 9433.
- 148 T. Lebleu and J.-F. Paquin, *Tetrahedron Lett.*, 2017, **58**, 442.
- 149 P. J. Goldsmith, S. J. Teat and S. Woodward, *Angew. Chem. Int. Ed.*, 2005, **44**, 2235.
- 150 J. Francos, S. Zaragoza-Calero and C. T. O'Hara, *Dalton Trans.*, 2014, **43**, 1408.
- 151 W. L. F. Armarego and D. D. Perrin, *Purification of Laboratory Chemicals*, Pergamon Press, 3rd Ed., 1998.
- 152 A. Krasovskiy and P. Knochel, *Synthesis*, 2006, **5**, 890.
- 153 B. E. Love and E. G. Jones, *J. Org. Chem.*, 1999, **64**, 3755.
- 154 K. Alder and J. Haydn, *Justus Liebigs Ann. Chem.*, 1950, **570**, 201.
- 155 L. Ackermann, S. Barfüsser and J. Pospesch, *Org. Lett.*, 2010, **12**, 724.
- 156 K. Ishizuka, H. Seike, T. Hatakeyama and M. Nakamura, *J. Am. Chem. Soc.*, 2010, **132**, 13117.
- 157 J. A. Kenar and A. Nickon, *Tetrahedron*, 1997, **53**, 14871.
- 158 J.-M. Fang, S.-F. Sun and M.-H. Rei, *J. Chem. Soc. Perkin Trans. 2*, 1989, 747.
- 159 E. A. Basso, C. Kaiser, R. Rittner and J. B. Lambert, *J. Org. Chem.*, 1993, **58**, 7865.
- 160 M. Hannaby and S. Warren, *J. Chem. Soc. Perkin Trans. 1*, 1992, 3007.
- 161 R. Liu, O. Gutierrez, D. J. Tantillo and J. Aubé, *J. Am. Chem. Soc.*, 2012, **134**, 6528.
- 162 Ignacio Pérez, and José Pérez Sestelo and L. A. Sarandeses, *J. Am. Chem. Soc.*, 2001, **123**,

- 4155.
- 163 Z. Jia, F. Zhou, M. Liu, X. Li, A. S. C. Chan and C.-J. Li, *Angew. Chem. Int. Ed.*, 2013, **52**, 11871.
- 164 A. Seifert, K. Rohr and R. Mahrwald, *Tetrahedron*, 2012, **68**, 1137.
- 165 A. Chevalley, J. Prunet, M. Mauduit and J.-P. Férézou, *Eur. J. Org. Chem.*, 2013, **36**, 8265.
- 166 A. I. Meyers, A. Susan V. Downing and M. J. Weiser, *J. Org. Chem.*, 2001, **66**, 1413.
- 167 A. Jerschow and N. Müller, *J. Magn. Reson. Ser. A*, 1996, **123**, 222.
- 168 P. Katai, *9 Month Report*, University of Strathclyde, 2016.
- 169 A. V. Malkov, F. Friscourt, M. Bell, M. E. Swarbrick and P. Kočovský, *J. Org. Chem.*, 2008, **73**, 3996.
- 170 A. V. Malkov, F. Friscourt, M. Bell, M. E. Swarbrick and P. Kočovský, *J. Org. Chem.*, 2008, **73**, 3996.
- 171 H.-J. Xu, F.-F. Zhu, Y.-Y. Shen, X. Wan and Y.-S. Feng, *Tetrahedron*, 2012, **68**, 4145.
- 172 T. Matsuda and I. Yuihara, *Chem. Commun.*, 2015, **51**, 7393.
- 173 M. Ni, J. Zhang, X. Liang, Y. Jiang and T.-P. Loh, *Chem. Commun.*, 2017, **53**, 12286.
- 174 Gaussian 09, Revision D.01, M. J. Frisch, G. W. Trucks, H. B. Schlegel, G. E. Scuseria, M. A. Robb, J. R. Cheeseman, G. Scalmani, V. Barone, B. Mennucci, G. A. Petersson, H. Nakatsuji, M. Caricato, X. Li, H. P. Hratchian, A. F. Izmaylov, J. Bloino, G. Zheng, J. L. Sonnenberg, M. Hada, M. Ehara, K. Toyota, R. Fukuda, J. Hasegawa, M. Ishida, T. Nakajima, Y. Honda, O. Kitao, H. Nakai, T. Vreven, J. A. Montgomery, J. E. Peralta, F. Ogliaro, M. Bearpark, J. J. Heyd, E. Brothers, K. N. Kudin, V. N. Staroverov, R. Kobayashi, J. Normand, K. Raghavachari, A. Rendell, J. C. Burant, S. S. Iyengar, J. Tomasi, M. Cossi, N. Rega, J. M. Millam, M. Klene, J. E. Knox, J. B. Cross, V. Bakken, C. Adamo, J. Jaramillo, R. Gomperts, R. E. Stratmann, O. Yazyev, A. J. Austin, R. Cammi, C. Pomelli, J. W. Ochterski, R. L. Martin, K. Morokuma, V. G. Zakrzewski, G. A. Voth, P. Salvador, J. J. Dannenberg, S. Dapprich, A. D. Daniels, Ö. Farkas, J. B. Foresman, J. V. Ortiz, J. Cioslowski, D. J. Fox. Gaussian, Inc., Wallingford CT, 2009.
- 175 Zhao, Y.; Truhlar, D. G., *Theor. Chem. Acc.* **2008**, *120*, 215-241.
- 176 Peng, C.; Schlegel, H. B., *Israel J. Chem.* **1993**, *33*, 449-454.
- 177 For a derivation of an equation analogous to [Eq. 1] see: Schneebeli, S. T.; Hall, M. L.; Breslow,

R.; Friesner, R., *J. Am. Chem. Soc.* **2009**, *131*, 3965-3973.